LONDON'S GLOBAL UNIVERSITY

Pyruvate Kinase M2 (PKM2) and Lactate Dehydrogenase A (LDHA) as Novel Diagnostic Markers and Therapeutic Targets for Pancreatic Cancer

Goran Hamid Mohammad

UCL Institute for Liver and Digestive Health
Medical School
Royal Free Campus
University College London

This thesis is submitted in fulfilment of the requirements for the degree of Doctor of Philosophy

Primary supervisor
Professor Stephen Pereira

Secondary supervisor
Dr Dipok Kumar Dhar

March 2016

DECLARATION

I, Goran Hamid Mohammad confirm that the work presented in this thesis is my own. Where information has been derived from other sources, I confirm that this has been indicated in the thesis. Parts of this thesis have been submitted for publication or are manuscripts in preparation or conference presentations.

- **Mohammad GH**, Olde Damink SW, Malago M, Dhar DK, Pereira SP "Pyruvate Kinase M2 and Lactate Dehydrogenase A are Overexpressed in Pancreatic Cancer and Correlate with Poor Outcome" PloS One, 2015, manuscript just accepted.
- **Mohammad GH**, Olde Damink SW, Malago M, Dhar DK, Pereira SP "Activation of Pyruvate Kinase M2 in Combination with Inhibition of Lactate Dehydrogenase A as a Novel Strategy for Pancreatic Cancer Treatment" manuscript in preparation.
- **Mohammad GH**, Dhar DK, Pereira SP "Pyruvate Kinase-M2 (PKM2) as a Novel Diagnostic Marker and Therapeutic Target for Pancreatic Cancer" Poster presented at UCL Division of Medicine Post-Graduate Student Research Day Conference, UK, 2015. The poster has won the best poster presentation award (see Appendix 1).

During my PhD work, I was also involved in the below research projects:

- Dhar DK, **Mohammad GH**, Vyas S, Broering DC, & Malago M. "A novel rat model of liver regeneration: possible role of cytokine induced neutrophil chemoattractant-1 in augmented liver regeneration". Annals of Surgical Innovation and Research, 2015: 9(1), 1-10.
- Pahk KJ, **Mohammad GH**, Malago M, Saffari N, Dhar DK "A Novel Approach to Ultrasound Mediated Tissue Decellularization and Intrahepatic Cell Delivery in Rats" Ultrasound in Medicine & Biology, 2015, manuscript just accepted.

Signature……  …

ACKNOWLEDGEMENTS

The work presented in this thesis is due in large part to many people who have given me advice and guidance over the last three years. First of all, I would like to thank my supervisor, Prof. Stephen Pereira, for accepting me into his group and consistently supporting me with his invaluable advice. I would also like to extend my great thanks to Dr. Dipok Dhar, who acted as my laboratory supervisor and provided invaluable training in immunohistochemistry and animal experiments as well as guidance and regular scientific advice. I would also like to warmly thank Dr. Virginie Cerec, who provided training in cell culture, isolation, extraction and quantification of proteins in cell culture and western blot technique.

I would like to acknowledge the support, advice and assistance rendered from my colleagues within the Hepatobiliary and Pancreatic Cancer Group in the UCL Institute for Liver and Digestive Health, especially thanks to Yuan Chen, Nasima Gharmoud, Geri Keane, Matthew Huggett, David Brown and the Director of the Institute Professor Massimo Pinzani.

I would like also to thank the staff of the Comparative Biology Unit / Royal Free Campus, especially Duncan Moore, Alison O'Hara and Mark Neal, for their help and support during the animal experiment work.

I also thank the Ministry of High Education and Scientific Research/ Kurdistan Region Government for giving me the opportunity to study abroad and for funding me during my study.

Finally, I would like to thank my dear wife and children for their continual support and encouragement during my study. And I dedicate this thesis to my family and souls of my parents.

ABSTRACT

Pancreatic cancer is one of the most lethal malignancies worldwide; the early diagnosis of this disease remains challenging and there are few effective therapies, with palliative chemotherapy being the main treatment option for patients with locally advanced or metastatic disease. Alteration of cellular energy metabolism is one of the hallmarks of tumours. Therefore, I proposed that the study of metabolic enzymes such as pyruvate kinase M2 (PKM2) and lactate dehydrogenase A (LDHA), which serve as key regulators of cellular energy metabolism in proliferating cells and mediators of aerobic glycolysis, could play an important role in the diagnosis and therapy of pancreatic cancer.

Expression of PKM2 and LDHA was evaluated by immunohistochemistry in pancreatic cancer specimens. I found that the majority of PDAC strongly expressed PKM2 and LDHA at significantly higher levels compared with normal pancreatic tissues and benign pancreatic disease. PKM2 and LDHA expression directly correlated with tumour size and were expressed at higher levels in poorly differentiated tumours compared to well differentiated ones. Tumour cell proliferation, as detected by Ki67 staining, was significantly higher in tumours with strong PKM2 and LDHA expression compared to those with weak PKM2 and LDHA expression. Conversely, the number of CD8+ tumour infiltrating lymphocytes (TILs) was significantly higher in tumours with weak PKM2 and LDHA expression than in those with strong PKM2 and LDHA expression. Patients with tumours that had strong PKM2 and LDHA expression had a significantly worse overall survival compared with those that had weak PKM2 and/or LDHA expression (7.0 months vs. 27.9 months, respectively, $p = 0.003$, log rank test). Plasma PK and LDH concentrations were also significantly higher in pancreatic cancer patients compared to healthy controls (45.5 vs 21.6 U/L and 685 vs 194 U/L respectively, $P < 0.0001$).

Shikonin (a Chinese herbal medicine) inhibited PKM2 activity and had a strong cytotoxic effect on pancreatic cancer cell proliferation with an IC_{50} of 2-3μM and 1-2 μM for 24 and 72 hours interaction time, respectively. Treatment of pancreatic cancer cell lines with combination of PKM2 activator IV (TEPP-46) and LDHA inhibitor

(FX11) was synergistically inhibited pancreatic cancer cell proliferation, with combination indices (CI) of 0.48 and 0.45 for Miapaca-2 and BxPc-3 cell lines, respectively. Additionally, in the pancreatic cancer xenograft model, TEPP-46 and FX11 in combination significantly delayed both subcutaneous and orthotopic tumour growth compared to the control group ($P < 0.0001$). The combination treatment also reduced expression of PKM2 and LDHA, and significantly decreased Ki-67 expression compared with controls ($P < 0.0001$). Orthotopic xenografts treated with the combination therapy had a high number of CD8+TIL cells around the tumours.

In conclusion, PKM2 and LDHA overexpression in pancreatic cancer is associated with poor outcome. As such, high expression of these two enzyme may contribute to the aggressiveness of pancreatic cancer and confer anergy against the host anti-tumour immune response. Tetramerisation of PKM2 in combination with inhibition of LDHA synergistically inhibited pancreatic cancer cell proliferation and growth both *in vitro* and *in vivo* and may represent a novel strategy for pancreatic cancer therapy.

TABLE OF CONTENTS

DECLARATION **2**

ACKNOWLEDGEMENTS **3**

ABSTRACT **4**

TABLE OF CONTENTS **6**

LIST OF FIGURES **9**

LIST OF TABLES **11**

LIST OF ABBREVIATIONS **12**

CHAPTER 1: PANCREATIC CANCER **14**

1.1: BACKGROUND: 14
1.2: PANCREATIC CANCER SYMPTOMS: 15
1.3: DEVELOPMENT OF PANCREATIC CANCER: 15
1.4: RISK FACTORS: 16
1.5: THE STAGES OF PANCREATIC CANCER: 17
1.6: DIAGNOSIS OF PANCREATIC CANCER: 18
1.6.1: Biomarkers: *18*
1.6.2: Imaging and tissue acquisition: *20*
1.6.2.1: Transabdominal ultrasound (TAUS): 20
1.6.2.2: Computerised tomography (CT): 20
1.6.2.3: Magnetic resonance imaging (MRI): 20
1.6.2.4: Endoscopic ultrasonography (EUS): 21
1.6.2.5: Endoscopic retrograde cholangiopancreatography (ERCP): 21
1.6.2.6: Positron emission tomography (PET): 22
1.7: TREATMENT OF PANCREATIC CANCER: 22
1.7.1: Surgery: *22*
1.7.2: Chemotherapy: *23*
1.7.3: Radiotherapy: *23*
1.8: GLYCOLYSIS AND AEROBIC GLYCOLYSIS: 25
1.9: INHIBITION OF GLYCOLYTIC ENZYMES AS A TARGET FOR CANCER THERAPY: 27
1.10: PYRUVATE KINASE: 30
1.10.1: Structure of pyruvate kinase: *33*
1.10.2: Regulation of pyruvate kinase M2: *34*
1.10.3: Non-metabolic function of PKM2 (or nuclear function of PKM2): *38*
1.10.4: PKM2 as a target therapy: *40*
1.11: LACTATE DEHYDROGENASE (LDH): 44
1.11.1: Lactate dehydrogenase A structure: *49*
1.11.2: Metabolic symbiosis and lactate acidosis: *51*
1.11.3: Inhibition of Lactate dehydrogenase A as a target therapy: *53*
1.12: COMBINATION THERAPY: 58
1.13: THE CELL CYCLE: 59
1.13.1: Proliferation marker Ki67: *60*
1.14: CD8 TUMOUR INFILTRATING LYMPHOCYTES (CYTOTOXIC T-LYMPHOCYTES): 61
1.15: HYPOTHESIS AND AIM: 62

CHAPTER 2: METHODOLOGY **64**

2.1: IMMUNOHISTOCHEMISTRY: 64

2.1.1: Principle: ... *64*
2.1.2: Patients: ... *67*
2.1.2.1: Pancreatic cancer: ... 67
2.1.2.2: Pancreatic cysts and normal pancreatic tissue: ... 68
2.1.2.3: Tissue microarrays (TMAs): ... 70
2.1.2.4: Plasma samples: ... 70
Protocol: ... *72*
2.1.2.5: Single staining: ... 72
2.1.2.6: Double staining: ... 73
2.1.3: Evaluation of immunohistochemical staining: ... *74*
2.1.3.1: Evaluation of PKM2: ... 74
2.1.3.2: Evaluation of CD8+ TILs and Ki-67 proliferation marker: ... 75
2.2: WESTERN BLOT ANALYSIS: ... 75
2.2.1: Principle: ... *75*
2.2.2: Method: ... *77*
2.2.2.1: Cell lines: ... 77
2.2.2.2: Cell culture: ... 77
2.2.2.3: Preparation of total cell protein extracts: ... 78
2.2.2.4: Total protein assay: ... 78
2.2.2.5: Western blot protocol: ... 79
2.3: IMMUNOCYTOCHEMISTRY: ... 82
2.4: MTS ASSAY: ... 82
2.5: STAINING CELLS WITH HAEMATOXYLIN: ... 83
2.6: ANIMAL EXPERIMENTS: ... 84
2.6.1: Subcutaneous tumour implantation: ... *84*
2.6.2: Orthotopic tumour model generation: ... *84*
2.6.3: Staining of Miapaca-2 cell line with DiR fluorescent dye: ... *85*
2.6.4: Drug preparation and treatment regimen: ... *86*
2.6.5: End of the experiment: ... *87*
2.7: BIOLUMINESCENT IMAGING: ... 87
2.7.1: Imaging procedure: ... *87*
2.7.2: In vitro Bioluminescent Assay: ... *88*
2.8: PROCESSING OF TUMOUR TISSUES: ... 88
2.9: PYRUVATE KINASE AND LACTATE DEHYDROGENASE ACTIVITY ASSAY: ... 88
2.9.1: PK and LDH activity assay in tumour tissues: ... *88*
2.9.2: PK and LDH activity assay in human pancreatic cancer cell line: ... *89*
2.9.3: Pyruvate Kinase Assay: ... *89*
2.9.4: Lactate Dehydrogenase Assay: ... *91*
2.10: STATISTICAL ANALYSIS: ... 92

CHAPTER 3: RESULTS ... 93

3.1: PYRUVATE KINASE M2 AND LACTATE DEHYDROGENASE A ARE OVEREXPRESSED IN PANCREATIC CANCER AND CORRELATE WITH POOR OUTCOME ... 93
3.1.1: RESULTS: ... *93*
3.1.1.1: Expression of PKM2 and LDHA in pancreatic cancer: ... 93
3.1.1.2: Association with clinicopathological parameters: ... 96
3.1.1.3: Correlation between PKM2 and LDHA expression and patient survival: ... 102
3.1.1.4: Association between tumour types, resection status and survival months: ... 104
3.1.1.5: PKM2 and LDHA expression in pancreatic cancer cell lines: ... 106
3.1.1.6: Plasma PK and LDH activity in pancreatic cancer and healthy controls: ... 107
3.1.2: DISCUSSION: ... *108*

3.2: ACTIVATION OF PKM2 IN COMBINATION WITH INHIBITION OF LDHA SYNERGISTICALLY INHIBIT PANCREATIC CANCER CELL PROLIFERATION *IN VITRO* 112
3.2.1: RESULTS: *112*
3.2.1.1: Expression of PKM2 and LDHA in pancreatic cancer cell lines: 112
3.2.1.2: Effect of PKM2 inhibition on pancreatic cancer cell proliferation: 114
3.2.1.3: Activation of PKM2 with inhibition of LDHA attenuate pancreatic cancer cell proliferation: 118
3.2.1.4: Combination of PKM2 activator III and FX11: 118
3.2.1.5: Combination of PKM2 activator IV and FX11: 121
3.2.1.6: Optimisation of PKM2 activator IV and LDHA inhibitor combination: 121
3.2.1.7: Combination therapy synergistically inhibits pancreatic cancer cell proliferation: 123
3.2.2: DISCUSSION: *126*
3.3: ACTIVATION OF PYRUVATE KINASE M2 (PKM2) COMBINED WITH INHIBITION OF LACTATE DEHYDROGENASE A (LDH-A) AS A NOVEL STRATEGY FOR THE TREATMENT OF PANCREATIC CANCER 129
3.3.1: RESULTS: *129*
3.3.1.1: Pancreatic cancer cell line selection: 129
3.3.1.2: Combination therapy synergistically inhibits pancreatic cancer cell proliferation: 129
3.3.1.3: PK and LDH activity measurement: 133
3.3.1.4: Combination therapy synergistically attenuates tumour xenograft growth: 134
3.3.1.5: Histopathological analysis of tumour sections: 143
3.3.1.6: PK and LDH activity in tumour lysate and plasma: 147
3.3.1.7: Toxicity: 149
3.3.2: DISCUSSION: *150*

CHAPTER 4: GENERAL DISDUSSION 153

4.1: DISCUSSION: 153
4.2: CONCLUSION: 164
4.3: FUTURE WORK: 165

CHAPTER 5: REFERENCES 165

APPENDIX 1 184

LIST OF FIGURES

Figure 1.1: Development of pancreatic cancer.. 15
Figure 1.2: Algorithm for management of pancreatic cancer. 24
Figure 1.3: Illustration of cancer cell metabolism. Oncogenes and tumour suppressor genes signalling pathways regulate cancer cell metabolism. 27
Figure 1.4: Summary of inhibition of glycolytic enzymes. These drugs have been shown to inhibit glycolysis and produce anticancer effects. 29
Figure 1.5: Illustration of pyruvate kinase gene transcription and alterative splicing of PKM1 and PKM2 mRNA. 31
Figure 1.6: Illustration of pyruvate kinase structure and binding sites. 34
Figure 1.7: Regulation of pyruvate kinase type M2 in glycolysis pathway by fructose 1.6-biphosphates 35
Figure 1.8: Illustration of glycolytic regulation of pyruvate kinase M2 activity 37
Figure 1.9: Illustration of non-metabolic function of PKM2. The scheme shows the mechanism of nuclear translocation and functions of PKM2. 40
Figure 1.10: Structures of the most popular PKM2 inhibitors and activators 44
Figure 1.11: Illustration of lactate dehydrogenase functions and gene expression 46
Figure 1.12: Human Lactate dehydrogenase A, LDHA isoform found in skeletal muscle. 46
Figure 1.13: Illustration of mitochondrial lactate dehydrogenase functions and localization 49
Figure 1.14: The LDHA active site structure and catalytic reaction 50
Figure 1.15: Illustration of metabolic symbiosis between aerobic and hypoxic tumour regions. 53
Figure 1.16: Chemical structure of the most popular lactate dehydrogenase A inhibitors 57
Figure 1.17: The cell cycle mechanism 60
Figure 1.18: Schematic explanation of perforin / granzyme mechanism. Cytotoxic T cell (CD8 T cell) kills target cells (tumour or infected cells) by perforin/granzyme pathway 62
Figure 2.1: Basic principle of immunohistochemistry double staining method. 66
Figure 2.2: Basic principle of western blot. 76
Figure 2.3: Structure of MTS tetrazolium and its formazan product. 83
Figure 2.4: Development of pancreatic cancer xenograft tumour model 85
Figure 3.1: Immunohistochemical staining of PKM2 expression in representative pancreatic tumour sections 94
Figure 3.2: LDHA expression pattern 94
Figure 3.3: Percentages of PKM2 and LDHA expression in different type of tissues are shown. 95
Figure 3.4: Double immunohistochemical staining of PKM2 and CD8+TIL 98
Figure 3.5: Correlation between PKM2 and LDHA expression with CD8+TIL. 99
Figure 3.6: Immunohistochemical staining of PKM2 and Ki67 in pancreatic cancer 100
Figure 3.7: Relationship between PKM2/LDHA expression and Ki67 in pancreatic cancer 101
Figure 3.8: PKM2 and LDHA expression in pancreatic cancer tissue microarrays and correlation with tumour size.. 101
Figure 3.9: Overall patient survival in relation to PKM2 and LDHA expression 103
Figure 3.10: Survival according to the tumour type and resection status 105
Figure 3.11: Expression of PKM2 and LDHA in pancreatic cancer cell lines as detected by western blot. 106
Figure 3.12: Immunocytochemical staining of Miapaca-2 cell line with PKM2 and LDHA 106
Figure 3.13: Plasma pyruvate kinase and lactate dehydrogenase activity in pancreatic cancer compared with healthy controls 107

Figure 3.14: PKM2 and LDHA expression in different pancreatic cancer cell lines and different stages of cell culture. 113
Figure 3.15: The effect of different concentrations of Shikonin on pancreatic cancer cell lines 115
Figure 3.16: The effect of different concentrations of Shikonin on the PK-1 and PANC-1 cell line after 96 hours interaction. 116
Figure 3.17: Effect of Shikonin on pyruvate kinase activity in the Miapaca-2 cell line. 117
Figure 3.18: Cytotoxicity of PKM2 activator III, LDHA inhibitor (FX11) and combination treatment at different time points 119
Figure 3.19: Optimization of PKM2 activator IV (TEPP-46) and LDHA inhibitor (FX11) combination and time of treatment. 122
Figure 3.20: Cytotoxicity of PKM2 activator IV (TEPP-46), LDHA inhibitor (FX11) and combination treatment on different pancreatic cancer cell line proliferation after 72 hours of treatment. 124
Figure 3.21: The effect of single and combination therapy on Miapaca-2 and BxPc-3 cell lines. 130
Figure 3.22: Effect of single and combination therapy on Miapaca-2 cell viability 131
Figure 3.23: Effect of single and combination therapy on BxPc-3 cell viability 132
Figure 3.24: Effect of single and combination treatment on the BxPc-3 cells compared to DMSO control 132
Figure 3.25: Effect of different concentrations of PKM2 activator IV (TEPP-46) and LDHA inhibitor (FX11) on PK and LDH activity in Miapaca-2 and BxPc-3 cell lines. 133
Figure 3.26: Tumour growth curve over 21 days treatment. 135
Figure 3.27: Miapaca-2 xenograft tumours in mice from different treatment groups 136
Figure 3.28: Tumour growth curve over 21 days treatment. 138
Figure 3.29: Effect of single and combination treatment on subcutaneous tumour growth compared to the control group 139
Figure 3.30: Effect of single and combination treatment on size of subcutaneous tumours after 21 days of treatment compared to the control group. 140
Figure 3.31: Effect of high-dose combination therapy on orthotopic tumour growth compared to the control group 141
Figure 3.32: Subcutaneous and orthotopic tumour weight after 21 days of treatment 142
Figure 3.33: Tumour volume, liver and spleen metastasis in orthotopic control group 142
Figure 3.34: Ki67 proliferation index in control and different treatment groups 144
Figure 3.35: H&E staining and PKM2, LDHA and Ki67 expression in BxPc-3 pancreatic cancer xenografts in response to therapy 145
Figure 3.36: Immunohistochemical staining of CD8+TILs in orthotopic tumours 146
Figure 3.37: Relative values of pyruvate kinase (PK) and lactate dehydrogenase (LDH) activity in tumour lysate and plasma from mice with subcutaneous or orthotopic BxPc-3 xenografts... 148
Figure 3.38: Toxicity evaluation in response to therapy 149

LIST OF TABLES

Table 2.1: Summary of clinicopathological characteristics of patients with pancreatic cancer, pancreatic cysts, pancreatitis and controls..... 69
Table 2.2: Summary of clinical data of pancreatic cancer tissue microarray. 71
Table 2.3: Evaluation of PKM2 and LDHA stained according to the intensity and extent..... 75
Table 3.1: Correlation of PKM2 and LDHA expression with clinicopathological factors 97
Table 3.2: Summary of the correlations between PKM2, LDHA expression and number of nucleus immunostained CD8+TIL and Ki67 proliferation index……. 98
Table 3.3: Multivariable analysis of prognostic factors. 104
Table 3.4: Summary of correlation between tumour types and resection status and patients survival. 105
Table 3.5: Plasma pyruvate kinase and lactate dehydrogenase activity in pancreatic cancer compared to the healthy control. 108
Table 3.6: The effect of Shikonin on pancreatic cancer cell lines proliferation at different time points, expressed by the half maximal inhibitory concentration (IC_{50}). 116
Table 3.7: The effect of PKM2 activator III, LDHA inhibitor (FX11) and combination treatmnet on Miapaca-2 and PK-59 cell lines proliferation at different time points, expressed by the half maximal inhibitory or activatory concentration (IC_{50}) or (AC_{50}). 120
Table 3.8: The effect of PKM2 activator IV (TEPP-46), LDHA inhibitor (FX11) and combination treatment on proliferation of different pancreatic cancer cell lines after 72 hours of interaction, expressed by the half maximal inhibitory or activatory concentration (IC_{50}) or (AC_{50}). 125
Table 3.9: Summary of the effects of single and combination treatment on pancreatic cancer cell proliferation at different time points expressed by the half maximal inhibitory or activatory concentration (IC_{50} or AC_{50})..... 131

LIST OF ABBREVIATIONS

ABC	Avidin biotin complex
ADM	Acinar ductal metaplasia
ADP	Adenosine diphosphate
ATP	Adenosine triphosphate
BCA	Bicinchoninic Acid
CA19-9	Carbohydrate antigen 19-9
CPA:	Chronic active pancreatitis
CT:	Computerised tomography
DMEM:	Dulbecco's modified eagle's medium
DNA	Deoxyribonucleic acid
EDTA	Ethylenediaminetetraacetic acid
ELISA	Enzyme Linked Immunosorbent Assay
ERCP	Endoscopic retrograde cholangiopancreatography
EUS	Endoscopic ultrasonography
EUS-FNA	Endoscopic ultrasound guided fine needle aspiration biopsy
FasL	Fas ligand
FasR	Fas receptor
FBS	Fetal bovine serum
GAPDH	Glyceraldehyde-3-phosphate dehydrogenase
HIF-1	Hypoxia inducible factor-1
HPF	High power field
IC_{50}	Inhibit Cellular Proliferation by 50% (Median Inhibition Concentration)
IgG	Immunoglobulin G
IHC	Immunohistochemistry
IPMN	Intraductal papillary mucinous neoplasms
LDH	Lactate dehydrogenase
LDH-A	Lactate dehydrogenase A
LDS	Lithium dodecyl sulphate
LSAB	Labelled streptavidin biotin
PKM2	Pyruvate kinase type M2
MCN	Mucinous cystic neoplasm
MCT	Mono-carboxylate transporter
MDCT	Multidetector row computerised tomography
MHC I	Major histocompatibility class I complex

miRNA	microRNA
MOPS	3-(N-morpholino) propane sulfonic acid
MRI	Magnetic resonance imaging
OCT-4	Octamer-binding transcription factor 4
PanInN	Pancreatic intraepithelial neoplasia
PAP	Peroxidase–antiperoxidase
PBS	Phosphate buffered saline
PBST	Phosphate buffered saline -Tween 20
PCR	Polymerase chain reaction
PDAC	Pancreatic ductal adenocarcinoma
PDK-1	Phosphoinositide-dependent kinase-1
PDVF	Polyvinylidene difluoride
PEP	Phosphoenolpyruvate
PET	Positron emission tomography
PI	Proliferation index
PK	Pyruvate kinase
PTC	Percutaneous transhepatic cholangiography
RNA	Ribonucleic acid
ROS	Reactive oxygen species
RPMI-1640	Roswell Park Memorial Institute (culture medium)
SD	Standard deviation
shRNA	Short hairpin RNA
SPPT	Solid pseudo-papillary tumour
TAUS	Transabdominal ultrasound
TBS	Tris buffered saline
TBST	Tris buffered saline tween-20
TIL	Tumour infiltrating lymphocyte
TMA	Tissue microarray

CHAPTER 1: PANCREATIC CANCER

1.1: Background:

Cancer is a leading cause of morbidity and mortality in the world. The World Health Organization (WHO) estimated that about 14 million people are diagnosed with cancer every year and 8.2 million died of cancer in 2012. According to WHO, new cancer cases are expected to rise by 70% over the next two decades (1). In the UK, more than 331,000 new cancer cases were diagnosed in 2011 and around 162,000 people died from cancer in 2012 (2). Pancreatic cancer is the 10^{th} most prevalent cancer worldwide and the 4^{th} most common cause of cancer death (1). According to Cancer Research UK statistics, 8,773 patients were diagnosed with pancreatic cancer in the UK in 2011 and 8,662 people died with pancreatic cancer during 2012, so approximately 24 people are diagnosed with and die of pancreatic cancer every day (3). The risk of pancreatic cancer increases with age; three-quarters of patients diagnosed with this disease are over the age 65 and the disease rarely occurs before the age of 40 (4).

Pancreatic ductal adenocarcinoma (PDAC) accounts for more than 90% of pancreatic cancer cases. Prognosis of pancreatic cancer is very poor; five-year survival is less than 4% and this has not changed over the last 40 years. Moreover, pancreatic cancer has the worst survival rate among the 21 most common cancers in the UK (3). The poor prognosis of patients with pancreatic cancer is attributed to late diagnosis when surgical resection is often not possible. However, if patients are diagnosed earlier and are able to undergo surgical resection, the 5 year survival improves dramatically to 25% (5). Surgical resection remains the only curative treatment for pancreatic cancer; however, this is feasible in less than 20% of patients. The management of locally advanced or metastatic disease is challenging with most patients just receiving palliative single-agent or combination chemotherapy (6-8).

1.2: Pancreatic cancer symptoms:

Symptoms of pancreatic cancer do not usually present until an advanced stage and generally depend on the location of the tumour. More than 50% of pancreatic tumours develop in the head of pancreas. The most important symptom that appears in patients with tumour of the head of the pancreas is painless jaundice, which occurs as a result of obstruction of the bile duct. Another symptom that presents in most patients in this group is upper abdominal and back pain (7). On the other hand, symptoms associated with tumours in the body and tail of pancreas are upper abdominal and back pain without jaundice. Rapid weight loss and new onset diabetes are two other symptoms that may occur, and may be associated with short survival of patients.

1.3: Development of pancreatic cancer:

PDAC develops in a similar manner to the common adenocarcinoma sequence in different solid organ tumours, such as the breast, cervix and colon (8,9). Invasive PDAC develops through a series of premalignant lesions, which are characterized by gradually increasing dysplasia (10). Precursor lesions include pancreatic intraepithelial neoplasia (PanIN), intraductal papillary mucinous neoplasms (IPMN) and mucinous cystic neoplasms (MCN). Within the pancreatic ducts, PanIN progresses from flat form (PanIN-1A) to papillary lesion without dysplasia (PanIN-1B), then to papillary lesion with dysplasia and finally to carcinoma in situ (PanIN-3) (4,10) (see Figure 1.1).

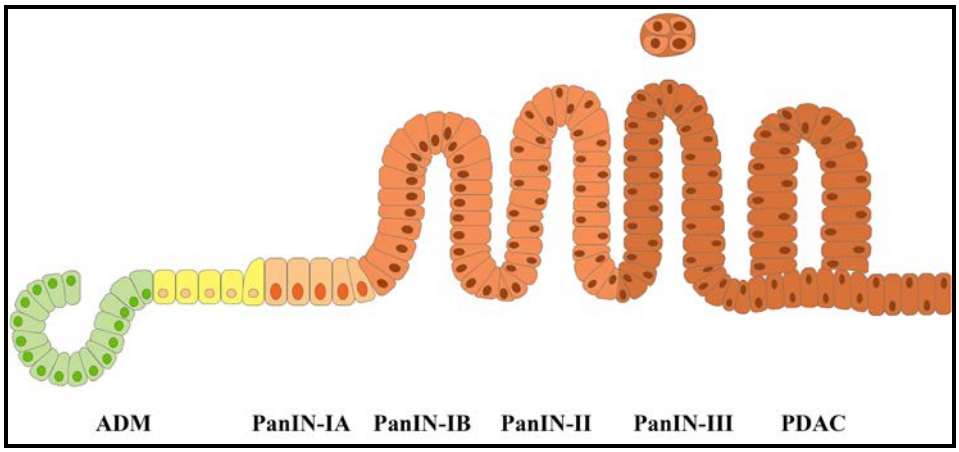

Figure 1.1: Development of pancreatic cancer. Adapted from *Herreros-Villanueva et al. 2013* (10).

The PanIN lesion model is the best understood mechanism for the development of PDAC in humans. Recent research has also indicated that pancreatic tumorigenesis could be generated through progression of tubular complexes, which develop from flat metaplastic lesions within the acinae (acinar ductal metaplasia, ADM). The development and progression of PanIN and ADM lesions into pancreatic adenocarcinoma is triggered by a series of genetic alterations. Mutations in the K-ras gene are the most common and tend to occur at an early stage, followed by mutations in the tumour suppressor gene p16 and mutations in p53, SMAD4 and BRCA2 in the later stages of the process (4,10–12).

1.4: Risk factors:

A number of risk factors have been identified for the development of pancreatic cancer. Similar to other cancers, age is one of the main risk factors for pancreatic cancer, with over 80% of pancreatic cancer cases developing between the ages of 60 and 80 (4,13). Family history of pancreatic cancer is also an important risk factor. The chance of developing pancreatic cancer is increased 2.3 fold in an individual with a first degree relative with pancreatic cancer and 16-64 fold if they have two or more first degree relatives with pancreatic cancer (4,13–15). Some other familial cancers such as melanoma and certain hereditary forms of breast, ovarian and colon cancer, as well as some rare familial cancer syndromes such as Lynch Syndrome (microsatellite instability), Li-Fraumeni Syndrome (P53 mutation), and Familial Adenomatous Polyposis (APC mutation), are associated with an increased risk of developing pancreatic cancer (4,13). These individuals are at increased risk of developing pancreatic cancer when compared to the general population and recent international guidelines recommend regular surveillance once patients are over the 40 years. In the UK, high risk patients are eligible to be screened as part of the pan-European EUROPAC registry (The European Registry of Hereditary Pancreatitis and Familial Pancreatic Cancer- http://www.europac-org.eu) which is evaluating the utility of surveillance in this group of patients (16). An estimated 4 out of 10 patients with hereditary pancreatitis will develop pancreatic cancer, while individuals with chronic pancreatitis have a nearly 15 fold increased risk. Obesity

and diabetes mellitus are also associated with a 2-fold risk of developing this disease (3,4,13). Smoking is another strong risk factor for the development of PDAC, with one out of four patients having a smoking history. Finally, high dietary meat and fat intake may contribute to the development of pancreatic cancer, while diets rich in vegetables and fruits may reduce that risk (17).

1.5: The stages of pancreatic cancer:

Staging of cancer is an important way to describe the extent of tumour growth, predict prognosis and plan treatment strategies. Cancer stages are classified in several ways. The American Joint Committee on Cancer (AJCC) stage pancreatic cancer by the TNM system, which gives information about the cancer through three key letters **T** (primary tumour), **N** (regional lymph nodes) and **M** (distant metastasis) (see Appendix 1 table 1). After the T, N and M categories are determined, the stage of pancreatic cancer is assigned by combining the TNM information. The stage grouping is expressed by combination of stage letter with Roman number from 0 to IV (see Appendix 1 table 2). Additional factors that are not formally part of TNM or stage system, such as the extent of resection (R), grades and or tumour proliferation are also useful in determining patient's prognosis.

1.6: Diagnosis of pancreatic cancer:

1.6.1: Biomarkers:

Due to the asymptomatic development of pancreatic cancer and lack of accurate biomarkers, the early diagnosis of pancreatic cancer remain extremely challenging. Therefore, the discovery of novel biomarkers, which can diagnose pancreatic cancer at an early stage when patients can undergo curative surgical resection, is of the upmost importance.

Blood is simple to obtain from the patient and can be easily analysed in clinical laboratories. However, the wide range of proteins in the blood complicated the protocol for discovery of new biomarker.

In theory, the discovery of biomarkers for detection of early stage pancreatic cancer could improve survival rates. In the last forty years many sensitive and selective biomarkers have been discovered for some cancers, which significantly improved survival rates, however, the early diagnosis of pancreatic cancer remain difficult and pancreatic cancer has the worst survival rate among most common cancer worldwide (3).

Carbohydrate antigen 19-9 (CA19-9) is the only standard serum biomarker that is in current use for diagnosis of pancreatic cancer and the only serum marker that has been approved by US Food and Drug Administration (FDA) for monitoring patients with pancreatic cancer (10).

CA19-9 has a sensitivity of 79–81% and specificity of 82-90% for the diagnosis of pancreatic cancer in symptomatic patients, however, CA19-9 can be elevated in chronic and acute pancreatitis, cholangitis, obstructive jaundice and liver cirrhosis (10,18). CA19-9 is a sialylated lewis antigen of the MUC1 protein. Approximately 7-10% of the population do not secrete the Lewis antigen, which is another limitation of CA19-9 in the diagnosis of pancreatic cancer (19).

Carcinoembryonic antigen (CEA) is another serum biomarker that has been used for more than a decade as a biomarker for the diagnosis of pancreatic cancer, with a sensitivity of 25-54% and specificity of 75-91%. Due to its low sensitivity and because it

is elevated in colorectal, stomach and breast cancer as well as pancreatic cancer, CEA is not currently used for the diagnosis of pancreatic cancer (10,20).

Many serum biomarkers have been studied so far, but none of them have shown better selectivity and sensitivity than CA19-9 for early diagnosis of pancreatic cancer. Recently, serum PKM2 has been identified as a diagnostic and prognostic marker with comparable sensitivity and selectivity to serum CA19-9 in pancreatic cancer (5,20,21). Serum PKM2 has some advantages over C19-9 for the diagnosis of pancreatic cancer. Blood PKM2 level is not affected by cholestasis and correlates with the presence of pancreatic cancer metastasis, the previous research studies have also shown a direct correlation between plasma PKM2 and stage of pancreatic cancer (5,20,22). PKM2 can also easily be quantified in blood by immune-enzymatic assay.

Recently, the combination of two or more tumour markers has been utilised for the early diagnosis of pancreatic cancer. Schulze *et al* (2000) found that the combination of PKM2 and CA19-9 significantly increased the sensitivity up to 96% without reducing specificity for the diagnosis of pancreatic cancer (23).

More recently, O'Brien *et al* (2015) studied the combination of multiple serum biomarkers and found that the combination of CA19-9 and CA125 elevated and was able to detect pancreatic cancer up to two years prior to clinical diagnosis in some patients (24).

To summarise, the identification of highly sensitive and selective blood biomarkers is likely to lead to early detection of pancreatic cancer, resulting in curative surgical resection and improves patient’s survival rate.

1.6.2: Imaging and tissue acquisition:

1.6.2.1: Transabdominal ultrasound (TAUS):

Transabdominal ultrasonography (TAUS) is the most commonly used technique for initial evaluation of abdominal pain and jaundice, the two most common symptoms of pancreatic cancer. The accuracy of TAUS for the diagnosis of pancreatic cancer is approximately 50 to 70% (25,26). The role of transabdominal ultrasonography is also limited to confirming the presence of a mass lesion, diagnosing a dilated biliary tree, excluding cholelithiasis and detecting ascites and hepatic metastases (27). Contrast-enhanced Doppler ultrasonography can improve the accuracy of pancreatic tumour diagnosis, with a reported sensitivity and specificity of 90% and 95%, respectively (25,28). On the other hand, intervening bowel gas and differential skill of the operator may decrease the sensitivity of ultrasonography for detection and staging of pancreatic tumours (25,27).

1.6.2.2: Computerised tomography (CT):

Computerised tomography (CT) is the most commonly used imaging technology for diagnosis and staging of pancreatic cancer. Typically a multidetector row computerised tomography (MDCT) with intravenous contrast is used, which takes just a few minutes. It has an accuracy for detection of pancreatic carcinoma of 85-100% and accurately predicts resectability in 80-90% of patients (25,27,29).

1.6.2.3: Magnetic resonance imaging (MRI):

Magnetic resonance imaging is another useful imaging technique for diagnosing pancreatic tumours. MRI images are formed from the radiofrequency signal obtained from the relaxation of hydrogen nuclei, which are present throughout the body, are exposed to strong magnetic field. Recently, contrast enhanced MRI has been confirmed as a useful imaging technique for identification of tumours. Pancreatic MRI can be combined with magnetic resonance cholangiopancreatography (MRCP) to evaluate biliary pathology including other causes of biliary obstruction (27). There are no significant differences between MRI and CT in pancreatic tumour detection and in

predicting resectability. However, MRI often less commonly available, is more expensive and takes longer than CT; as well, it is less effective at looking for the presence of lung metastases (30,31). MRI is a useful imaging technique for staging of pancreatic tumours, differentiation of an inflammatory pancreatic mass from PDAC and detection of liver metastasis. The sensitivity of MRI for detection of pancreatic tumour ranges from 88-96% (32).

1.6.2.4: Endoscopic ultrasonography (EUS):

Endoscopic ultrasonography was initially developed in the 1980s with mechanical radial scanning transducers. EUS is highly sensitive for pancreatic cancer lesions and is more accurate than MDCT and MRI for detection of tumours, especially for tumours less than 2cm (25,27). Furthermore, it is highly sensitive for detecting vascular infiltration by the tumour and lymph node metastasis (25,33). The main disadvantage of EUS is that it is an invasive technique and has limited visualization for detecting metastatic spread to the peritoneum and liver (25). On the other hand, EUS when combined with fine needle aspiration or biopsy can enable cytological diagnosis at the same time, with a sensitivity and specificity of 91% and 95%, respectively (34). EUS-FNA is now the main mode of obtaining a cytological diagnosis of pancreatic carcinoma (35).

1.6.2.5: Endoscopic retrograde cholangiopancreatography (ERCP):

Endoscopic retrograde cholangiopancreatography is a common procedure for acquisition of diagnostic material in pancreatic carcinoma, which is typically obtained via biliary brush cytology (25,27). At the time of the ERCP the ampulla, duodenum and stomach are also visualized, so any signs of tumour invasion or gastric outlet obstruction can be diagnosed. In patients with obstructive jaundice a biliary stent can also be placed at the same time. The main disadvantages of these invasive methods are the potential complications of acute pancreatitis, infection, bleeding and visceral perforation (<3%). The sensitivity of biliary brush cytology for the diagnosis of pancreaticobiliary malignancy is low. Recently, some cytological techniques have improved sensitivity of pancreaticobiliary malignancy diagnosis to approximately 43 to 60% (36,37). Pancreatic

duct brushing has also been reported, with one study showing a sensitivity and specificity of 66% and 100%, respectively (38).

1.6.2.6: Positron emission tomography (PET):

Positron emission tomography is a non-invasive imaging technique, which uses different radiolabeled compounds such as the radiolabeled glucose analogue ^{18}F-fluorodeoxyglucose, which can detect metabolic active tissues. A malignant tumour is characterized by an increased concentration of intracellular glucose due to upregulation of glucose transporters, hexokinase and phosphofructokinase activity. The sensitivity and specificity of FDG-PET for detection of pancreatic tumours is 71-100% and 64-90%, respectively (25,39). FDG-PET may also be useful for detecting distant metastasis in pancreatic cancer (25). PET can be superimposed with computed tomography (PET-CT) to further improve diagnosis of pancreatic tumour lesions, with a sensitivity of 87% and specificity of 83%. Furthermore, contrast-enhanced PET-CT has shown better performance with a sensitivity and specificity of 91% and 88%, respectively (40).

1.7: Treatment of pancreatic cancer:

1.7.1: Surgery:

Complete removal of the tumour by surgery is the most effective treatment for pancreatic cancer. However, only 10-20% of patients are eligible to undergo radical surgery because pancreatic cancer is usually diagnosed at an advanced stage (5,41). The survival rate after resection is still very low with a median survival of only 10 to 20 months and a five year survival of around 25% (5,42). For tumours in the head of the pancreas, a Whipple's operation (Pancreatoduodenectomy) is the most common type of surgery performed (43). For tumours in the tail of the pancreas a distal pancreatectomy is undertaken. However, at the time of surgery if patients are found to have locally advanced disease involving the arteries or metastatic disease, curative surgical resection is usually not possible and a palliative gastric and biliary bypass may be performed. An alternative is subsequent endoscopically placed duodenal and biliary stents.

1.7.2: Chemotherapy:

Chemotherapy is used for the palliative treatment of pancreatic cancer, as well as in the neoadjuvant and adjuvant setting (44,45). Chemotherapy may improve the quality of life and survival length. Gemcitabine is the most commonly used chemotherapy in the USA and Europe and generally shows better efficacy over 5-fluorouracil (46). GemCap (Gemcitabine given with Capecitabine) combination chemotherapy is also used (47). Recently, the combination chemotherapy FOLFIRINOX (5-fluorouracil, leucovorin, irinotecan, oxaliplatin) has shown significant improvement in survival length in patients with metastatic disease when compared to Gemcitabine alone, albeit with considerable toxicity (6).

1.7.3: Radiotherapy:

Radiotherapy is a type of cancer therapy that uses high energy radiation to kill cancer cells. Radiotherapy is used less frequently when compared with chemotherapy and surgery. In some cases radiotherapy is offered to patients with metastatic pancreatic cancer to relieve symptoms. Combination chemotherapy with radiotherapy (chemoradiation) has been shown to have better results than chemotherapy alone for the treatment of locally advanced disease.

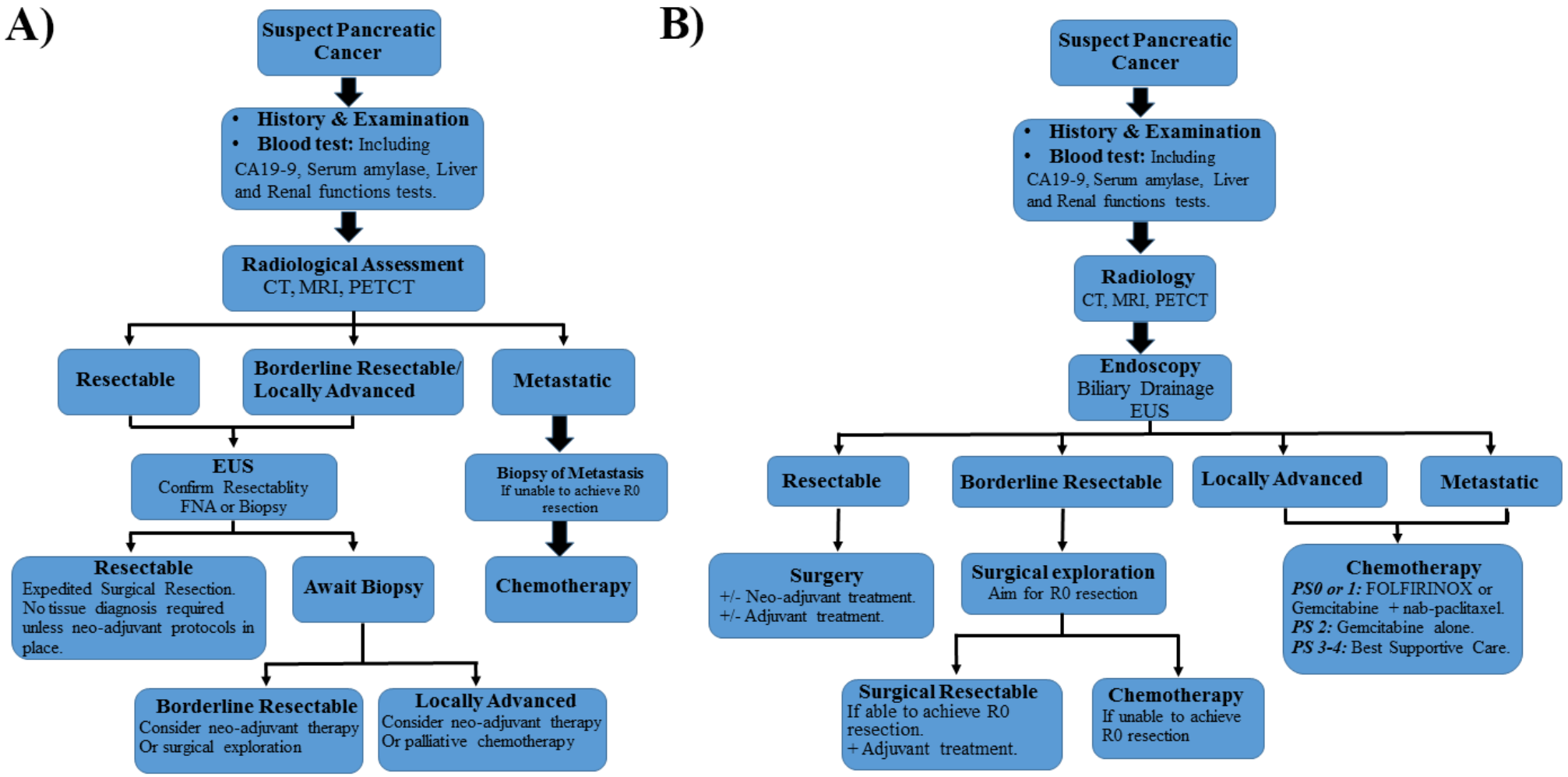

Figure 1.2: Algorithm for management of pancreatic cancer. **(A)** Clinical assessment and diagnosis of pancreatic cancer. **(B)** Treatment algorithm for patients with pancreatic cancer.

1.8: Glycolysis and aerobic glycolysis:

Glucose plays an essential role as an energy source for cell survival and as a carbon source for anabolic pathways. Catabolism of glucose, called glycolysis, is a central pathway in metabolism. In the presence of ample amounts of oxygen, most normal cells rely on the energy (ATP) that is generated from oxidative phosphorylation in mitochondria. During this process, pyruvate generated from the degradation of glucose is transported to the mitochondria and used as a substrate in the TCA cycle to generate ATP for biological activity of the cell. In contrast to normal cells, cancer cells have adapted to generate significant amounts of their ATP in the conversion of glucose to lactate, even in the existence of adequate amount of oxygen, a process known as the Warburg effect or aerobic glycolysis (48–50). In 1920, Otto Heinrich Warburg explained metabolism in tumour cells and discovered that the cancer cells utilize high quantities of glucose and produce lactate even in the presence of sufficient amounts of oxygen (51,52). Warburg considered the impairment of cellular respiration to be caused by defects in mitochondria and enhanced utilization of the high amounts of glucose to cope with the high energy demand by cancer cells (53). Later, the observation of high glucose uptake by malignant cells was emphasized by the use of ^{18}F-fluorodeoxyglucose as a tracer for positron emission tomography to detect occult tumour masses (48,53,54). Warburg also proposed that the defect of mitochondrial respiration was a primary cause of malignancy. However, modern research findings showed that mitochondrial dysfunction is not common in most types of cancer. Accumulating evidence supports the hypothesis that mutations in oncogenes and tumour suppressor genes (which activate oncogenes or inactivate tumour suppressors) lead to altered metabolism and cause the development of a tumour (50,55–57).

Mutations have a significant effect on metabolic enzymes activities and have a crucial role in aerobic glycolysis of cancer. Mutations of oncogenes and tumour suppresser genes such as Myc, phosphatidylinositol 3-kinase (PI3K), phosphatase and tensin homolog (PTEN), and p53 are commonly shown to be altered and have a great impact on reprogramming cell metabolism and tumorigenesis (Figure 1.2) (49,56,58,59). Alteration

of the PI3K/Akt pathway has been frequently found in cancer and has a key role in various tumours (56). Activated PI3K phosphorylates (activates) AKT and stabilizes hypoxia inducible factor-1 (HIF-1). PTEN tumour suppresser gene is inactivated by the PI3K enzyme antagonise and stimulate glycolysis through AKT and HIF-1 activation (60). The activated Akt directly controls glycolytic enzymes and enhances glucose uptake through activation of glycolysis enzymes, for instance phosphofructokinase (PFK) and hexokinase (HK) (56,61). Mammalian target of rapamycin (mTOR) is also activated by AKT, which indirectly affects other metabolic pathways by activating HIF-1, even under normal concentrations of oxygen (61). Pyruvate dehydrogenase kinases (PDKs) is then activated by HIF-1 and inhibit the access of pyruvate into the TCA cycle (56). Transcription of most glycolytic enzymes, including LDHA and glucose transporter-1 (GLUT-1), are activated by the oncogenic transcription factor (myc), which consequently increase both glucose uptake and production of lactate, it can also regulate genes associated with glutamine metabolism. Taken together, alteration of myc oncogene enhances both glycolysis and glutaminolysis, which are associated with tumour aggressiveness (49,50,56).

The tumour suppressor protein p53 is also one of the most crucial mutated proteins involved in the alteration of glycolysis in various types of cancer. Besides its role in controlling cell cycle and death, p53 also has an inhibitory effect on the glycolytic pathway (56,62). p53 upregulates TIGAR (TP53-induced glycolysis and apoptosis regulator) expression, causes reduction of the level of fructose-2,6- bisphosphatase and decreases the rate of glycolysis (63). Additionally, p53, in normal cells, directly induces oxidative phosphorylation by up-regulation of cytochrome c oxidase 2 (SCO2), which is necessary for the appropriate assembly of the SCO complex of the electron transport chain. Accordingly, the loss of p53 function, as shown in cancer cells, directs metabolism from mitochondrial respiration towards glycolysis (Figure 1.2) (56,64).

Another factor that further promotes alteration of metabolism in cancer cells is the expression of the spliced variant form of PKM2, which is characterized by the low activity toward its substrate leading to the reduction of oxygen consumption and

increased lactate production (53,57,59). The expression of spliced form of PKM2 also enhances glucose uptake, increases the rate of glycolysis and directs glycolysis toward production of glycolytic intermediates, such as amino acids, lipid and nucleotides, which are required for biosynthesis of new cells (51,52,55).

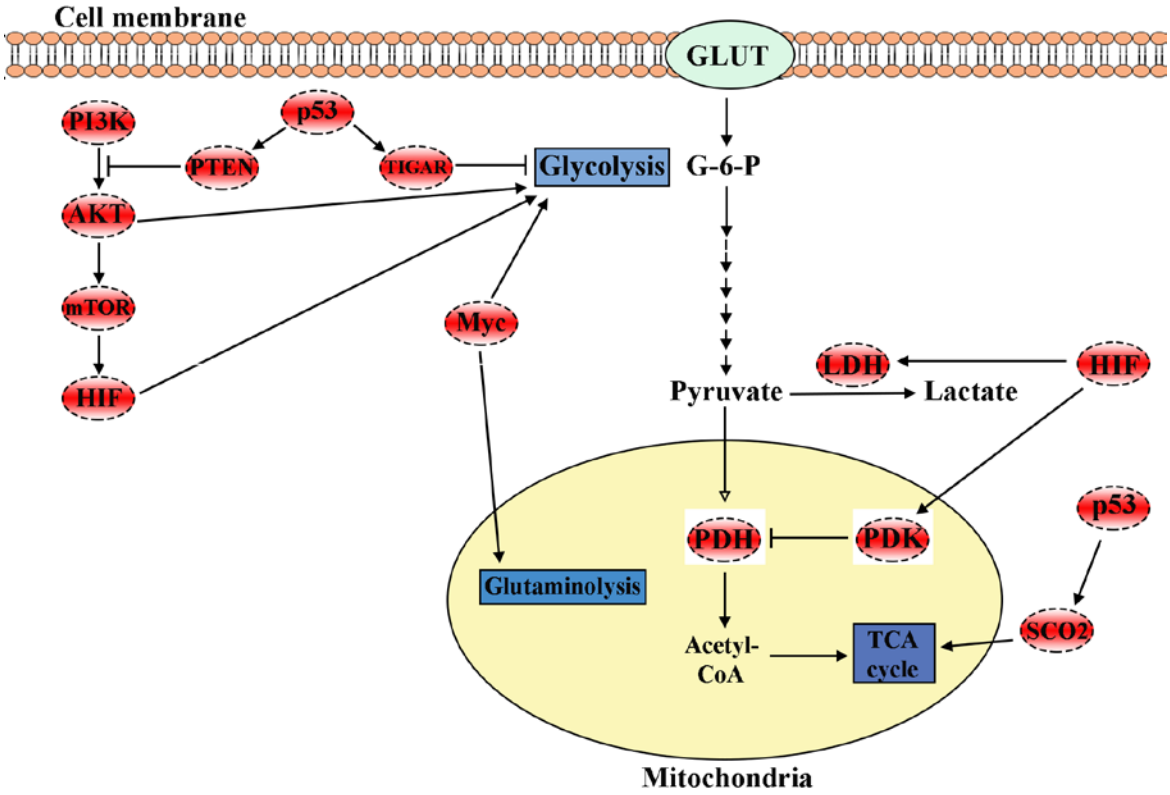

Figure 1.3: Illustration of cancer cell metabolism. Oncogenes and tumour suppressor genes signalling pathways regulate cancer cell metabolism. Adapted from *Jang et al. 2013* (56).

1.9: Inhibition of glycolytic enzymes as a target for cancer therapy:

Alteration of glucose metabolism is one of the features of cancer cells. In contrast to normal cells, tumours rely on glycolysis for energy (ATP) generation rather than mitochondrial oxidative phosphorylation (48–50). There is increasing evidence that glycolysis is required for proliferation, invasion and metastasis of tumour cells. Thereby, the inhibition or attenuation of glycolysis may restrict the capacity of tumour to proliferate, invade adjacent tissues and migrate to distant organs (56,65).

The inhibition of hexokinase (HK), phosphofructokinase (PFK) and pyruvate kinase (PK) enzymes, which are regulated irreversible and rate limiting steps of glycolysis, can

attenuate the increased rate of glycolysis in the cancer cells. Similarly, pyruvate dehydrogenase kinase (PDK), pyruvate dehydrogenase (PDH) and lactate dehydrogenase (LDH) enzymes also play a crucial role in glycolysis and mitochondrial oxidation phosphorylation. Inhibition of these enzymes is another strategy for attenuating the increased rate of glycolysis in tumour cells (65,66).

Hexokinase is the first rate limiting step of glycolysis that catalyses the conversion of glucose to glucose-6-phosphate. Lonidamine is an indazole-3-carboxylic acid derivate that can inhibit phosphorylation of glucose through inhibition of hexokinase II (HK-II). Lonidamine has been evaluated in phase III trials but widespread clinical application has been limited by significant hepatic and pancreatic toxicities (56,65,66). 3-bromopyruvate (3-BrPA) is another anticancer and strong alkylation agent, which has recently been shown to have a potent glycolysis and mitochondrial oxidative phosphorylation inhibitory effect through targeting HK-II and LDH enzymes. Moreover, 3-BrPA is a pyruvate and lactate analogue that has shown potent anticancer activity in preclinical studies (67–69). Similar to Lonidamine and 3-BrPA, 2-deoxyglucose (2-DG) is another glycolysis inhibitor; it is a glucose analogue and acts as a competitive inhibitor of glucose metabolism. Hexokinase II phosphorylates 2-DG to 2-DG-phosphate, but unlike glucose-6-phosphate, cannot be further metabolized and is not converted to fructose-6-phosphate by the action of phosphohexokinase isomerase enzyme. As a result, significantly reduced ATP generation leads to inhibition of cell cycle progression and finally cell death. 2-DG also showed promising anticancer activity effects in pre-clinical and early clinical phase trials (66,68–70).

Several other glycolysis inhibitor drugs have been developed and shown to have anti-cancer activity both in cell culture and in xenograft models, and some drugs have entered clinical trials (56,65,66,69,70) (Figure 1.3).

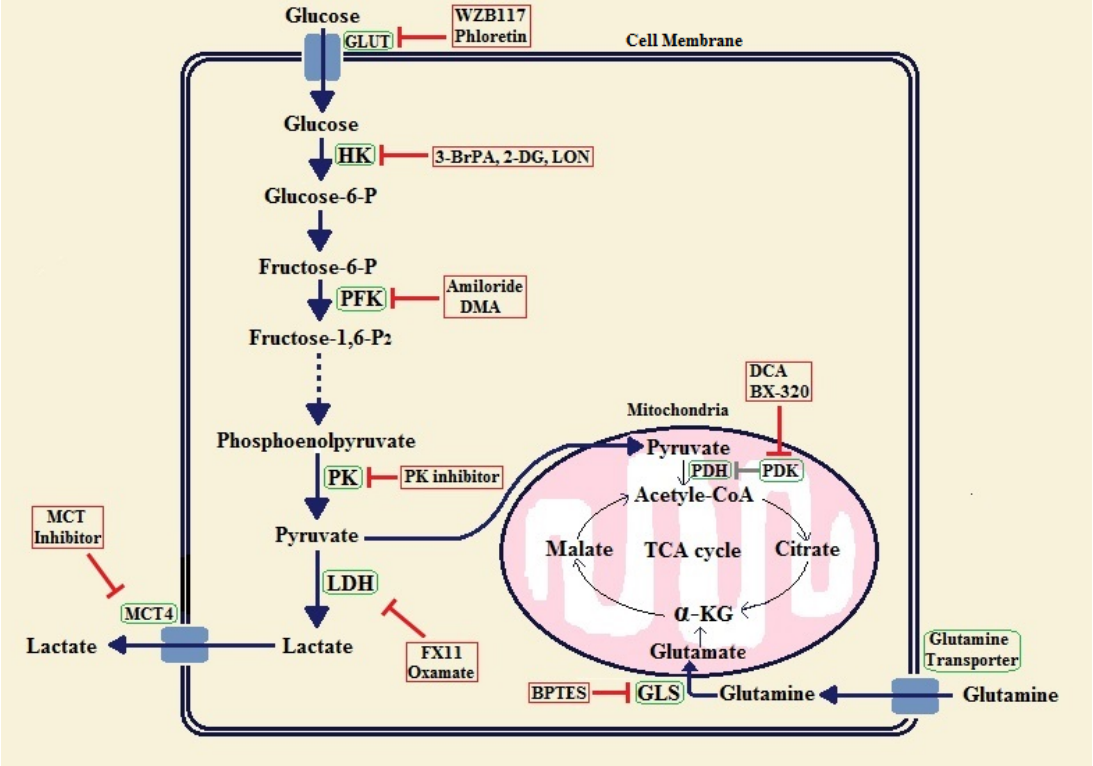

Figure 1.4: Summary of inhibition of glycolytic enzymes. These drugs have been shown to inhibit glycolysis and produce anticancer effects. (**WZB117:** 3-Fluoro-1,2-phenylene bis(3-hydroxybenzoate), **3-BrPA:** 3-bromopyruvate, **2-DG:** 2-deoxyglucose**, LON:** lonidamine, **DMA:** 5,5-dimethylamiloride, **FX11:** 2,3-Dihydroxy-6-methyl-7-(phenylmethyl)-4-propyl-1-naphthalenecarboxylic Acid, **DCA:** dichloroacetate , **BX-320:** N1-[3-[[5-Bromo-2-[[3-[(1-pyrrolidinylcarbonyl)amino]phenyl]amino]-4-pyrimidinyl]amino]propyl]-2,2-dimethylpropanediamide **, BPTES:** Bis-2-(5-phenylacetamido-1,3,4-thiadiazol-2-yl)ethyl sulphide).

There are several potential obstacles to the use of glycolysis enzyme inhibitors as an anticancer therapy. Indeed, glycolysis enzymes are required for glucose metabolism in normal cells, so that inhibition of glycolysis severely depletes ATP generation and can cause serious disorders through the impairment of glucose consumption. Some normal tissues such as brain, testis and retina use glucose as the main source of energy. In this case, the inhibition of glycolysis may have a toxic effect for these particular tissues (50).

In line with this observation, I focused on the study of PKM2 and LDHA enzymes in PDAC. Activation of PKM2 and inhibition of LDHA can inhibit cancer cell proliferation and might not be harmful for normal cells (50,52,54). Interest in PKM2 and LDH-A as a target for pancreatic cancer treatment comes from the observation that these enzymes are frequently upregulated during tumorigenesis and offer the possibility of a therapeutic intervention aimed at correcting these altered activities (52,59,71–74).

1.10: Pyruvate kinase:

Pyruvate kinase (PK, EC: 2.7.1.40) is a highly regulated glycolytic enzyme found in all living organisms. This enzyme catalyses the last step of glycolysis and mediates the transferring of a phosphate group from phosphoenolpyruvate (PEP) to adenosine diphosphate (ADP) to produce pyruvic acid and adenosine triphosphate (ATP) (21,75–78)**.**

PK has four different isoenzymes, which mainly depends upon the metabolic response of various cells and tissues. Both L and M genes encode PK isoenzymes (75,76,78,79). The L gene encodes both L- and R-PK isoenzymes. Tissues with high gluconeogenesis, for instance liver and kidney, are characterized by the expression of L-PK isoenzyme; however, erythrocytes express R-isoenzyme. The M gene encodes both M1 and M2 isoenzymes. Those tissues that require a high amount of energy, for instance brain and muscle, express M1-PK. However, M2-PK is found in lung tissues and all cells with high proliferation, such as tumour cells, embryonic cells and adult stem cells (21,75,78–81).

The PKM gene consists of 12 exons and 11 introns and encodes both M1 and M2 pyruvate kinase isoenzymes. M1- and M2- PK isoenzymes are different splicing products (exon 10 for PKM2 and exon 9 for M1PK)(57,71,77). The amino acid composition of human M1- and M2-PK is very similar and the homology between these two isoenzymes is about 96%. The differences are only in 23 amino acids within 56 amino acids stretch (aa 378-434) at the carboxy terminus of the M2-PK protein. Notably, 44 amino acids of the 56 amino acids belong to the C-domain of the M2-PK protein and is involved in the formation of a tetrameric isoform of PKM2 from two dimers (77,82,83). Furthermore, this difference in C-domain amino acids is responsible for the different regulation mechanism and kinetic characteristics between M1- and M2-PK (Figure 1.4A).

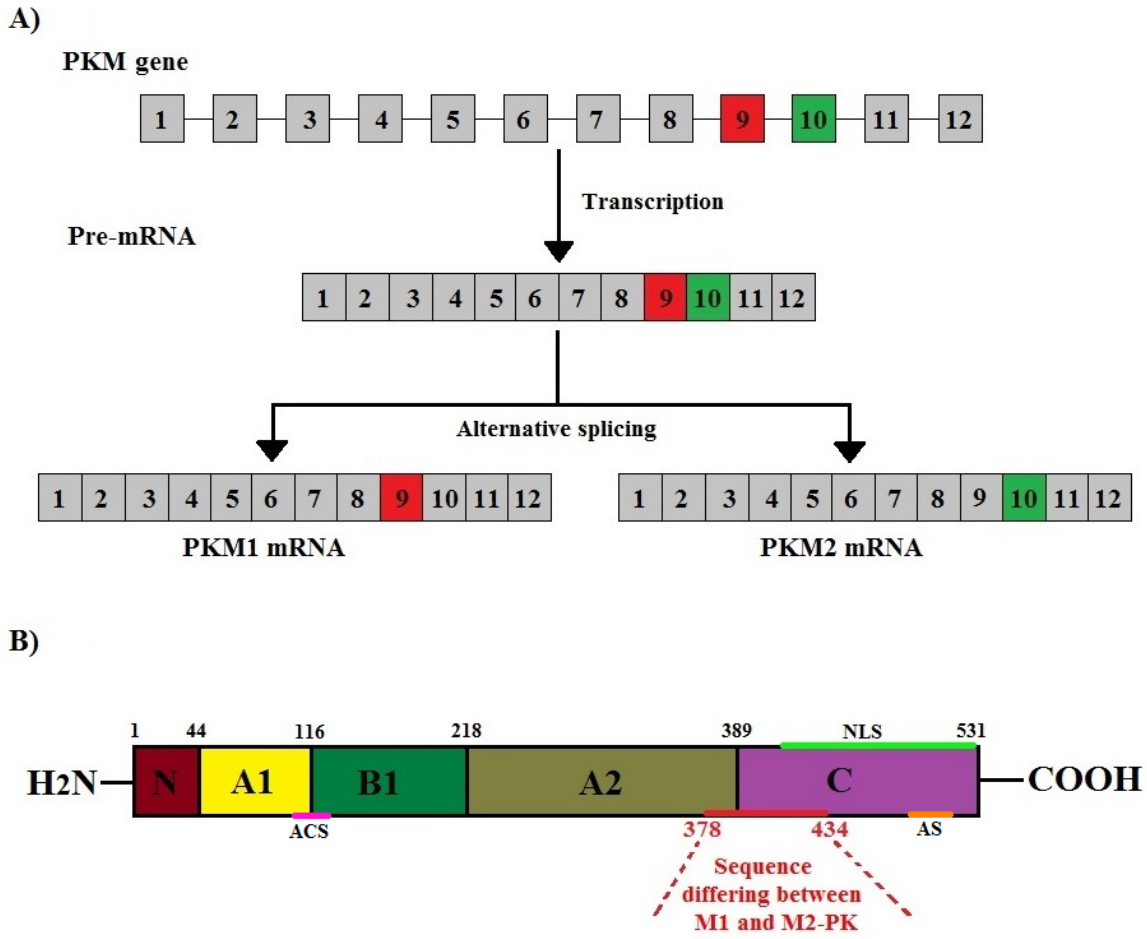

Figure 1.5: Illustration of pyruvate kinase gene transcription and alterative splicing of PKM1 and PKM2 mRNA. **A)** The PKM-gene consists of 12 exons and 11 introns and encodes both of M1 and M2-PK isoenzymes, these two isoenzymes are different splicing products, exon 10 for PKM2 and exon 9 for M1PK. **B)** The structure and differences between PKM1 and PKM2 proteins, both proteins consist of 531 amino acids and the compositions are very similar and have about 96% homology. (ACS: PKM2 active site, AS: allosteric activator FBP, and, NLS: nuclear localisation signal sequence.)

The PKM2 monomer is composed of 531 amino acids and divided into four domains which are the N (aa 1-43), A (aa 44-116 and 219-389), B (aa 117-218) and C (aa 390-531) domains (Figure 1.4B). In contrast to the other PK isoenzymes which are characterized by tetrameric structures, PKM2 occurs either in dimeric or tetrameric isoform. The dimeric structure of PKM2 is formed by the intracellular interaction of two monomers in the A-domain region, while the tetrameric structure occurs as a result of the association of the interface of the C-domain of two dimers. Moreover, the tetrameric isoform of PKM2 is characterised by high affinity to its substrate PEP (Km, 0.03mM); however, the dimeric isoform has a low affinity for PEP (Km, 0.46mM) (57,71,77,83–85). PKM2 is mainly in the tetrameric isoform in normal cells, whereas the dimeric

isoform of PKM2 is usually found in cancer cells and has therefore been known as tumour PKM2.

Tumour cell metabolism differs substantially from normal cell metabolism. As well as other characteristic differences of cancer, tumours show increases in glycolysis and glutaminolysis rates, whereas gluconeogenesis is decreased. The most important advantages for an increasing rate of glycolysis in tumour cells are production of energy without oxygen consumption and glycolytic intermediates, such as amino acids, nucleotides, phospholipids and triglycerides, which are used as precursors of new cells (see Figure 1.6) (51–53,86).

During tumorigenesis, the specific PK isoenzymes, for instance PKM1 in the brain and L-PK in the liver, disappear and the expression of PKM2 predominates (87). PKM2 plays a key role in the regulation of cellular metabolism and the balance between energy generation and production of glycolytic intermediates. In the presence of ample amounts of oxygen, tumour cells obtain energy from the degradation of glutamine by glutaminolysis but when oxygen is absent, glutaminolysis is inhibited and tetramerisation of PKM2 occurs by increasing the level of fructose 1,6 biphosphate, and glycolysis shift toward energy production (21).

Egenbrodt *et al*. first described the inactive dimeric form of PKM2 as a characteristic metabolic marker of tumour. He studied the level of PKM2 in patients with pancreas, lung, kidney, liver and breast cancer and found high level of the inactive dimeric form of PKM2 in the blood and tissues, and termed it tumour PKM2 (21).

1.10.1: Structure of pyruvate kinase:

The structure of pyruvate kinase (PK) structure has been studied in both eukaryotic and prokaryotic cells and in most cases has been observed to exist primarily as a hetero-tetramer of four identical subunits (50-60 kDa). Each subunit consists of an approximately 531 amino acid residues and is assembled to form a tetrameric structure with 2-2-2 symmetry. Each PK subunit is also composed of four different domains, which are A, B and C and the N- terminal domains (75,88,89). The active site pocket is located between the A and B domains and based about 39 Å from the effector site, which is positioned in the C-domain. In the tetrameric structure, neighbouring C-domains build the C–C or 'small' interface, and adjacent A-domains build the A–A or 'large' interface. The B-domain contributes a mobile lid at one end of the (α/β)8-barrelled A-domain and modulates access to the active site (89) (Figure 1.5).

PK is a highly conserved homo-tetrameric enzyme across distant phylogenetic groups, whereas, the mechanism of PK activity regulation differs between various species (77,90,91). In the tetrameric structure of PK, three different binding pockets with affinities for a variety of molecules have been identified and are well defined in mammals, bacteria, yeast and trypanosomatids. The binding site pockets are composed of the active site pocket, the effector site pocket and the amino acid binding site pocket (89). Most PK isoenzymes show binding of the PEP substrate at the active site pocket and fructose 1, 6 biphosphates (FBP) binds at the effector site pocket. FPB is an allosteric activator of PK and can modulate the activity of PK through binding (activation) or release (inhibition) of the effector binding site pocket. FBP can regulate the activity of three out of four mammalian PK isoenzymes, including R-PK, L-PK and PKM2, while the M1PK isoenzyme is constitutively in an active form. The activity of M1-PK can be inhibited by binding of phenylalanine or proline amino acid at the amino acid binding site pocket (92,93).

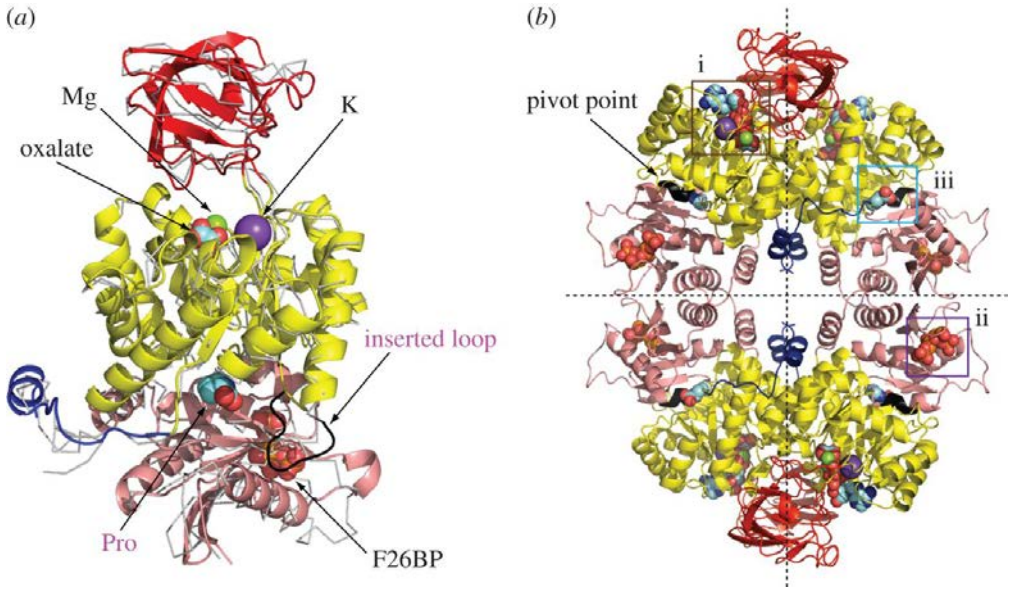

Figure 1.6: Illustration of pyruvate kinase structure and binding sites. **A)** X-ray crystallographic structure of pyruvate kinase monomer complex (PK-FBP-OX-Mg complex). PK monomer consists of N domain (blue colour), A domain (yellow colour), B domain (red colour) and C domain (pink colour). **B)** Tetrameric structure of PK and the binding sites. (i) Represents the active site which has bound with oxalate, ATP, K and Mg. (ii) Represents the effector sit that hosts FBP, and (iii) represents the amino acid binding site which has bound proline. The dashed lines represent the interaction sites between monomers (A-A and C-C domains interaction), *Morgan HP et al. 2014* (89).

1.10.2: Regulation of pyruvate kinase M2:

PKM2 occurs either in a highly active tetrameric or nearly inactive dimeric isoform. PKM2 is mainly in the tetrameric form in normal cells, whereas the dimeric form is usually found in tumour cells (81). The ratio of tetrameric to dimeric isoform of PKM2 is not a fixed value and depends greatly upon the level of metabolic intermediates, especially the intracellular concentration of FBP. FBP is an allosteric activator of PKM2 and upon elevation induces re-association of the highly active tetrameric form from the combination of two molecules of an inactive dimeric form of PKM2 (21,81). As a result of tetramerisation of PKM2, energy is produced by the conversion of glucose to lactate, until the level of FBP decreases to a minimal level. The dimeric form of PKM2 is then re-produced from the dissociation of the tetrameric form, and the levels of metabolic intermediates increase and become available for synthesis of macromolecules for new cells. These processes continue until the level of FBP increases to a sufficient point to begin another cycle of tetramerisation (Figure 1.6) (21,81).

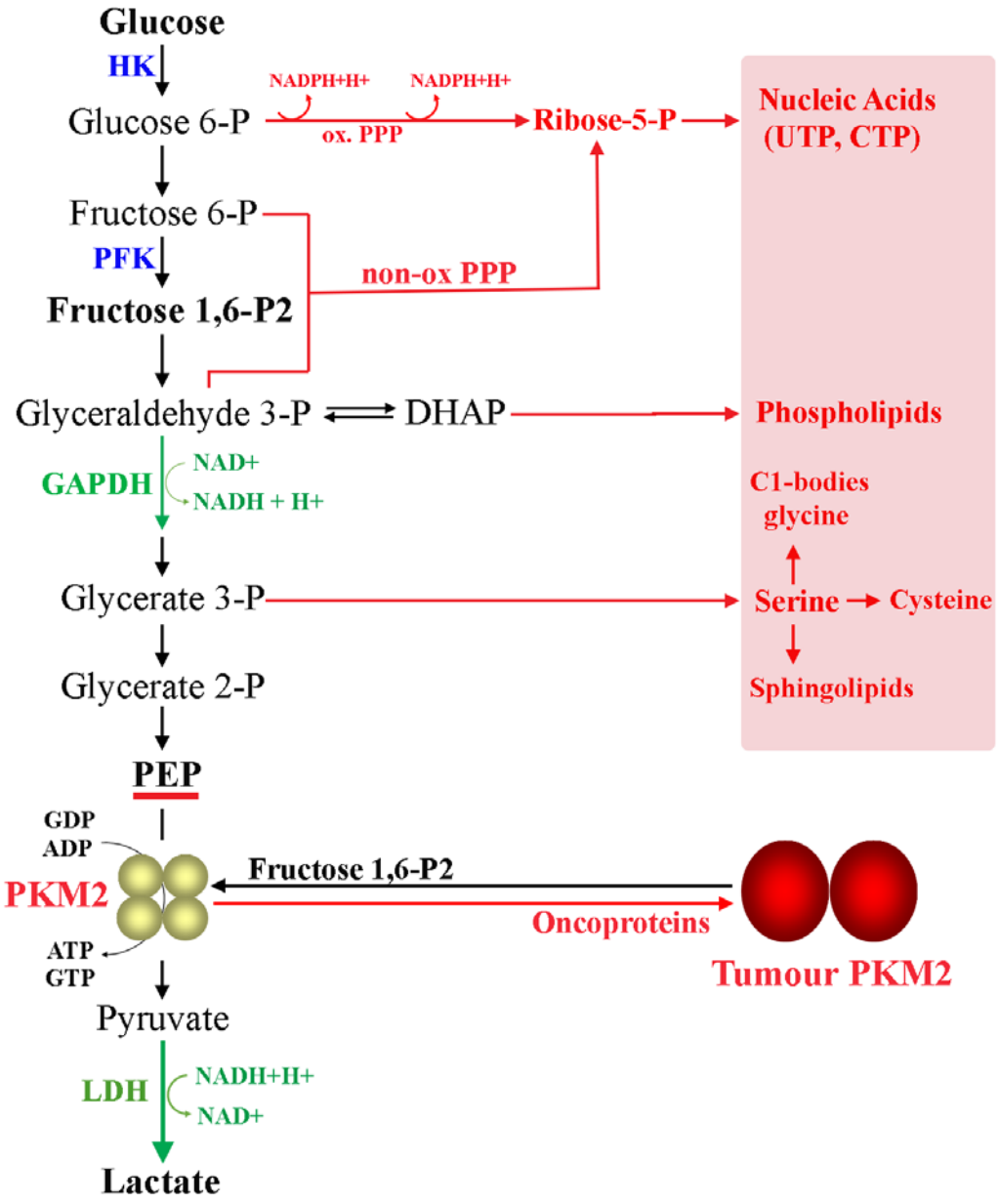

Figure 1.7: Regulation of pyruvate kinase type M2 in glycolysis pathway by fructose 1.6- biphosphates (77). (HK: hexokinase, PFK: 6-phosphofructo 1-kinase, GAPDH: glyceraldehyde 3-dehydrogenase, LDH: lactate dehydrogenase, PPP: pentose-P-pathway). Adapted from *Mazurek S et al. 2011* (77).

Similar to FBP, the amino acid serine has been also identified as an allosteric activator of PKM2. Serine can activate PKM2 in a similar manner to PFB but the interaction occurs independently and in a different location of the FPB active pocket. Serine biosynthesis is an anabolic pathway required for cell proliferation and growth (93). In the presence of sufficient amounts of serine, PKM2 is completely active and facilitates the utilization of maximum amount of glucose through glycolysis, whereas, when the intracellular

concentration of serine decreases, the activity of PKM2 is rapidly decreased and directs glycolysis toward the anabolic pathway for biosynthesis of serine to compensate the low concentration of serine (57). Additionally, decreasing PKM2 activity alters the glycolytic pathway from the production of lactate in the cytosol to the production of citrate in the mitochondria and this switch provides a sufficient amount of energy required for rapid cell proliferation. Interestingly, succinyl-amino-imidazole-carboxamide-ribose-5-phosphate (SAICAR), an intermediate of the de-novo purine nucleotide synthesis pathway, has also emerged to regulate PKM2 activity. The binding pocket of SAICAR is close to the binding site of FBP on PKM2 (94). Upon starvation of glucose, cellular concentration of SAICAR has been observed to elevate in an oscillatory manner. Increased concentration of SAICAR induces PKM2 activity, elevates rate of glucose and glutamine utilization and also promotes cancer cell proliferation and survival.

The tetrameric to dimeric ratio of PKM2 is also regulated by post translational modifications (PTM) as well as interaction with oncoproteins which facilitates dissociation of the tetrameric to dimeric form of PKM2. PTM in the A-domain of PKM2 plays a crucial role in dissociation of subunits and reduction of PKM2 activity. Fibroblast growth factor receptor 1 (FGFR1) directly phosphorylates PKM2 at tyrosine 105 (Y 105) and inhibits the formation of tetrameric form of PKM2 by disruption of the allosteric activator and FBP binding (Figure 1.7). Animal studies have shown that the phosphorylated tyrosine 105 suppress PKM2 activity and promotes tumorigenesis (53,57,95). Acetylation is another common modification used in the regulation of various cellular processes, including metabolic enzymes. Acetylation of PKM2 at lysine 305 occurs under high concentrations of glucose and suppresses PKM2 activity to direct glycolysis toward the anabolic pathway and tumorigenicity. PKM2 also contributes to the elimination of excess amounts of intracellular reactive oxygen species (ROS) (96). An elevation of intracellular concentration of ROS can damage cell components and compromise viability of the cell. Therefore, control of ROS level is very important for proliferation and survival of the cells. Research findings have shown that the sharp elevation in cellular ROS, suppresses PKM2 activity through oxidation of PKM2 at

cysteine 358, which then drives glucose flux toward the pentose phosphate pathway and induce tumorigenesis (96) (Figure 1.7).

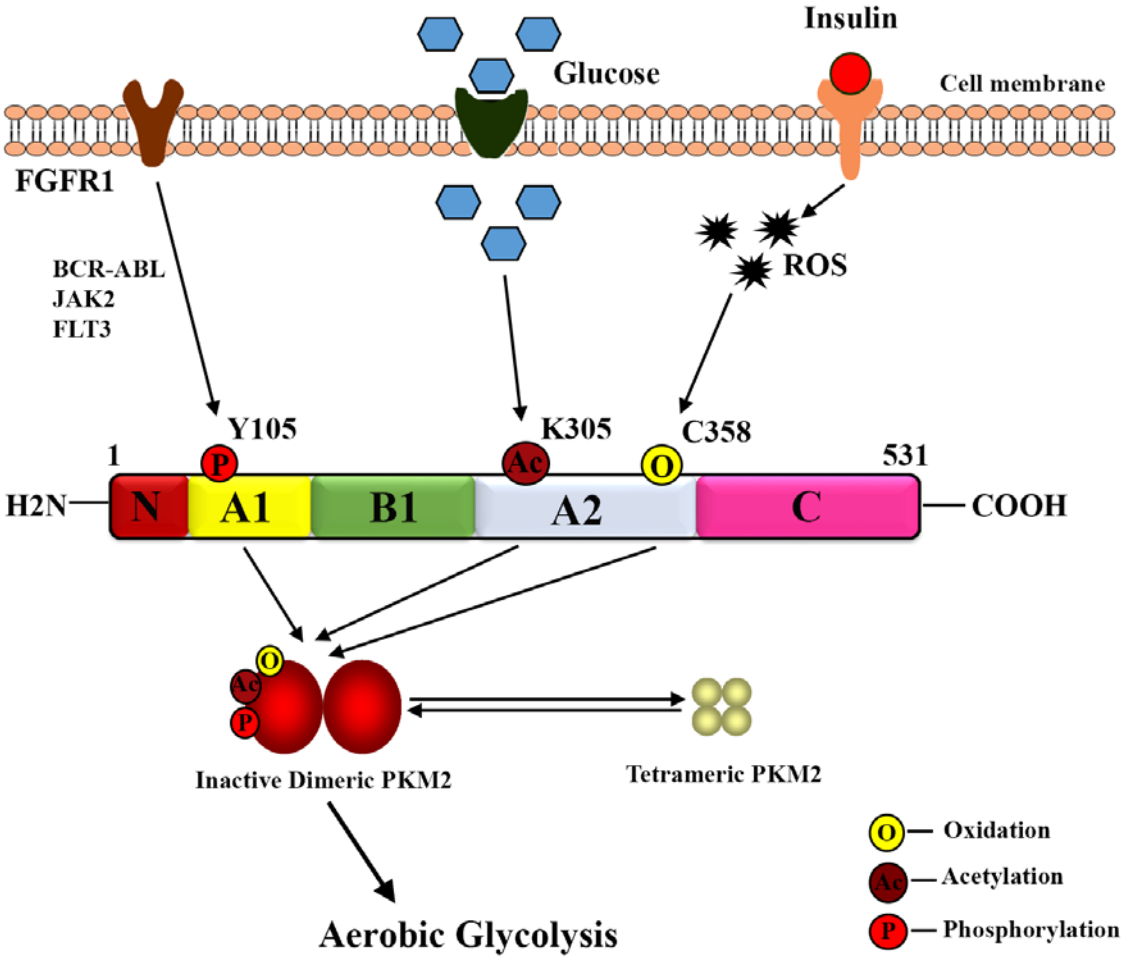

Figure 1.8: Illustration of glycolytic regulation of pyruvate kinase M2 activity. PKM2 activity is not only regulated by glycolytic intermediates, but also various factors stimulate different post translational modifications of PKM2. Adapted from *Iqbal et al. 2014* (53).

In addition to the PTM, numerous viral oncoproteins can control oscillation between dimeric to tetrameric PKM2 in tumour cells. Direct interaction of PKM2 with different oncoproteins, such as human papilloma virus type 16 (HPV-16 E7) and tyrosine kinase pp60v-src, induces dimerization of PKM2 by different mechanisms. The human papilloma virus type 16 produces the E7 oncoprotein that binds directly to PKM2 and the tyrosine kinase pp60v-src phosphorylates PKM2, as a result, the tetrameric form of PKM2 dissociates to the dimer and promotes tumorigenesis (21,81,84).

1.10.3: Non-metabolic function of PKM2 (or nuclear function of PKM2):

In addition to its role in cancer metabolism, PKM2 has been shown to have a nuclear function that further contributes to tumorigenesis. PKM2 is translocated into the nucleus as a response to apoptotic and interleukin-3 signals (51,97,98). Nuclear PKM2 interacts with Oct-4 through the C-terminal residues (residues 307-531) and enhancing Oct-4 mediated transactivation (99). Oct-4 is a crucial protein for the maintenance of pluripotent embryonic stem cells. Nuclear PKM2 has also been shown to act as an HIF-1 co-activator. Luo *et al.* observed that nuclear PKM2 interacts with HIF-1α in a prolylhydroxylase-3 (PHD-3) dependent manner and increases transcription activity of HIF-1α, resulting in an increase in expression of its target genes such as GLUT-1, LDH and PKM2 (53,100). Recently, Jumonji C domain-containing dioxygenase (JMJD5) has been identified to bind directly to PKM2, causing disruption of PKM2 tetramerisation and promoting translocation into the nucleus. Moreover, nuclear JMJD5-PKM2 is a heterodimeric protein and promotes HIF-1α mediated transactivation activity for metabolic reprogramming (101).

Yang *et al.* demonstrated that PKM2 (not M1-PK) can translocate into the nucleus under the activation of epidermal growth factor receptor (EGFR) in human cancer cells. The EGFR signaling induces activation of Src tyrosine kinase and phosphorylates β-catenin at Y333. PKM2 then binds to phosphorylated tyrosine peptides of β-catenin via K433, leading to the recruitment of both proteins to the cyclin D1 (CCND1) and MYC promoters and transactivation of both genes (102). PKM2- β-catenin complex enhances expression of c-MYC and cyclin D1 through dissociation of histone deacetylase 3 (HDAC3) from cyclin D1 promoter. PKM2 dependent β-catenin transactivation is involved in EGFR and promotes tumorigenesis. PKM2 also up-regulates expression of c-MYC, which in turn up-regulates the transcription of hnRNPs (heterogeneous nuclear ribonucleoproteins) that promotes the alternative splicing of PKM2 over M1-PK (53,103). Moreover, in response to EGFR signaling, PKM2 phosphorylates histone H3 at threonine 11 position, resulting in dissociation of HDAC3 from CCND1 and c-MYC promoter and acetylation of histone H3 at K9. Upon EGF stimulation, PKM2, as a

protein kinase, also involves in histone modification to control CCND1 and c-Myc expression in tumour cells (104) (Figure 1.8). Furthermore, the levels of nuclear PKM2 were found to be correlated with histone H3 phosphorylated threonine 11 status in brain tumour and reduced patient survival.

However, the mechanism of switching PKM2 function between protein kinase and pyruvate kinase remained controversial. A recent study found that the dimeric form of PKM2 is a protein kinase and regulates gene transcription. Gao *et al.* also demonstrated that the dimeric from of PKM2 is an active protein kinase, while the tetrameric form is an active pyruvate kinase. They also showed that nuclear PKM2 is in a dimeric form and the expression of mutant PKM2 promotes cell proliferation, indicating that protein kinase activity is essential for cell proliferation (86). This study found a crucial link between metabolic transformation and gene expression.

Another study reported that the acetylation at K433 promotes PKM2 to act as a protein kinase rather than pyruvate kinase and induces accumulation of PKM2 in the nucleus. Lv *et al.* observed that PKM2 is acetylated at K433, under mitogenic or oncogenic stimulation, by p300 acetyltransferase. Consequently, acetylated PKM2 interferes with FBP binding, prevents PKM2 activation, promotes protein kinase activity and accumulation of PKM2 in nuclear. Moreover, acetylated PKM2 promotes tumour cell proliferation and progression through phosphorylation of STAT-3 at Y705 and histone-3 (57,105) (Figure 1.8).

In summary, PKM2 translocates into the nucleus under certain circumstance, accumulating in the dimeric form and functioning as a protein kinase to promote tumour cell proliferation and progression.

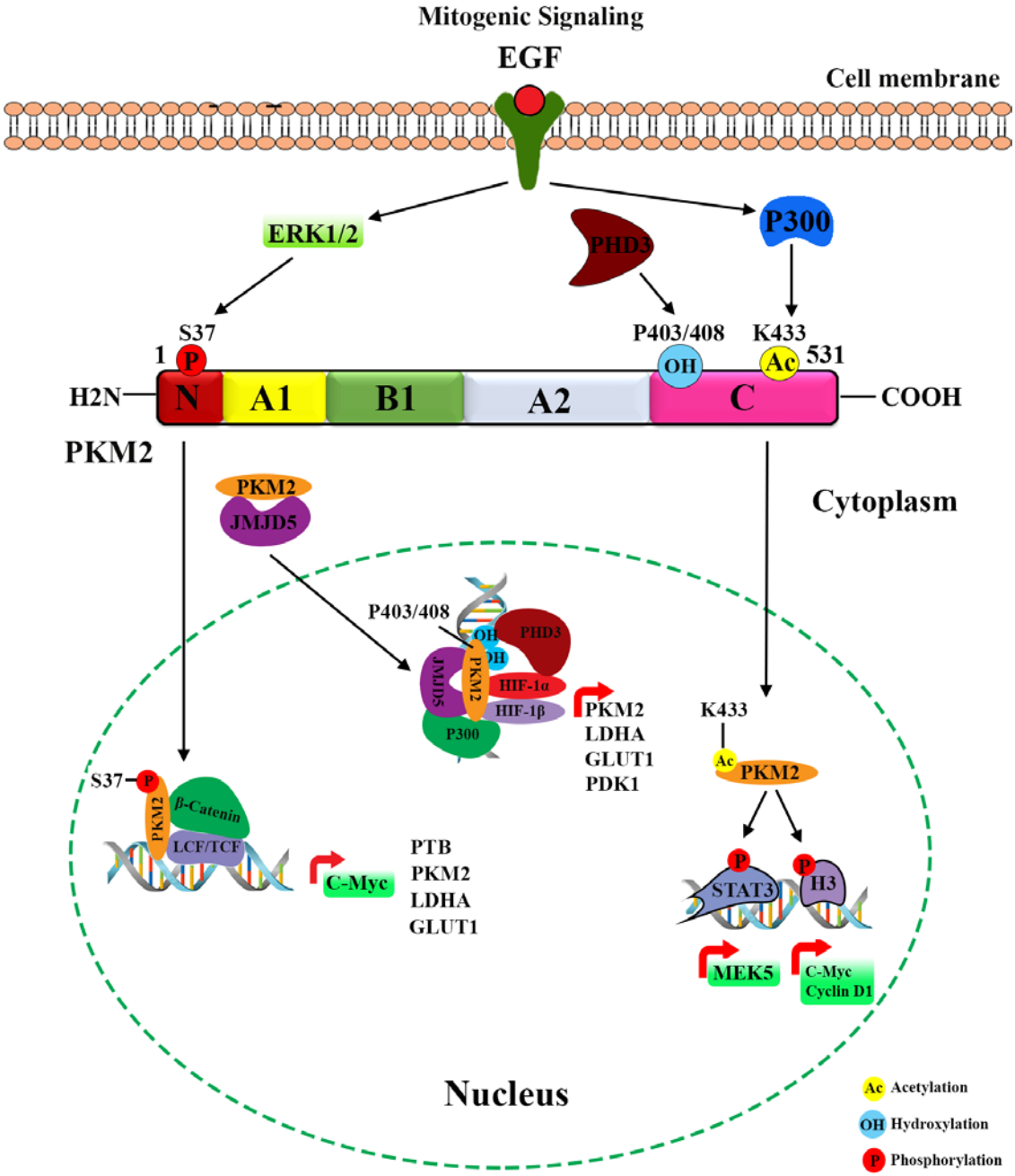

Figure 1.9: Illustration of non-metabolic function of PKM2. The scheme shows the mechanism of nuclear translocation and functions of PKM2. Nuclear PKM2 acts as a protein kinase or transcriptional coactivator to promote tumour cell proliferation and growth. Adapted from *Iqbal et al. 2014* (53).

1.10.4: PKM2 as a target therapy:

Cell division and proliferation require high amounts of glycolytic intermediates, such as nucleotides, lipids and amino acids, on one side, and generation of energy on the other. Therefore, blocking of either energy production or production of glycolytic intermediates may lead to inhibition of cell proliferation (83,106). PKM2 plays an important role in tumour progression and could be a potential therapeutic target for inhibition of tumour

cell proliferation and growth. Fixation of PKM2 in either form may lead to inhibition of tumour progression (77,83,106). In the presence of high amount of glucose, fixation of PKM2 in dimeric form leads to inhibition of energy production and tumour progression. However, in the presence of glutamine, accumulation glycolytic intermediates induce cell proliferation, therefore, fixation of PKM2 in tetrameric form can lead to inhibition of cell proliferation due to the block of production of glycolytic intermediates which required for cell division (77,83,106). Various studies have demonstrated that interfering PKM2 expression by short hairpin RNA (shRNA) and microRNA (miRNA) can induce apoptosis, reduce glycolysis activity and tumorigenicity (83,107,108), and also enhance the sensitivity of tumour toward the treatment (83,109,110).

In the past several years much work has been done to identify PKM2 inhibitors. The active derivate of leflunomide (ARAVA), also known as A77 1726, was a first compound identified as a PKM2 inhibitor. ARAVA is well known in rheumatology as a pyrimidine synthesis inhibitor. ARAVA was firstly described as a dihydroorotate dehydrogenase inhibitor which is a key enzyme in pyrimidine denovo synthesis. However, ARAVA can also inhibit PKM2, resulting in inhibition of glycolytic flux rate and cell proliferation (111).

Recently, Vander Heiden *et al.* (2010) screened more than 100,000 small organic molecules to identify a suitable inhibitor for PKM2. In the presence of 125 μM fructose 1, 6 biphosphate, approximately 5,500 compounds inhibited 50% of PKM2 activity and the lowest IC_{50} compound called compound 3 was used in cell culture. After 36 hours of interaction between compound 3 (250μM) and the H1299 cell line, cell death was increased, at least a part of cytotoxicity was due to the PKM2 inhibition by compound 3 (78). Shikonin and its analogues are another class of PKM2 inhibitor. Shikonin is a Chinese herbal medicine and has well-known anti-inflammatory, anti-bacterial and anti-tumour effects (Figure 1.9). Shikonin inhibited tumour cell glycolysis with an approximately 100 times lower IC_{50} than compound 3, and had selectivity toward PKM2 over the other PK isoenzymes (106,112).

In contrast to the inhibitors, PKM2 activators induce intense glycolysis in tumour by tetramerisation of PKM2 and reduction of glycolytic intermediates. Several studies have shown that restoring PKM2 activity may revert the metabolic state of tumours towards that in normal cells. PKM2 activator can reduce production of glycolytic intermediates and inhibit translocation of the dimeric form into the nucleus, causing inhibition of cancer cell proliferation and progression (52,113). Therefore, discovery and development of small molecule activator could be important for cancer treatment (Figure 1.9).

The first class of small molecule activators were identified by high throughput screening (HTS) of 300,000 compounds of the NIH molecular library. Two main classes of chemical compounds were identified. The two chemical compounds were substituted thieno [3, 2-b] pyrrolo [3, 2-d] pyridazinone and substituted *N.N'*-diarylsulfonamide with an AC_{50} of 63nM and the maximum PKM2 activation of 122%. The pyridazinone molecule initially did not require significant optimization as a small molecule activator of PKM2, but solubility was low (< 0.2 µg/ml). After several substitutions and optimization of the molecular probe, the solubility was significantly increased (29.6 µg/ml), but the activity slightly decreased (AC_{50} =92nM). The PKM2 activator identified from this effort known as TEPP-46. On the other hand, the substituted *N.N'*-diarylsulfonamide compound developed and optimized to the several molecular activators, however, the only molecular activator with an identity of DASA-58 was shown the high selectivity and potency toward activation of PKM2. DASA-58 has not only improved potency (38 nM) but also significantly increased its aqueous solubility (51.2 µg/ml). The two small molecular activators were tested against all PK isoenzymes and found to have a specific activity toward PKM2 over the other isoenzymes (113–115).

Following the identification of TEPP-46 and DASA-58, further studies of the characteristics of these two molecules as PKM2 activator were done. Interestingly, the activators efficiently induced tetramerisation of PKM2 in cell culture. Initially, it was suggested that the activators would interact with the allosteric activator binding site, but structure analysis showed the PKM2 tetramer in a complex with two molecular

activators and four FBP molecules. Interestingly, the molecular activators bind to the pocket on the PKM2 subunit interface (binding on the C-C` interface of two opposing dimers) away from the FBP binding site, so that the interaction enhanced association of PKM2 subunits and stabilized tetrameric structure. Furthermore, TEPP-46 was showed to impair tumour growth in xenograft model in a dose of 50 mg/kg twice a day. (113).

The same research group has developed a third class of PKM2 activator from 2-oxo-N-aryl-tertrahydroquinoline-6-sulfonanide. The activator was identified from the previous HTS and initially had an AC_{50} of 790nM. Several derivatives were developed but only one of them showed to have a low nanomolar potency (AC_{50} = 90 nM), selective over the other PK isoforms and good cellular permeability (116).

Another research group identified nine small PKM2 activators by screening 13,000,000 small molecules in silico against the PKM2 structure. After several modification a more promising PKM2 activator has developed. The PKM2 activator is derived from 5-((2,3-dihydrobenzo[b][1,4]dioxin-6-yl)sulfonyl)-2-methyl-1-(methylsulfonyl) indoline scaffold, with low nanomolar potency (AC_{50} =17 nM), selectivity over the other PKM2 isoenzymes, good cellular permeability and liver microsome stability (117).

In addition, two further PKM2 activators were identified from two HTS of small molecules. The first PKM2 activator was based on the sulphonamide scaffold and the lead compound was modified and synthesised several derivatives, the AC_{50} of most promising one was lower than 14 nM (118). The other HTS has identified benzodiazolopyrimidinone as a lead compound with AC_{50} of 3.5 µM and the maximum activity of 148%. The lead compound was modified by using structure based approach, as a result PKM2 activator was synthesised with an AC_{50} of 86 nM (119). Moreover, the x-ray crystallography study showed that the binding site location of these two molecular activators were similar binding site location of DASA-58 on PKM2 enzyme (118,119).

Finally, another PKM2 activator was recently identified by using fragment based screening. The lead compound was pyrrolo-carboxy amide fragment with AC_{50} of 36 µM. The initial compound was modified and synthesised a series of compounds with an AC_{50} of lower than 11 nM. The molecular activators identified from this effort were

examined both *in vitor* and *in vivo*. In the absence of serine, the molecular activators inhibited cell proliferation in a lung cancer cell line and impeded tumour growth in an A549 xenograft tumour model (120).

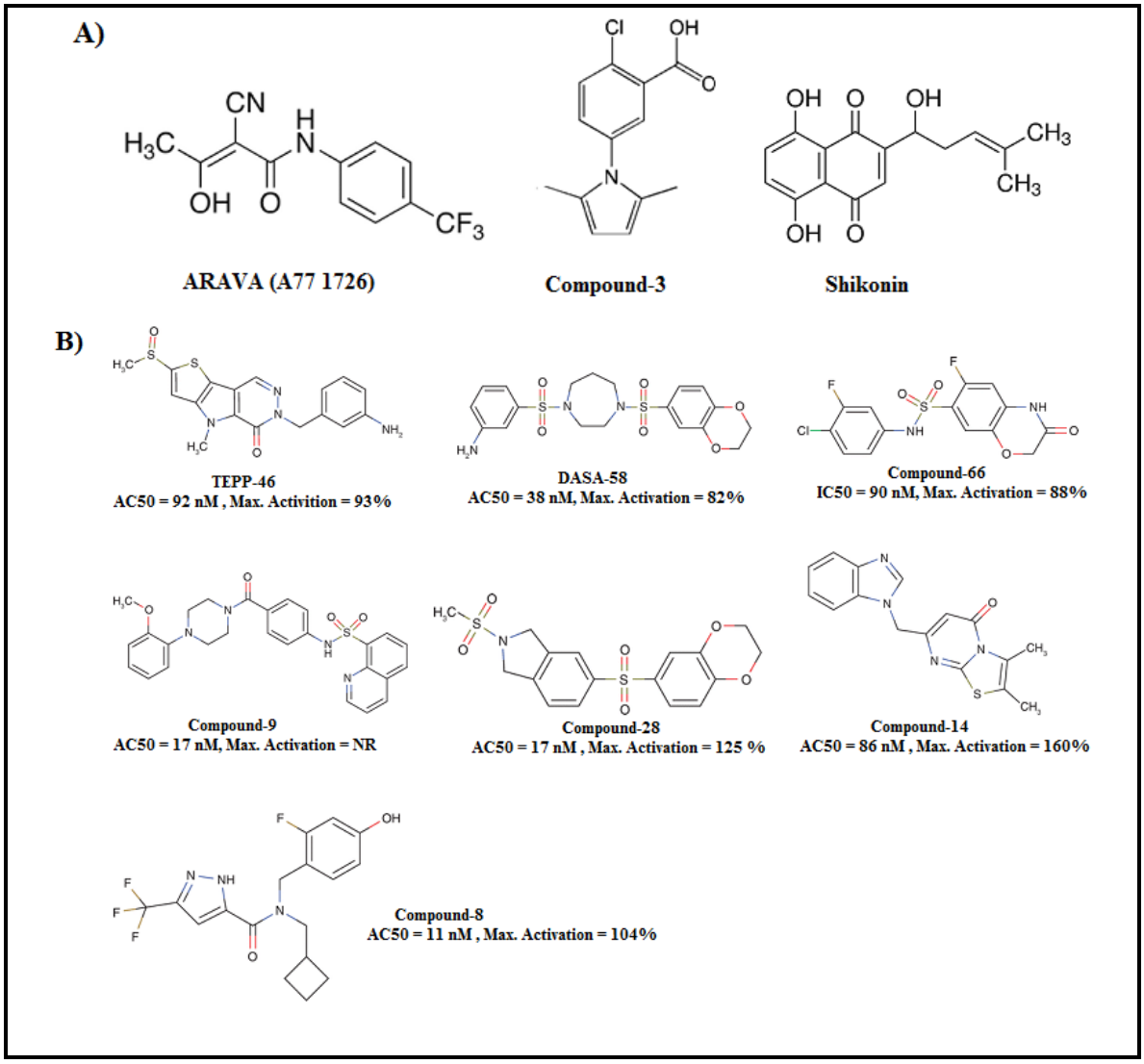

Figure 1.10: Structures of the most popular PKM2 inhibitors and activators. **A)** Chemical structure of the most common PKM2 inhibitors. **B)** Chemical structures, half-maximum activating concentrations and maximum activation vales of most common PKM2 activators.

1.11: Lactate dehydrogenase (LDH):

Lactate dehydrogenase (LDH, EC 1.1.1.27) mediates inter-conversion of pyruvate and lactate using nicotinamide adenine dinucleotide (NAD+) as a cofactor (Figure 1.10A). Lactate dehydrogenases (LDHs) are a family of 2-hydroxyacid oxidoreductases that are found in almost all animal tissues, as well as in microorganisms, bacteria and plants

(121). Lactate dehydrogenase is a homo- and hetero- tetrameric (144 kDa) enzyme comprised of two major subunits A and B (36 kDa), resulting in five isoenzymes that catalyse the reversible conversion of pyruvate and lactate (Figure 1.10). LDHA (also known as LDH-5, LDH-M or A4) is encoded by the *ldh-a* gene and predominates in skeletal muscle and liver, while, LDHB (also known as LDH-1, LDH-H or B4) is encoded by the *ldh-b* gene and is mainly found in heart and brain (Figure 1.10) (49,121,122). LDH-C is another type of lactate dehydrogenase, which is mainly composed of X-subunits. LDH-C is a less common type of lactate dehydrogenase, which is encoded by the *ldh-c* gene. LDH-C is found in human spermatozoa and has been proposed to play a role in male fertility (121,123). The genetic loci of the three LDH isoforms show about 75% sequence identity, indicating extensive conservation in amino acid composition of the LDH subunits (121).

LDH isoenzymes have different electrophoretic mobility depending on the availability of the B subunit. Therefore, LDHB is the faster and LDHA the slowest moving LDH isoenzyme. LDHA and LDHB show different kinetic properties, of which LDHA needs a higher concentration of pyruvate substrate to reach maximum activity. The Km value for pyruvate is about 158 and 58 µM for both LDHA and LDHB, respectively. Additionally, at a concentration of pyruvate substrate required for optimum activity of LDHA, the LDHB isoenzyme is inhibited with Ki for pyruvate substrate of 3900 and 770 µM for LDHA and LDHB, respectively (50,121,124). Accordingly, a high Km value for LDHA indicates a low affinity for pyruvate substrate and is suited to the tissues frequently exposed to oxygen limitation; however, a low Km value of LDHB indicates a high affinity for pyruvate and is more suited to the aerobic metabolism. This so called “aerobic anaerobic theory” was hypothesized in 1975 by Kaplan. However, later research showed that human erythrocytes, which lack mitochondria, primarily express LDHB. LDH isoenzymes also have a different distribution pattern between individual organs of the same type in different animal species, which was not clearly explained by the Kaplan theory (50,121).

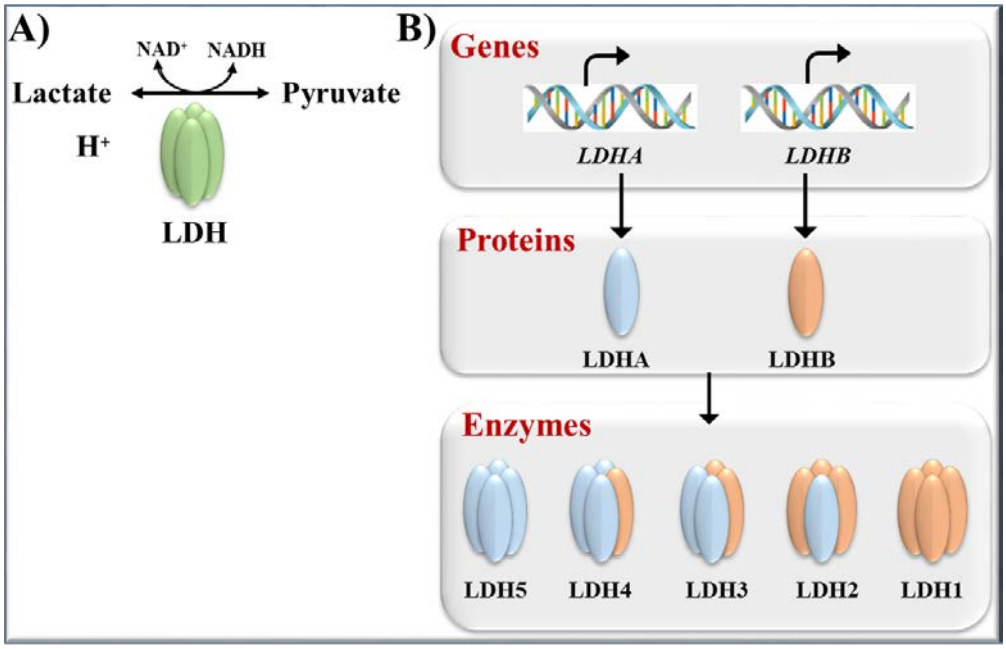

Figure 1.11: Illustration of lactate dehydrogenase functions and gene expression. (A) LDH catalyses inter-conversion of pyruvate and lactate with regeneration of NAD+. (B) LDH is a homo- and hetero-tetrameric enzyme consisting of A and/or B subunits, resulting in five different isoenzymes. Adapted from *Doherty JR et al. 2013* (49).

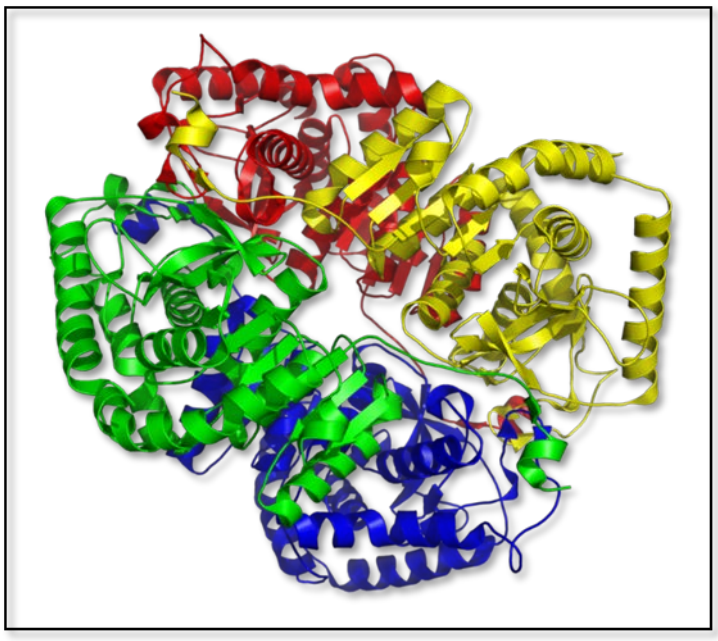

Figure 1.12: Human Lactate dehydrogenase A, LDHA isoform found in skeletal muscle.

Despite the different kinetic properties of LDHA and LDHB in cytosol, both catalyse the inter-conversion of pyruvate to lactate. In most tissues, LDH isoenzyme activity depends on the glycolytic flux and is always close to equilibrium. The LDH equilibrium reaction may significantly deviate when extensive change occurs in cell glycolytic flux and

energy metabolism. This is the only situation where the different physiological roles of LDH isoenzymes have been observed. For instance, during exercise or overworking of muscle, glucose uptake and glycolytic flux significantly increase. In this situation LDHA isoenzyme is highly activated to overcome the high glycolytic flux and energy demand by conversion of pyruvate to lactate with regeneration of NAD+ to sustain glycolysis (50). A similar situation has been detected in tumour, overexpression of LDHA in cancer is required for progression and growth of tumour (54). In contrast to muscle and cancer cells, LDHB is predominately expressed in brain cells (50).

LDH is mainly detected in cytosol and involved in cytosolic glycolysis. LDH is also detected in peroxisomes, mitochondria and nuclei with performing different biological functions.

LDHA predominates in peroxisomes and is mainly found in the matrix (125,126). The main function of peroxisomes is shortening of long chain fatty acids that cannot be handled by mitochondria. The long chain fatty acid is degraded to butyryl-CoA by β-oxidation, then transfer from peroxisomes into mitochondria. Research findings showed that mitochondrial respiratory chain cannot re-oxidize NADH which is generated from peroxisomes β-oxidation, however, in the presence of pyruvate, LDHA can reconvert NADH to NAD+. Lactate and pyruvate exchange is possibly done through monocarboxylate transporter (MCT) complex display on the peroxisome membrane (125,126).

In mitochondria, lactate derived from glycolysis can be reused as fuel or as a precursor of gluconeogenesis (50,127,128). The re-oxidation of lactate occurs in mitochondria of the original cells, in adjacent cells or in distant cells, after release of lactate into the extracellular medium. For instance, the heart takes up and re-oxidates lactate produced during muscle overworking, whilst, that originating in astrocytes is an important energy substrate for adjacent neurons (50). MCT proteins facilitate the transfer of released lactate across the cell membranes. Moreover, mitochondria can take up lactate through MCT proteins and oxidized to pyruvate by mitochondrial LDH (127,128). In

mitochondria, PDH quickly metabolizes and decreases pyruvate concentration, favoring the oxidation of lactate by LDH (50).

LDH isoenzyme activity varies with tissue types. LDHA is predominantly expressed in the liver mitochondria; however, myocardium mitochondria was characterized by expression of LDHB (129). This difference in LDH isoenzymes was due to the predominant pathway in different organs, for instance, lactate is taken by liver more likely to undergo gluconeogenesis, whereas in the myocardium is more likely to undergo oxidation. Despite these differences, it is thought that the redox state of the mitochondria dictates the ability of the tissues to oxidize lactate, not the particular LDH isoform (129).

Mitochondrial LDH is based in the intermembrane space, matrix fraction and inserted also into the inner membrane (Figure 1.12) (129). The mitochondrial and cytosolic LDH has different kinetic properties.

Besides the crucial role in cellular energy metabolism, LDHA shows additional functions in nucleus. The subunit of LDH-A binds to single stranded DNA (ssDNA) and functions similarly to the other ssDNA-binding proteins, which are involved in nuclear enzymatic activities for DNA transcription and/ or replication (130). This observation was confirmed by recent research that identified the location of nuclear LDH in a transcriptional active region of chromosomes. RNA in polytenic chromosomes was also stimulated when LDHA enzyme was injected into the *Chironomus* Salivary gland cells (50). Recently, Zhang and co-work explained the role of nuclear LDH in DNA transcription and showed that nuclear LDH is one of the main components of the transcriptional complex of histone 2B gene (H2B) (131). LDHA subunit, in this transcriptional complex, is in association with GAPDH and through the coordination of the activity of these two enzymes, maintain the ratio of NAD/NADH, which is required for optimum expression of H2B.

In contrast to cytoplasmic LDH, in which the minimum functional unit was shown to be a dimer, the nuclear LDH is mainly a monomer. The supramolecular structure formed with GAPDH or with other components of the transcriptional complex presumably maintains catalytic activity of nuclear LDH. *In vitro* studies have shown that the

monomers of LDH and GAPDH can form catalytically active complexes in the nucleus (50). Due to being widely distributed in cell nuclei, the LDHA subunit could be involved in regulation of gene transcription and participates in cell survival pathways.

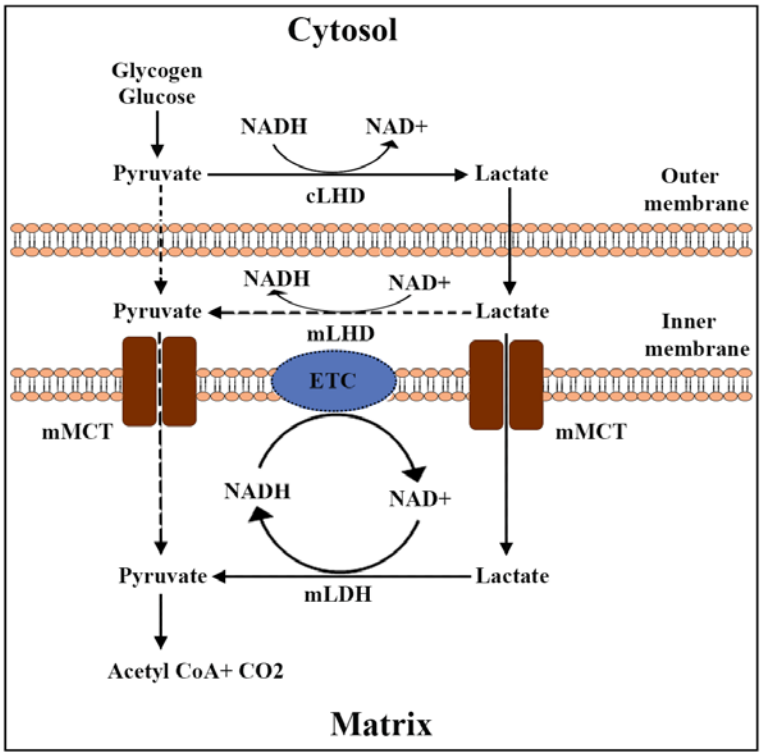

Figure 1.13: Illustration of mitochondrial lactate dehydrogenase functions and localization. Adapted from *Brooks G et al. 1999* (129).

1.11.1: Lactate dehydrogenase A structure:

Crystallography of LDHA shows that this enzyme is usually in a tetrameric form with an arrangement of 2-2-2 symmetric structure. Each subunit of LDHA consists of approximately 330 amino acids with bilobal structure, and also each monomer of LDHA independently has full biological functions (124,132). The study of crystal structure of LDHA have identified two domains, the larger domain adopts Ross-mann fold and is located in 20-162 and 248-266 residues regions, which provides a binding site for NADH cofactor. The smaller domain is a substrate binding pocket, which is located at the interface with the adjoining mixed α/β domain (50,121). The mechanism of enzyme substrate reaction is started by interaction of NADH cofactor with LDHA in a His195, which prepares the binding site for pyruvate binding. Subsequently, substrate gains

access to the binding site cavity through the interaction with Arg109 and His195. The main functions of His195 are proton exchanger and to facilitate the orientation of pyruvate for its interaction with NADH. Arg109 is a polarized carbonyl group of pyruvate substrate by forming H-bond, followed by closure of the active site loop (restudies 99-110). As a consequence, the active site loop facilitates transformation of hydride and prevent the access of solvent (50,121,124,132).

The crystallography study also shows that the active site of human LDHA is located in a deep position within the enzyme and accessibility to this cavity is very narrow. In normal condition, both pyruvate substrate and NADH cofactor are hosted by active site cavity. Furthermore, the LDHA active site loop is very polar and rich in cation residue particularly arginine and this characteristic explained why the inhibitors discovered so far contains carboxylate groups (50,122) (figure 1.13).

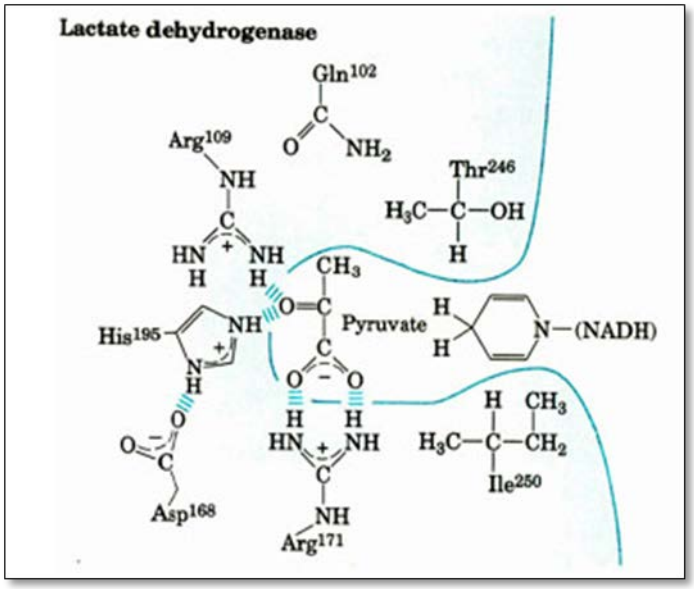

Figure 1.14: The LDHA active site structure and catalytic reaction. The LDH-A active side loop naturally hosts both pyruvate and NADH. The picture illustrates the catalytic reaction and hydrogen bond between pyruvate substrate, NADH cofactor with active site loop and the most important amino acids in the active site cavity.

1.11.2: Metabolic symbiosis and lactate acidosis:

The first step in glucose metabolism is the generation of two molecules of pyruvate with reduction of NAD+ from one molecule of glucose, a similar process in both normal and cancer cells. In the normal cell, pyruvate enters into the mitochondria and TCA cycle after decarboxylation to acetyl-CoA and NADH is re-oxidized by highly active mitochondrial respiratory chain. However, in the cancer cell, LDHA converts pyruvate to lactate with regeneration of NAD+ to sustain energy production by glycolysis (51,52). Oxidation of one mole of glucose through aerobic glycolysis generates two moles of lactate and two of ATP. In contrast to the normal cell, which relies on the catabolic pathway to generate maximum energy through full oxidation of glucose to CO_2 and H_2O. The tumour cell is characterized by anabolic pathway aiming at obtaining macromolecules for building new cells. PKM2 plays a crucial role in the regulation of glucose metabolism and the balance between energy generation and the production glycolytic intermediates (51,53,57,59).

Catabolic metabolism pathway is not only specific to the tumour cells, but also observed in some circumstance of normal cells especially during requirement of rapid cell division, for instance, during development of embryonic cells, wound healing or during immune response activation (50). In contrast to the past thought, normal proliferating cells and a large fraction of cancer cells depend mainly on glycolysis for production of new macromolecules, and gain a significant fraction of their energy (ATP) from mitochondrial oxidative phosphorylation. Moreover, glycolytic energy becomes one of the major energy source when the hypoxic microenvironment prevent mitochondria functions, such as in hypo-vascularized tumour region or in the healing wound bed (50). The increased rate of lactate production is regulated by the activity of LDHA. High levels of lactate production contribute to the development of extracellular acidosis, which strongly participates in tumour invasion, migration, angiogenesis, metastasis and resistance to the chemotherapy (50,133). Lactate is not only the end product of aerobic glycolysis, but can also be used as a metabolic fuel by oxidative cancer cells. This

phenomenon resembles a process that have been described for brain and skeletal muscle that involve what are known as cell-cell and intracellular lactate shuttles (50,134).

Cancer cells can be categorized into two types: aerobic tumour cells, which are located near to the blood vessels and hypoxic tumour cells, which are further away from vascular network (Figure 14). The symbiosis between hypoxic tumour cells, which produce lactate, and aerobic tumour cells, which consume lactate, was observed. Generally, hypoxic tumour cells actively uptake glucose through GLUT1 and glucose then converts to pyruvate through series glycolytic enzymes activity. Finally, pyruvate is converted to lactate by the action of LDHA activity (135,136). Hypoxic tumour cells generate two moles of lactate and two ATP from glycolysis of one mole of glucose. Lactate is then extruded from the hypoxic tumour cell into the extracellular milieu by MCT4. Lactate derived from hypoxic tumour cells can be used as a major source of metabolic fuel in well oxygenated tumour cells. Aerobic tumour cells then take up lactate through MCT1 and use as a main source of energy generation. Aerobic tumour cells convert lactate to pyruvate through the action of LDHB activity and pyruvate then enter into the TCA cycle in mitochondria and generate energy through mitochondrial oxidation phosphorylation. As a result, aerobic tumour cells generate 18 mole ATP from the re-use of one mole of lactate and spare glucose, which can then diffuse longer distance into the tumour to feed glycolytic cells (50,134–136). MCT1 and MCT4 play a key role in this process. The details of metabolic symbiosis between hypoxic and aerobic tumour cells are described in Figure 1.14.

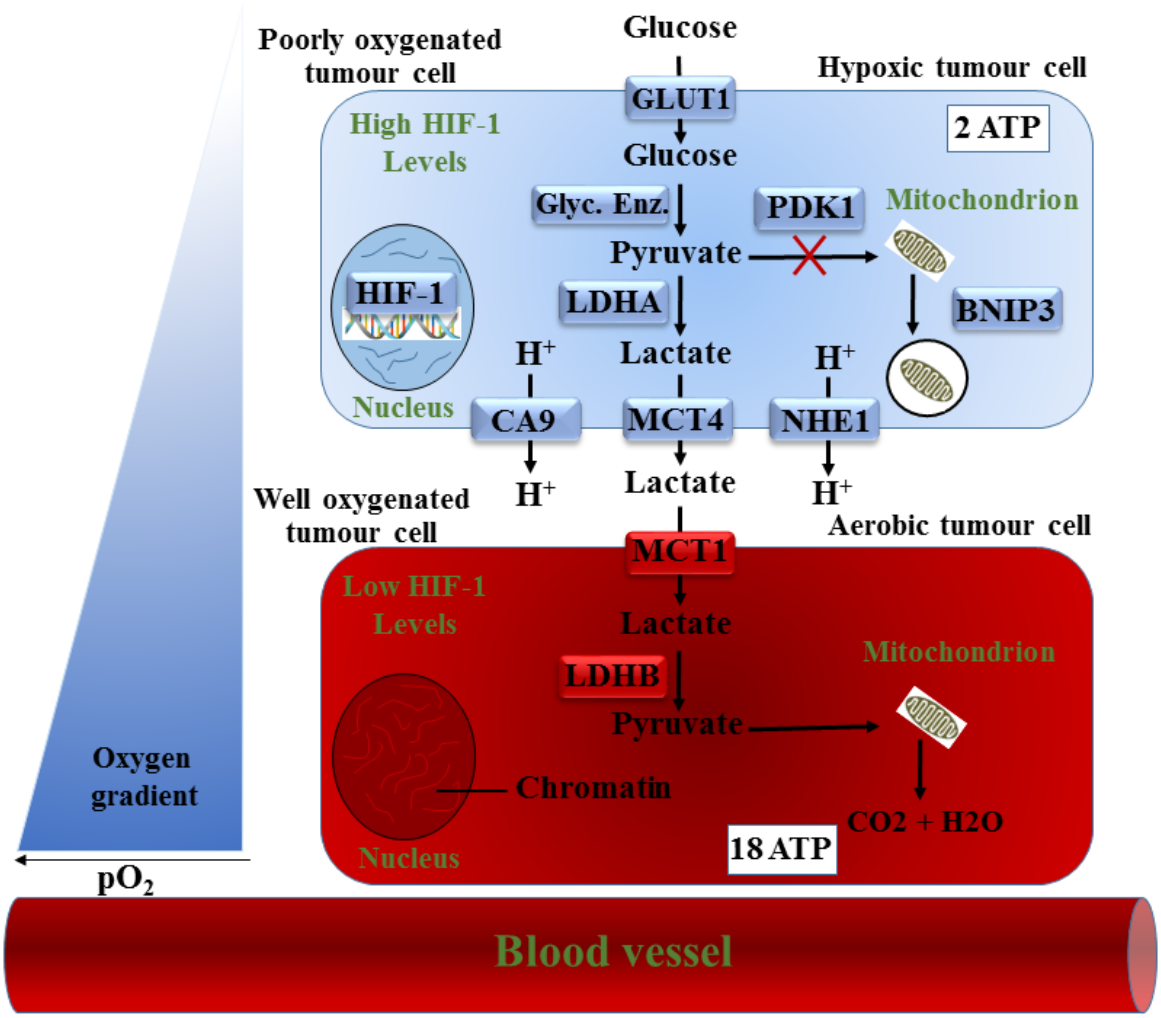

Figure 1.15: Illustration of metabolic symbiosis between aerobic and hypoxic tumour regions. Hypoxic tumour cells utilize high amount of glucose and produce lactate, however, aerobic tumour cells can use lactate as an energy source for bioactivity and spares the glucose for hypoxic tumour cells. Adapted from *Semenza GL et al. 2008* (136).

1.11.3: Inhibition of Lactate dehydrogenase A as a target therapy:

Up-regulation of LDHA has been observed in many types of cancer and has a crucial role in tumour progression (49,54,133). Targeting LDHA is commonly considered as a potential therapeutic target for cancer treatment. Previous research findings have proven that the inhibition of LDHA by using siRNA or small molecule inhibitors, increase the rate of oxygen consumption, reduce glucose uptake and lactate production and also attenuate tumour growth and progression (49,54,72,137). However, the most currently

available LDHA inhibitors have low potency with high doses are required and potentially have high level of systemic toxicity (Figure 1.15).

Oxamate and gossypol are two chemical compounds that have long been known as LDHA inhibitors. Oxamate is an analogue of pyruvate substrate and a competitive inhibitor of LDHA. Oxamate is not toxic in healthy animals up to 3 g/kg, but has poor selectivity and potency toward LDHA (50,122,138). Oxamate also shows very low cell membrane permeability, therefore, the inhibition of cancer cell glycolysis requires high concentrations of oxamate *in vitro* and has little effect *in vivo*. Interestingly, oxamate is still considered to be one of the most important LDHA reference inhibitors. Several oxamate derivatives later have been synthesised aiming to improve selectivity and potency of LDHA inhibition, but none of them shows anticancer activity effect (50).

Gossypol is a natural poly-phenol di-aldehyde derivative found in cotton seeds and can inhibit LDHA through competition with NADH cofactor. Gossypol is not specific to LDHA but can interact with other cell components, interrupting some biological activity and causing nonspecific toxicity (50). In contrast to oxamate, gossypol shows an inhibitory effect at low concentrations (micro-molar) *in vitro*. Several analogues of gossypol have been synthesised. The 8-deoxyhemigossylic acid derivatives, which were originally synthesised as anti-malarial agents, have been found to be the most selective LDHA inhibitors. Among these compounds, 2,3-dihydroxynaphtalen-1-carboxylic acid (which is known as FX11) has a high selectivity and potency toward LDHA inhibition (49,50,122). Previous research findings showed that the FX11 can inhibit cancer cell proliferation *in vitro* and impede tumour growth in xenografts model (54,72,122). Ann Le *et al.* (2010) found that the FX11 can enhance oxygen consumption, reduce ATP generation and lactate production, induce oxidation stress and finally cancer cell death (72). On the basis of *in vitro* and *in vivo* inhibitory effect and availability in market, I chose FX11 in combination with PKM2 activator as a potential therapeutic approach in pancreatic cancer.

Galloflavin, another LDH inhibitor was found by a structure-based virtual screening strategy. Galloflavin is a derivate of garlic acid that can inhibit both LDHA and LHDB

(139). The inhibitory effect of Galloflavin was tested in several cancer cell lines and the results showed that Galloflavin inhibit LDH with an IC_{50} of 90-150µM and also reduce lactate production. Moreover, Galloflavin has good cellular permeability with little toxicity to mitochondrial respiration or the normal cell metabolism. Apoptosis is the main reason for cell death in most cancer cell lines treated with Galloflavin; however, in some other cell lines, Galloflavin induces oxidative stress due to an increase of ROS production and finally cell death (50,139,140).

Another chemical compound that shows moderate potency toward LDHA inhibition is 2-thio-6-oxo-1,6-dihydropyrimidine, which was identified by HTS of library small molecules (141). Later, several modifications were made to the molecular structure of this compound to improve its selectivity and potency toward LDHA inhibition; however, none of the modified compounds were shown to decrease lactate production in cell culture. Recently, the discovery of quinolone 3-sulfonamides as a potent LDHA inhibitor has been announced. Despite its high potency (nano-molar) and 10-80 fold selectivity over the LDHB, these chemical compounds are not acceptable for *in vivo* use because of their low clearance. One of the other limitations of these chemical compounds is a direct effect of mitochondrial function rather than inhibition of LDHA at doses of 10µM and above (48).

Ex-novo design is another strategy that has been used to design a potent LDHA inhibitors. A new LDHA inhibitor was synthesised by adding hydroxyl (-OH) and carboxyl (COOH) into an N-hydroxyindole (NHI) scaffold (122). A number of derivatives were synthesised and tested *in vitro*. NHI-1 derivative was found to have the most promising anticancer activity effect. Later, a methyl ester of NHI-1 was designed, which showed a better cellular permeability and inhibited 80% of lactate production in a concentration of 200µM (142). Subsequently there were no further experiments done on these compounds.

Fragment based lead generation (FBLG) is another strategy that has been used to design potent LDHA inhibitors. This method is based on screening of chemical compounds to identify small chemical fragments, which may bind weakly to the biological target. This

preliminary test was done with the aid of NMR spectroscopy and/or surface Plasmon resonance. The identified chemical fragments were then grown or combined to generate compounds with high selectivity and potency. Moorhouse *et al.* (2011) was the first to use this strategy for finding an LDHA inhibitor (143). More recently, a research team at AstraZeneca has found some high potent LDHA inhibitors by using this strategy. The most potent compound was shown to have an IC_{50} of lower than 0.27µM in an enzymatic activity assay but there was no any inhibitory effect in cell culture assay. This inactivity in cell culture probably related to the low cellular permeability. Moreover, the dimethyl ester derivate showed less potency toward LDHA inhibition compared to the original molecule, but it could inhibit production of lactate in cell culture with an IC_{50} of 4.8µM (144). Similarly, a research team at ARIAD Pharmaceuticals used this approach to identify LDHA inhibitors. One of the most promising compounds they reported had an IC_{50} of 13µM of enzymatic activity assay, and was able to decrease lactate production in cell culture at a concentration of 200µM (132).

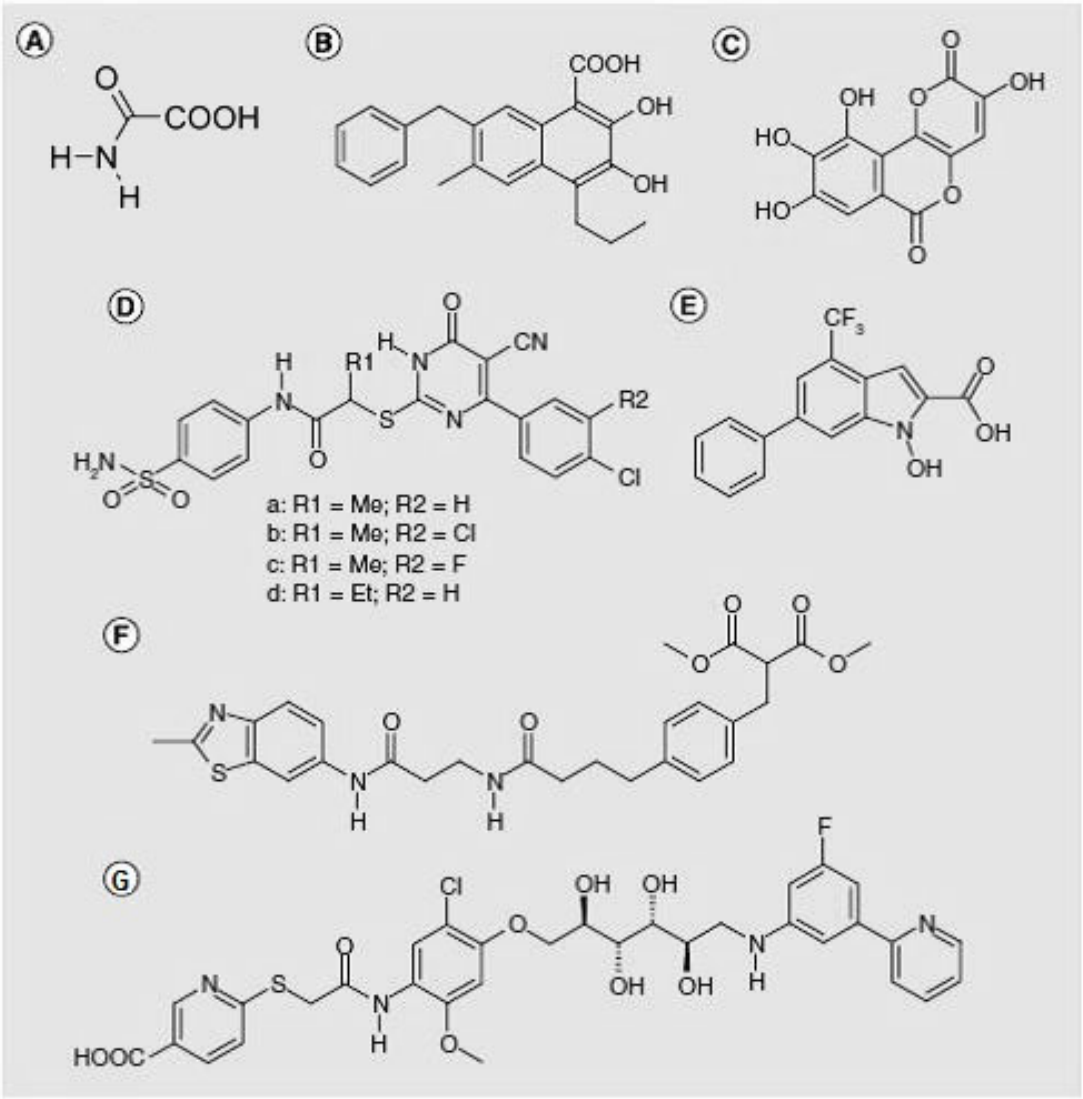

Figure 1.16: Chemical structure of the most popular lactate dehydrogenase A inhibitors. **(A)** Oxamate. **(B)** FX-11, 2, 3-dihydroxynaphtalen-1-carboxylic acid. **(C)** Galloflavin, **(D)** 2-thio-6-oxo- 1, 6-dihydropyrimidine derivative, **(E)** NHI-1, obtained from N-hydroxyindole. Inhibitors obtained through the fragment-based approach at **(F)** AstraZeneca and **(G)** ARIAD Laboratories.

1.12: Combination therapy:

Although pancreatic cancer is very aggressive and is often resistant to chemotherapy, ongoing studies have aimed to develop better adjuvant, neoadjuvant and combination (two or more chemotherapy drugs) agents to improve outcomes. The combination of chemotherapy with glycolytic enzyme inhibitors or inhibition of two glycolytic enzymes together have recently been tried in experimental studies. Aberrant glucose metabolism is one of the main differences between cancer and normal cells; therefore, targeting glycolytic enzymes is considered a feasible strategy for inhibition of cancer cell proliferation and growth. Zhou *et al.* (2010) observed that combination of Taxol and Oxamate (LDHA inhibitor) overcame the resistance of therapy, increased the inhibitory effect and promoted cell apoptosis in breast cancer (145). Similarly, Zhao *et al.* (2011) found that combination of Trastuzumab with a glycolytic inhibitor, such as 2-deoxy glucose or oxamate, synergistically inhibits breast cancer cell proliferation and growth both *in vitro* and *in vivo* (146). In addition, Ann Le *et al.* (2010) found that the combination of FX11 (LDHA inhibitor) and FK866 (NAD+ synthesis inhibitor) blocks pancreatic cancer cell progression in cell culture and a xenograft model (72). Furthermore, Maftouh *et al.* (2014) reported that combination of Gemcitabine with LDHA inhibitor (*N*-hydroxyindole derivative, NHI) synergistically inhibit cell proliferation, growth and induce apoptosis in pancreatic cancer. Combination of Gemcitabine with LDHA inhibitor also inhibits pancreatic cancer cell invasion and migration (74). However, studies evaluating the use of both PKM2 and LDHA together have not been undertaken and is the focus of this study.

1.13: The cell cycle:

The cell cycle involves the duplication of the cell contents and division of cells through a tightly controlled sequence of events that takes place inside the cell. The cell cycle is an essential mechanism for reproduction in all living organisms from unicellular to multicellular species. In the adult body cell division occurs and is necessary for replacing dead cells. The mechanism of cell cycle differs from one organism to another and it occurs at various times of the organism's lifespan. However, certain characteristics of the cell cycle is common between all organisms (147). The most crucial and common feature of cell division between all organisms is the transfer of genetic information from the original cell to the next generation of cells. For production of two genetically equivalent daughter cells, first of all, chromosomal DNA must be faithfully duplicated into two identical and complete copies, and then the duplicated chromosomes should be precisely divided into two daughter cells (147,148).

The cell cycle in eukaryotic cell is more complex and very tightly controlled. The cell cycle has four major phases, which are gap 1 phase (G1), S-phase, gap 2 phase (G2) and M phase. The first three phases (G1, S, and G2) together are known as interphase. The S and M phases are the most important phase of cell division. During the S phase duplication of DNA occurs and requires approximately 12 hours (147). However, the M phase takes much less time in the mammalian cell cycle and usually lasts about one hour. In this phase all the energy of the cell focuses on division into two identical daughter cells. In M phase both nucleus and cytoplasmic divisions occur. Distribution of duplicated chromosomes between two daughter nuclei occur during division of the nucleus (or mitosis), followed by division of the cytoplasm (or cytokinesis) and finally two identical daughter cells are produced (Figure 16), (147–149).

Between the S and M phases, the cell cycle has two extra gap phases. These two phases provide extra time for the cell to grow, duplicate its proteins and organelles that are necessary for chromosome duplication and prepare the cell for division (Figure 1.16). G1 phase is the first phase of interphase, in which the cell grows and biosynthesis of proteins

activated. Restriction point is the last step of G1 phase that controls the cell cycle mechanism. However, if the extracellular conditions are unfavourable the cell cycle is delayed and may enter into the resting state called G_0. On the other hand, G2 is a second gap phase after S phase, in which cell growth continues and provides time to prepare suitable conditions to enter M phase (147,148). Any deregulation of the cell cycle or defect in G1 and G2 gap checkpoints lead to uncontrolled cell proliferation and this phenomenon is a characteristic feature of tumour development (150,151).

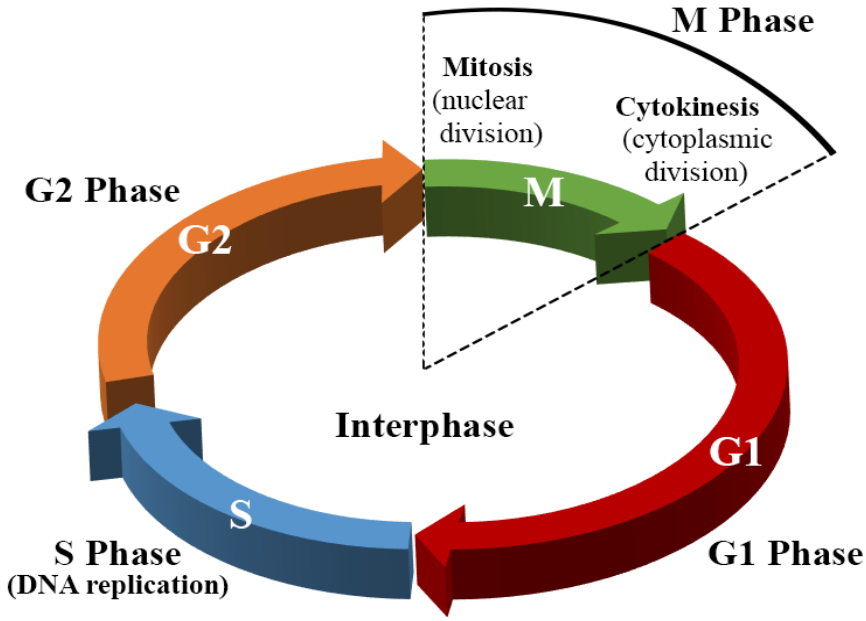

Figure 1.17: The cell cycle mechanism. Adopted from *Alberts B et al. 2008* (147).

1.13.1: Proliferation marker Ki67:

Ki67 is a nonhistone nuclear protein that is strongly associated with cell proliferation and known as a cell proliferation marker. It was first identified by Gerdes in Kiel, Germany (after which was named "Ki"); after immunisation of mice with the Hodgkin's lymphoma cell line L428 (67 comes from the clone number in the 96-well plate in which it was found). In human the Ki67 gene is detected on the long arm of chromosome 10 (10q25) and consists of 15 exons and 14 introns (152,153). The expression of Ki67 antigen varies during the different phases of cell cycle. The location of Ki67 in a cell depends on the cell cycle, during interphase Ki67 antigen is essentially found in the nucleolar cortex and in the dense fibrillar components of the nucleolus. However, during

mitosis Ki67 is located in the periphery of the condensed chromosomes (152). Overall research evidence demonstrated that the expression of Ki67 is low during G1 and early S phases, but reaches a maximum during mitosis. On the other hand, a sharp decrease in Ki67 expression is seen during anaphase and telophase, while Ki67 does not express in resting G_0 phase (152–155).

In spite of the information about location, sequence and nature of the Ki67 protein, little is known about its function. Ki67 protein is phosphorylated via serine and threonine and it plays a crucial role in cell proliferation. The inhibition of Ki67 leads to arrest of cell proliferation as shown either by microinjection of blocking antibodies or by inhibition of dephosphorylation (152,153).

1.14: CD8 tumour infiltrating lymphocytes (Cytotoxic T-lymphocytes):

The host immune response is one of the most crucial weapons against tumour cells; however, the failure of this system to find and eliminate cancer cells may lead to tumour development (156,157). CD8-T cells (Cytotoxic T lymphocytes) are important components of tumour infiltrating lymphocytes that play a crucial role in the anti-tumour immune response. Immunohistochemistry studies have shown anti-tumour activity and favourable effects of tumour infiltrating CD8- lymphocytes on survival of patients with pancreatic, lung, ovarian, colorectal, renal and esophageal tumours (158). Furthermore, several studies have shown a direct correlation between increasing number of CD8+TIL and tumour cell apoptosis (158,159). These results clearly indicate that the tumour infiltrating CD8 lymphocytes inhibit tumour growth and induce apoptosis in cancer cells. The CD8 molecule is a heterodimer transmembrane glycoprotein with alpha and beta chains that covalently bonded together by disulfide linkage. Every chain has a single immunoglobulin like domain which is bound by a polypeptide segment to the cell membrane (160). CD8 cells work as a co-receptor for T-cell receptor and have a specific affinity for the major histocompatibility class I complex (MHC I) (160). CD8 stabilises the interaction between T-cell and cell presenting antigen through the MHC I. When CD8 cell and T-cell receptor attach to the MHC I molecule, the T-cell receptor becomes

more sensitive to antigen and approximately increase its sensitivity by 100-fold more than in the absence of CD8 (160).

CD8+TILs can eliminate infected and tumour cells (target cells) through the perforin/granzyme and FasL/Fas pathways (161). In the former pathway, when a cytotoxic CD8-T cell attaches to the target cell, CD8 cells secrete a cytoplasmic granule that contains perforin and granzyme proteins. The perforin protein plays an important role in their cytotoxic activity by forming pores on the plasma membrane of the target cell to facilitate the delivery of granzyme which induces apoptosis (Figure 1.17), (161,162). In the FasL/Fas pathway, cytotoxic CD8-T cells attach to the target cells through Fas receptor on the target cells and induce apoptosis through activation of caspase cascade pathway (161,162).

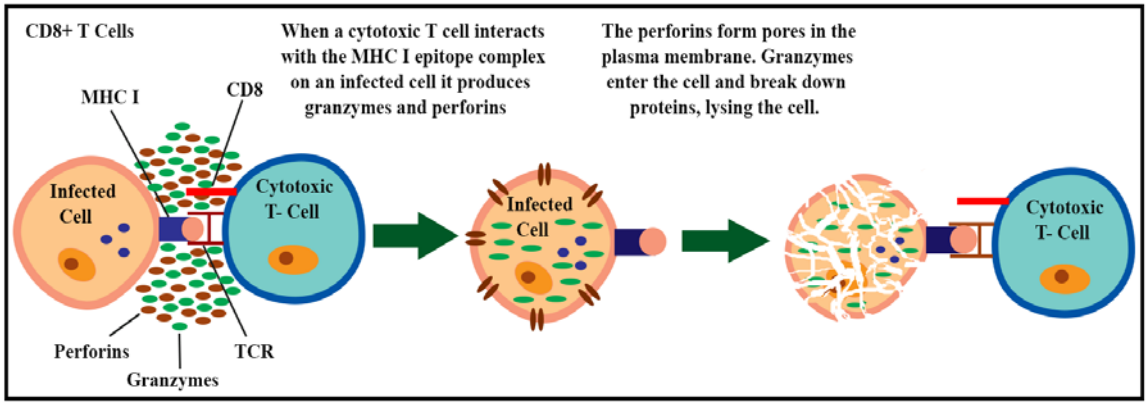

Figure 1.18: Schematic explanation of perforin / granzyme mechanism. Cytotoxic T cell (CD8 T cell) kills target cells (tumour or infected cells) by perforin/granzyme pathway. Adopted from *OpenStax College* 2013 (163).

1.15: Hypothesis and Aim:

Pancreatic cancer has one of the worst survival rates of the most common cancers worldwide and effective therapy of this disease is rather limited. Therefore, early diagnostic markers and new therapeutic option are urgently required to improve survival in this disease. PKM2 and LDHA are two crucial glycolytic enzymes which may play a role in initiation and progression of pancreatic cancer. In this thesis, I will focus on the study of the PKM2 and LDHA enzymes and propose the following hypothesis:

“Pyruvate Kinase M2 (PKM2) and Lactate Dehydrogenase A (LDHA) as Novel Diagnostic Markers and Therapeutic Targets for Pancreatic Ductal Adenocarcinoma (PDAC)”

In order to achieve this hypothesis the following aims were set:

1. To determine expression and localization of PKM2 and LDHA in pancreatic cancer specimens compared to normal and benign pancreatic disease tissues and also correlate the expressions of these two glycolytic enzymes with clinicopathological parameters.
2. To study the expression pattern of PKM2 and LDHA in relation to the host immune response and cell proliferation by counting nuclear immunostaining of CD8 tumour infiltrating lymphocytes (CD8+ TIL) and the Ki67 proliferation marker in pancreatic cancer specimens.
3. To correlate positive nuclear immunostaining of CD8+ TIL and the Ki67 proliferation marker with pancreatic cancer clinicopathological parameters.
4. To measure the plasma activity of PKM2 and LDHA in pancreatic cancer patients compared to the normal healthy controls.
5. To study the expression pattern of PKM2 and LDHA in pancreatic cancer cell lines.
6. To study the cytotoxicity effect of PKM2 inhibition, PKM2 activation and LDHA inhibition treatment and compare the effect of single and combination treatment on the pancreatic cancer cells viability.
7. To study the effect of single and combination of PKM2 activation (tetramerisation) and LDHA inhibition treatments on tumour growth in mice bearing subcutaneous and orthotopic pancreatic cancer xenograft tumours.

CHAPTER 2: METHODOLOGY

2.1: Immunohistochemistry:

2.1.1: Principle:

Immunohistochemistry (IHC) is a widely used technique that combines immunology, anatomy, physiology and biochemistry together to identify tissue constituents by the interaction of specific antibodies with target antigens. This technique is routinely used in research and in the clinic. It provides a good sensitivity and specificity and can identify a wide range of antigens in tissues (164,165). One of the most important advantages of IHC over other techniques is its capability to detect and localise an antigen in a cell or tissue (166).

Immunohistochemistry is extensively used as a diagnostic and prognostic tool. It is used to diagnose benign or malignant cells and also for tumour staging by using specific tumour markers. Furthermore, IHC can provide useful information about cell type and site of origin of metastasis to identify the primary location of the tumour. Moreover, IHC can be used to assess the activity and efficacy of specific drugs given for particular diseases, immunohistochemically (164–166).

The basic principle of IHC involves the binding of a specific antibody to a target antigen, followed by the amplification and visualization of that antigen-antibody link. The target immunogen may be physically “hidden” from the antibody because of protein folding caused during fixation. A pre-treatment or antigen-retrieval step, where enzymes or heat are used to remodel the protein structure and make the antigen accessible, may be required to visualize some antigens.

Target antigen detection can be accomplished by a direct or an indirect method. In the direct method the labeled antibody directly interacts with the target immunogen in the tissue section. Despite the simplicity and rapidity in this one-step staining method, it is rarely used because there is no signal amplification, and the antigen–antibody binding appears very weak. However, the indirect immunostaining protocol is the most commonly used method for the detection of target antigens. This method can be

subdivided into several steps / layers. Firstly, the unlabelled primary antibody (first layer) binds to the target antigen in the tissue section and then a labeled secondary antibody (second layer) is applied which interacts with the primary antibody (164,165). The secondary antibody must be raised against the immunoglobulin G (IgG) of the animal species in which the primary antibody was produced. Secondary antibodies may be labeled with fluorescent dyes (immunofluorescence or immunoenzyme technique). The two-step immunostaining protocol is more sensitive than the one-step protocol because the antigen-antibody binding signal can be amplified (164).

Further amplification and improvement in sensitivity of an antigen-antibody signal can be achieved by a three-layer immunostaining technique. In this method, an unlabelled secondary antibody is conjugated to several biotin molecules or anti-enzyme antibody to produce more stable complexes (165). The most commonly used are the Avidin-Biotin Complex (ABC), Labelled Streptavidin Biotin (LSAB) and peroxidase–antiperoxidase (PAP) method. However, more recently, a peroxidise-labelled polymer method has been introduced to further improve sensitivity of antigen-antibody signal (164).

For many years, the Peroxidase-antiperoxidase (PAP) method was the most commonly used method, but now this procedure is rarely used and replaced by more sensitive techniques (164,167). For instance, Streptavidin is used instead of the avidin molecule which was originally isolated from Streptococcus avidini. The Streptavidin molecule unlike avidin is uncharged relative to animal species; consequently, electrostatic linking to tissue section is eliminated (164,167). Furthermore, the use of Streptavidin instead of avidin eliminates background staining, since carbohydrate groups, which might bind to lectins in tissue sections and are associated with background staining, are not found in the Streptavidin molecule. These characteristics of the Streptavidin molecule have made this method highly sensitive and approximately 5-10 times more sensitive than the standard ABC method (164,167).

On the other hand, the direct and indirect immunostaining protocols are only able to identify one target antigen. However, the identification of two or more antigens in the same tissue section can be done by multiple immunostaining (double staining is most

common) and different fluorescent dyes or enzymes for visualization of stained antibodies (see Figure 2.1).

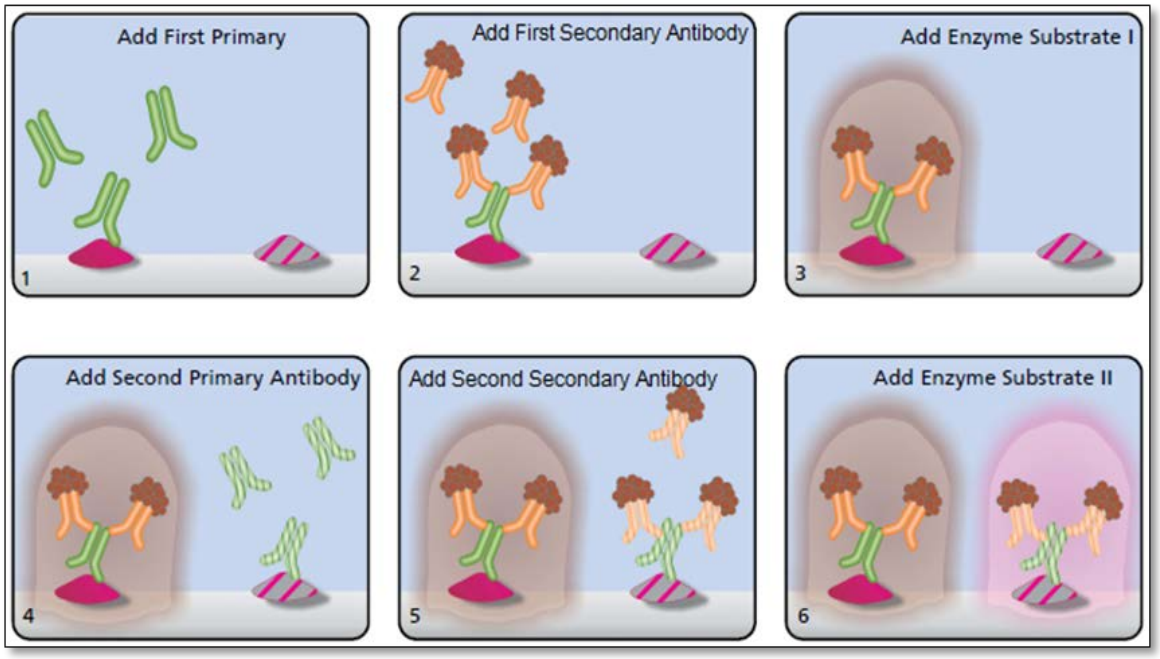

Figure 2.1: Basic principle of immunohistochemistry double staining method.

2.1.2: Patients:

2.1.2.1: Pancreatic cancer:

This study included tissue sections from pancreatic biopsies or surgical resection specimens from 72 patients with confirmed pancreatic ductal adenocarcinoma (n=61) or ampullary adenocarcinoma (n=11) treated during the period January 2005 to January 2010 at University College Hospital, London. An experienced histopathologist examined and confirmed the presence of pancreatic cancer and identified areas of tumour from haematoxylin and eosin (H&E) stained sections. Clinical information was obtained through the CoPath histology database, and a database was created which included the following clinicopathological parameters: gender, age at diagnosis, sample type (biopsy or resection), type of tumour (ampulla or ductal), outcome (alive or dead), cause of death, length of follow-up if alive, presence or absence of metastatic disease at the time of histological diagnosis, whether resection was carried out, residual disease (R) status, post-resection recurrence, time to post-resection recurrence (if any), histological stage, lymph node involvement, presence of perineural or lymphovascular invasion, degree of tumour differentiation, and whether chemotherapy was administered (see summary in Table 2.1). All data were collected from the date of histological diagnosis to the date of death or the end of data collection on 1/2/2015.

A total of 39 males and 33 females were included in this study with a median age at diagnosis of 65 years (range of 34-84 years). Sixty-one samples were identified as pancreatic ductal adenocarcinoma, and 11 samples were confirmed as ampullary adenocarcinoma. Forty-five samples were biopsy specimens, whereas the other 27 were from resection. Furthermore, 20 patients had metastatic disease at the time of diagnosis. The R-status was defined in the patients that had surgical resection as: R0=10, R1=15 and R2=2. Twenty of the 27 patients (74%) who had undergone resection developed recurrent disease during the follow-up period. The median time to recurrence was 9.6 months (range of 0.3-27.1 months).

Sixty-six patients had died, 64 from terminal-stage disease, and two from pulmonary emboli. The median survival of the patients who had died was 8.8 months (ranging from 0.8 to 59.7 months) and the median follow-up of the remaining seven patients who were alive was 50.9 months (range of 27.5.1-73.2 months). Ethics committee approval was obtained from the Central London REC 3 Research Ethics Committee to perform immunohistochemistry on stored biopsy and resection specimens linked with a clinical database, with the need for consent waived (REC reference 06/Q0512/106, amendment date 30 July 2010). All patient samples were anonymised and de-identified prior to analysis.

2.1.2.2: Pancreatic cysts and normal pancreatic tissue:

A set of 72 patients with pancreatic cysts and normal pancreatic tissue were identified from a search of the histology database of the Royal Free and University College Hospital. Due to lack of clinical data, 8 patients were excluded from the study. In total, 64 patients were included in the study and all these patients had undergone surgical resection for pancreatic cysts or a benign condition during 2006 to 2012. The patients were followed up for at least one year after surgery to ensure that they did not develop pancreatic cancer. Forty-nine patients were diagnosed with pancreatic cysts (19 IPMN, 14 SCA, 7 MCN, 2 SPPT and 7 pseudo-cysts), eleven patients had chronic pancreatitis and four patients were found to have normal histology (Table 2.1). All H&E-stained slides were reviewed by an experienced histopathologist, and diagnosis was reconfirmed.

Table 2.1: Summary of clinicopathological characteristics of patients with pancreatic cancer, pancreatic cysts, pancreatitis and controls.

Variables	Pancreatic Ductal Adenocarcinoma (n=61) % (*n*)	Ampullary Adenocarcinoma (n=11) % (*n*)	Pancreatic Cystic Tumour (n=42) %(*n*)	Chronic Pancreatitis (n=11) % (*n*)	Pseudocyst (n=7) %(*n*)	Normal Pancreas (n=4) %(*n*)	Total (n=136) % (*n*)
Sex							
Male	59% (36)	27% (3)	33.4% (14)	55.5% (7)	71.4% (5)	50% (2)	49.3% (67)
Female	41% (25)	73% (8)	66.6% (28)	44.5% (4)	28.6% (2)	50% (2)	50.7% (69)
Age at Diagnosis (years)							
Median (Range)	63 (34-84)	67 (36-78)	62 (17-83)	54 (34-82)	48 (30-54)	80 (32-83)	62 (17-84)
Histological Samples							
Biopsy	74% (45)	0.0% (0)	0.0% (0)	0.0% (0)	0.0% (0)	0.0% (0)	33% (45)
Resected samples	26% (16)	100% (11)	100% (42)	100% (11)	100% (7)	100% (4)	67% (91)
Tumour Differentiation							
Well	1.65 % (1)	9% (1)	---	---	---	---	2.7% (2)
Well/Mod	0.0 % (0)	9% (1)	---	---	---	---	1.3% (1)
Moderate	14.75 % (9)	54.6% (6)	---	---	---	---	21% (15)
Mod/Poor	65.6% (40)	27.3% (3)	---	---	---	---	60% (43)
Poor	18% (11)	0.0% (0)	---	---	---	---	15% (11)
Survival status							
Alive at last contact	1.6% (1)	45.5% (5)	95.2% (40)	100% (11)	100% (7)	100% (4)	50% (68)
Dead	98.4% (60)	54.5% (6)	4.8% (2)	0.0% (0)	0.0% (0)	0.0% (0)	50% (68)
Median Survival (Months)	8.5 (95% CI: 7.7-13.1)	29.5 (95% CI: 23-49.9)	---	---	---	---	9.3 (95% CI: 10.8 -18.2)
Metastasis Status							
Patients with metastasis	32.8 % (20)	0.0% (0)	---	---	---	---	27.8% (20)
Patients without metastasis	67.2% (41)	100% (11)	---	---	---	---	72.2% (52)
Lymph Node Involvement							
Positive lymph node	18% (11)	45.5% (5)	---	---	---	---	22.2% (16)
Negative lymph node	8.3% (5)	54.5% (6)	---	---	---	---	15.3% (11)
Unknown	73.7% (45)	0.0% (0)	---	---	---	---	62.5% (45)
Clinical T-Stage Classification							
T1	0.0% (0)	0.0% (0)	---	---	---	---	0.0% (0)
T2	0.0% (0)	63.6% (7)	---	---	---	---	9.7% (7)
T3	18% (11)	0.0% (0)	---	---	---	---	15.3% (11)
T4	8.3% (5)	36.4% (4)	---	---	---	---	12.5% (9)
Unknown	73.7% (45)	0.0% (0)	---	---	---	---	62.5% (45)
Staging							
Stage I	0.0% (0)	27.3% (3)	---	---	---	---	4.2% (3)
Stage II	14.75% (9)	36.4% (4)	---	---	---	---	18% (13)
Stage III	8.2% (5)	36.4% (4)	---	---	---	---	12.5% (9)
Stage IV	3.3% (2)	0.0% (0)	---	---	---	---	2.8% (2)
Unknown	73.75% (45)	0.0% (0)	---	---	---	---	62.5% (45)

2.1.2.3: Tissue microarrays (TMAs):

Commercially available tissue microarrays (TMAs) were purchased as paraffin embedded sections (TMA 1 and 2, AccuMaxArray, ISU ABXIS CO., LTD, USA, A207V and A307 (II), TMA 3, Insight Biotechnology Limited, UK, BIC14011). TMA tissue sections were stained with anti-PKM2 and anti-LDHA antibodies by immunohistochemistry as described in **2.1.3.1**. A total of 206 tissue cores from 130 patients were presented in the TMAs, which included 63 cases of pancreatic ductal adenocarcinoma in duplicate, 19 pancreatic intraepithelial neoplasia (10 PanIN-1, 7 PanIN-2 and 2 PanIN-3), 10 chronic pancreatitis and 38 normal pancreatic tissue cores. Histology was verified by H&E staining. There were 83 male and 47 female patients with a median age of 59 (range of 32-80 years). The clinical data that was provided included tumour size, stage, degree of tumour differentiation, lymph node involvement, metastatic status and tumour sites. Table 2.2 describes the clinicopathological characteristics of the patients.

2.1.2.4: Plasma samples:

Plasma samples from 51 patients with pancreatic cancer and 20 healthy individuals were obtained. Following the confirmation of cancer diagnosis by an experienced histopathologist, blood samples were obtained during treatment from patients at the Royal Free Hospital, University College Hospital (UCL, London, UK), and Charing Cross Hospital (IC, London, UK). Blood samples were collected in heparinised tubes, which were then centrifuged at 10,000 rpm for 15 minute at 4^{O}C, the plasma carefully separated and collected in new tubes and stored in -80C for later analysis. Patient information included age (median =68, range 41-94 years), gender (27 male and 24 female), histological stage of pancreatic cancer (Stage I=1, Stage II=7, Stage III=13, Stage IV=20, NA=10) and whether chemotherapy was given. The study was approved by the Central London REC 3 Research Ethics Committee, and all patients had given written informed consent. The trial was conducted in accordance with the Declaration of Helsinki.

Table 2.2: Summary of clinical data of pancreatic cancer tissue microarray.

Variables	Pancreatic Adenocarcinoma (n =63) *n* (%)	PanIN (*n* =19) % (*n*)	Chronic Pancreatitis (*n* = 10) % (*n*)	Non-neoplastic (*n* =38) % (*n*)	Total (*n* = 130) % (*n*)
Sex					
Male	60.3% (38)	68.4% (13)	60% (6)	68.4% (26)	63.8% (83)
Female	39.7% (25)	31.6% (6)	40% (4)	31.6% (12)	36.2% (47)
Age					
Median (Range)	61 (32-80)	51 (33-76)	54 (33-67)	61 (38-73)	59 (32-80)
Tumour Differentiation					
Well	3.2% (2)	---	---	---	3.2% (2)
Moderately	63.5% (40)	---	---	---	63.5% (40)
Poorly	27% (17)	---	---	---	27% (17)
Mucinous	3.2% (2)	---	---	---	3.2% (2)
Undifferentiated	1.6% (1)	---	---	---	1.6% (1)
Unknown	1.6% (1)	---	---	---	1.6% (1)
Lymph Node Involvement					
Positive lymph node	54% (34)	---	---	---	54% (34)
Negative lymph node	46% (29)	---	---	---	46% (29)
Metastasis Status					
Patients with metastasis	1.6% (1)	---	---	---	1.6% (1)
Patients without metastasis	98.4% (62)	---	---	---	98.4% (62)
Clinical T-Stage Classification					
T1	1.6% (1)	---	---	---	1.6% (1)
T2	9.5% (6)	---	---	---	9.5% (6)
T3	81% (51)	---	---	---	81% (51)
T4	7.9% (5)	---	---	---	7.9% (5)
Staging					
Stage I	6.3% (4)	---	---	---	6.3% (4)
Stage II	84.1% (53)	---	---	---	84.1% (53)
Stage III	8% (5)	---	---	---	8% (5)
Stage IV	1.6% (1)	---	---	---	1.6% (1)
Tumour Size (cm)					
≤ 2.5	36.7% (22)	---	---	---	36.7% (22)
2.6-3.9	45% (27)	---	---	---	45% (27)
≥ 4	18.3% (11)	---	---	---	18.3% (11)
Tumour Site					
Head	66.6% (42)	---	---	---	66.6% (42)
Body	16% (10)	---	---	---	16% (10)
Tail	12.7% (8)	---	---	---	12.7% (8)
Unknown	4.7% (3)	---	---	---	4.7% (3)

Protocol:

2.1.2.5: Single staining:

The expression of PKM2, LDHA, CD8 and Ki-67 in specimens was evaluated by standard immunohistochemistry. Paraffin embedded tissue sections were warmed in a heated oven for 30 minutes at 60℃ (Memmert, Beschickung-loading model 100-800, Germany), then the samples were deparaffinised in xylene and hydrated through a series of graded ethanol (70%-95%). Tissue sections were subjected to a heat mediated antigen retrieval method by using an autoclave (Autoclave medical device, Prestige Medical Limited, Blackburn, England). After cooling to room temperature and rinsing in phosphate buffered saline (PBS), endogenous peroxidase activity was inhibited by incubation with 3% hydrogen peroxide for 20 minutes. The sections were washed in PBS and then incubated with 2.5% normal horse blocking serum (Ready-to-use normal horse serum blocking solution, ImmPRESSTM UNIVERSAL KIT, Vector Laboratories, UK, Cat# MP-7500) for 20 minutes at room temperature. The sections were then incubated with primary antibody (for one hour at room temperature for both CD8 and Ki-67, overnight at 4℃ for PKM2, LDHA) at a dilution of 1/200 for CD8, 1/300 for Ki-67, 1/100 for PKM2 and 1/250 for LDHA in PBS. After three washes with PBST (PBS-T, 0.05% Tween-20 in 1 × PBS), the sections were incubated with horseradish peroxidase (HRP) - conjugated secondary antibody (ImmPRESSTM UNIVERSAL anti-mouse/rabbit IgG Reagent, ImmPRESSTM UNIVERSAL KIT, Vector Laboratories, UK, Cat# MP-7500) for 30 minutes. The sections were washed thrice with PBST and the primary antibody was detected using the DAB detection system kit (Dako RealTM EnVisionTM Detection System, Peroxidase/DAB+, Rabbit/Mouse, UK, Cat# K5007). The sections were placed in a haematoxylin solution for 3 minutes, then gently washed in running water to remove excess haematoxylin, and then mounted with aqueous mounting media.

2.1.2.6: Double staining:

The expression of PKM2/CD8 and PKM2/Ki-67 in pancreatic cancer tissue sections were evaluated by using a double immunohistochemical staining kit (ImmPRESSTM Universal Reagent, Anti-Mouse/Rabbit IgG, Vector Laboratories, Cat# MP-7500). The deparaffinisation, rehydration, antigen retrieval and peroxidase quenching steps were carried out as described above for the single staining section method. Sections were then incubated for 20 minutes with 2.5% normal horse blocking serum, followed by the first primary antibody (monoclonal mouse anti-human and rat pyruvate kinase type M2 (M2-PK), DF-4, ScheBO®Biotech, Germany, Cat# S-1) at a dilution of 1/100 in PBS overnight at 4℃. After three washes with PBST, the sections were incubated with horseradish peroxidase (HRP) - conjugated secondary antibody for 30 minutes. The sections were then washed thrice with PBST and the primary antibody was detected using the DAB detection system kit. After that the sections were washed with PBS and incubated for 20 minutes with blocking solution (ready to use blocking solution Reagent 1, PicTure^{TM} double staining kit, Invitrogen, UK, Cat# 87-9999), followed by incubation with the next primary antibody [either CD8 (CD8A Rabbit polyclonal antibody, Abnova , UK , Cat# PAB11235) or Ki-67 (Rabbit polyclonal to Ki-67 - Proliferation Marker, Abcam, UK, Cat# ab15580)] at a dilution of 1/200 for CD8 and 1/300 for Ki-67 in PBS for 1 hour. The sections were then washed thrice with PBST and incubated for 30 minutes with the secondary antibody for the second primary antibody (ready-to-use Gt anti-Rabbit IgG-alkaline phosphatase (AP) polymer conjugate, PicTureTM double staining kit, Invitrogen, UK, Cat# 87-9999). After washing thrice with TBST the second primary antibody was visualized using fast-red chromogen detection system kit (fast-red chromogen tablets, reagent 5B, and ready-to-use alkaline phosphatase substrate/buffer, Reagent 5A, PicTureTM double staining kit, Invitrogen, Cat# 87- 9999). The sections were placed in a haematoxylin solution for 3 minutes, followed by a gentle wash in running tap water to remove excess haematoxylin, and then mounted with aqueous mounting media.

In this study, two different systems of substrate/chromogen/enzyme were used; DAB chromogen system produced brown colour (PKM2) with immunoglobulin G (IgG)-horseradish peroxidase, and fast red chromogen system with immunoglobulin G (IgG)-alkaline phosphatase produced red colour (CD8 or Ki-67).

Errors can occur in any steps of the immunohistochemistry, especially in concentration of antibodies and time of interaction of antibodies and tissue sections. In our experiment, I minimised those errors by optimisation of antibody concentration and interaction times before starting the experiments.

2.1.3: Evaluation of immunohistochemical staining:

2.1.3.1: Evaluation of PKM2:

Immunohistochemical staining was evaluated using a light microscope (AXIO Scope, Carl Zeiss Micro-Imaging GmbH, Gottingen, Germany). The assessment of the immunostained slides was done independently by two observers and any disparity between the results resolved by using a conference microscope. A comprehensive scoring formula was used for the semi-quantitative evaluation of PKM2 expression as described previously (168). The PKM2 and LDHA staining score is explained in the following table (Table 2.3). The intensity of staining was scored as: 1, weak expression; 2, moderate expression; or 3, strong expression and the extent of staining scored as 1, <33% of tumour cells stained positive; 2, 33% to 67% of tumour cells stained positive or; 3, >67% tumour cells stained positive. The intensity and the extent scores were then multiplied to obtain a single scale of score of 1, 2, 3, 4, 6, and 9. Scores of 1, 2 and 3 were defined as a weak (or negative) staining, whereas scores 4, 6 and 9 were considered as strong (or positive) staining.

Table 2.3: Evaluation of PKM2 and LDHA stained according to the intensity and extent.

Degrees of	Intensity of PKM2 staining	Extend of PKM2 staining
0	No expression	0
1	Weak expression	Less than 33%
2	Moderate expression	33% to 67%
3	Strong expression	More than 67%

2.1.3.2: Evaluation of CD8+ TILs and Ki-67 proliferation marker:

The number of CD8+ TILs and the number of cells which stained positively for Ki-67 was determined independently by two observers. Initially, the entire tumour section was scanned at low magnification (x100) to identify the region with highest density of CD8+/Ki-67 cells and then five random areas within that region were counted at high magnification (x400). The average number of CD8+ TILs was calculated and expressed as count per high power field (HPF). The cell proliferation index (PI) was expressed as a percentage of positive-stained nuclei for Ki-67 among 1000 tumour cells using a standardised grid.

Potential errors can occur during observation and assessment of stained tissue sections and counting of nuclear staining. To avoid bias and minimize error, assessment was done independently and blindly to the patient's status by two observers and any differences between the results resolved by conference microscope.

2.2: Western blot analysis:

2.2.1: Principle:

Western blot or immunoblotting is a widely used analytical technique for the detection of specific proteins in a mixture of extracted proteins or homogenated tissues. This method is based on the separation of proteins according to the electric charge, isoelectric point, molecular weight or a combination of them, through gel electrophoresis. Negatively charged, low molecular weight, denatured proteins

migrate faster through the polyacrylamide gel than high molecular weight proteins (169,170). Separated proteins on the gel are transferred to a membrane (either nitrocellulose or Polyvinylidene difluoride (PVDF)), and then the target protein is stained with a specific antibody. The detection of the target protein takes place either in one step or in two steps. In the one step process, the target protein is stained with a labelled primary antibody. Whereas, in the two step method, the target protein is exposed to the unlabelled primary antibody, then a secondary labelled antibody binds to the primary antibody (169–171). The most commonly used conjugations are biotin or enzyme such as horseradish peroxidase or alkaline phosphatase. The two-step process is more commonly used due to higher sensitivity of antigen-antibody reaction (see figure 2.2) (169,170).

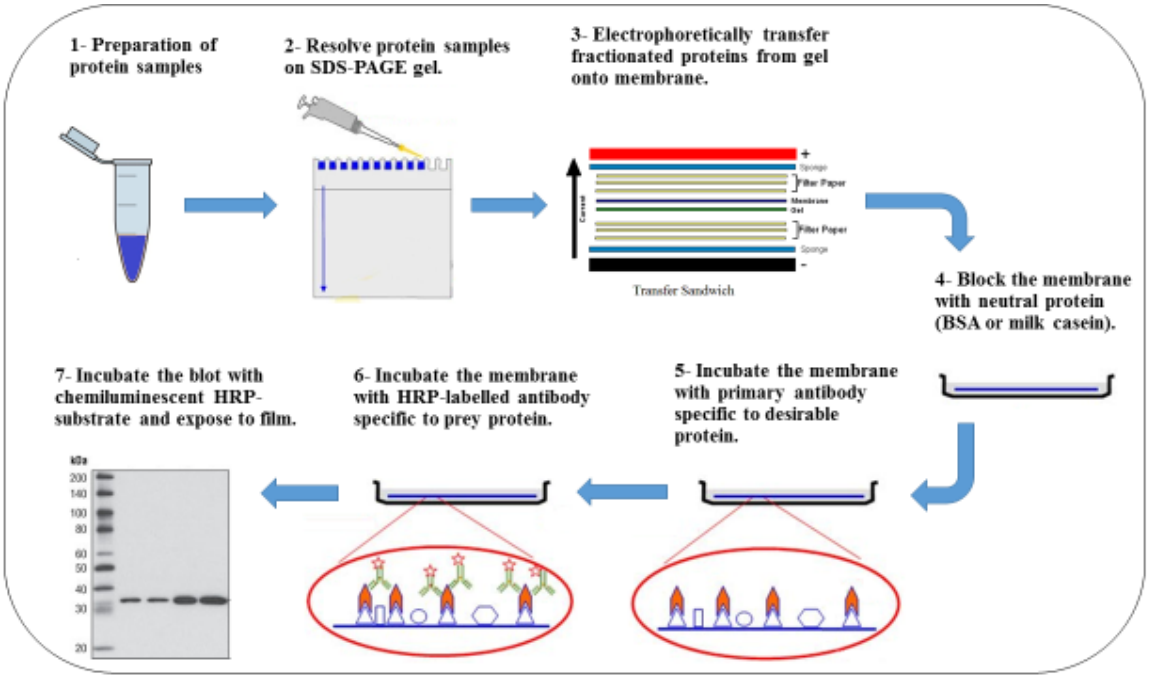

Figure 2.2: Basic principle of western blot.

2.2.2: Method:

2.2.2.1: Cell lines:

Human pancreatic cancer cell lines were purchased either from RIKEN BioResource Center (RIKEN BRC, Tsukuba, Japan) or PerknElmer (Caliper LifeSciences, Hopkinton, MA, USA). MIApaca-2, PANC-1, PK-1, PK-59, PK-45H, PK45P, KP-4, KLM-1, NOR-P1 cell lines were purchased from RIKEN BioResource Center, however, BxPc-3^{Luc2} cell line was purchased from Caliper LifeSciences, PerkinElmer LTD. The BxPc-3^{Luc2} Bioware Ultra-Light Producing Cell Line is a luciferase expressing cell line, stably transfected with the firefly luciferase gene (luc2). The cell line was established by transducing lentivirus-containing luciferase 2 gene under the control of the human ubiquitin C promoter. PANC-1, PK-1, PK-59, PK-45H, PK45P, KLM-1, NOR-P1 and BxPc-3 were maintained in RPMI-1640 supplemented with 10% FBS, 1% penicillin/streptomycin and 2mM glutamine (Gibco, Life technologies, UK). Miapaca-2 was maintained in DMED and KP-4 in DMEM/F12 media. All media were supplemented with 10% FBS, 1% penicillin/streptomycin and 2mM glutamine. Cells were maintained in a humidified atmosphere of 21% O2, 5% CO2 at 37 °C (Binder incubator, Germany, Serial# 10-09701) and harvested with trypsin-EDTA.

2.2.2.2: Cell culture:

All pancreatic cancer cell lines were maintained in cell culture media supplemented with 10% FBS, 1% penicillin/streptomycin and 2mM glutamine and maintained in a humidified atmosphere of 21% O2, 5% CO2 at 37 °C until reach approximately 80% confluent, then the cells subcultured for the next experiment. Cell culture media was changed, with a pre-warmed solution, every 2-3 days. Adherent cells were washed twice with PBS then detached using 0.25% Trypsin-EDTA and then the cells were counted under a microscope (Primo Vert, Carl Zeiss Ltd, Gottingen, Germany) by using disposal haemocytometer (C-Chip, Disposable Haemocytometer, Digital Bio, Korea). For each experiment, approximately one million cells were plated in 75 cm2 flasks and cultured for 48 hours (proliferation phase) and 120 hours (confluent phase).

Adherent cells were washed twice with cold PBS, and scraped with rubber policeman cell scraper in 10ml cold PBS. Cells were then centrifuged at 3000 rpm in a pre-cooled centrifuge (4℃) for 5 minutes (Eppendorf Centrifuge 5810R, Hamburg, Germany) and pelleted. The cell pellets were then directly used for isolation and extraction of proteins. To avoid and minimize a potential errors, all experiments were done in duplicate.

2.2.2.3: Preparation of total cell protein extracts:

Cell pellets were re-suspended in complete lysis buffer [lysis buffer (M-PER® Mammalian Protein Extraction Reagent, Thermo Scientific, Cat# 78501) + Protease Inhibitors Cocktail (Thermo Scientific, Cat# 87785)]. The solution was placed on a shaker for 10-15 minutes (Stuart gyro-rocker, BIBBY Sterilin LTD, UK, Cat# SSL3), then transferred to micro-centrifuge tubes. Samples were centrifuged at 14000 rpm for 15 minutes at 4℃ (Centrifuge, Thermo Fisher Scientific, Thermo electron LED GmbH LR56495, Germany), and then transferred the supernatant to new tubes for analysis. To minimize any error occurring during experiments, each sample was analysed in duplicate and the experiments were also done in duplicate.

2.2.2.4: Total protein assay:

The total protein concentration of samples was measured by using micro BCA protein assay kit (Micro BCA™ Protein Assay Kit, Thermo Scientific, USA, Cat # 23235). As per manufacturer's protocol, preparation of working reagent was done by mixing 25 portions of the Micro BCA reagent MA and 24 portions of reagent MB with 1 portion of MC reagent. Albumin (BSA) standard was serially diluted using deionized water for preparation of a standard curve (0.5, 1, 2.5, 5, 10, 20, 40µg/ml). Samples were diluted 150, 200 and 300 times with deionized water. After that 150 µl of the samples, standards and a blank were pipetted into the 96 well plate in duplicates, then 150 µl of working solution was added into the wells. The plate was incubated at 37℃ for 2 hours, then the protein concentration was analysed according to the standard curve using MARS Data Analysis Software, FLUOstar Omega-BMG Labtech

microplate reader (FLUOstar Omega-BMG Labtech microplate reader, BMG Labtech GmbH, Allmendgruen 8, D-77799 Ortenberg, Germany). To avoid a potential errors, each sample was analysed in duplicate and experiments were also done in duplicate.

2.2.2.5: Western blot protocol:

- **Sample preparation:**

For 10 wells pre-cassette SDS-polyacrylamide gel, 15 µg of total protein in 20 µl solution was used per well. The samples were prepared by mixing the appropriate amount of protein solution with 2 µl of Sample Reducing Agent (10X), (Invitrogen, USA, Cat# NP0004), and 5 µl of LDS (lithium dodecyl sulphate) sample loading buffer (4X), (Invitrogen, USA, Cat# NP0007) and the solution was then adjusted to 20 µl by adding molecular grade water.

- **Gel electrophoresis:**

The protein solution was denatured at 70℃ for 10 minutes; followed by brief centrifugation of the mixture. For gel electrophoresis, NuPAGE 4-12% Bis-Tris gel 1.0 mm, 10 well gels (Life technologies, USA, REF# NP0321BOX) precast gels were used with MOPS SDS Running Buffer (20X),(Life technologies, USA, Cat# NP0001). Samples were loaded along with a protein ladder (Novex® Sharp pre-stained protein standards, Life technologies, USA, Cat# 57318) and then run at 200 V for approximately 1 hour (until the marker reached the bottom of the gel).

- **Transferring proteins to PVDF membrane:**

Polyvinylidene fluoride (PVDF) membranes (InvitrolonTM PVDF Filter Paper Sandwich, 0.45µm Pore Size, Invitrogen, USA, Cat# LC2005) were activated by rinsing in absolute methanol for 1- 2 minutes, followed by washing twice with distilled water and then incubated in transfer buffer (NuPAGE® Transfer Buffer (20X), Invitrogen, USA, Cat# NP0006) for 30 minutes. Blotting pads were prepared by soaking in cold transfer buffer. Then the air bubbles were removed by squeezing the pads while they submerged in the buffer. Immediately after gel electrophoresis, the

proteins were transferred electronically from the gel to the polyvinylidene fluoride (PVDF) membrane by using the transfer sandwich system. The transfer sandwich system consists of blotting pads, filter paper; gel and PVDF membrane were assembled in an Xcell blot-Module as illustrated below.

The Xcell blot-Module was placed into the assembly tray of the western blot tank (Xcell SureLockTM , InvitrogenTM Novex Mini-Cell, USA). The blotting module was filled with transferring buffer solution, whereas the tank (outer of blotting module) was filled with water. Then the system was run at a constant voltage of 20 V for 1 hour.

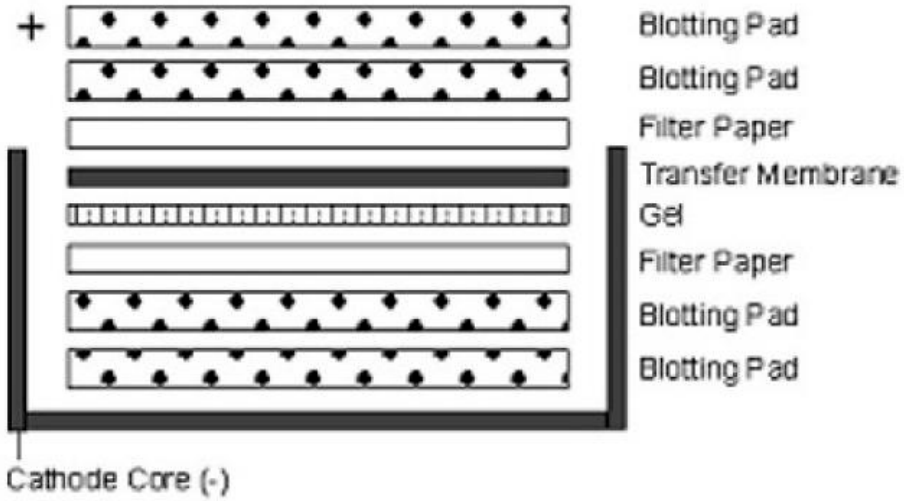

- **Blocking membrane:**

Following protein transfer, the PVDF membrane was rinsed in TBS (Tris Buffered Saline 10X, GBiosciences, USA, Cat# R030) and stained with Ponceau S solution (Sigma- Aldrich, St. Louis, MO, USA) to ensure successful transfer, washed 3 times with tap water before incubating in 10 ml blocking solution (5% Albumin from Bovine Serum BSA in TBST), (Albumin from bovine Serum BSA, Sigma, USA, Cat# A2153-100G) for 1 hour at room temperature to block the non-specific binding of the primary antibody.

- **Incubation with primary and secondary antibody:**

After the blocking process, the PVDF membrane was incubated overnight at 4℃ with 10 ml diluted primary antibody [mouse anti-PKM2 (DF-4, ScheBo®Biotech, Giessen, Germany) or rabbit anti-LDHA antibodies (Cell Signaling, UK)] 1:1000 in 5%BSA. The following day the PVDF membrane was washed twice with TBS-Tween 20 (TBS-T, 0.05% Tween-20 in 1 × TBS) and twice with a diluted blocking solution (diluted Blocking solution 1:1 with TBST) for 10 minutes each time. The membrane was then incubated with appropriate horseradish peroxidase (HRP) - conjugated secondary antibody (Anti-mouse IgG or anti-rabbit, HRP-linked Antibody, Cell Signaling Technology, UK) 1:2000 in 5%BSA for 1 hour. Anti- β actin antibody (Cell Signaling, UK) was used as a protein loading control.

- **Signal development:**

The PVDF membrane was then washed thrice with TBST for 5 minutes and thrice with TBS for 10 minutes. After washing, the chemiluminescent signal was developed by incubating the PVDF membrane with ECL chemiluminescent substrate (according to the manufacturer's instructions, the ECL substrate working solution was prepared by mixing equal parts of the stable peroxidase with luminal/enhancer solution), (Thermo Scientific, USA) for 5 minutes at room temperature. The developed chemiluminescent signal was detected and the intensity of the bands were measured (FlourChem E digital dark room, Cell Biosciences, Inc. Santa Clara, CA, USA). The intensity of the PKM2 and LDHA bands in the different pancreatic cancer cell lines were normalized with the intensity of the loading control.

The error can occur in any steps of western blot experiment, to avoid any error, all the experiments were done in duplicate.

2.3: Immunocytochemistry:

The Miapaca-2 cell line was immunocytochemically stained with anti-PKM2 or anti-LDHA antibodies. Briefly, $25x10^4$ Miapaca-2 cells were seeded in sterilized 2-well cell culture chamber slide (Fisher Scientific, UK) and left to grow for 24 hours. Cells were washed with cold PBS, and fixed with cold absolute methanol for 15 minutes, and then permeabilized in 0.25% triton X-100 in PBS. Cells were then blocked with 3% BSA for 1 hour at room temperature, following by an overnight incubation at 4°C with a primary antibodies specific for PKM2 (1:100 dilution, DF-4, ScheBo®Biotech, Giessen, Germany) or LDHA (1:250 dilution, Cell Signaling, UK). Cells were further incubated with appropriate secondary antibodies and antigen-antibody reaction was visualized using the DAB detection system kit. Cells were incubated in a haematoxylin solution for 1 minute, followed by a gentle wash in running water to remove excess haematoxylin, and then mounted with aqueous mounting media. All experiments were done in duplicate.

2.4: MTS Assay:

The effect of single and combination treatment was evaluated in the pancreatic cancer cell lines by the MTS assay. Briefly, 3000 cells were plated per well in 96-well plates and incubated overnight. LDHA inhibitor (FX11, Toronto Research Chemicals Inc., North York, Ontario, Canada), PKM2 activators [PKM2 activator III and IV (TEPP-46), Cayman Chemical, Ann Arbor, MI, USA) or inhibitor (Shikonin, Calbiochem, Merck Millipore, UK) were added alone or in combination for 24, 48, 72 and 96 hours. After an indicated time points, 20µl of MTS tetrazolium compound [3-(4, 5–dimethythiazol-2-yl)] -5-(3-carboxymethoxyphenyl)-2-(4-sulfophenyl)-2H-tetrazolium) was added to each well in 100µl of fresh culture medium and plates were incubated at 37ºC for 1 hour. Absorbance of formazan was measured at 490 nm to measure the percentage of viable cells. The IC_{50}, AC_{50} and combination index (CI) of the different treatment regimens calculated using Origin or CompuSyn software from the dose-response curves.

To avoid and minimize any error occurring during experiments, each sample was analysed in duplicate and the experiments were also done in duplicate.

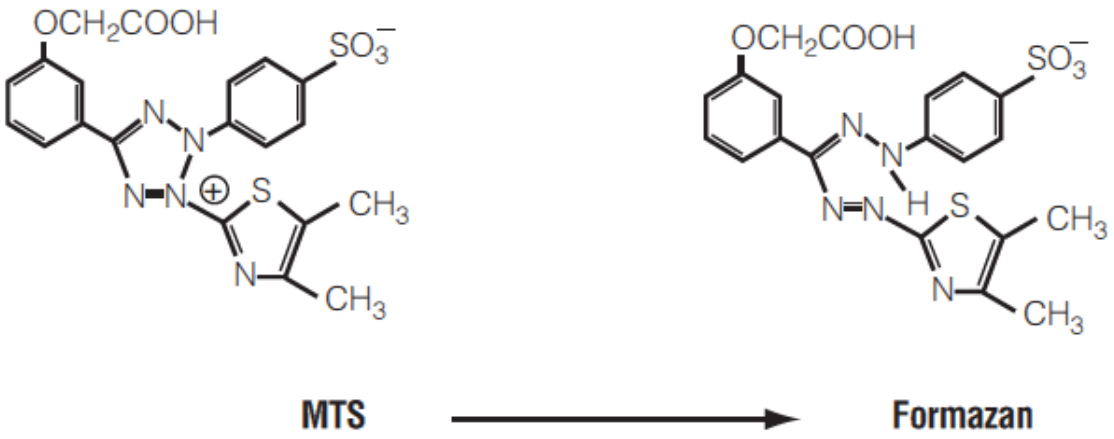

Figure 2.3: Structure of MTS tetrazolium and its formazan product.

2.5: Staining cells with haematoxylin:

After measuring cytotoxicity of the single-agent and combination treatment by the MTS assay, pancreatic cancer cell lines were stained with haematoxylin. Briefly, cell culture media was aspirated and cells were washed twice in cold PBS. The cells were then fixed with ice-cold absolute methanol for 15 minutes and permeabilized with 0.25% triton X-100 in PBS for 10 minutes at room temperature. Cells were then washed twice in 0.25% triton X-100 in PBS and incubated for 1 minute with haematoxylin. Cells were then washed in a running tap water to remove excess haematoxylin and left to dry and then captured using a light microscope. All experiments were done in duplicate.

2.6: Animal Experiments:

All animal experiments were carried out in the Comparative Biology Unit (CBU), School of medicine, Royal Free campus, University College London. Sixty-five, 4-6 week-old male nude mice (weighing approximately 25g) were purchased from Charles River Ltd (Charles River UK Ltd., Margate, Kent, UK), and maintained on a standard diet, at a temperature of 19–23°C, and humidity of approximately 50%. All animal experiments were conducted according to Home Office guidelines under the Animals in Scientific Procedures Act 1986.

2.6.1: Subcutaneous tumour implantation:

The human pancreatic cancer cell lines, Miapaca-2 and BxPc-3^{Luc2} were used to generate subcutaneous xenografts in nude mice. Briefly, $6x10^6$ cells of Miapaca-2 or BxPc-3^{Luc2} were injected subcutaneously into the right flank of mice, using 27-gage needle (figure 2.4 A). Xenografts generated by the Miapapca-2 cell line were allowed to grow for two weeks and then mice were randomly divided into the following four groups (n=5 per group): 1) untreated control, 2) high combination treated, 3) low combination treated, and 4) LDHA inhibitor (FX11) treated groups. A second experiment used the BxPc-3^{Luc2} cell to generate subcutaneous xenografts. Four days post tumour cell inoculation, mice were randomly divided into following five groups (n=6 per group) : 1) untreated control, 2) high combination treated, 3) low combination treated, 4) single FX11 treated and 5) single PKM2 activator IV (TEPP-46) treated groups.

Body weight and tumour volume were measured thrice a week. Tumour volumes were measured using a digital Caliper and calculated using the following formula: [Tumour Volume = length (mm) x width (mm) x width (mm) x 0.52].

2.6.2: Orthotopic tumour model generation:

Twelve 4-6 week-old male nude mice underwent an established surgical method for orthotopic injection of human pancreatic cancer cells into the pancreas. The implantation was carried out under sterile conditions. Mice were anaesthetised under

2-3% isoflurane gas, the abdominal was cleaned with iodine solution, and an incision was made in the abdominal cavity off the midline and directly above the pancreas to allow visualization of the pancreas. Then the pancreas was gently retracted and positioned to allow for direct injection of $6x10^6$ BxPc-3^{Luc2} cells in 50µl PBS mixed with 50µl matrigel using a 27-gage needle (figure 2.4 B). Successful delivery of cells into the pancreas was observed under magnification using a dissection microscope (Leica Wild M691, Wetzlar, Germany). The pancreas was then placed back within the abdominal cavity and both the muscle and skin layers sutured (figure 2.4 B). Following recovery from surgery, mice were monitored and weighed thrice a week.

Figure 2.4: Development of pancreatic cancer xenograft tumour model. **A)** Subcutaneous xenograft tumour model. **B)** Orthotopic xenograft tumour model.

2.6.3: Staining of Miapaca-2 cell line with DiR fluorescent dye:

Miapaca-2 cells were trypsinised in 0.25% Trypsin-EDTA and counted. The cell solution was centrifuged at 1100 rpm for 5 minutes at 4°C and the pellet resuspended in 50ml PBS containing 10µM DiR fluorescent dye (XenoLight DiR, Perkin Elmer, USA, Cat# 125964). The cell solution was then incubated in 21% O2, 5% CO2 at 37 °C incubator for 20 minutes. Cells were re-counted and re-suspended in cold PBS at a concentration of $6x10^7$cells/ml. Subcutaneous or orthotopic xenografts were generated

using $6x10^6$ cells. The fluorescence signal was detected at the beginning and the end of the experiment by using IVIS instrument.

2.6.4: Drug preparation and treatment regimen:

PKM2 activator IV (TEPP46, 6-[(3-aminophenyl)methyl]-4,6-dihydro-4-methyl-2-(methylsulfinyl)-5H-thieno[2',3':4,5]pyrrolo[2,3-d]pyridazin-5-one) and LDHA inhibitor (FX11, 2,3-Dihydroxy-6-methyl-7-(phenylmethyl)-4-propyl-1-naphthalenecarboxylic Acid) were dissolved and prepared in 40% (2-hydroxypropyl) beta-cyclodextrin solvent. The desired dose of single or combination treatment were freshly prepared and injected intraperitoneally on a daily basis for three weeks. In the first animal experiment, the untreated (control) animals were injected with 100µl vehicle [40% (2-hydroxypropyl) beta-cyclodextrin] and in the high combination treated group, mice were injected with a 100µl solution of PKM2 activator IV (TEPP-46) and LDHA inhibitor (FX11) at a concentration of 25mg/kg and 2mg/kg, respectively. Mice in the low combination treated group were administered at a concentration of 13mg/kg and 1mg/kg for TEPP-46 and FX11, respectively. In the single LDHA inhibitor treated group, mice administered with FX11 at concentration of 2mg/kg FX11. Osmotic pumps (Alzet micro-osmotic pump, model 1004, Cupertino, CA, USA) were used for administered of low combination and single FX11 treated mice group and implanted intraperitoneally. The osmotic pump had a reservoir volume of 100 µl and delivered drug solution at a rate of 0.11 µl/hr. over 28 days. Pumps were filled with 100 µl of FX11 and TEPP-46 (1.9 mg/100µl and 23.5 mg/100µl, respectively) or with 100µl of FX11 (1.9 mg) for the low combination and the single LDHA inhibitor treated groups, respectively.

In the second animal experiment: the control group animals were injected daily with 100µl vehicle [40% (2-hydroxypropyl) beta-cyclodextrin], the high combination treated group received daily injections of 100µl TEPP-46 and FX11 at a concentration of 30mg/kg and 2.1mg/kg, respectively. Animal from the low combination treated group received daily injections of 100µl TEPP-46 and FX11 at a concentration of 15mg/kg and 1.05mg/kg, respectively. The single LDHA inhibitor treated group

received daily injection of 100µl FX11 at a concentration of 2.1mg/kg and the single PKM2 activator IV treated group received daily injections of 100µl TEPP-46 at a concentration of 30mg/kg.

Therapy was administered for three weeks; body weight and tumour volume were measured thrice a week using digital Caliper and calculated using the following formula: [Tumour Volume = length (mm) x width (mm) x width (mm) x 0.52].

2.6.5: End of the experiment:

Following three weeks of treatment, mice were sacrificed approximately after one hour post the last injection; the tumours were harvested and blood samples were collected by heart puncture. Tumours were weighed and half were flash-frozen in liquid nitrogen and half were fixed in formalin. Blood samples were collected in heparinised polystyrene tubes and plasma was immediately separated by centrifuging samples at 10,000 rpm, for 15 minutes at 4◦C; plasma samples were stored in -80 for later analysis.

In animal studies, error can occur in several steps, especially during injection of cell lines, injection of drugs and measurement of tumour volume. To minimize errors, all animal experiments were done under supervision of an experienced project license holder. The animals were also randomly divided into the groups, blindly to the size of the tumour. All the animals were consistently treated with the drugs and the tumour volumes precisely measured by bioluminescence imaging as well as manually.

2.7: Bioluminescent imaging:

2.7.1: Imaging procedure:

Luciferin (VivoGlo™ Luciferin, *In Vivo* Grade, Promega UK Ltd, UK) was dissolved in PBS and a stock solution of 37.5mg/ml was prepared and sterilised. Mice were injected intra-peritoneally with 100µl (150 mg/kg) luciferin solution; 10 minutes later, mice were anaesthetised with 2-3% isoflurane gas. Mice were then transferred to the IVIS imaging chamber, and anaesthesia gas was reduced to 1.5%. Images were

acquired for 5 to10 minutes and in auto-exposure time with both small and medium binning.

2.7.2: *In vitro* Bioluminescent Assay:

BxPc-3^{Luc2} cells were washed with sterilised PBS, trypsinised and counted using trypan blue exclusive assay. Cells were re-suspended in fresh complete media and seeded in 12 well-plates at a concentration of 30,000 cell/well, and incubated overnight. LDHA inhibitor (FX11) and PKM2 activator IV (TEPP46) were added either alone or in combination to the cell cultures and incubated for 72 hours. All drugs were freshly prepared in complete media and the cell cultures were replaced each day with fresh drug solution. At the end of treatment, 150µg/ml D-Luciferin was added to each well and cells were imaged after 10 minutes with the IVIS machine.

2.8: Processing of tumour tissues:

Tumour samples were fixed in 10% formalin, processed with 70%, 80%, 95% and 100% ethanol, xylenes and paraffin in tissue processer (LEICA TP1020 tissue processor, Nussloch, Germany). Tumour tissues were embedded in paraffin, cut into 5 µm thick sections and mounted onto Superfrost plus glass slides (Fisher Scientific, Loughborough, UK). For histological analysis, slide sections were deparaffinised in xylene and hydrated through a series of graded ethanol (70%-95%) followed by routine H&E staining. The expression of PKM2, LDHA, CD8 and Ki-67 in tumour xenografts was evaluated by standard immunohistochemistry staining methods as described in **2.1.3.1** (single staining section).

2.9: Pyruvate kinase and Lactate dehydrogenase activity assay:

2.9.1: PK and LDH activity assay in tumour tissues:

Proteins from the tumour xenograft tissues were extracted by TissueLyser LT instrument (Qiagen, USA). Approximately 25mg of tumour tissue was homogenized and proteins extracted using TissueLyser LT for 5 minutes at 50 Hertz with one 5mm stainless steel bead. Proteins in the tumour tissues were extracted with 500µl of either pyruvate kinase or lactate dehydrogenase assay buffer. The tumour tissue lysate was

cleared by centrifugation at 13,000 rpm for 15 minutes at 4◦C, and protein concentration measured using BCA assay method. Pyruvate kinase and lactate dehydrogenase activity assays were performed using PK and LDH assay kits (BioVision Incorporated, Milpitas, CA, USA) as per manufacturer's instructions (as described in **2.9.3** and **2.9.4** sections) and activity was normalized to the total protein concentration.

2.9.2: PK and LDH activity assay in human pancreatic cancer cell line:

One million cells (Miapaca-2 or BxPc-3) were plated per well in 6-well tissue culture plates in DMEM or PRMI-1640 media and allowed to attach overnight. The following morning, media were replaced with medium containing a DMSO control or the indicated doses (5, 10, 25, 50, 100µM) of PKM2 activator IV (TEPP-46) or LDHA inhibitor (FX11) then the cells were incubated at 37°C for 6 hours. Following the incubation, cells were washed twice with cold PBS on ice, scraped into 200µl of cold pyruvate kinase or lactate dehydrogenase assay buffer and sonicated on ice for 4 cycles of 5 seconds with intervals of 20 seconds, using QSONICA sonicator (Qsonica LLC, Newtown, CT, USA). The sonicated cells were centrifuged at 13,000 rpm for 15 minutes at 4 °C, then the protein concentration quantified by a BCA assay kit. Pyruvate Kinase and Lactate Dehydrogenase activity was determined using PK and LDH activity assay kit as per manufacturer's instructions (as described in **2.9.3** and **2.9.4** sections) and normalized to the total protein concentration.

2.9.3: Pyruvate Kinase Assay:

Pyruvate kinase activity in plasma, cell lines and tumour tissue lysates was measured by a pyruvate kinase assay kit (BioVision, USA, Cat# K709-100). The kit consisted of PK assay buffer, OxiRed Probe, PK enzyme Mix, PK substrate Mix, PK positive control and pyruvate standard. All the reagents were prepared according to the manufacturer's instructions, stored at -20 ^{o}C and used within one week.

Standard curve: A stock solution of pyruvate standard was prepared by diluting 10µl pyruvate standard to 1ml pyruvate assay buffer to prepare 1nmol/µl of stock solution. A standard curve was prepared by 10 fold dilutions of pyruvate stock solution to obtain

0.1nmole/µl; the series pyruvate standard was then prepared by adding 0, 2, 4, 6, 8 and 10µl of pyruvate standard into 96-wells plates in duplicate to obtain 0, 0.2, 0.4, 0.6, 0.8 and 1nmole/well pyruvate standard solution. The volume was then adjusted to 50µl with PK buffer.

Sample preparation: Human and mouse plasma samples were directly added to the assay well plate following a 5-10 times dilution. Cells and tissues were extracted with pyruvate assay buffer as described above; 10µl of samples were added to the assay well plate and volume of the samples was adjusted to 50µl using pyruvate assay buffer.

Reaction Mix preparation: For each well, 50µl reaction mix was prepared by mixing 44µl of assay buffer, 2µl substrate mix, 2µl enzyme mix and 2µl OxiRed probe.

After preparing appropriate amount of reaction mix, 50µl of this solution was added into each well of samples, standards and control using 8 channel pipette, and mixed gently. The optical density was then measured at 570nm using FLUOstar Omega-BMG Labtech microplate reader (FLUOstar Omega-BMG Labtech microplate reader, BMG Labtech GmbH, Allmendgruen 8, D-77799 Ortenberg, Germany). The initial optical density (A_1) was measured after 2-3 minutes (T_1), and the plate was then incubated at 25℃ for 10-30 minutes (T_2) to measure the final optical density (A_2). The pyruvate kinase activity was calculated according to the below formula.

$$\text{PK activity} = \frac{B}{(T2 - T1) \times V} \times \text{Sample dilution factor} = \text{nmol/min /ml} = \text{mU/ml}$$

B: is the amount of pyruvate generated by PK $(\Delta A = A2 - A1)$ between T_1 and T_2 and measured on pyruvate standard curve.

T_1: is the time of the initial measurement (A_1) in minutes.

T_2: is the time of the final measurement (A_2) in minutes.

V: is the volume of the sample that added into the assay well in milliliter.

One unit of pyruvate kinase activity was defined as the amount of the PK enzyme that transferred a phosphate group from phosphoenolpyruvate to adenosine diphosphate to produce 1 µmole of pyruvate per minute at 25°C.

2.9.4: Lactate Dehydrogenase Assay:

Lactate dehydrogenase activity in plasma, cell lines and tumour tissue lysate was measured by a lactate dehydrogenase assay kit (BioVision, USA, Cat# K726-500). The assay kit consisted of LDH assay buffer, LDH substrate Mix, NADH standard and an LDH positive control. All reagents were prepared according to the manufacturer's instructions and stored at -20°C and used within two weeks.

NADH standard curve: A standard solution of NADH was prepared by dissolving NADH in 400µl deionized distilled water (ddH_2O) to obtain 1.25mM NADH solution. A standard curve was prepared by adding 0, 2, 4, 6, 8 and 10µl of NADH standard into 96-well plates in duplicate to obtain 0, 2.5, 5, 7.5, 10 and 12.5nmole/well NADH standard solution. The volume was then adjusted to 50µl with LDH buffer.

Sample preparation: Human and mouse plasma samples were directly added to the plate following a 5-10 time dilution; cells and tissues were extracted with LDH assay buffer as described above. Then 10µl of each sample was added into the assay well plate in duplicate and sample volume was adjusted to 50µl with LDH assay buffer.

Reaction Mix preparation: For each assay plate well, 50µl reaction mix was prepared by mixing 48µl of assay buffer with 2µl substrate mix solution.

After preparing appropriate amount of reaction mix, 50µl of this solution was added into each assay plate well containing the samples, standard and control using 8 channel pipette and mixed gently. Optical density was then measured at 450nm using an LT-4000 microplate reader (LT-4000 microplate reader, Labtech International Ltd, UK). The initial optical density (A_1) was measured after 2-3 minutes (T_1), and the plate was then incubated at 37℃ for 10-30 minutes (T_2) to measure the final optical density (A_2). The LDH activity was calculated according to the below formula.

$$\text{LDH activity} = \frac{B}{(T2 - T1) \times V} \times \text{Sample dilution factor} = \text{nmol/min /ml} = \text{mU/ml}$$

B: is the amount of the NADH generated by LDH $(\Delta A = A2 - A1)$ between T_1 and T_2 and measured on NADH standard curve.

T_1: is the time of the initial measurement (A_1) in minutes.

T_2: is the time of the final measurement (A_2) in minutes.

V: is the volume of the sample that added into the assay well in milliliter.

One unit of lactate dehydrogenase activity was defined as the amount of the LDH enzyme that produced 1 µmole of NADH per minute at 37°C.

To avoid and minimize any error occurring during measurement of PK and LDH activity, each sample was analysed in duplicate and all experiments were also done in duplicate.

2.10: Statistical analysis:

IBM SPSS Statistical software (Version 22, SPSS Inc., Chicago, IL, USA) was used for statistical tests, data analysis and graphics. The Kaplan-Meier method and log-rank test were used for analysis of survival time and to identify differences between the groups. One-way ANOVA or Kruskal Wallis test was used for comparison of multiple groups. Mann-Whitney U-test was used for a nonparametric test. Chi square test was used to identify differences between categorical data. Non-parametric correlation analyses between continuous variables were performed by Spearman test. A Cox proportional hazard regression model was used for univariate and multivariate analysis, and multivariate analysis was perform using backword, stepwise Cox regression model. The Origin software (OriginLab Corporation, Northampton, MA, USA) and CompuSyn software (ComboSyn, Inc., Paramus, NJ. USA) were used for drug dose response analysis and calculation of the dose effect curve, IC_{50}, AC_{50} and combination index (CI) of the drugs. All test results were two tailed, with effects summarized using 95% confidence intervals. Statistical significance was set at $p<0.05$.

CHAPTER 3: RESULTS

3.1: Pyruvate Kinase M2 and Lactate Dehydrogenase A are overexpressed in pancreatic cancer and correlate with poor outcome

3.1.1: RESULTS:

3.1.1.1: Expression of PKM2 and LDHA in pancreatic cancer:

Both PKM2 and LDHA were overexpressed in tumour cells compared with normal pancreatic tissue. A variable expression pattern of PKM2 was observed in tumour tissues, with relatively higher expression in less differentiated areas, in advancing margins of tumour nodules and in invasive (muscular and blood vessel) tumours (Figure 3.1A,B,E and F). Overall, PKM2 expression was predominantly associated with aggressive tumours. Preferential expression of PKM2 was observed in binucleated proliferating cells in tumour nodules (Figure 3.1D). Expression of PKM2 was noted in all cell compartments, including the cell membrane, cytoplasm and/or nucleus (Figure 3.1C and F). In contrast, LDHA expression was generally high in tumour as well as in preneoplastic tissues and pancreatitis without a specific pattern (Figure 3.2). LDHA expression was also detected in the cell membrane and/or cytoplasm and occasionally in the nucleus.

Similar expression of PKM2 and LDHA was observed in the UCLH cohort and TMA samples, with a staining score of > 3 in 64% and 73% of tumours, respectively, for PKM2, and in 76% of tumours for LDHA in both cohorts. In both cohorts, pancreatitis samples also highly expressed LDHA compared with PKM2 expression (Figure 3.3).

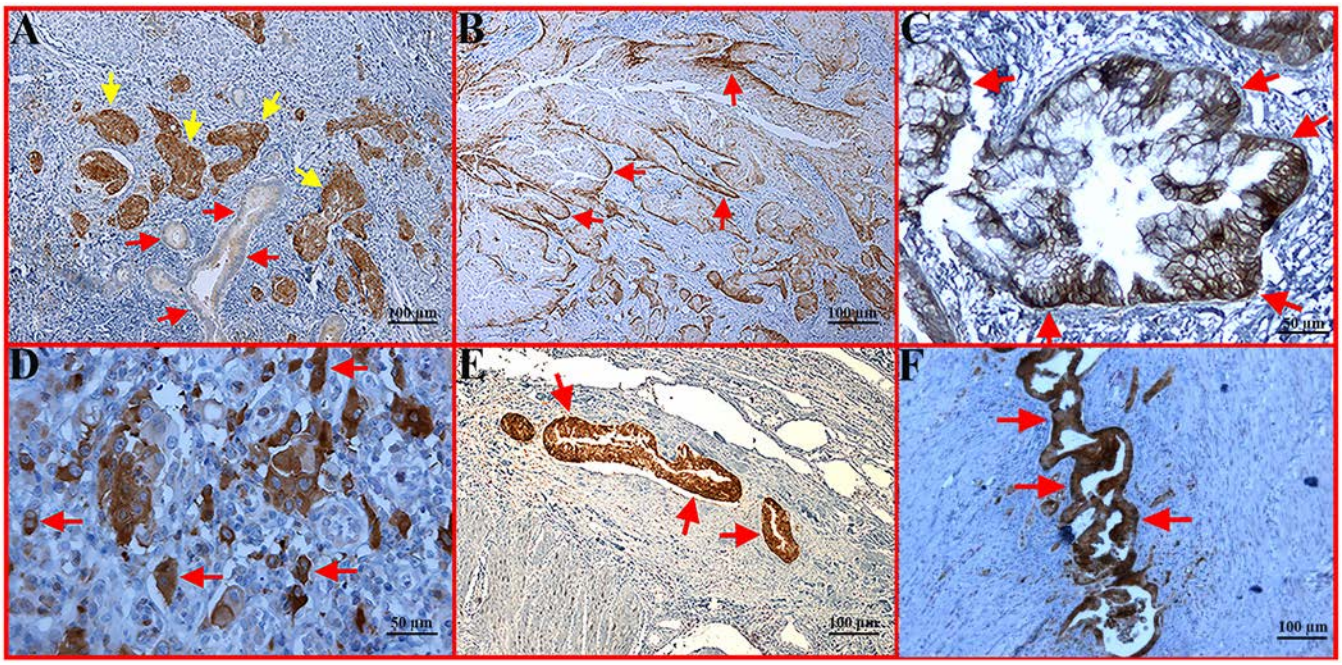

Figure 3.1: Immunohistochemical staining of PKM2 expression in representative pancreatic tumour sections. **(A)** Well differentiated area of tumour showing weak PKM2 expression (red arrow), with high expression in poorly differentiated areas (brown colour, yellow arrow). **(B)** Growing margin of tumour nodules with strong expression of PKM2 (red arrow). **(C)** Membranous expression of PKM2 (red arrow). **(D)** Heterogeneous expression of PKM2 with predominant expression in the proliferating cells (red arrow). **(E)** Strongly positive tumour expression of PKM2 in vascular invasion (red arrow). **(F)** Strongly positive tumour expression of PKM2 with muscular invasion (red arrow).

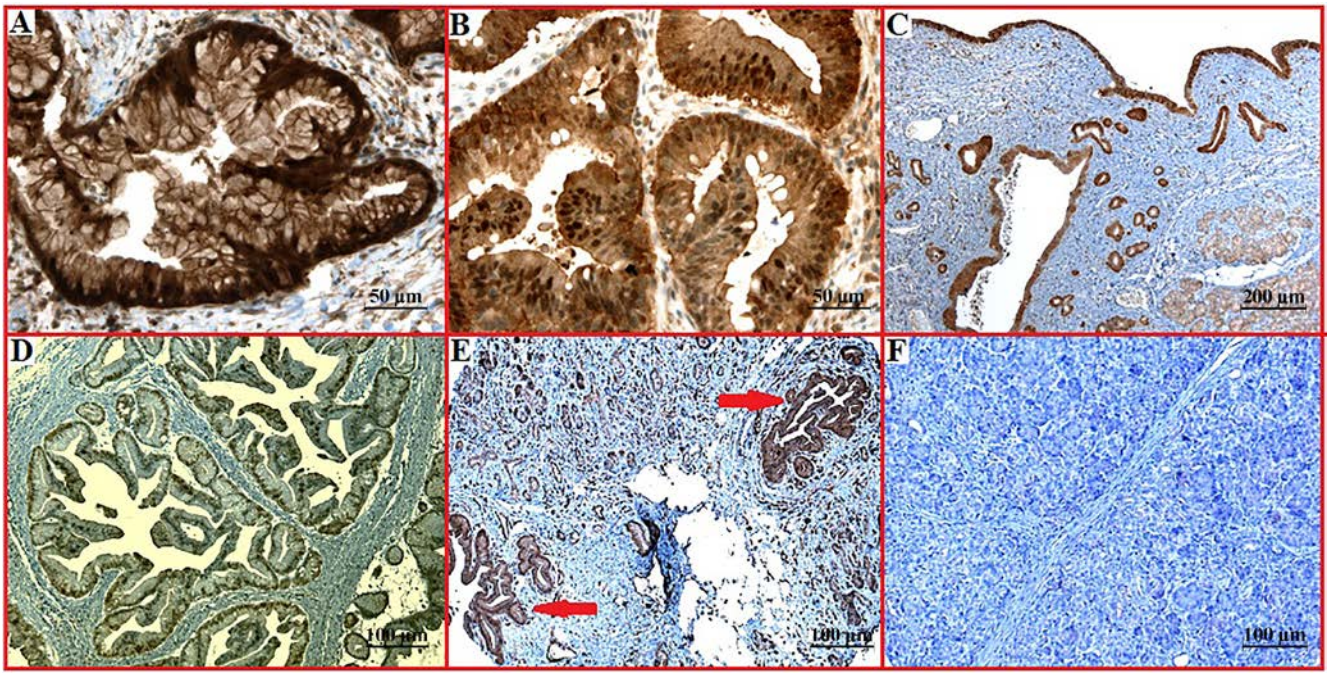

Figure 3.2: LDHA expression pattern. **(A)** Membranous expression of LDHA. **(B)** Cytoplasmic and nuclear expression **(C)** Strong expression in pancreatic cyst with mild expression in the surrounding normal pancreatic tissue. **(D)** Nuclear expression of LDHA in pancreatic cancer. **(E)** Strong expression in PanIN lesion. **(F)** Negative staining in normal pancreas

As shown in Fig 3.3, progressively higher PKM2 expression was observed along the tumorigenic pathway, with the lowest expression in pancreatic cysts (19%), intermediate in PanIN (37%) and highest in cancers (68%). PKM2 expression was approximately four-fold higher in pancreatitis (29%) compared with normal pancreatic tissue. Although LDHA expression was also significantly increased in cancers compared with normal pancreatic tissue ($p < 0.0001$, ANOVA), there were no significant differences between chronic pancreatitis, pancreatic cysts, PanIN and cancer samples (67%, 59%, 73% and 76%, respectively, Figure 3.3).

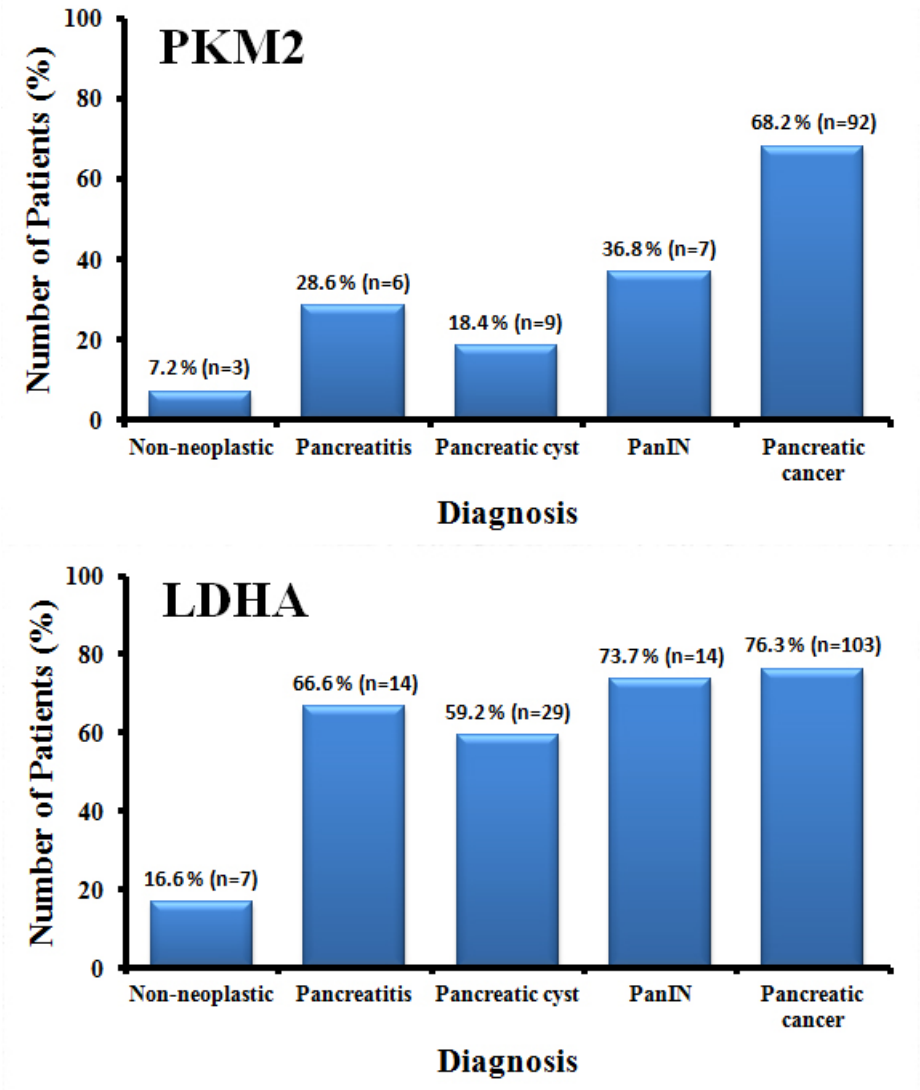

Figure 3.3: Percentages of PKM2 and LDHA expression in different type of tissues are shown. PKM2 was strongly expressed by pancreatic cancer tissue specimens and was significantly higher than normal, pancreatitis, pancreatic cyst and PanIN ($P<0.001$). Expression of LDHA was significantly high in pancreatic cancer than in normal pancreas ($P<0.001$), whereas, there was no signification differences in LDHA expression between pancreatic cancer, PanIN, pancreatic cysts and pancreatitis.

3.1.1.2: Association with clinicopathological parameters:

The correlation between PKM2 and LDHA expression with clinicopathological characteristics is shown in Table 3.1. There was a significant inverse correlation between PKM2 expression and tumour differentiation in the UCLH cohort, with 83% of PKM2 positive tumours being less differentiated compared with 64% of PKM2 negative tumours (p= 0.047, Chi-square test).

A significantly higher number of CD8+ TIL was found in tumours with weak PKM2 or LDHA expression compared with tumours that had a strong expression (PKM2: 42.4±43.1 vs. 16.3±24.3, p=0.0001, LDHA: 44.3±40.1 vs. 20.1±30.7, p=0.005 respectively, Table 3.1). Furthermore, a significant association between tumour cell proliferation and expression of both PKM2 and LDHA was observed; the number of tumour nuclei expressing Ki-67 was more than 2-fold higher in PKM2 and LDHA expressing tumours compared with negative tumours (PKM2: 27.8 ± 12.9 vs. 12.2 ± 14, p=0.0001 and LDHA: 25.1 ± 14 vs. 12.3 ± 15.1, p=0.004, Table 3.1). When staining scores, CD8+ TIL count and the number of Ki-67 positive cells were considered as continuous variables, a significant inverse correlation between the staining scores and CD8+ cell count was observed (PKM2: $p<0.001$ and LDHA: p= 0.004, Spearman rank correlation, Table 3.2, Figures 3.4 and 3.5). A significant direct correlation was noticed between the staining scores and Ki-67 count (PKM2: $p<0.001$ and LDHA: p= 0.001, Spearman rank correlation test, Table 3.2, Figures 3.6 and 3.7).

In the TMA cohort, the expression of PKM2 and LDHA correlated with tumour size. PKM2 expression was observed in 54.5%, 77.8% and 90.9% of tumours that were ≤ 2.5, 2.6-3.9 and ≥ 4 cm in size, respectively. Positive LDHA expression was found in 59.1%, 77.8% and 100% in tumours that were ≤ 2.5, 2.6-3.9 and ≥ 4 cm in size, respectively (Table 1, Figure 3.8). There were no significant differences between PKM2 or LDHA expression and tumour location, lymph node involvement, T-stage and metastatic status.

Table 3.1: Correlation of PKM2 and LDHA expression with clinicopathological factors. (UCLH cohort and TMA samples).

Variable		Total N (n=266)	PKM2 Expression		P-Value	LDHA Expression		P-Value	Combined Expression		P-Value
			Positive (High) (n=117) n (%)	Negative (Low) (n=149) n (%)		Positive (High) (n=167) n (%)	Negative (Low) (n=99) n (%)		Positive* (High) (n=104) n (%)	Negative** (Low) (n=162) n (%)	
Tumour Types	PDAC	124	87 (74.4)	37 (24.8)	**0.0001**	96 (57.5)	28 (28.3)	**0.0001**	80 (76.9)	44 (27.2)	**0.0001**
	Ampullary	11	5 (4.3)	6 (4)		7 (4.2)	4 (4)		4 (3.8)	7 (4.3)	
	Pancreatic cyst	42	8 (6.8)	34 (22.8)		27 (16.2)	15 (15.2)		8 (7.7)	34 (21)	
	PanIN	19	7 (6)	12 (8.1)		14 (8.4)	5 (5.1)		6 (5.8)	13 (8)	
	Pancreatistis	21	6 (5.1)	15 (10.1)		14 (8.4)	7 (7.1)		5 (4.8)	16 (9.9)	
	Pseudocyst	7	1 (0.9)	6 (4)		2 (1.2)	5 (5.1)		1 (1)	6 (3.7)	
	Normal (Non-neoplastic)	42	3 (2.6)	39 (26.2)		7 (4.2)	35 (35.4)		0 (0)	42 (25.9)	
Sex	Male	150	65 (55.6)	85 (57)	0.809	87 (52.1)	63 (63.6)	0.067	55 (52.9)	95 (58.6)	0.357
	Female	116	52 (44.4)	64 (43)		80 (47.9)	36 (36.4)		49 (47.1)	67 (41.4)	
Age at Diagnosis (Years)	Median (Range)	135	61 (32-84)	66 (41-82)	0.266	62 (34-84)	64 (32-82)	0.878	61 (34-84)	65 (32-82)	0.552
Tumour Differentiation	Well/Moderate	5	4 (4.3)	1 (2.3)	0.83	3 (2.9)	2 (6.3)	0.454	2 (2.4	3 (5.9)	0.141
	Moderate	55	36 (39.1)	19 (44.2)		41 (39.8)	14 (43.8)		32 (38.1)	23 (45.1)	
	Moderate/Poor	71	50 (54.3)	21 (48.8)		55 (53.4)	16 (50)		48 (57.1)	23 (45.1)	
	Unknown	4	2 (2.2)	2 (4.7)		4 (3.9)	0 (0)		2 (2.4)	2 (3.9)	
Metastasis status	Patients with metastasis	21	16 (17.4)	5 (11.6)	0.393	16 (15.5)	5 (15.6)	0.99	15 (17.9)	6 (11.8)	0.34
	Patients without metastasis	114	76 (82.6)	38 (88.4)		87 (84.5)	27 (84.4)		69 (82.1)	45 (88.2)	
Lymph node involvment	Positive lymph node	49	34 (37)	15 (34.9)	0.646	37 (35.9)	12 (37.5)	0.615	30 (35.7)	19 (37.3)	0.89
	Negative lymph node	43	30 (32.6)	13 (30.2)		34 (33)	9 (28.1)		27 (32.1)	16 (31.4)	
	Unknown	43	28 (30.4)	15 (34.9)		32 (31.1)	11 (34.4)		27 (32.1)	16 (31.4)	
Clinical T-stage classiffication	T1	1	1 (1.1)	0 (0)	0.214	1 (1)	0 (0)	0.78	1 (1.2)	0 (0)	0.248
	T2	13	6 (6.5)	7 (16.3)		9 (8.7)	4 (12.5)		5 (6)	8 (15.7)	
	T3	62	46 (50)	16 (37.2)		49 (47.6)	13 (40.6)		41 (48.8)	21 (41.2)	
	T4	14	9 (9.8)	5 (11.6)		10 (9.7)	4 (12.5)		8 (9.5)	6 (11.8)	
	Unknown	45	30 (32.6)	15 (34.9)		34 (33)	11 (34.4)		29 (34.5)	16 (31.4)	
Staging	Stage I	7	4 (4.3)	3 (7)	0.592	5 (4.9)	2 (6.3)	0.751	4 (4.8)	3 (5.9)	0.573
	Stage II	66	46 (50)	20 (46.5)		51 (49.5)	15 (46.9)		40 (47.6)	26 (51)	
	Stage III	14	9 (9.8)	5 (11.6)		10 (9.7)	4 (12.5)		8 (9.5)	6 (11.8)	
	Stage IV	3	3 (3.3)	0 (0)		3 (2.9)	0 (0)		3 (3.6)	0 (0)	
	Unknown	45	30 (32.6)	15 (34.9)		34 (33)	11 (34.4)		29 (34.5)	16 (31.4)	
Tumour Size	≤ 2.5	22	12 (13)	10 (23.2)	**0.019**	13 (12.6)	9 (28.1)	**0.009**	11 (13.1)	11 (21.5)	**0.01**
	2.6-3.9	27	21 (23)	6 (14)		21 (20.4)	6 (18.8)		16 (19)	11 (21.5)	
	≥ 4	11	10 (11)	1 (2.3)		11 (10.7)	0 (0)		10 (11.9)	1 (2)	
	Unknown	75	49 (53)	26 (60.5)		58 (56.3)	17 (53.1)		47 (56)	28 (55)	
Tumour Site	Head	42	27 (29.3)	15 (34.9)	0.17	28 (27.2)	14 (43.8)	0.087	21 (25)	21 (41)	**0.016**
	Body	10	9 (9.8)	1 (2.3)		9 (8.7)	1 (3.1)		9 (10.7)	1 (2)	
	Tail	8	7 (7.6)	1 (2.3)		8 (7.8)	0 (0)		7 (8.3)	1 (2)	
	Unknown	75	49 (53.3)	26 (60.5)		58 (56.3)	17 (53.1)		47 (56)	28 (55)	
Mean of CD8/HPF	Mean±SD	72	16.3±24.3	42.4±43.1	**0.0001**	20.1±30.7	44.3±40.1	**0.005**	16.4±24.9	39.5±41.7	**0.001**
Ki67 Proliferation Index (%)	Mean±SD	72	27.8±12.9	12.2±14	**0.0001**	25.1±14	12.3±15.1	**0.004**	27.8±12.8	13.7±14.7	**0.0001**

* Both PKM2 and LDHA Positive **Either PKM2 or LDHA Positive and Both Negative

Table 3.2: Summary of the correlations between PKM2, LDHA expression and number of nucleus immunostained CD8+TIL and Ki67 proliferation index.

			M2PK Expression	LDHA Expression	Number of CD8/HPF	Ki67 PI
Spearman's rho	M2PK Expression	Correlation Coefficient	1.000	.716**	.435**	-.481**
		Sig. (2-tailed)	.	.000	.000	.000
		N	72	72	72	72
	LDHA Expression	Correlation Coefficient	.716**	1.000	.346**	-.384**
		Sig. (2-tailed)	.000	.	.004	.001
		N	72	72	72	72
	Number of CD8/HPF	Correlation Coefficient	.435**	.346**	1.000	-.034
		Sig. (2-tailed)	.000	.004	.	.780
		N	72	72	72	72
	Ki67 PI	Correlation Coefficient	-.481**	-.384**	-.034	1.000
		Sig. (2-tailed)	.000	.001	.780	.
		N	72	72	72	72

**. Correlation is significant at the 0.01 level (2-tailed).

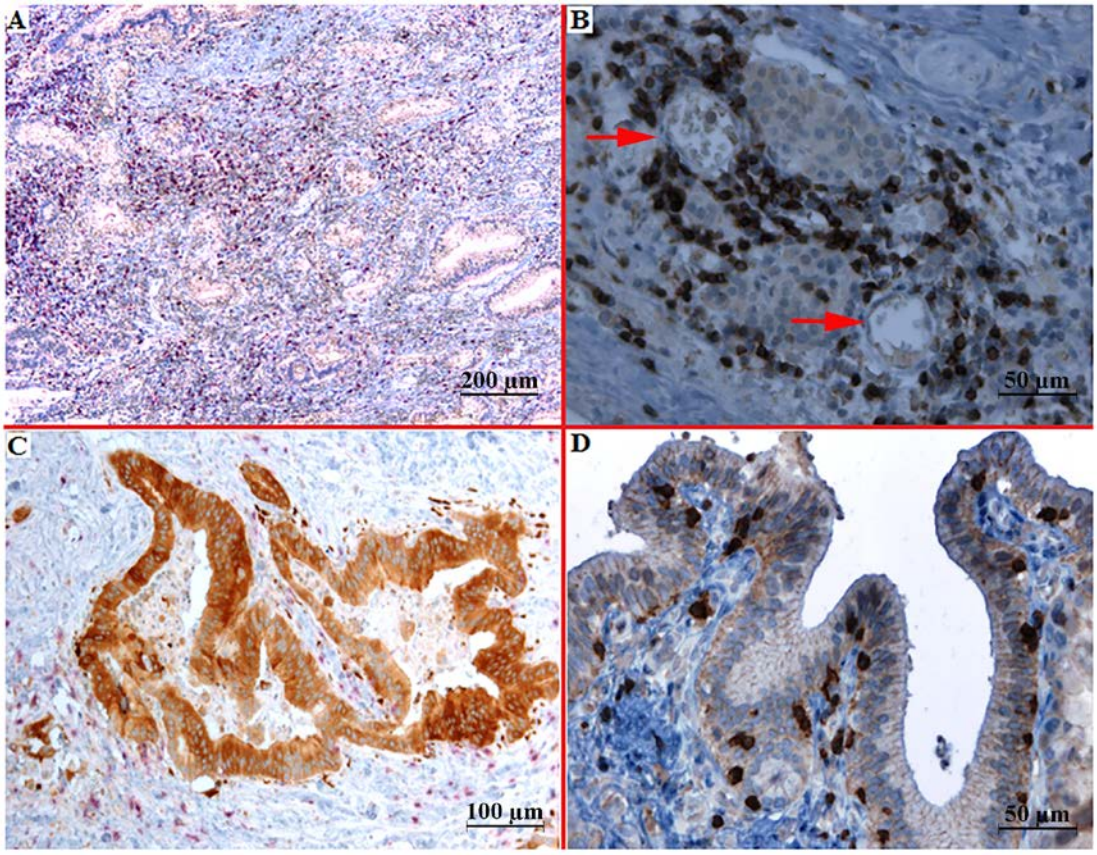

Figure 3.4: Double immunohistochemical staining of PKM2 and CD8+TIL. Relationship between tumour differentiation, PKM2 expression and stained CD8 cells. **(A)** Well differentiated tumour with negative PKM2 expression and high infiltration by CD8+ positive T-lymphocytes. **(B)** Well differentiated tumour with weak PKM2 expression had strong infiltration by CD8+ positive T-lymphocytes. Shows tumour autolysis (red arrows). **(C)** Poorly differentiated tumour strongly positive for PKM2 had sparse infiltration by CD8+ positive T-lymphocytes. **(D)** Intratumoural infiltration by CD8+ cells in a well differentiated and PKM2 weakly positive tumour.

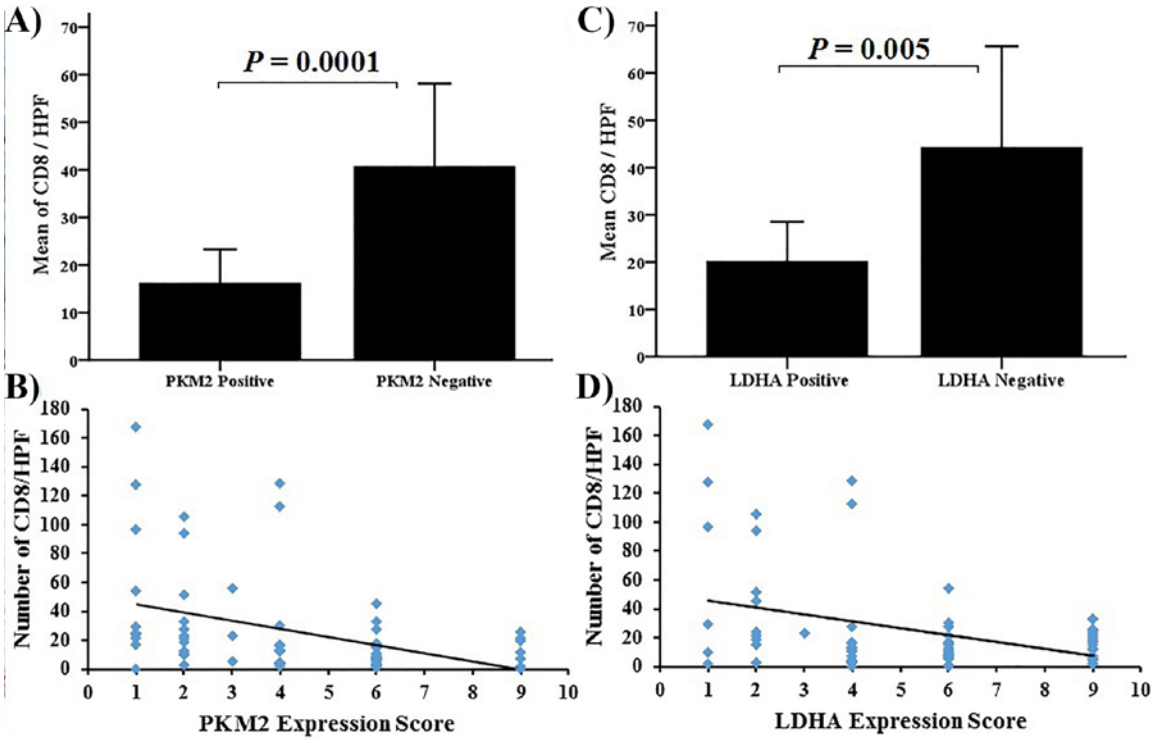

Figure 3.5: Correlation between PKM2 and LDHA expression with CD8+TIL. **(A)** Correlation between CD8+ tumour infiltrating lymphocytes and PKM2 expression. Tumours with weak PKM2 expression had significantly higher number of CD8+TIL than those with strong PKM2 expression (Bar chart, 95% CI). **B)** Number of nucleus stained CD8+TIL significantly decreased with increasing PKM2 expression score (R=0.4, p=0.002, Linear Regression Test). **C)** Pancreatic cancer specimens with weak LDHA expression had significantly higher number of nucleus stained CD8+TIL than those with strong LDHA expression (Bar chart, 95% CI). **D)** Number of nucleus stained CD8+TIL significantly decreased with increasing LDHA expression in pancreatic cancer specimens (R=0.37, p=0.009, Linear Regression Test).

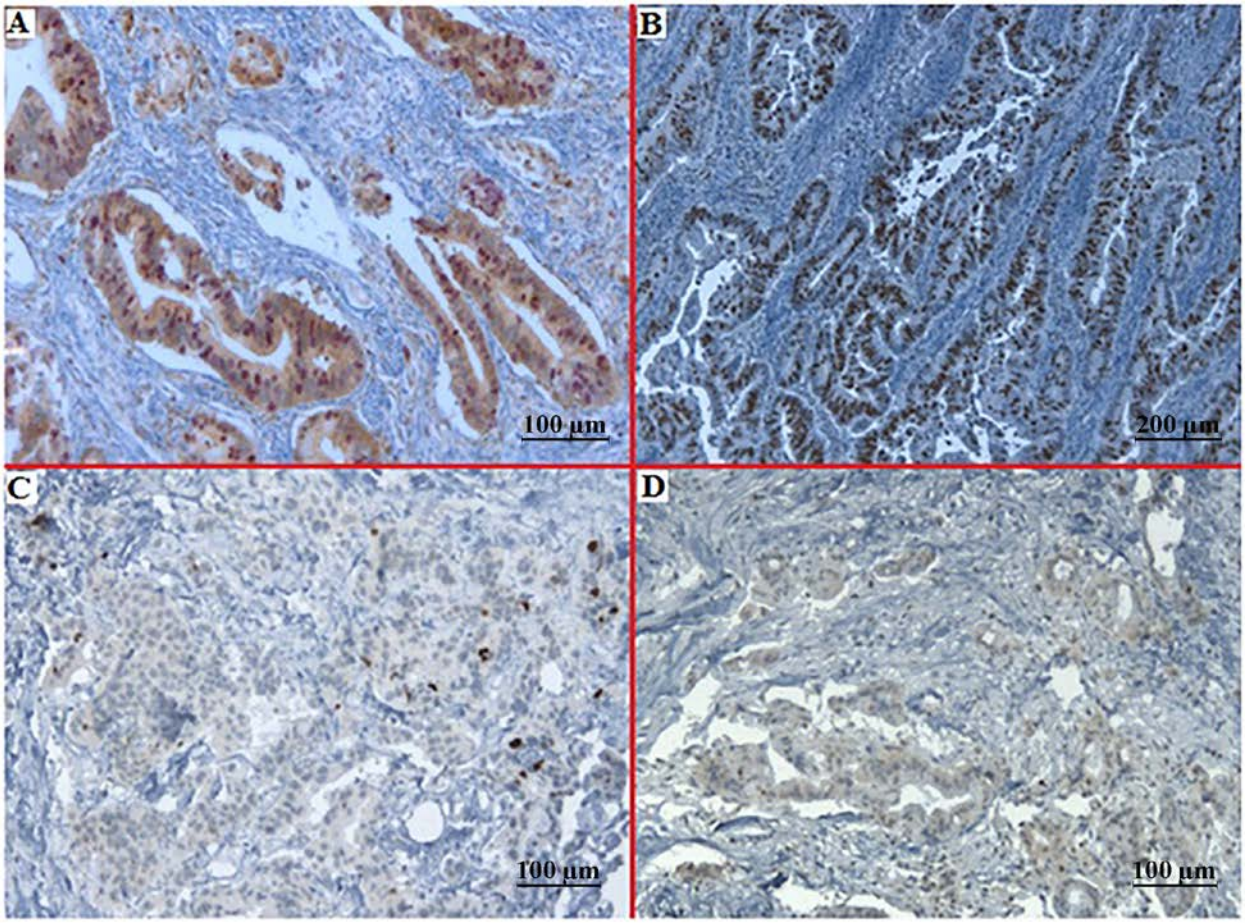

Figure 3.6: Immunohistochemical staining of PKM2 and Ki67 in pancreatic cancer. **(A)** Double immunohistochemical staining of Ki67 (red colour, nuclear) and PKM2 (brown colour, cytoplasmic). Strongly positive tumour for PKM2 expression had most of the nucleus stained for Ki-67. **(B)** Single Ki67 immunostaining with high positive number in tumour area. **(C, D)** Weak PKM2 expression with few Ki67 stained cells.

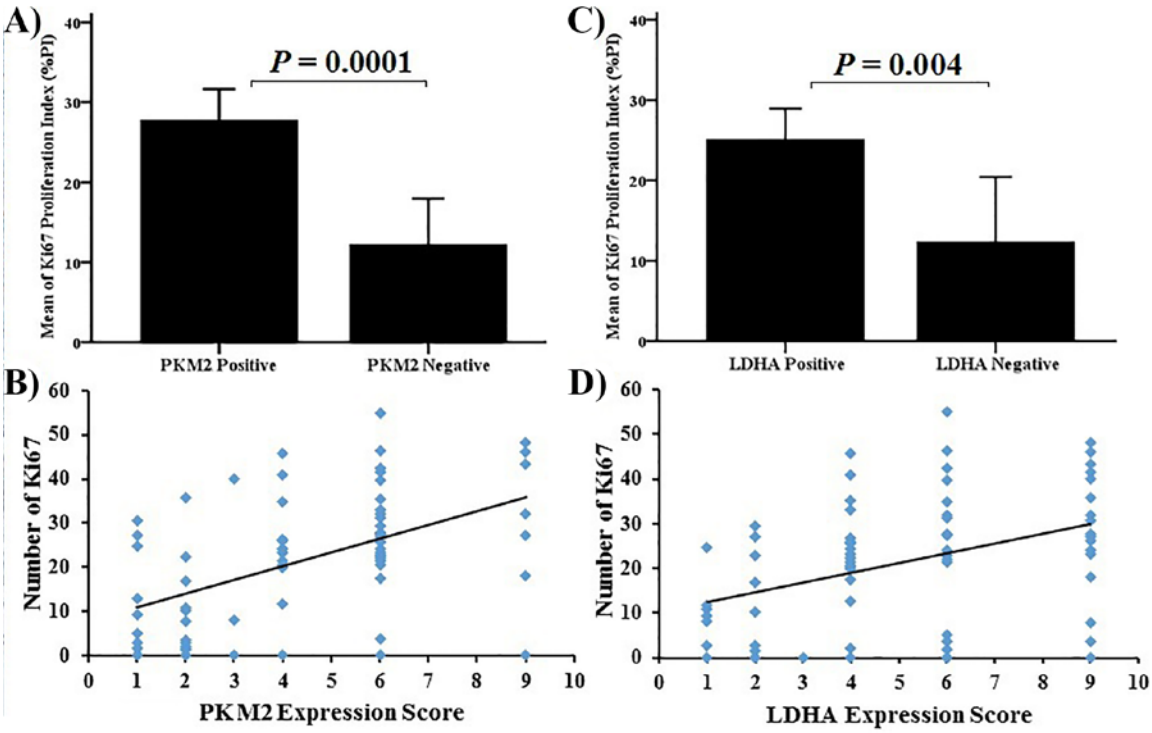

Figure 3.7: Relationship between PKM2/LDHA expression and Ki67 in pancreatic cancer. **A)** Correlation between mean of Ki-67 proliferation index and PKM2 expression. Tumours with strong PKM2 expression were characterized by high number of Ki-67 proliferation index (Bar chart, 95% CI). **B)** Number of Ki67 proliferation index was significantly increased with increasing of PKM2 expression score (R=0.485, p<0.0001, Linear Regression Test). **(C)** Pancreatic cancer specimens with strong LDHA expression had significantly high number of nucleus stained Ki67 than weak LDHA expression (Bar chart, 95% CI). **(D)** Number of Ki67 proliferation index was significantly increased with increasing LDHA expression score (R=0.395, p=0.004, Linear Regression Test).

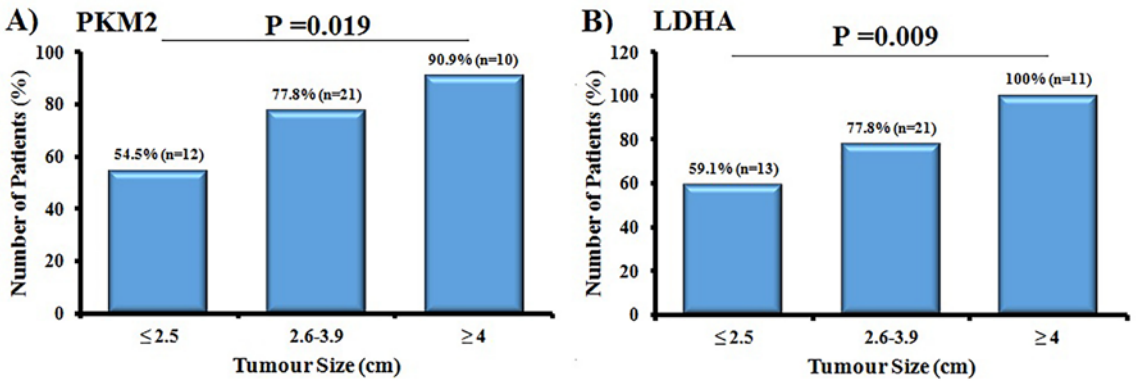

Figure 3.8: PKM2 and LDHA expression in pancreatic cancer tissue microarrays and correlation with tumour size. **(A)** PKM2 expression highly correlate with tumour size and significantly increase with increasing of tumour size. **(B)** Expression of LDHA directly correlate with tumour size and significantly increase with increasing tumour size.

3.1.1.3: Correlation between PKM2 and LDHA expression and patient survival:

I next examined whether the expression profile of PKM2 and LDHA predicted survival. Patients with tumours scoring > 3 for PKM2 or LDHA expression had significantly worse survival compared with those that weakly expressed PKM2 and/or LDHA. Of the 72 pancreatic cancer samples (UCLH cohort), 46 (64%) strongly expressed PKM2 and these patients had a median survival of only 8.9 months compared with 28.9 months in the 26 (36%) patients with weak (negative) PKM2 tumour expression (p=0.016, log-rank test, Figure 3.9). Similarly, 55 (76.4%) patients with positive LDHA tumour expression had a median survival of 10.9 months compared with 34.5 months of the 17 (23.6%) patients with weak (negative) LDHA tumour expression (p = 0.029, log-rank test, Figure 3.9). Moreover, when the expression profile of PKM2 and LDHA was combined, the survival of patients with negative expression for both or positive for one was four times longer than those with a positive status for both (27.9 months vs. 7.0 months, respectively, p = 0.003, log rank test). Among the several survival predictors by the univariate analysis (T-stage; p = 0.006, tumour differentiation; p = 0.003, metastatic status; p = 0.000), by Cox regression analysis only the combined PKM2 / LDHA expression status and tumour differentiation status were independent survival predictors (p= 0.003, Hazard ratio (HR) = 4.96 and p=0.015, HR= 3.31, respectively) (Table 3.3).

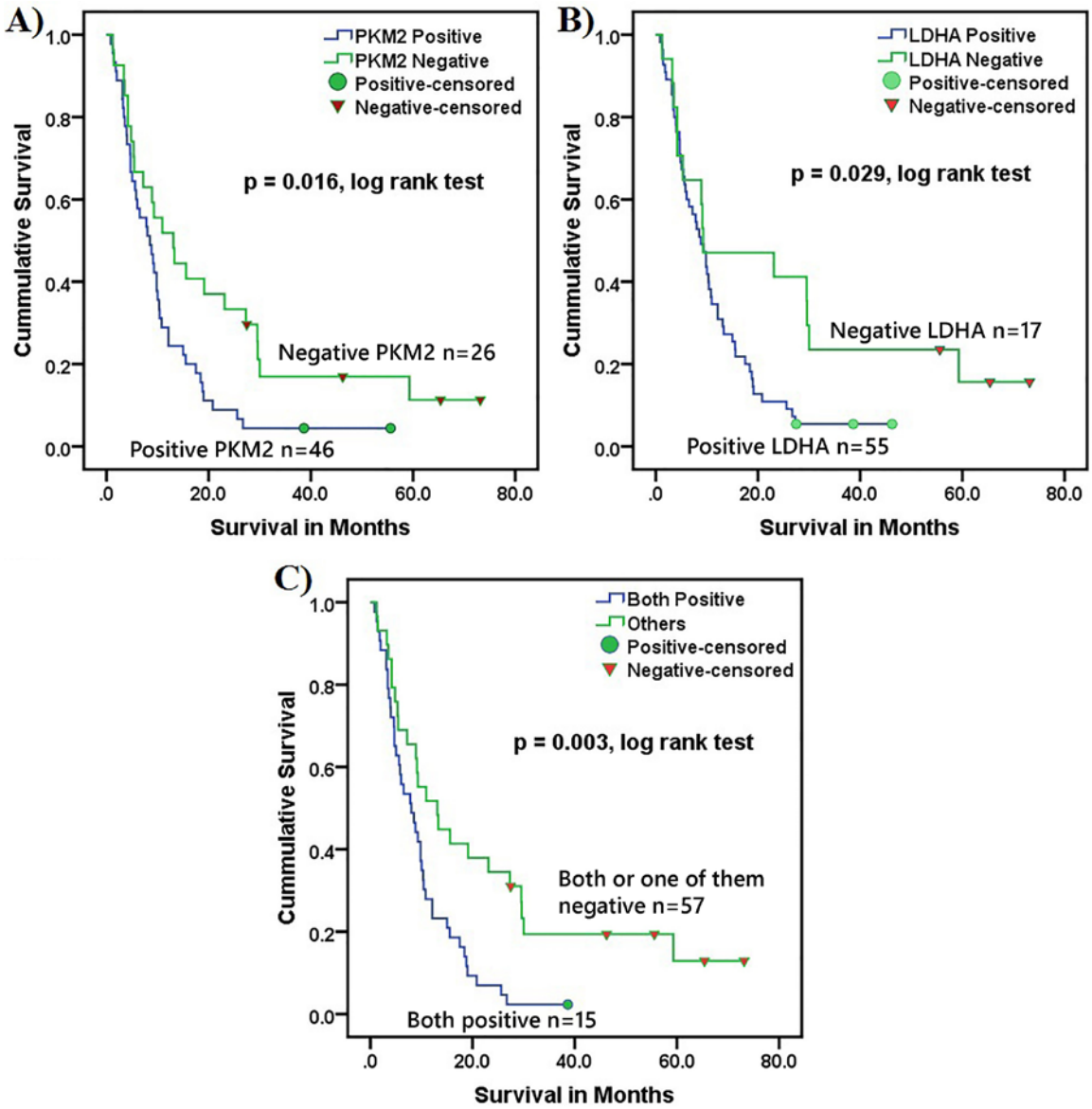

Figure 3.9: Overall patient survival in relation to PKM2 and LDHA expression. Both PKM2 (A) and LDHA (B) had a significant prognostic impact on patient survival and the combined expression for both markers further stratified the patients into significant groups (C).

Table 3.3: Multivariable analysis of prognostic factors.

	Variables in equation	p-value	Hazard ratio
Step 1	Tumour differentiation	0.096	3.372
	T-stage	0.877	0.937
	Metastatic status	0.223	0.333
	PKM2 and LDHA combined expression	0.007	4.538
Step 2	Tumour differentiation	0.024	3.109
	Metastatic status	0.203	0.324
	PKM2 and LDHA combined expression	0.005	4.642
Step 3	Tumour differentiation	0.015	3.314
	PKM2 and LDHA combined expression	0.003	4.959

3.1.1.4: Association between tumour types, resection status and survival months:

To further investigate PKM2 and LDHA expression pattern in pancreatic cancer, I evaluated the correlation between expressions of these two important glycolytic enzymes with tumour types, resection status and survival rate.

Twenty-seven of the 72 patients underwent surgical resection for PDAC (n=16) or ampullary adenocarcinoma (n=11). Those who underwent surgical resection had a significantly longer survival than those who did not undergo surgery (26.5 vs 7.0 months, P<0.0001; log rank test, Figure 3.10, Table 3.4). As expected, patients with ampullary adenocarcinoma had a better prognosis after surgery than those with PDAC, with 5 of 11 (45.5%) ampullary carcinoma patients alive at last contact, compared with only 1 out of 16 (6.3%) patients with PDAC (P<0.0001; log rank test, Figure 3.10, Table 3.4). The association of PKM2 and LDHA expression with tumour types, resection status and survival in months are described in figure 3.10 and table 3.4.

Table 3.4: Summary of correlation between tumour types and resection status and patients survival.

Variables	N	Survival month Mean ± SD	P- value
Tumour Types			
PDAC	61	10.41 ± 10.36	**0.0001**
Ampullary	11	36.5 ± 19.96	
Resection status			
YES	27	26.54 ± 18.72	**0.0001**
No	45	6.95 ± 4.98	

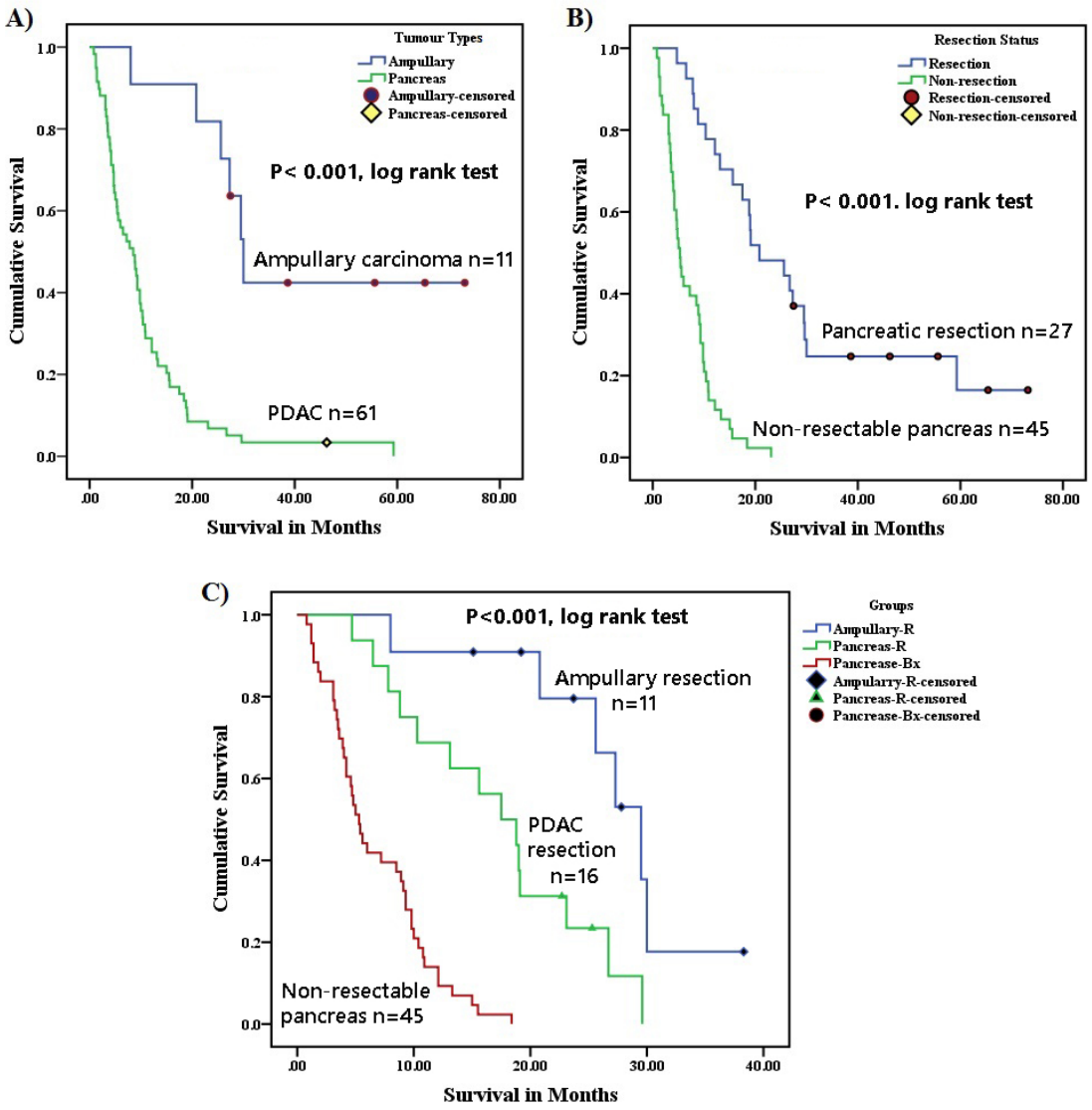

Figure 3.10: Survival according to the tumour type and resection status. **(A)** Patients with ampullary tumours had longer survival time than pancreatic adenocarcinoma (p<0.001, log rank test). **(B)** Resectable tumour patients had longer survival time than who did not undergo resection treatment (p<0.001, log rank test). **(C)** Comparing survival time according to the resection in pancreatic adenocarcinoma and ampullary resection tumours.

3.1.1.5: PKM2 and LDHA expression in pancreatic cancer cell lines:

I also evaluated the level of PKM2 and LDHA expression in pancreatic cancer cell lines by western blot. Of 10 pancreatic cancer cell lines, 8 highly expressed PKM2 and 9 highly expressed LDHA, as defined by intensity of western blot bands (Fig 3.11). The PK-59 cell line exhibited weak expression of both LDHA and PKM2, while the KP4 cell line weakly expressed PKM2. By immunocytochemistry, both PKM2 and LDHA had strong cytoplasmic and nuclear expression (Fig 3.12).

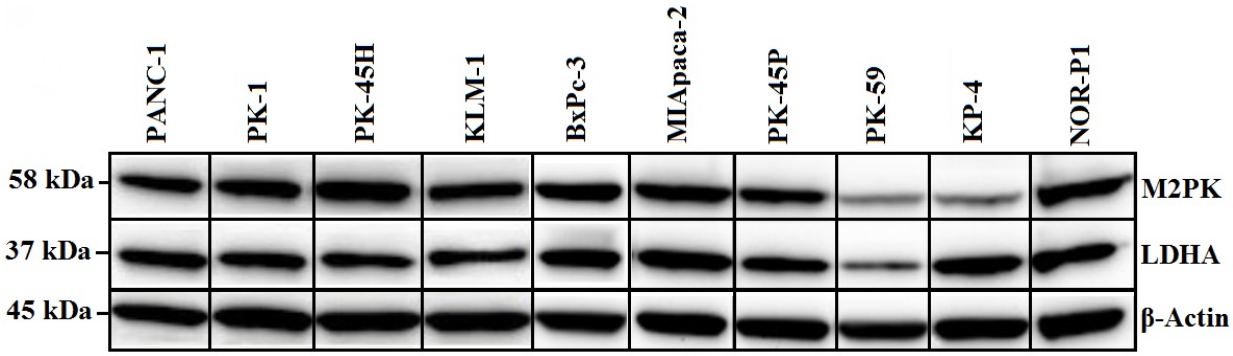

Figure 3.11: Expression of PKM2 and LDHA in pancreatic cancer cell lines as detected by western blot.

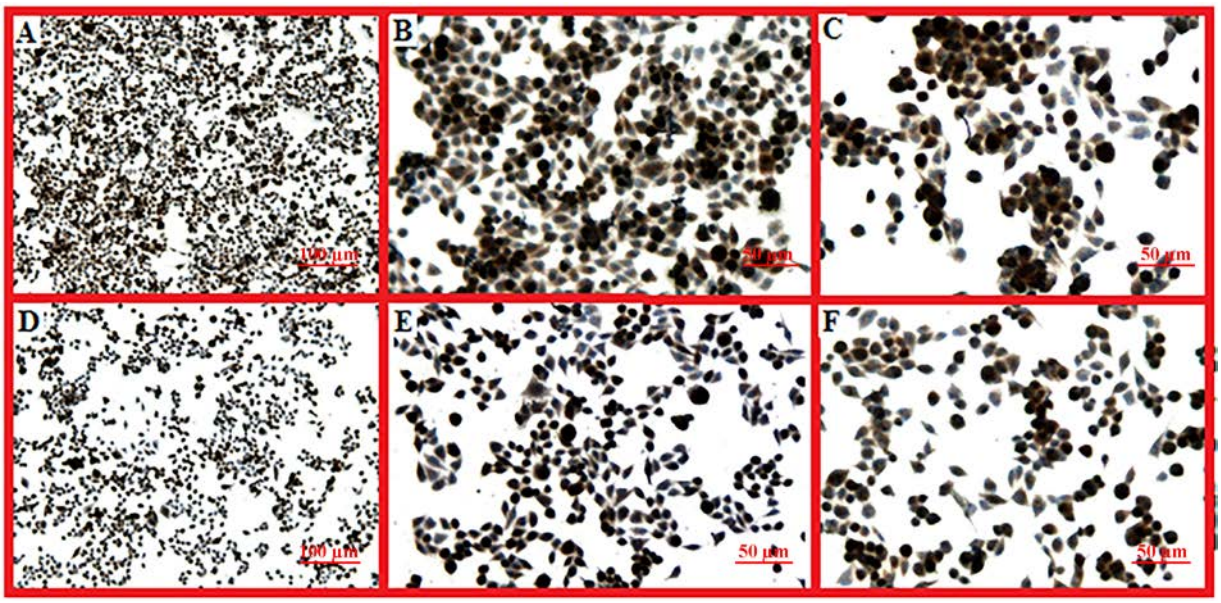

Figure 3.12: Immunocytochemical staining of Miapaca-2 cell line with PKM2 **(A,B,C)** and LDHA **(D,E,F).** Strong cytoplasmic and nuclear staining is noticed in proliferating cells.

3.1.1.6: Plasma PK and LDH activity in pancreatic cancer and healthy controls:

Besides studying the expression of PKM2 and LDHA in pancreatic cancer specimens and pancreatic cancer cell lines, I also assessed the plasma activity of these two glycolytic enzymes. Plasma samples from 51 patients (median age 68 years) with pancreatic cancer and 20 healthy controls with a median age of 69 years were obtained. Pancreatic cancer patients included 27 men and 24 women with different histological stages (Stage I=1, Stage II=7, Stage III=13, Stage IV=20, NA=10), whereas, healthy controls included 12 men and 8 women. The activity of PK and LDH in plasma samples was measured by using a commercially available PK and LDH activity assay kit (BioVision, USA).

Plasma PK and LDH enzyme activity was significantly higher in patients with pancreatic cancer compared to the healthy controls ($p < 0.0001$, Kruskal-Wallis Test, Figure 3.13), and are described in Figure 3.13 and Table 3.5. The activity of PK in pancreatic cancer plasma was approximately 2 fold higher than in healthy controls, with mean PK activities of 45.5 U/L and 21.6 U/L, respectively. LDH activity in pancreatic cancer plasma was approximately 3.5 fold higher than in healthy controls, with values of 685 U/L and 194 U/L, respectively.

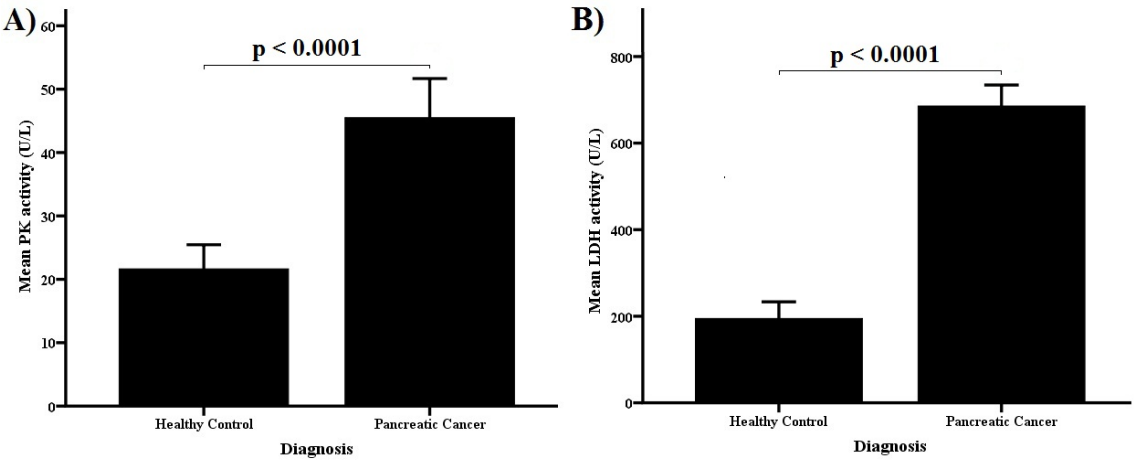

Figure 3.13: Plasma pyruvate kinase and lactate dehydrogenase activity in pancreatic cancer compared with healthy controls ($P < 0.0001$, Kruskal-Wallis Test, Bar chart, 95% CI).

Table 3.5: Plasma pyruvate kinase and lactate dehydrogenase activity in pancreatic cancer compared to the healthy control.

Diagnosis	N	Age Median (Range)	PK activity (U/L) (Mean ± SD)	P-Value	LDH activity (U/L) (Mean ± SD)	P-Value
Pancreatic cancer	51	68 (41-94)	45.5 ± 18.7	**0.0001**	685.78 ± 167.74	**0.0001**
Healthy Control	20	69 (41-80)	21.65 ± 8.5		194.75 ± 77.17	

3.1.2: DISCUSSION:

There is mounting evidence that cancer cells have elevated glucose uptake with a concomitant increase in lactate production through sequential catalytic enzyme mediated processes (59,172). PKM2 and LDHA are two crucial glycolytic enzymes that facilitate these processes to confer cancer cells with a growth advantage over normal cells. To date, serum PKM2 has been identified as a diagnostic and prognostic marker with comparable sensitivity and specificity to serum CA19-9 marker in pancreatic cancer (5,173,174). However, there are limited data on the expression pattern and prognostic impact of PKM2 and LDHA in pancreatic cancer (73,175). To the best of our knowledge, our study is the first to evaluate the prognostic impact of combined PKM2 and LDHA expression in the initiation and progression of pancreatic cancer. A recent study showed overexpression and phosphorylation of both of these enzymes in thyroid cancer compared with benign goitre (176). Our results concur with their findings showing significant overexpression of PKM2 and LDHA in pancreatic cancers compared with normal pancreatic tissue.

The step-wise initiation and development of pancreatic cancer often begins with pancreatitis, ductal metaplasia, cyst formation or PanIN lesions, leading to pancreatic cancer. Interestingly, our results demonstrate overexpression of LDHA at a very early stage along the carcinogenic pathway from pancreatitis through cyst/PanIN to cancer with the highest expression in the most aggressive tumours. In contrast, PKM2 expression increased progressively along the tumorigenic pathway and was lowest in cysts, intermediate in PanIN lesions and highest in cancers. Although the exact mechanism of this differential expression pattern remains to be elucidated, it is possible that the pre-neoplastic lesions acquire the glycolytic phenotype through LDHA overexpression and then LDHA itself or other oncogenes induce PKM2 overexpression

at later stages when tumour cell proliferation rates are higher. In fact, it has been recently shown that the epidermal growth factor receptor (EGFR) induces β-catenin transactivation and c-myc expression, upregulating LDHA, which in turn induces upregulation of PKM2 expression by alternating splicing of the gene from M1 to M2 type (177). These findings might partially explain the consistent overexpression of LDHA throughout the tumorigenic process and the progressive overexpression of PKM2 along the carcinogenetic pathway. The expression and enzymatic activity of LDHA and PKM2 can also be modulated by tyrosine phosphorylation at various residues (Y10 and Y105, respectively) by the oncogenic tyrosine kinase fibroblast growth factor receptor-1 (178). The differential expression pattern suggests that PKM2 (or a combination of PKM2 and LDHA) would be a better choice for discriminating cancer from pre-neoplastic lesions compared with LDHA alone, except in pancreatitis where both markers are highly expressed.

The main reason for using several pancreatic cancer cell lines was to study the level of PKM2 and LDHA expression alongside tissue sections and plasma samples, and to compare the expression levels of these two glycolytic enzymes in order to select a suitable cell line for both in vitro and in vivo study. The western blot is a semi-quantitative analysis and is a suitable method for comparing the expression level of these two enzymes.

Interestingly, we noticed consistently high expression of both PKM2 and LDHA in Miapaca-2, PK-1 and BxPc-3 cell lines in different stages of cell culture. In fact, these pancreatic cancer cell lines are more aggressive and exhibit faster growth than other cell lines used in this study. A possible explanation for this is the high expression of the two glycolytic enzymes PKM2 and LDHA, which are necessary for cell proliferation and growth.

Treating pancreatic cancer is highly challenging due to late diagnosis, and lack of appropriate prognostic markers and effective therapies. Our results demonstrate that both PKM2 and LDHA are significant prognostic markers in pancreatic cancer and the combination provides improved stratification of outcome. These results are in line with

previous publications showing a significant prognostic effect of LDHA or PKM2 in other tumour types, including squamous cell carcinoma, cholangiocarcinoma and gastric cancer (168,179,180). The exact mechanisms associated with the overexpression of PKM2 and LDHA that lead to poor prognosis remain unclear. Very recently, Rajeshkumar *et al.* (2015) found that the LDHA small molecule inhibitor FX11 can impede tumour growth, reduce tumour cell proliferation and induce apoptosis in a patient-derived mouse xenograft model of pancreatic cancer with mutant TP53, while tumours harbouring wild-type TP53 were completely resistant to FX11 (181). In this study, I noticed a significant direct correlation between staining scores and the tumour cell proliferation index, and by using the double labelling technique, I was able to identify Ki-67 positive proliferating cells topographically co-localising in PKM2 positive areas. It has been well recognised that these glycolytic enzymes translocate to the nucleus and interact with several other oncogenic transcription factors and transcribe several cell proliferating signaling pathways including Stat3, β-catenin, HIF-1, Oct-4, cyclin D1 (182). Moreover, PKM2 has been implicated in the phosphorylation of the chromosomal spindle checkpoint protein Bub3-Bub1-Blinkin complex, which ensures fidelity of chromosomal segregation during cell proliferation (183). Although I could not find any significant correlation with tumour stage and metastasis status, strong expression of PKM2 was observed in metastatic tumours invading muscle and blood vessels, indicating the aggressive phenotype of pancreatic tumours expressing the glycolytic enzymes. We and others have previously shown in cholangiocarcinoma and lung cancer, respectively, that tumour-associated angiogenesis is induced by PKM2 and LDHA, which could be another contributing factor to poor prognosis (168,184).

Host immune evasion is a hallmark of the aggressive tumour phenotype. Although a limited number of studies have provided evidence of a link between host immune suppression and the tumour glycolytic phenotype, to date, there is no concrete evidence showing a correlation between the expression of PKM2, LDHA and CD8+ effector cell infiltration. Interestingly, I noticed a significant inverse correlation between the PKM2 and LDHA expression and CD8+ cell infiltration, with an accumulation of CD8+ cells in

tumours that did not express PKM2. Recently, Crane *et al.* (2014) reported that LDHA secreted by glioblastoma cells downregulated the Natural Killer group 2, member D receptor on natural killer cells and thus subverted host immune surveillance (185). Similarly, Liu *et al*. (2015) reported that PKM2 expression was related to increased infiltration of primary and metastatic tumours by myeloid derived suppressor cells, responsible for the suppression of NK cells and induction of host immune suppression by regulatory T cells (186). I postulate that the compromised immune surveillance induced by enhanced expression of PKM2 and LDHA, and reduced CD8+ effector T-cells might be another contributing factor associated with poor prognosis of the glycolytic phenotype of pancreatic cancer.

There are some limitations to the studies; these include limited sample size and lack of some clinicopathological information. The scoring system of PKM2 and LDHA expression is another limitation, as various scoring systems have been reported (168,187–190), and an optimal scoring system for PKM2 and LDHA expression has not yet been established. In my study, the PKM2 and LDHA expression score was classified as negative or positive, which was based on the intensity and extent of PKM2 and LDHA expression across tumour areas. Moreover, surgical resection and chemotherapy might have affected the correlation of PKM2 and LDHA expression with overall survival of patients.

In conclusion, I have shown a differential expression pattern for PKM2 and LDHA from cysts through PanIN lesions to pancreatic cancer, with upregulation of LDHA throughout the carcinogenetic process and a progressive upregulation of PKM2 expression along the carcinogenetic pathway. Moreover, the combined expression of these glycolytic enzymes is a strong independent marker of poor prognosis, attributable to increased cell proliferation, larger tumour size and host immune evasion. Further studies are underway to evaluate these markers as possible targets for therapy in pre-clinical models of pancreatic cancer.

3.2: Activation of PKM2 in combination with inhibition of LDHA synergistically inhibit pancreatic cancer cell proliferation *in vitro*

3.2.1: RESULTS:

3.2.1.1: Expression of PKM2 and LDHA in pancreatic cancer cell lines:

The expression of PKM2 and LDHA was evaluated in ten different pancreatic cancer cell lines (Miapaca-2, BxPc-3, PANC-1, PK-1, PK-59, PK-45P, PK-45H, KLM-1, KP-4, NOR-P1) by Western blot. The levels of PKM2 and LDHA expression was measured when cells reached approximately 50% (proliferation stage) or 90% (confluent stage) confluency. The total protein was then quantified and equal amounts of protein were loaded into the gel. The intensity of PKM2 and LDHA expression was detected and measured using an image grabber.

I found that the majority of the pancreatic cancer cell lines highly expressed both PKM2 and LDHA. Out of the 10 cell lines, 9 had high LDHA expression and 8 had high PKM2 expression, as indicated by intensity of the Western blot bands (Figure 4.1). The PK-59 cell line exhibited weak expression of both LDHA and PKM2, while the KP4 cell line had a weak expression of PKM2 only. The expression of PKM2 was high in the PANC-1, PK-45H and KLM-1 cell lines during proliferation stage compared to the confluent stage. However, there was no difference in PKM2 expression between these two different stages in the other pancreatic cancer cell lines. There was no difference in LDHA expression between the proliferation and confluent culture stages in all pancreatic cancer cell lines. The Miapaca-2, BxPc-3 and PK-1 cell lines highly expressed both PKM2 and LDHA at both stages of cell culture confluency. Therefore, the Miapaca-2 and BxPc-3 cell lines were selected for further studies and for the development of tumour xenografts in nude mice. The expression of PKM2 and LDHA in the various pancreatic cancer cell lines are shown in figure 4.1.

The expression of both PKM2 and LDHA was further examined by immunocytochemistry in the Miapaca-2 cell line (Figure 3.12). Immunocytochemistry staining showed that PKM2 and LDHA were strongly expressed by Miapaca-2 cells.

LDHA expression was relatively higher in the nucleus of the cell, whereas expression of PKM2 was mostly cytoplasmic (Figure 3.12).

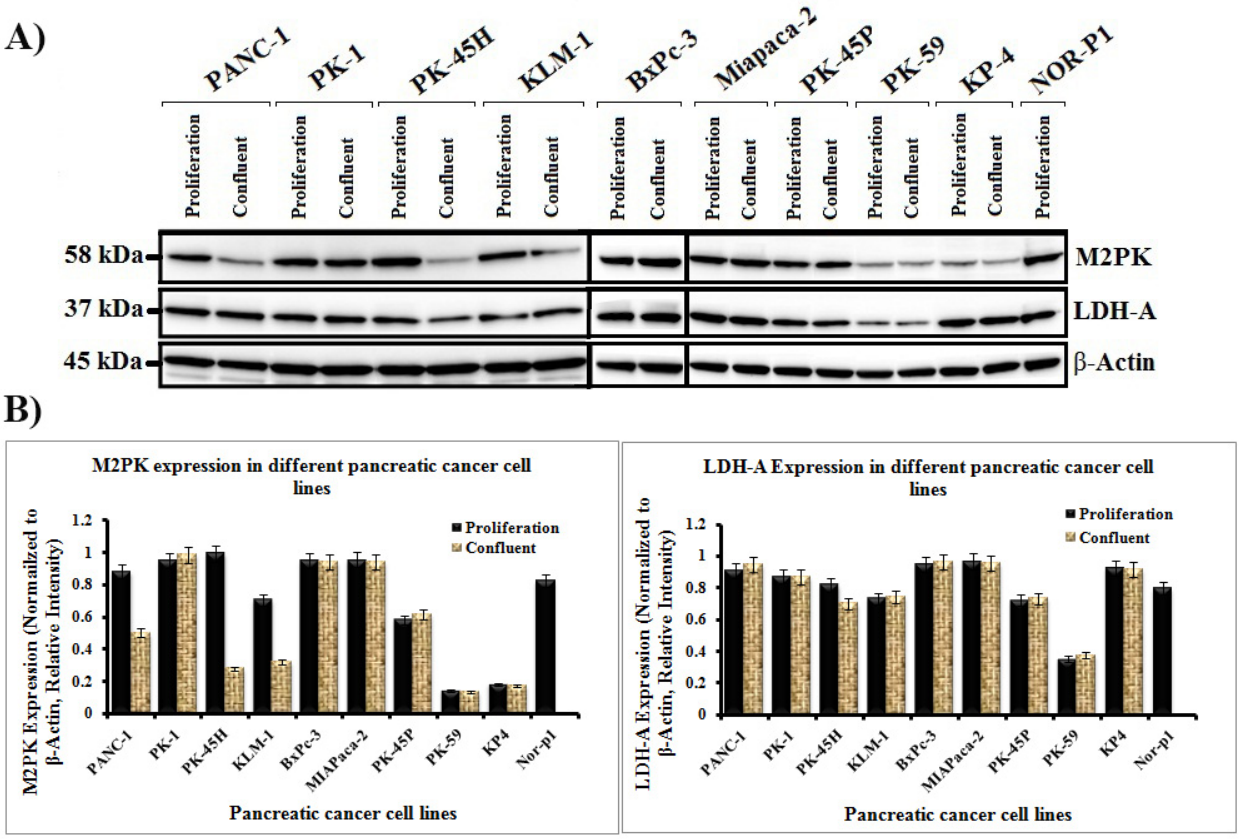

Figure 3.14: PKM2 and LDHA expression in different pancreatic cancer cell lines and different stages of cell culture. **A)** Western blot analysis and comparison between band intensity in different pancreatic cancer cell lines. **B)** Intensity of PKM2 and LDHA expression normalized with β-actin, represented by bar chart.

3.2.1.2: Effect of PKM2 inhibition on pancreatic cancer cell proliferation:

Shikonin was used as the PKM2 inhibitor in our studies. In order to investigate the effect of Shikonin on pancreatic cancer cell proliferation, PK-1 cells were treated with different concentrations (2.5 to 80 µM) of Shikonin over the period of 24, 48, 72 and 96 hours (see Appendix 1). The results of this study showed that the Shikonin had a strong cytotoxic effect on the viability of PK-1 cells.

Based on these results, a range of Shikonin concentrations from 1 to 5 µM were selected over two time intervals, either 24 and 72 hours or 24 and 96 hours, for further evaluation. As shown in the figure 4.2 and table 4.1, Shikonin had high cytotoxicity in the PK-1, PK-45H, and KLM-1, Miapaca-2, KP4, PK-45 H and PK-59 cell lines, with an IC_{50} of 2-3 µM for 24 hour exposure time. Whereas, Shikonin had lower cytotoxicity in PANC-1 cell line for the 24 hour exposure time, with an IC_{50} of 3.97µM. The effect of Shikonin treatment was then investigated over 72 or 96 hour exposure times in pancreatic cancer cell lines. The results showed that Shikonin was highly potent and had the high cytotoxic effect in all pancreatic cancer cell lines, with an IC_{50} of 1-2 µM for both 72 and 96 hours exposure times (Figure 4.2 and Table 4.1).

Shikonin had a high cytotoxic effect on pancreatic cancer cells. As shown in figure 3.16, treatment of pancreatic cancer cells with Shikonin lead to morphological change and shrinkage of pancreatic cancer cells, which in turn may finally lead to cell death by both apoptosis and necrosis.

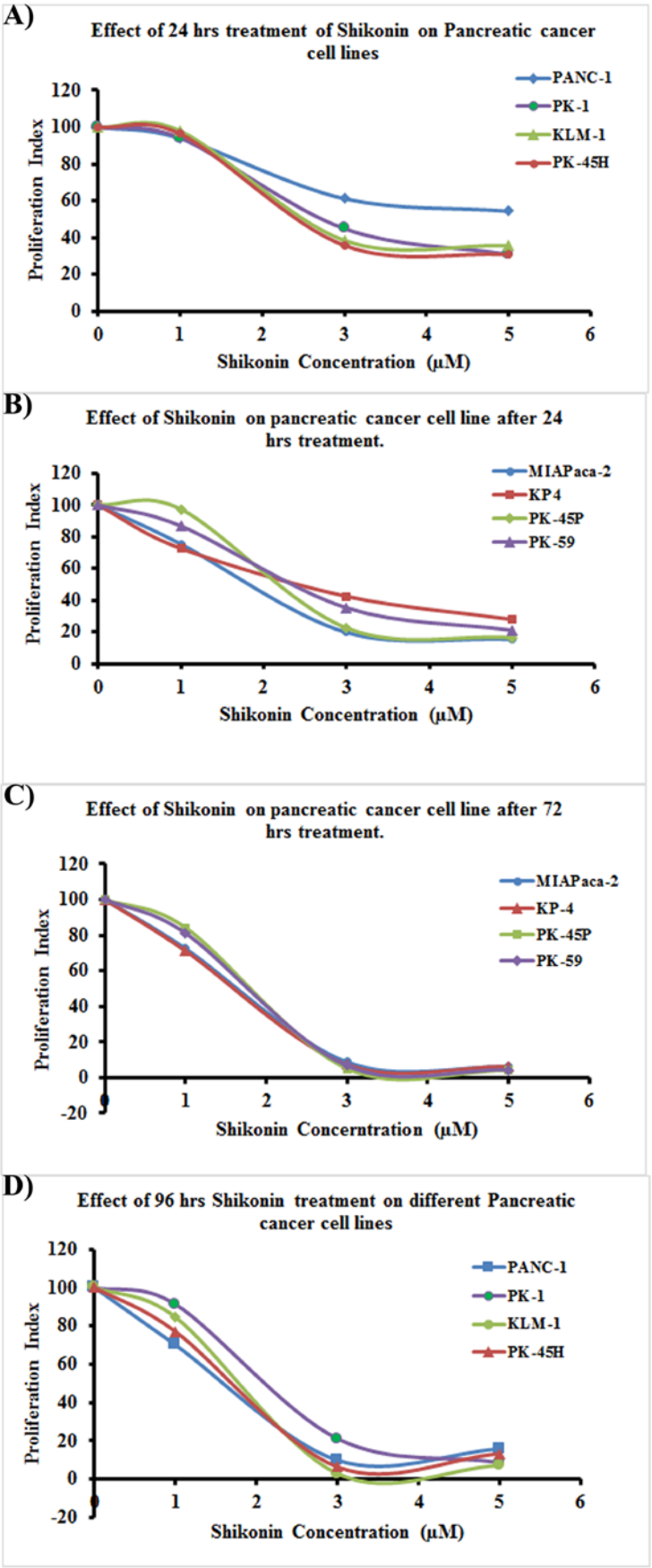

Figure 3.15: The effect of different concentrations of Shikonin on pancreatic cancer cell line proliferation after 24, 72 and 96 hours interaction.

Table 3.6: The effect of Shikonin on pancreatic cancer cell lines proliferation at different time points, expressed by the half maximal inhibitory concentration (IC_{50}).

Pancreatic cancer cell lines	Shikonin treatment (µM)		
	IC_{50} of 24 hrs. (IC_{50} ± SE)	**IC_{50} of 72 hrs. (IC_{50} ± SE)**	**IC_{50} of 96 hrs. (IC_{50} ± SE)**
PK-1	2.98 ± 0.14639	-----	1.976 ± 0.09787
PANC-1	3.97 ± 1.487	-----	1.422 ± 0.37
PK-45H	2.836 ± 0.717	-----	1.471 ± 0.373
KLM-1	3.022 ± 0.726	-----	1.461 ± 0.514
MIAPaca-2	1.81 ± 3.08	1.77 ± 2.92	-----
KP4	2.255 ±7.68	1.747 ± 2.85	-----
PK-45P	1.88 ± 3.16	1.743 ± 2.84	-----
PK-59	2.015 ± 4.93	1.76 ± 2.88	-----

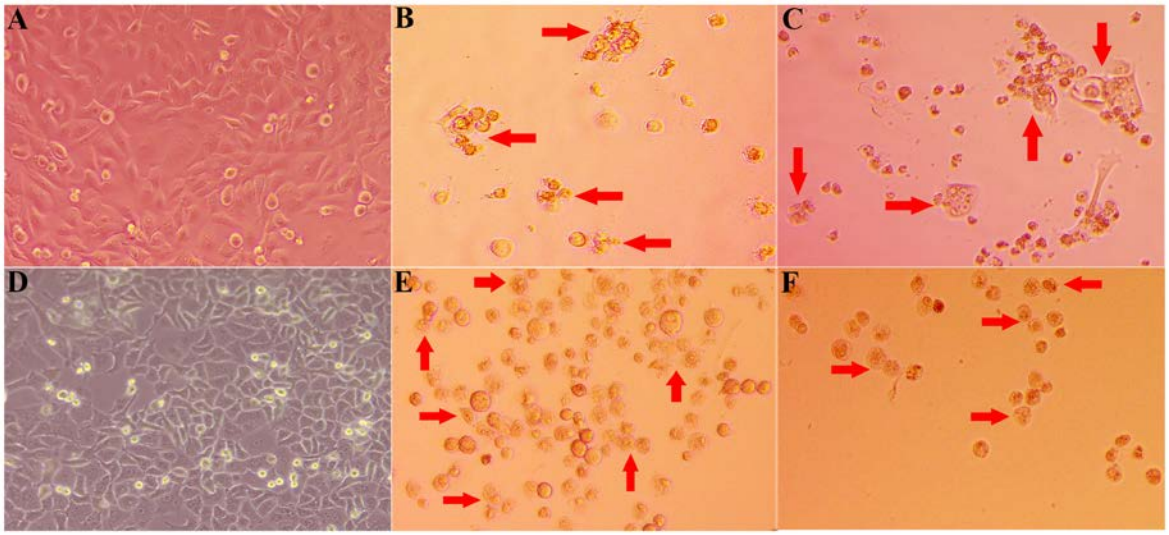

Figure 3.16: The effect of different concentrations of Shikonin on the PK-1 and PANC-1 cell line after 96 hours interaction. **(A)** PK-1 control (DMSO). (**B, C)** PK-1 cells treated with 2.5µM and 5µM Shikonin for 96 hours, red arrows show shrink, morphological change, nuclear breakdown, breakdown of the cell and rupture of cell membrane of PK-1 cells as a response to treatment. **(D)** PANC-1 control (DMSO). **(B, C)** PANC-1 treated with 3µM and 5µM Shikonin for 96 hours, red arrows show shrinkage, morphological change, nuclear breakdown of PNAC-1 cells as a response to treatment.

The enzymatic activity of PKM2 was also evaluated in response to Shikonin treatment in the Miapaca-2 cell line. The Miapaca-2 cells were treated with various concentrations of Shikonin for an hour, following which protein was extracted and the activity of PK measured. As shown in the figure 3.17, PK activity indirectly correlated with Shikonin concentrations and decreased with increasing concentrations of Shikonin. At 40µM of Shikonin concentration, an approximate 70% inhibition of PK activity was observed.

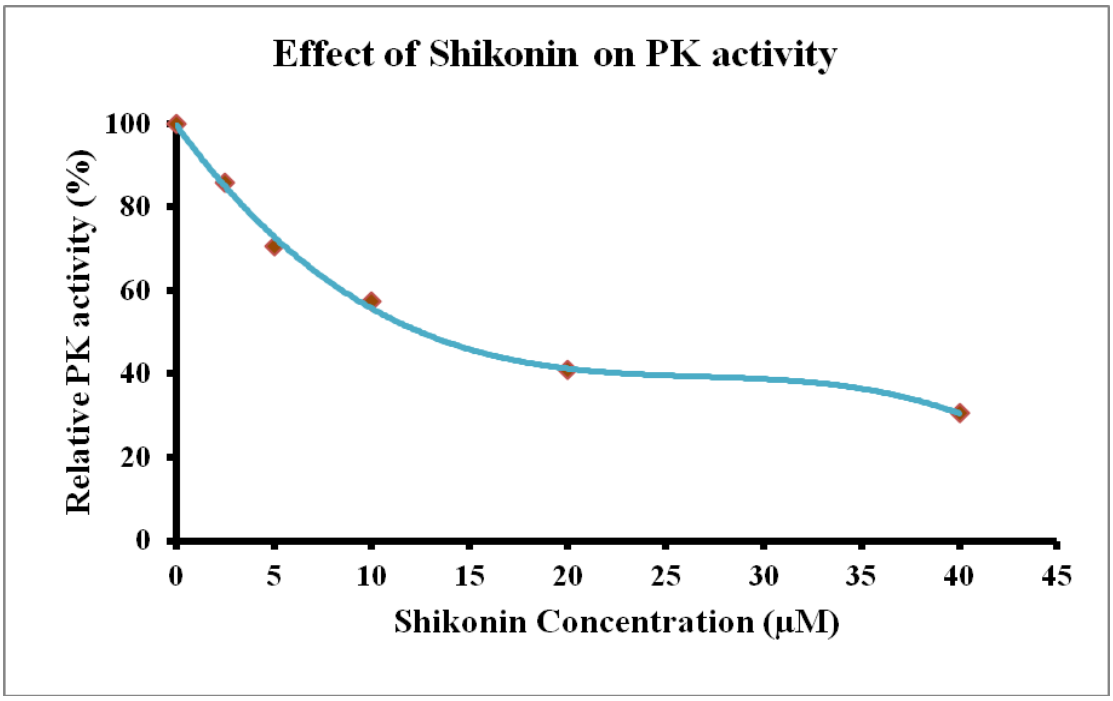

Figure 3.17: Effect of Shikonin on pyruvate kinase activity in the Miapaca-2 cell line.

3.2.1.3: Activation of PKM2 with inhibition of LDHA attenuates pancreatic cancer cell proliferation:

Tetramerisation of PKM2 in combination with LDHA inhibition is a novel strategy for inhibition of pancreatic cancer cell proliferation. To test our hypothesis, I used and optimized two commercially available PKM2 activators (PKM2 activator III, and IV) with an LDHA inhibitor (FX11) to get a maximum inhibitory effect.

3.2.1.4: Combination of PKM2 activator III and FX11:

Pancreatic cancer cell lines were treated with PKM2 activator III (Calbiochem-Merck Millipore Ltd, UK) and LDHA inhibitor (FX11, Toronto Research Chemicals Inc., North York, Ontario, Canada) or a combination of both (concurrent treatment). PKM2 activator III is an N-(4-(4-(2-Methoxyphenyl) piperazine-1-carbonyl) phenyl) quinoline-8-sulfonamide compound and FX11 is a 2, 3-dihydroxy-6-methyl-7-(phenylmethyl)-4-propyl-1-naphthalenecarboxylic acid compound. Miapaca-2 and PK-59 pancreatic cancer cell lines were used for this study, since Miapaca-2 cells have a high expression of both PKM2 and LDHA and the PK-59 cells have a low expression of both. Cells (3000 per well) were plated in 96-well plates and treated at a range of concentrations (0-75 µM) with either PKM2 activator III or FX11 or combination of both for 24, 48, 72 and 96 hours. I found that, activation of PKM2 in combination with LDHA inhibition synergistically inhibited both pancreatic cancer cell lines (Figure 4.5 and Table 4.2). Notably, the combination therapy had a high inhibitory effect and strong synergism in Miapaca-2 cell line for 72 hour exposure time. Treatment with PKM2 activator III alone had minimal effect on pancreatic cancer cell proliferation (IC_{50}< 75 µM), however, when combined with LDHA inhibitor (FX11), a significant reduction in proliferation was observed.

As PKM2 activator III has a very low solubility in DMSO, it was difficult to determine the precise concentration of this agent; therefore, I did not pursue further studies with it.

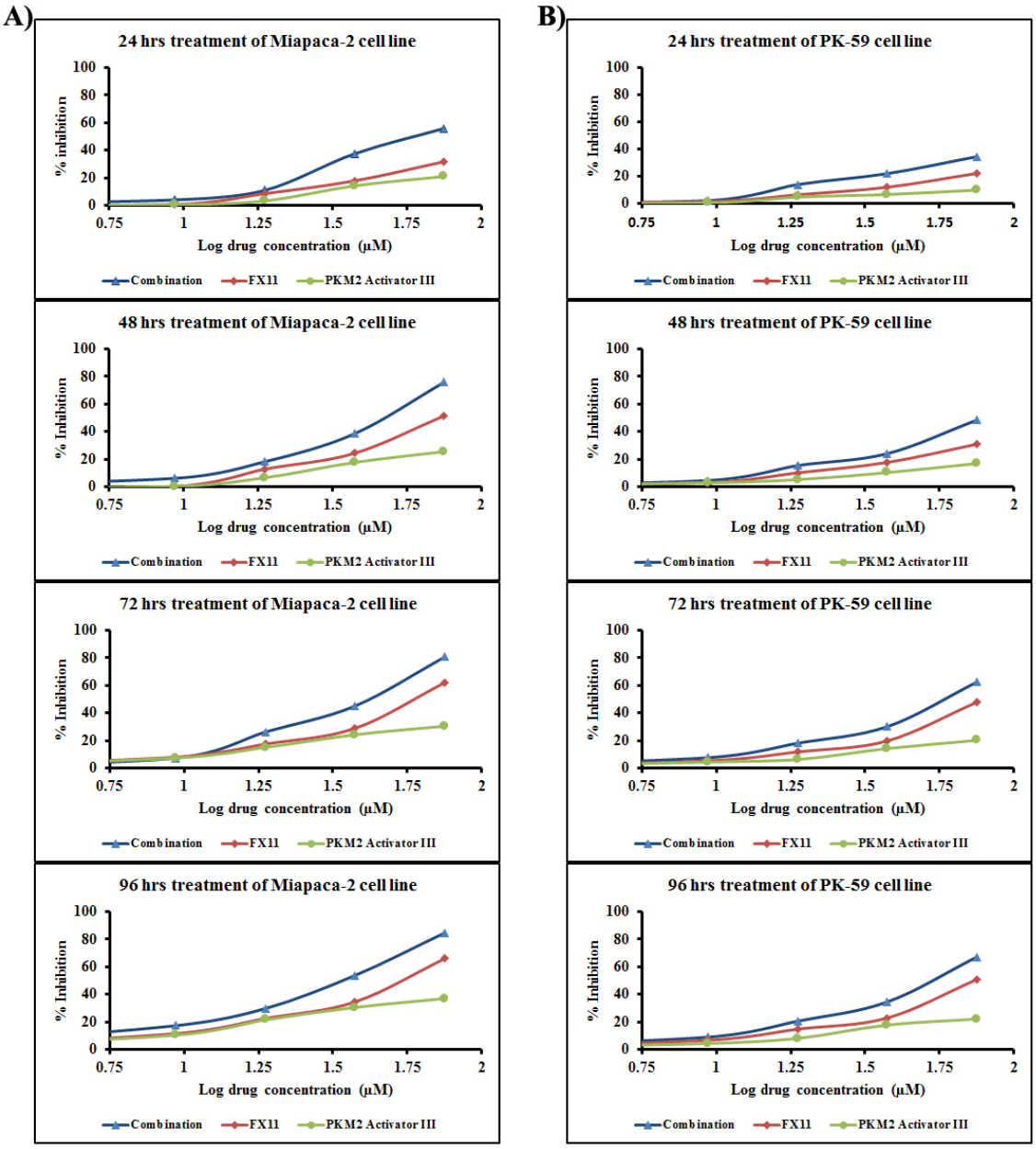

Figure 3.18: Cytotoxicity of PKM2 activator III, LDHA inhibitor (FX11) and combination treatment at different time points.

Table 3.7: The effect of PKM2 activator III, LDHA inhibitor (FX11) and combination treatmnet on Miapaca-2 and PK-59 cell lines proliferation at different time points, expressed by the half maximal inhibitory or activatory concentration (IC_{50}) or (AC_{50}).

Cell line	Time of Interaction	AC_{50} (µM) ± SE	IC_{50} (µM) ± SE	IC_{50} (µM) ± SE	Combination Index	Pharmacological Interaction Results
		PKM2 Activator III	FX11	Combination		
MIAPaca-2	24 hrs	> 75	> 75	60.21 ± 4.25	0.571	Synergism
	48 hrs	> 75	70.14 ± 5.5	44.27 ± 2.24	0.572	Synergism
	72 hrs	> 75	60.54 ± 4.78	39.53 ± 2.42	0.41	Synergism
	96 hrs	> 75	53..93 ± 9.69	33..98 ± 4.7	0.49	Synergism
PK-59	24 hrs	> 75	> 75	> 75	0.67	Synergism
	48 hrs	> 75	> 75	> 75	0.55	Synergism
	72 hrs	> 75	76.92 ± 7.25	64.1 ± 3.63	0.58	Synergism
	96 hrs	> 75	73.1 ± 7.55	59.38 ± 3.37	0.59	Synergism

3.2.1.5: Combination of PKM2 activator IV and FX11:

I sought an alternative activator of PKM2 that has better solubility than PKM2 activator III; I found another commercially available PKM2 activator (PKM2 activator IV), which had a higher aqueous solubility. PKM2 activator IV (TEPP-46) is a 6-((3-Aminophenyl) methyl)-4-methyl-2-methylsulfinylthieno [3, 4] pyrrolo [1, 3-d] pyridazin-5-one compound from Calbiochem-Merck Millipore Ltd, UK. The effects of PKM2 activator IV (TEPP-46) alone or in combination with LHDA inhibitor (FX11) was then evaluated in different pancreatic cancer cell lines.

3.2.1.6: Optimisation of PKM2 activator IV and LDHA inhibitor combination:

In order to obtain maximum effect of the combination therapy on pancreatic cancer cell proliferation *in vitro*, I optimised exposure time and the ratio of PKM2 activator to LDHA inhibitor combination. The Miapaca-2 cell line was used for this study, based on its high expression of both PKM2 and LDHA as described above. The Maipaca-2 cells were treated with PKM2 activator IV (TEPP-46) or LDHA inhibitor (FX11) alone or in combination at a range of concentrations from 2.5µM to 100µM, for 24, 48, 72 and 96 hours exposure times. Our results demonstrate that the maximum inhibitory and synergistic effect was obtained at a combination ratio of one-to-one with a 72-hour exposure time. The details of optimisation are shown in figure 4.6 and Appendix 1.

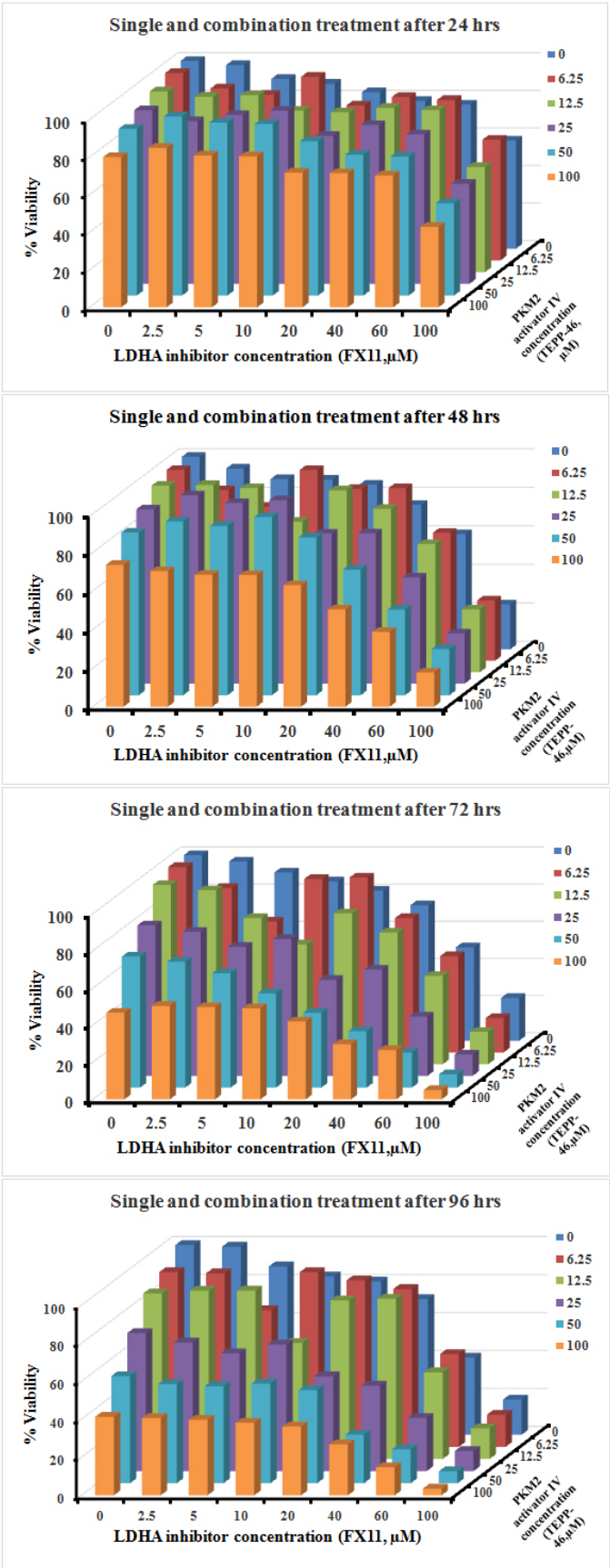

Figure 3.19: Optimization of PKM2 activator IV (TEPP-46) and LDHA inhibitor (FX11) combination and time of treatment.

3.2.1.7: Combination therapy synergistically inhibits pancreatic cancer cell proliferation:

The synergistic effect of combination treatment with PKM2 activator IV (TEPP-46) and LDHA inhibitor (FX11) was investigated in 9 pancreatic cancer cell lines. Based on our results above, a one-to-one concentration ratio of the drugs and 72 hour exposure time was used for treatment of pancreatic cancer cell lines. The AC_{50} and IC_{50} values for TEPP-46, FX11 and combination were then determined. Treatment with TEPP-46 alone, had no significant effect on cell proliferation; however, when combined with FX11, there was a significant reduction in pancreatic cancer cell proliferation (Figure 4.7). The combination treatment had a high inhibitory effect in the Miapaca-2 and BxPc-3 cell lines with an IC_{50} of 40.2 µM and 30.3 µM, respectively.

Further evaluation of synergism of the combination treatment was conducted by calculating the combination index (CI), where 50% growth inhibition was achieved with the treatments. Table 4.3 summarizes the AC_{50} and IC_{50} of TEPP-46, FX-11 and combined drugs, along with the CI of the combination treatment. Combination indices were <1, which indicates synergism for the combination treatment with TEPP-46 and FX-11. The CI for the combination therapy in the Miapaca-2 and BxPc-3 cell lines was 0.48 and 0.45, respectively, which is representative of a strong synergistic effect.

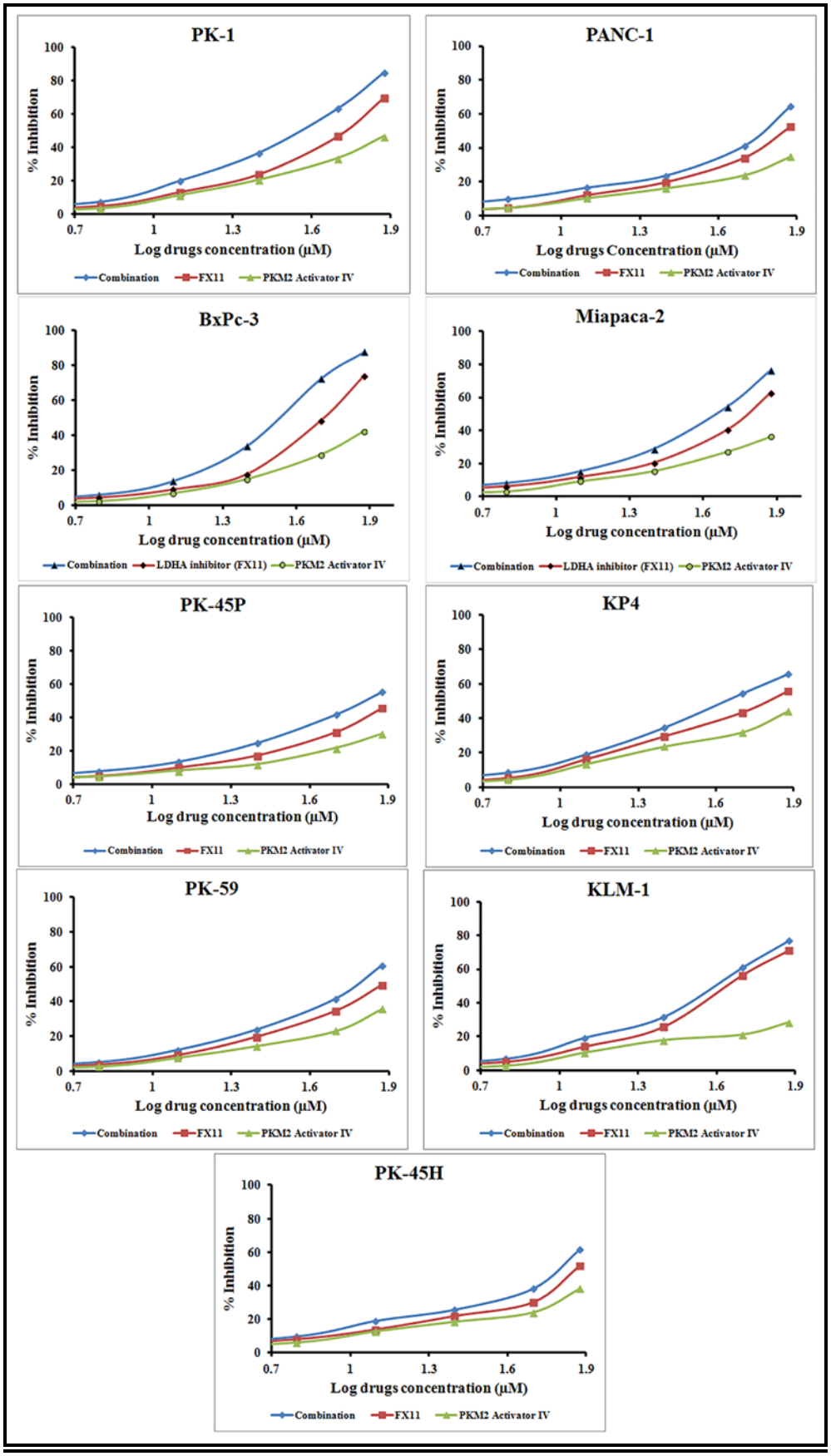

Figure 3.20: Cytotoxicity of PKM2 activator IV (TEPP-46), LDHA inhibitor (FX11) and combination treatment on different pancreatic cancer cell line proliferation after 72 hours of treatment.

Table 3.8: The effect of PKM2 activator IV (TEPP-46), LDHA inhibitor (FX11) and combination treatment on proliferation of different pancreatic cancer cell lines after 72 hours of interaction, expressed by the half maximal inhibitory or activatory concentration (IC_{50}) or (AC_{50}).

Cell line	Time of Interaction	AC_{50} (µM) ± SE	IC_{50} (µM) ± SE	IC_{50} (µM) ± SE	Combination Index	Pharmacological Interaction Results
		PKM2 Activator IV	FX11	Combination		
Miapaca-2	72 hrs	> 75	60.54 ± 3.1	40.21 ± 1.82	0.48	Synergism
BxPc-3	72 hrs	> 75	49.27 ± 1.53	30.32 ± 1.05	0.45	Synergism
KP-4	72 hrs	> 75	58.4 ± 2.25	43.05 ± 1.3	0.61	Synergism
PK45P	72 hrs	> 75	> 75	66.07 ± 2.2	0.51	Synergism
PK-59	72 hrs	> 75	76.92 ± 3.32	59.03 ± 1.53	0.61	Synergism
KLM-1	72 hrs	> 75	43.3 ± 3.66	36.05 ± 2.5	0.52	Synergism
PANC-1	72 hrs	> 75	76.7 ± 3.28	58 ± 1.85	0.59	Synergism
PK-1	72 hrs	> 75	48.8 ± 2.8	30.8 ± 3.18	0.51	Synergism
PK-45H	72 hrs	> 75	> 75	56 ± 2.9	0.516	Synergism

3.2.2: DISCUSSION:

Pancreatic cancer is one of the deadliest malignancies worldwide. Due to the asymptomatic development of pancreatic cancer, early diagnosis of this disease remains a challenge. Palliative chemotherapy is the main treatment option for patients with locally advanced or metastatic disease. Targeting metabolic enzymes, such as PKM2 and LDHA, could be an effective and novel treatment strategy for pancreatic cancer.

The use of PKM2 inhibitor (Shikonin) as a treatment of pancreatic cancer comes from the observation that the down-regulation of the PKM2 gene by siRNA inhibits cancer cell proliferation. Our results demonstrate that inhibition of PKM2 by Shikonin has a strong cytotoxic effect in a number of pancreatic cancer cell lines with an IC_{50} of 1-4 µM. Shikonin can inhibit pancreatic cancer cell proliferation by inhibition of PKM2 enzyme and halt glycolysis, which may finally lead to cell death. The enzymatic activity assay provided the evidence of inhibition of PKM2 by Shikonin in a dose-dependent (Figure 3.17). Our data are consistent with a previous report showing that Shikonin and its analogue can effectively inhibit cancer cell proliferation by the selective inhibition of tumour PKM2 (112). Shikonin not only inhibits the PKM2 enzyme but also affects mitochondrial function, inducing reactive oxygen species (ROS) generation and cell death by apoptosis (191,192).

Shikonin has been shown to induce cell death by apoptosis in several cancer cell lines, including gastric cancer (193), breast cancer (194), bladder cancer (195), ovarian cancer (196), prostate cancer (197) and osteosarcoma cells (192). Wu *el al* (2004) found that high dose Shikonin induces programmed cell death by apoptosis in the early stages of the melanoma cells treatment, while necrosis play a major role in cell death after 48 hour of treatment of those cells (198). Similarly, Yeh *et al* (2015) found that low-dose Shikonin reduces cell viability and induces apoptosis and cellular senescence through the up-regulation of cell cycle expression and apoptosis signaling pathway, while both necrosis and apoptosis were responsible for lung cancer cell death with high dose Shikonin (199). The results of the present study concur with these findings showing pancreatic cancer cell death by both apoptosis and necrosis as a response to Shikonin treatment.

Since inhibition of glycolysis (by inhibiting PKM2) can be toxic to both normal and tumour cells, I decided to evaluate the effects of an PKM2 activator on pancreatic cancer cell proliferation and this strategy might be less toxic to normal cells.

I have previously reported high expression of PKM2 and LDHA in pancreatic cancer patient samples and in pancreatic cancer cell lines. In this context, I hypothesized that targeting PKM2 (activation) and LDHA (inhibition) could effectively reduce pancreatic cancer cell proliferation.

Indeed, our results demonstrate that activation or tetramerisation of PKM2 in combination with the inhibition of LDHA synergistically inhibited pancreatic cancer cell proliferation *in vitro*. As described in the introduction section, PKM2 can be a dimer or tetramer. Its tetrameric isoform is predominately found in normal cells and is involved in direct glycolysis toward energy production, however, its dimeric isoform is generally found in cancer cells, replacing the main pyruvate kinase isoform, driving glycolysis towards the anabolic pathway (76,77,87).

Similarly, LDHA is a key glycolytic enzyme that catalyses the conversion of pyruvate to lactate, which is extruded to the extracellular milieu through the mono-carboxylate transporter 4 (MTC4). Lactate derived from hypoxic tumour cells can be used as a major source of metabolic fuel in well-oxygenated tumour cells. Aerobic tumour cells take up lactate through the MCT1 transporter and use it as a main source of energy, sparing glucose for hypoxic tumour cells. This mechanism provides an alternate source of energy for the survival of tumour cells (135,136).

Therefore, tetramerisation of PKM2 can inhibit the anabolic pathway and deplete glycolytic intermediates, which are precursors for cancer cell proliferation. Inhibition of LDHA can also reduce lactate production, causing a depletion of extracellular lactate, which is used as an energy source in well oxygenated tumour cells and as a consequence, cancer cell proliferation is inhibited.

Finally, the high expression of PKM2 and LDHA can result in chemoresistance and the combination of PKM2 activator and LDHA inhibitor in conjunction with chemotherapy

could be an effective therapy for patients with metastatic pancreatic cancer, prolong survival and overcome chemoresistance.

3.3: Activation of Pyruvate kinase M2 (PKM2) combined with inhibition of Lactate dehydrogenase A (LDH-A) as a novel strategy for the treatment of pancreatic cancer

3.3.1: RESULTS:

3.3.1.1: Pancreatic cancer cell line selection:

To find the suitable pancreatic cancer cell lines for *in vitro* and *in vivo* studies, the expression of PKM2 and LDHA were studied in 10 different pancreatic cancer cell lines (Miapaca-2, BxPc-3, PANC-1, PK-1, PK45H, PK-45P, PK-59, KP-4, KLM-1, NOR-P1) at two different stages of cell culture. The expression of these two enzymes was evaluated by Western blot in the proliferative and non-proliferative stage (50% and ~ 90% confluency, respectively).

I found that Miapaca-2, BxPc-3 and PK-1 cell lines had a stable and relatively high expression of PKM2 and LDHA in both stages of cell culture (see Figure 4.1). Therefore, I conducted the remainder of the studies in the BxPc-3 and Miapaca-2 cell lines. Moreover, BxPc-3 cells were stably transfected with the firefly luciferase gene (luc2), to help assess *in vivo* tumour growth.

3.3.1.2: Combination therapy synergistically inhibits pancreatic cancer cell proliferation:

The effect of TEPP-46 and FX11 alone or in combination on BxPc-3 and Miapaca-2 cell proliferation were assessed. Briefly, TEPP-46 and FX11 alone or in combination were applied for 72 hour to both cell lines. Half maximal inhibitory (IC_{50}) and activatory (AC_{50}) concentration of FX11, TEPP-46 and combination were assessed and compared to each other. Treatment with PKM2 activator IV, TEPP-4, did not have a significant effect on a pancreatic cancer cell proliferation; however, when combined with the LDHA inhibitor, FX11, a significant reduction in pancreatic cancer cell proliferation was observed. As shown in figure 5.1, the combination therapy curve was shifted to the left compared to single treatment curves. The IC_{50} of the combination therapy was 40.2 and 30.3 µM for the Miapaca-2 and BxPc-3 cell lines, respectively (Table 5.1).

To further evaluate synergism of combination treatment, the combination index (CI) of 50% inhibitory was calculated. Combination index values were < 1, indicating synergism for the combination of TEPP-46 and FX11 in both Miapaca-2 and BxPc-3 cell line (Table 5.1).

Miapaca-2 and BxPc-3 cell lines were also stained with haematoxylin to microscopically show the effect of the combined treatment on cell histology and viability (Figures 5.2 and 5.3). As shown in figures 5.2 and 5.3, combination therapy was highly toxic, in a concentration of 75 µM significantly reduced the number of viable cells compared to the DMSO control or single treatment.

The inhibitory effect of single and combination treatment was also evaluated by evaluating bioluminescence in BxPc-3 cells. Following single or combin9bation treatment for 72 hour, cells were incubated with D-luciferin (VivoGlo™ Luciferin, *In Vivo* Grade, Promega UK Ltd, UK) for 10 minutes and bioluminescence was detected with IVIS (IVIS Lumina 100, PerkinElmer, Caliper LifeSciences, USA) (Figure 5.4). Consistent with the MTS assay and haematoxylin staining, the combination treatment had a high cytotoxic effect on BxPc-3 cells, and only few viable cells were detected at a concentration of 75µM.

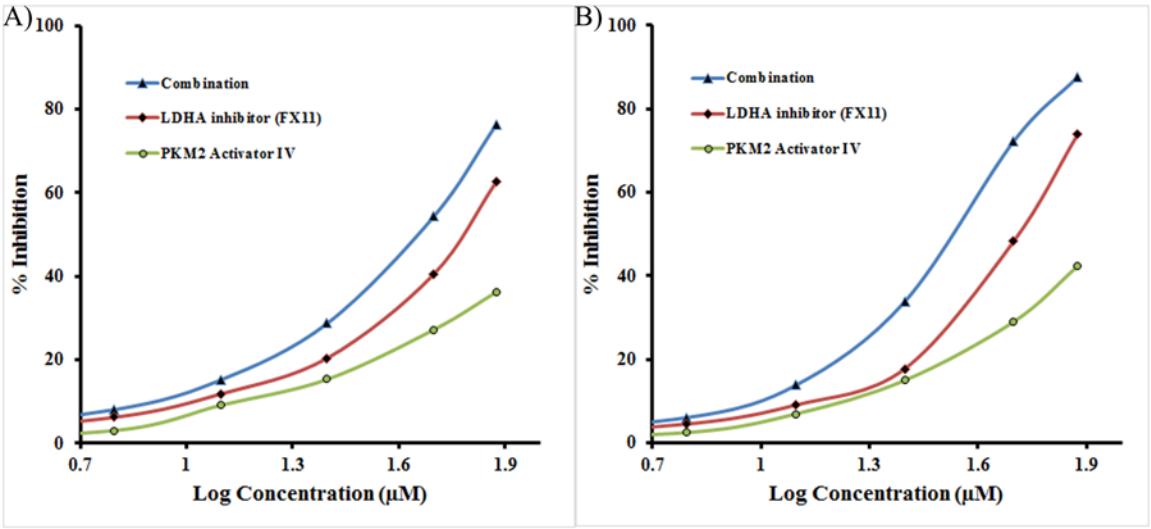

Figure 3.21: The effect of single and combination therapy on **(A)** Miapaca-2 and **(B)** BxPc-3 cell lines. Combination therapy synergistically attenuated cell proliferation and the curve shifted to the left compared to the single treatment.

Table 3.9: Summary of the effects of single and combination treatment on pancreatic cancer cell proliferation at different time points expressed by the half maximal inhibitory or activatory concentration (IC_{50} or AC_{50}).

Cell line	Time of Interaction (Hours)	AC_{50} (µM) ± SE	IC_{50} (µM) ± SE	IC_{50} (µM) ± SE	Combination Index	Pharmacological Interaction Results
		PKM2 Activator IV	FX11	Combination		
MIAPaca-2	72	> 75	60.54 ± 3.1	40.21 ± 1.82	0.48	Synergism
BxPc-3	72	> 75	49.27 ± 1.53	30.32 ± 1.05	0.45	Synergism

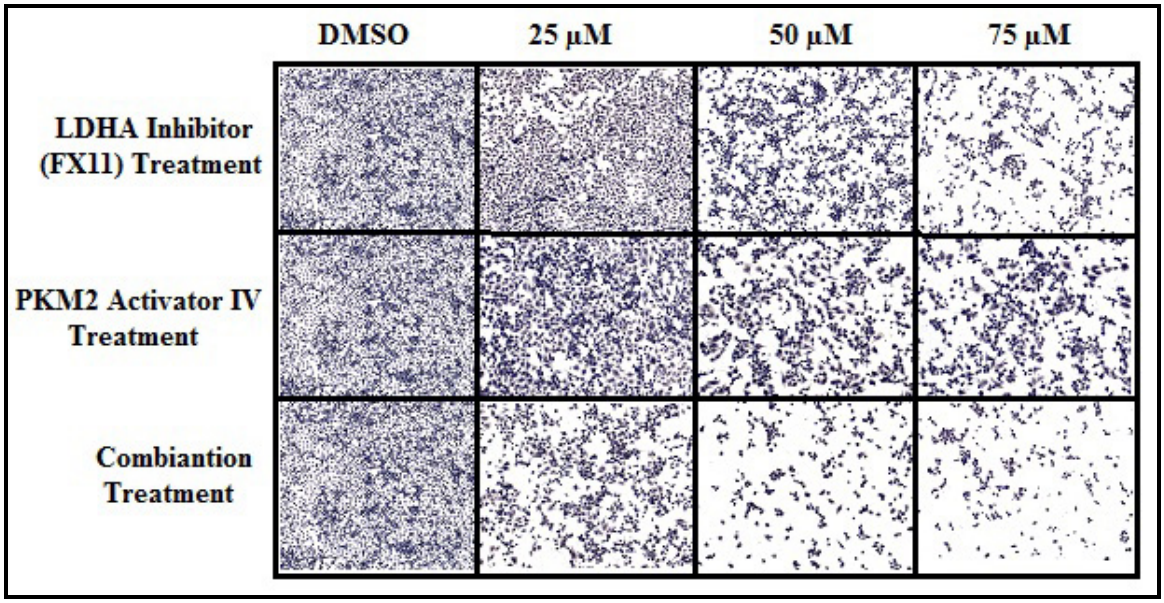

Figure 3.22: Effect of single and combination therapy on Miapaca-2 cell viability. After 72 hours of treatment, cells were washed and fixed in ice cold absolute methanol and permeabilized with 0.25% triton X-100 in PBS and stained with haematoxylin.

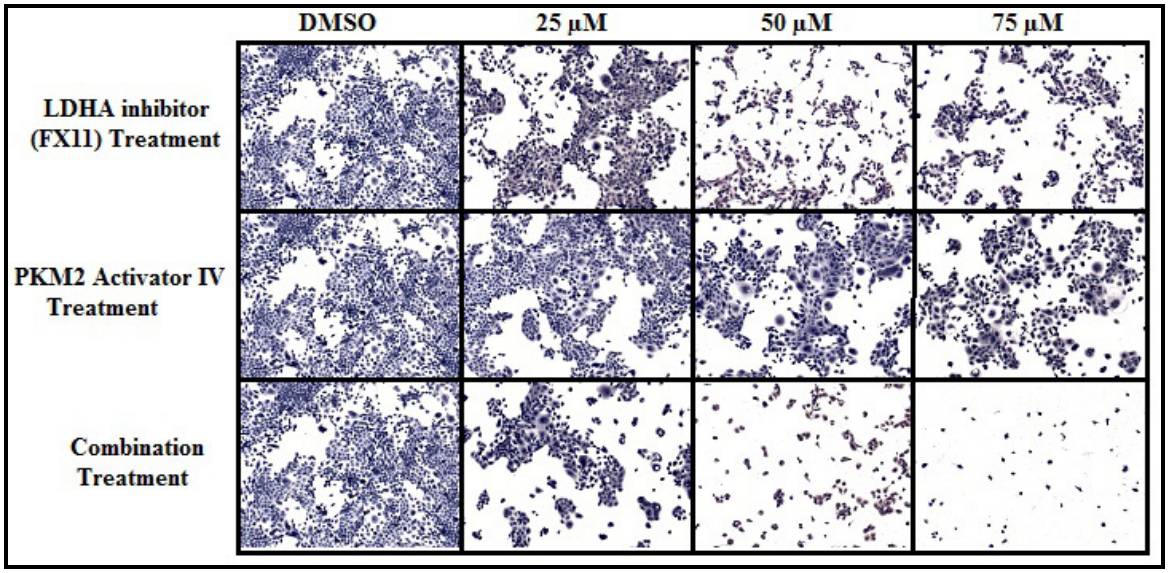

Figure 3.23: Effect of single and combination therapy on BxPc-3 cell viability. After 72 hours of treatment, cells were washed and fixed in ice cold absolute methanol and permeabilised with 0.25% triton X-100 in PBS and stained with haematoxylin.

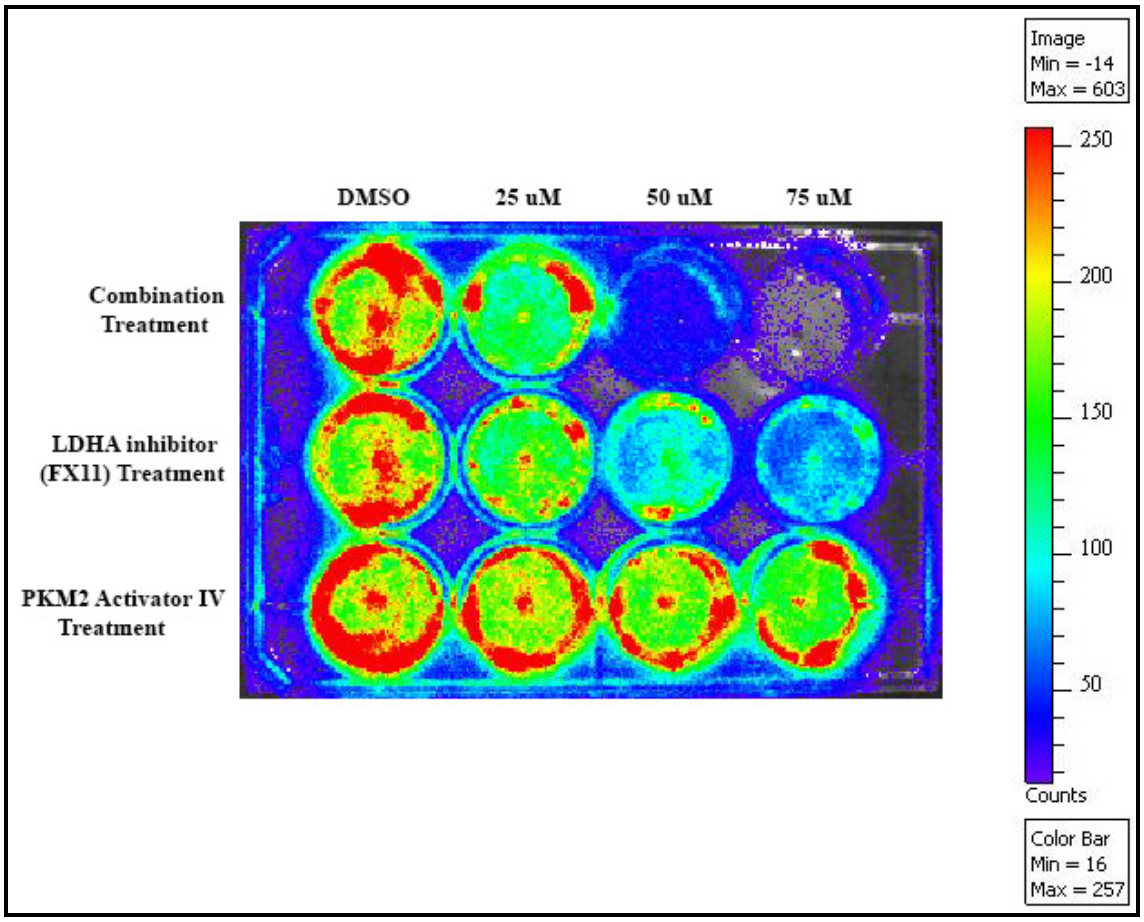

Figure 3.24: Effect of single and combination treatment on the BxPc-3 cells compared to DMSO control. After 72 hours of treatment cells were incubated for 10 min with D-luciferin; bioluminescence was detected by using IVIS.

3.3.1.3: PK and LDH activity measurement:

To confirm that the inhibitory effect of pancreatic cancer cell proliferation was due to the activation of PKM2 and inhibition of LDHA, PK and LDH activity was evaluated in treated and in DMSO control cells. Miapaca-2 and BxPc-3 cells were seeded in 6 well-plates and treated with different concentrations of either TEPP-46 or FX11 (from 0-100 µM) for 6 hours, PK and LDH activity were then measured by a commercially available PK and LDH activity assay Kit (BioVision, USA) and compared with control. A positive correlation between PKM2 activator IV (TEPP-46) concentration and PK activity was observed. PK activity gradually increased with increasing TEPP-46 concentration; at a concentration of 100µM, PK activity was increased by ~2.5 fold in both Miapaca-2 and BxPc-3 cells compared to DMSO treated cells (Figure 5.5). However, LDH activity in treated cells gradually decreased with increasing FX11 concentrations; at a concentration of 100 µM, LDH activity in both Miapaca-2 and BxPc-3 cells decreased by ~70% compared to DMSO treated cells (Figure. 5.5).

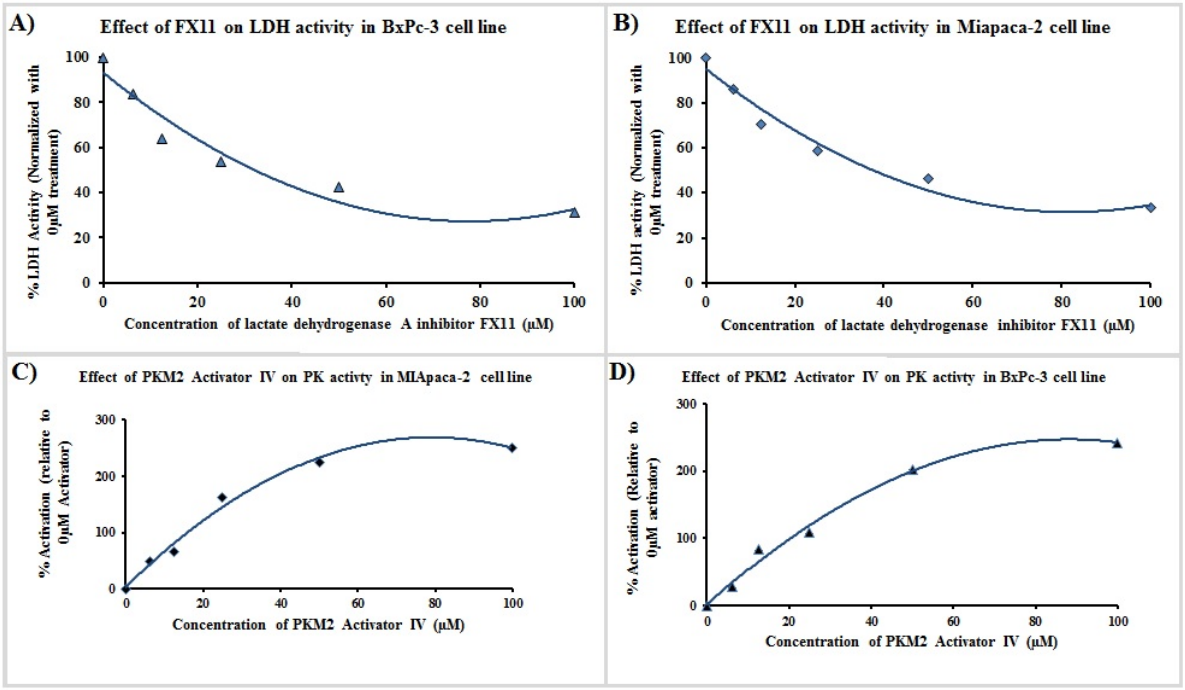

Figure 3.25: Effect of different concentrations of PKM2 activator IV (TEPP-46) and LDHA inhibitor (FX11) on PK and LDH activity in Miapaca-2 and BxPc-3 cell lines.

3.3.1.4: Combination therapy synergistically attenuates tumour xenograft growth:

The effect of the combination therapy was further investigated *in vivo*, in mice bearing Miapaca-2 or BxPc-3 tumour xenografts. Mice were treated with single or combination agent therapy and compared to vehicle control groups. Miapaca-2 xenografts were relatively aggressive and fast growing compared with the BxPc-3^{Luc2} xenografts.

3.3.1.4.1 : Mice bearing Miapaca-2 tumour xenografts:

Immunocompromised mice were injected with $6x10^6$ Miapaca-2 cells in the right flank. Tumours were left to grow for 2 weeks and mice were randomly divided into following four groups: (1) high-dose combination therapy (25 mg/kg TEPP-46 + 2 mg/kg FX11), (2) low-dose combination therapy (13 mg/kg TEPP-46 + 1 mg/kg FX11), (3) LDHA inhibitor therapy (2 mg/kg FX11) and (4) vehicle control. Mice in the high-dose combination and vehicle control groups received daily intraperitoneal (IP) injections of drugs and solvent, respectively. Mice in the low-dose combination and LDHA inhibitor therapy groups had an osmotic pump (Alzet micro-osmotic pump, model 1004, Cupertino, CA, USA) implanted intraperitoneally for drugs delivery. The osmotic pumps were characterized by reservoir volume of 100µl and a pumping rate of 0.11µl/hr for the duration of 28 days. Briefly, pumps were filled with 100µl of FX11 (53.8mM) or with 100 µl of FX11 and TEPP-46 (53.8mM and 0.47M, respectively). Mice were weighed and tumour volumes measured (digital Caliper) twice weekly throughout the duration of therapy, which lasted 3 weeks.

The combination therapy significantly delayed tumour growth compared to the vehicle control ($p < 0.0001$, Kruskal-Wallis test, Figures 5.6). As shown in the figure 5.6, no significant differences between tumour volumes were observed between high-dose combination and vehicle control groups up to day 13; however, past that day, the high-dose combination treatment significantly delayed tumour grow and tumour volume was significantly smaller than in vehicle control group ($p < 0.0001$, Kruskal-Wallis test, Figures 5.6 and 5.7).

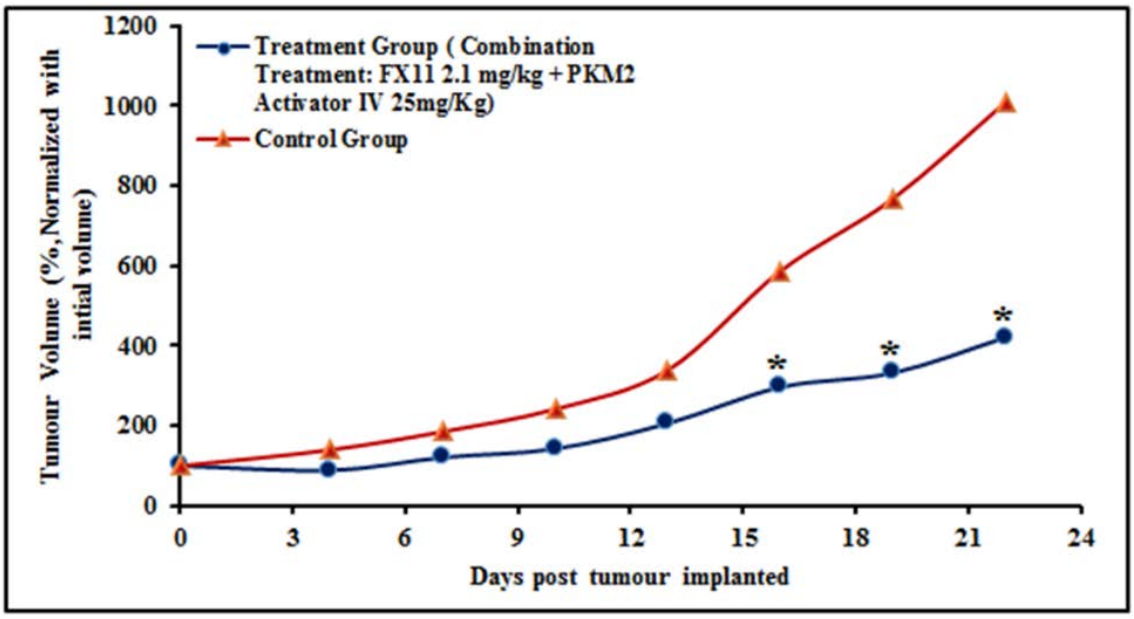

Figure 3.26: Tumour growth curve over 21 days treatment.

No significant differences were detected in tumour volume between low-dose combination and LDHA inhibitor groups compared to the vehicle control group. It is likely that the drug formulation (FX11 and TEPP-46) crystallised inside the osmotic pumps as a result of poor solubility, which could have altered drug release. Furthermore, the physiological body temperature of the mice and the duration of the study could have promoted drug crystallisation inside the osmotic pumps, as observed upon mouse sacrifice at the end of the study. Blood sample analysis and IHC staining for PKM2 and LDHA also showed no effect of low-dose combination and FX11 treatment on activity of these two glycolytic enzymes in the blood and the expression in tumour tissues, confirming a lack of drug delivery through the osmotic pumps.

IHC analysis of tumour sections from the high-dose combination group showed lower expression of PKM2 and LDHA compared with the vehicle control group. Similarly, activity of PK and LDH in plasma samples was significantly different in the high-dose combination group compared with vehicle control group ($P < 0.0001$, Kruskal-Wallis Test). Plasma PK and LDH activity was 2-fold higher and ~60% lower, respectively, in the high-dose combination group compared with the vehicle control group. No significant differences in PKM2 and LDHA expression were observed in tumour

sections nor in plasma activity of PK and LDH in the low-dose combination or LDHA inhibitor treated groups compared to the vehicle control group.

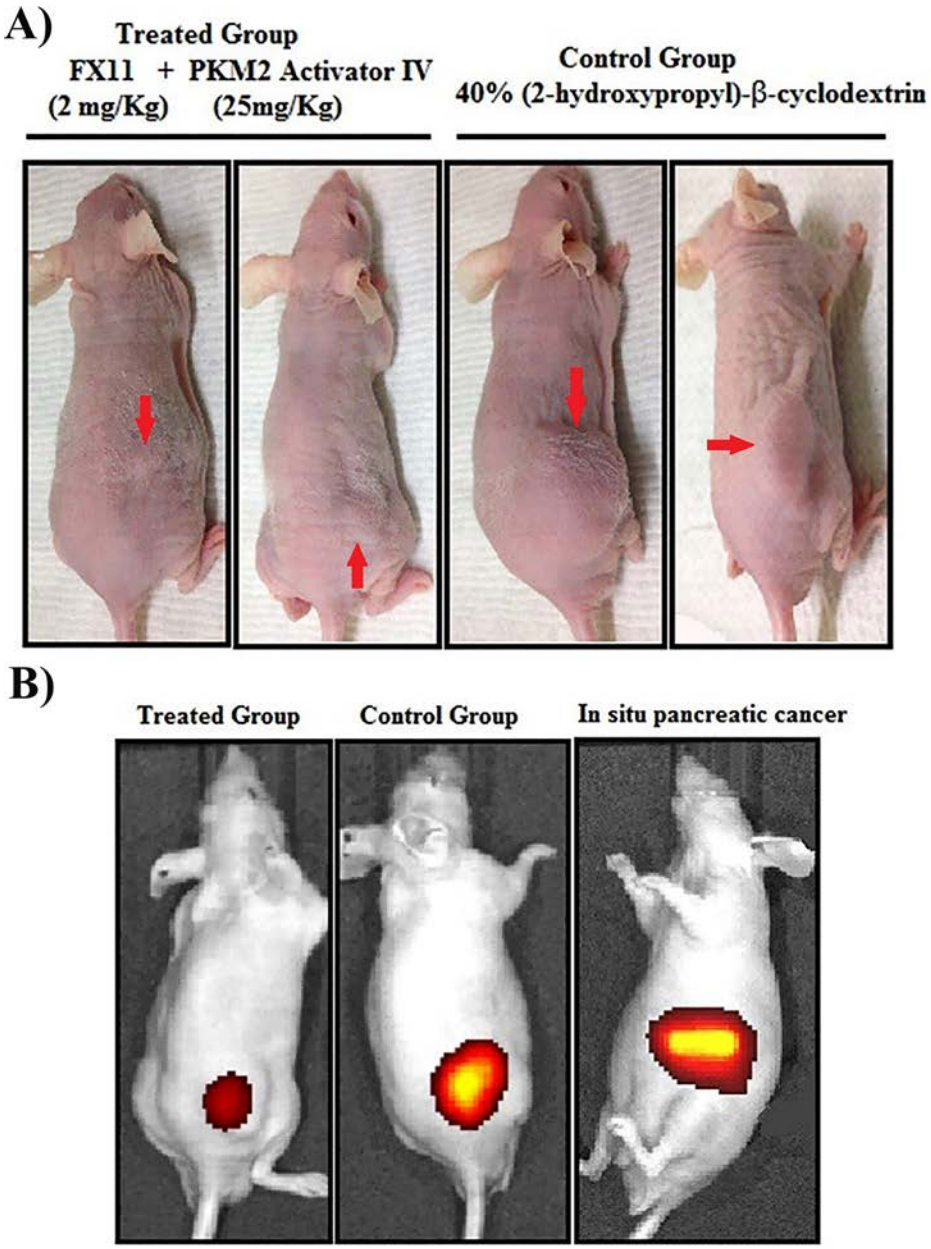

Figure 3.27: Miapaca-2 xenograft tumours in mice from different treatment groups. **A)** Xenograft tumour size (red arrow) of high-dose combination group compared to the vehicle control group. **B)** Tumour xenografts in high-dose combination, vehicle control and in situ pancreatic cancer groups, the cell line was stained with DIL fluoresce dye and the fluorescence signal was detected by IVIS machine.

3.3.1.4.2 : Mice bearing BxPc-3 tumour xenografts:

To further confirm the effect of the combination therapy, subcutaneous and orthotopic tumour xenografts were established with BxPc-3^{Luc2} cells. Briefly, $6X10^6$ BxPc-3 cells were injected in the right flank of mice for subcutaneous xenografts or surgically implanted into the pancreas for the generation of orthotopic xenografts.

In this experiment, mice bearing subcutaneous BxPc-3 xenografts were treated with vehicle control, high-dose combination (30 mg/kg TEPP-46 + 2.1 mg/kg FX11), low-dose combination (15 mg/kg TEPP-46 + 1.5 mg/kg FX11), LDHA inhibitor (2.1 mg/kg FX11) and PKM2 activator IV (30 mg/kg TEPP-46). Mice bearing BxPc-3 orthotopic xenografts were administered either vehicle control or high-dose combination treatment. The treatment regimen was continued for three weeks; mice were weighed and tumour volumes measured thrice per week; bioluminescent images were obtained at the beginning and end of the therapy.

High-dose and low-dose combination therapy and FX11 treatment significantly delayed tumour growth compared to the vehicle control ($p < 0.0001$, Kruskal-Wallis Test, Figure 5.8). Tumour volume in high-dose combination treated group was also significantly smaller than tumour volume in low-dose combination, FX11 and PKM2 activator IV treated groups ($p= 0.03$, $p= 0.018$ and $p < 0.001$, respectively, Kruskal-Wallis Test, Figures 5.8, 5.9 and 5.10).

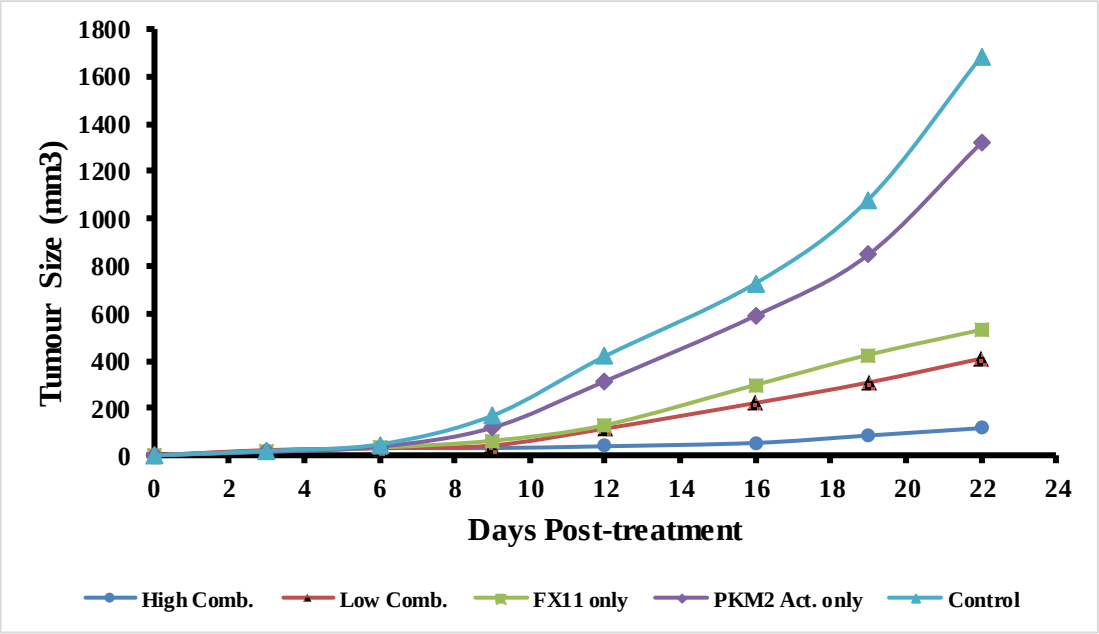

Figure 3.28: Tumour growth curve over 21 days treatment.

As shown in figure 5.8, high-dose combination was effectively impaired tumour growth and the tumour volume remained static over the experiment. However, there were no significant differences in tumour growth between PKM2 activator IV and vehicle control groups. Bioluminescence imaging revealed similar results (Figures 5.9 and 5.10). At the end of therapy, tumour weights from the high-dose and low-dose combination therapy and FX11 treatment groups were significantly lower compared with vehicle control group tumours ($p < 0.0001$ and $p = 0.001$, respectively, Kruskal-Wallis Test, Figures 5.10 and 5.12A). Tumour weight in high-dose combination treated group was also significantly lower than tumour weights in low-dose combination, FX11 and PKM2 activator IV treated groups ($p= 0.023$, $p= 0.016$ and $p < 0.001$, respectively, Kruskal-Wallis Test, Figures 5.10 and 5.12A). No significant differences were observed in tumour weight from the PKM2 activator IV treated and vehicle control groups (Figures 5.10 and 5.12A).

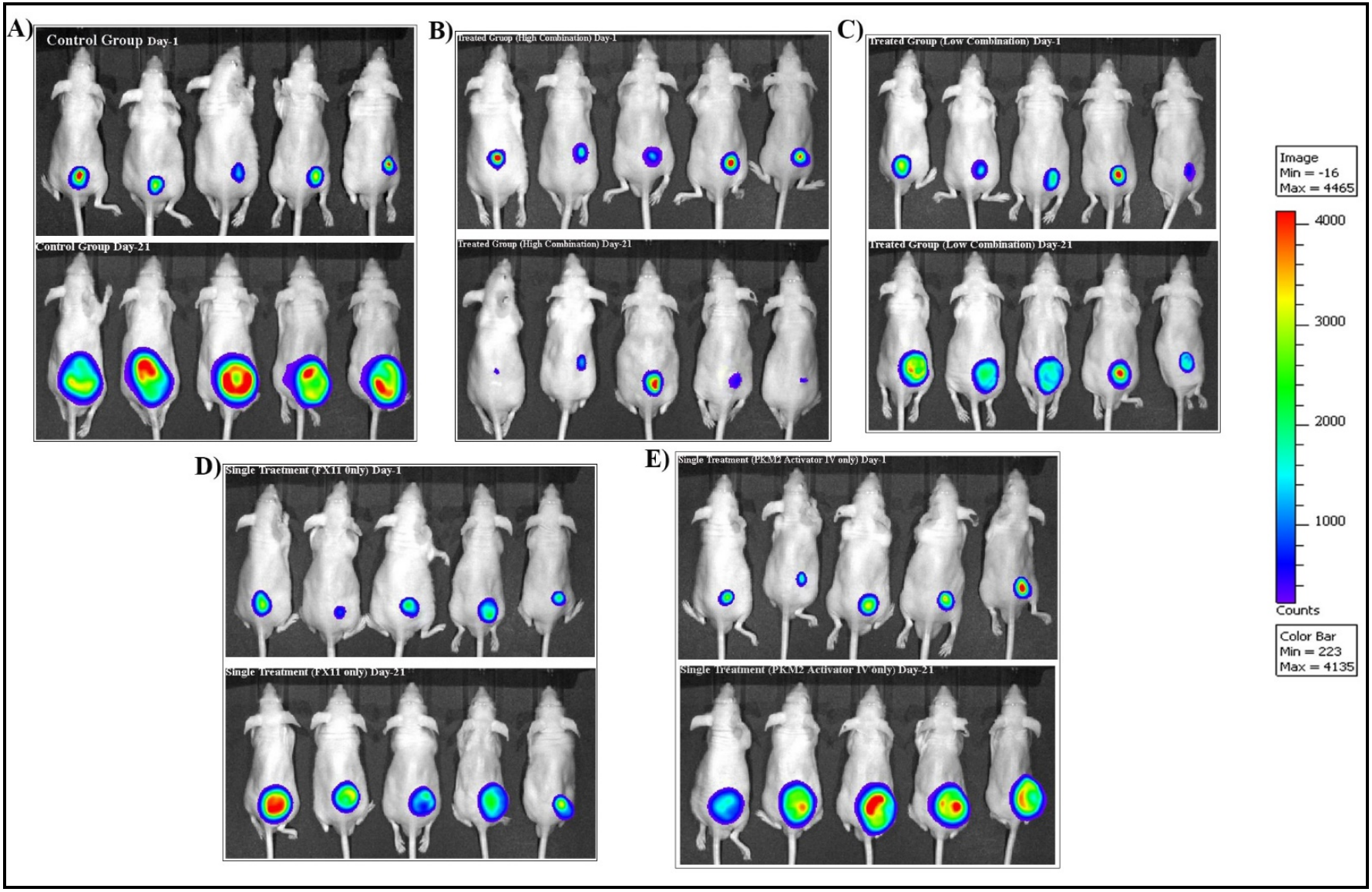

Figure 3.29: Effect of single and combination treatment on subcutaneous tumour growth compared to the control group. A) vehicle-control group. B) High-dose combination treated group. C) Low-dose combination treated group. D) Lactate dehydrogenase inhibitor treated group. E) PKM2 activator treated group. In the beginning and after 21 days of treatment.

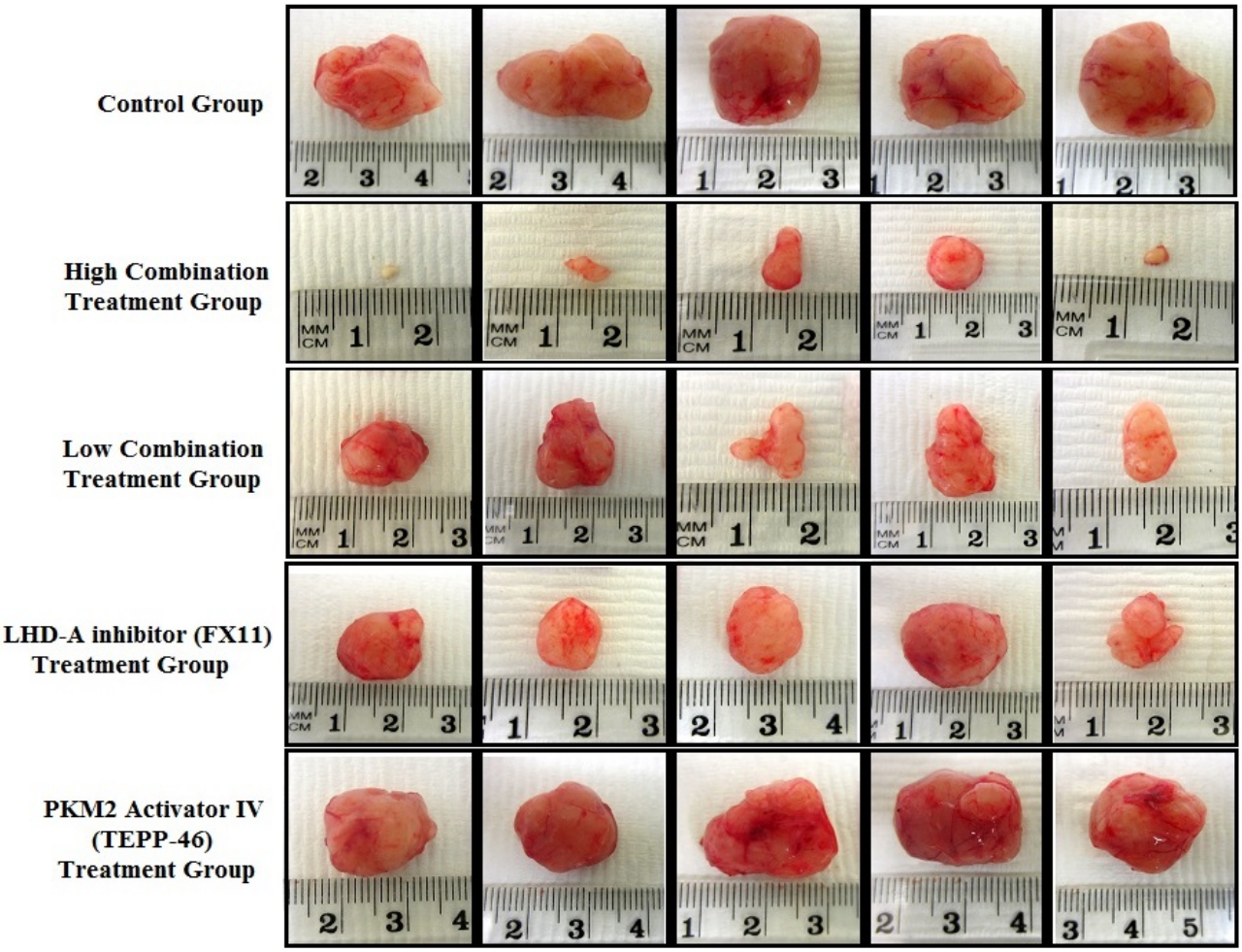

Figure 3.30: Effect of single and combination treatment on size of subcutaneous tumours after 21 days of treatment compared to the control group.

Similarly, the high-dose combination therapy significantly impaired tumour growth in the orthotopic tumour model and the tumour weight was significantly lower than in orthotopic control group (p=0.014, Kruskal-Wallis Test, Figures 5.11 and 5.12B). As shown clearly in the figure 3.33, the high-dose combination therapy also abolished liver and spleen metastases in orthotopic treated group and metastases were only found in the orthotopic control group, while there was no metastases detected in any animal in orthotopic treated group.

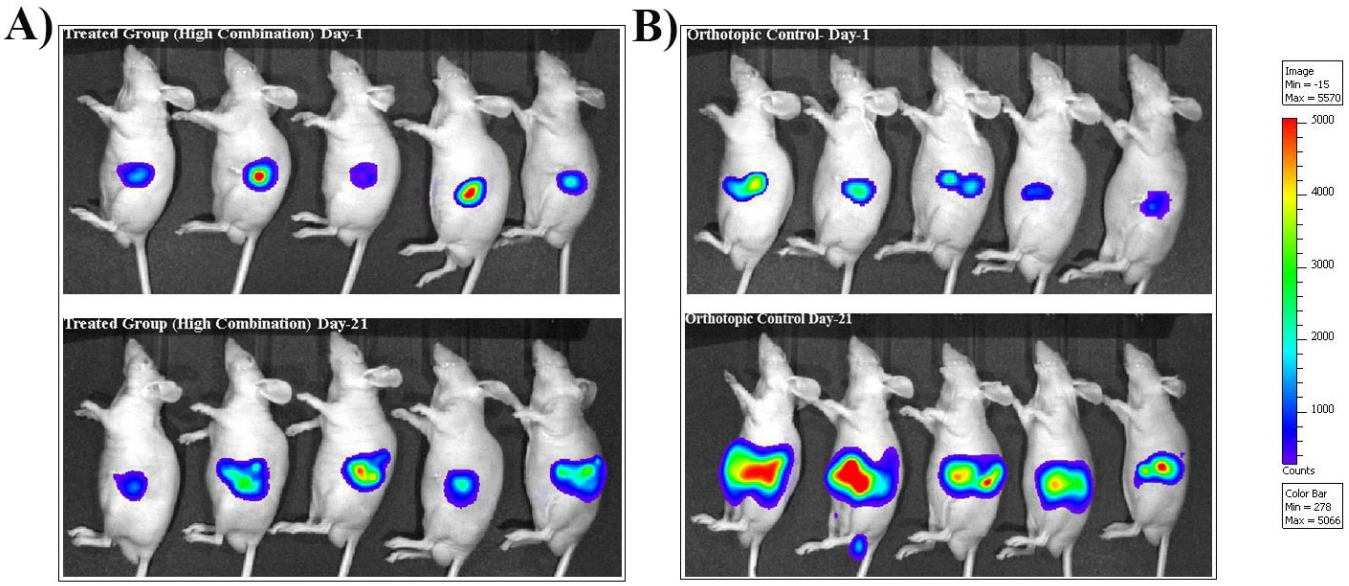

Figure 3.31: Effect of high-dose combination therapy on orthotopic tumour growth compared to the control group. A) High-dose combination treated group. B) Vehicle-control group. In the beginning and after 21 days of treatment.

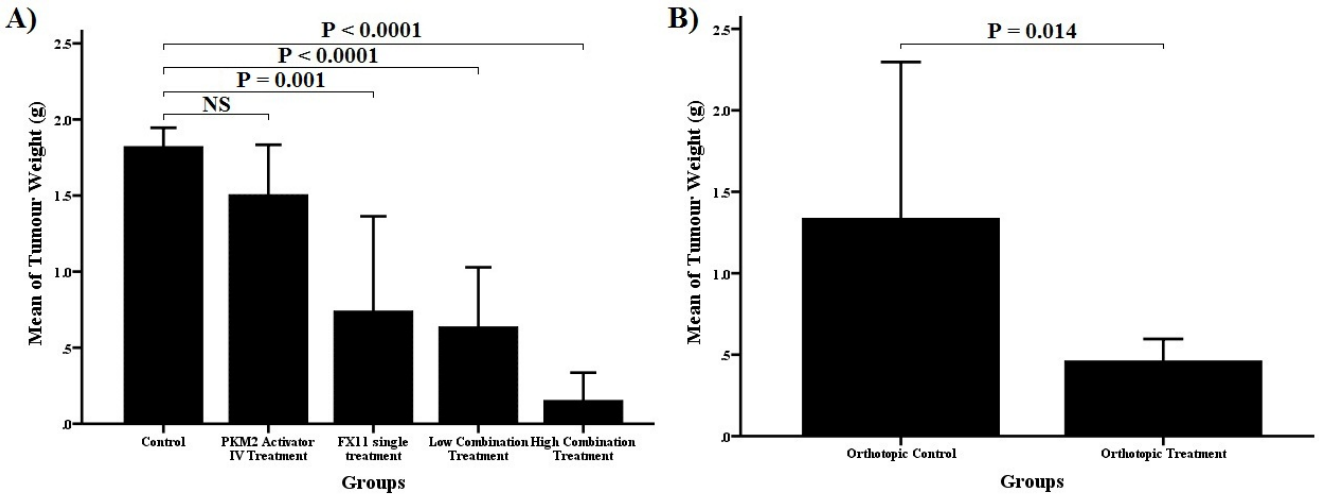

Figure 3.32: Subcutaneous and orthotopic tumour weight after 21 days of treatment. Effect of single and combination therapy on tumour weight compared with vehicle control group (Bar chart, 95% CI).

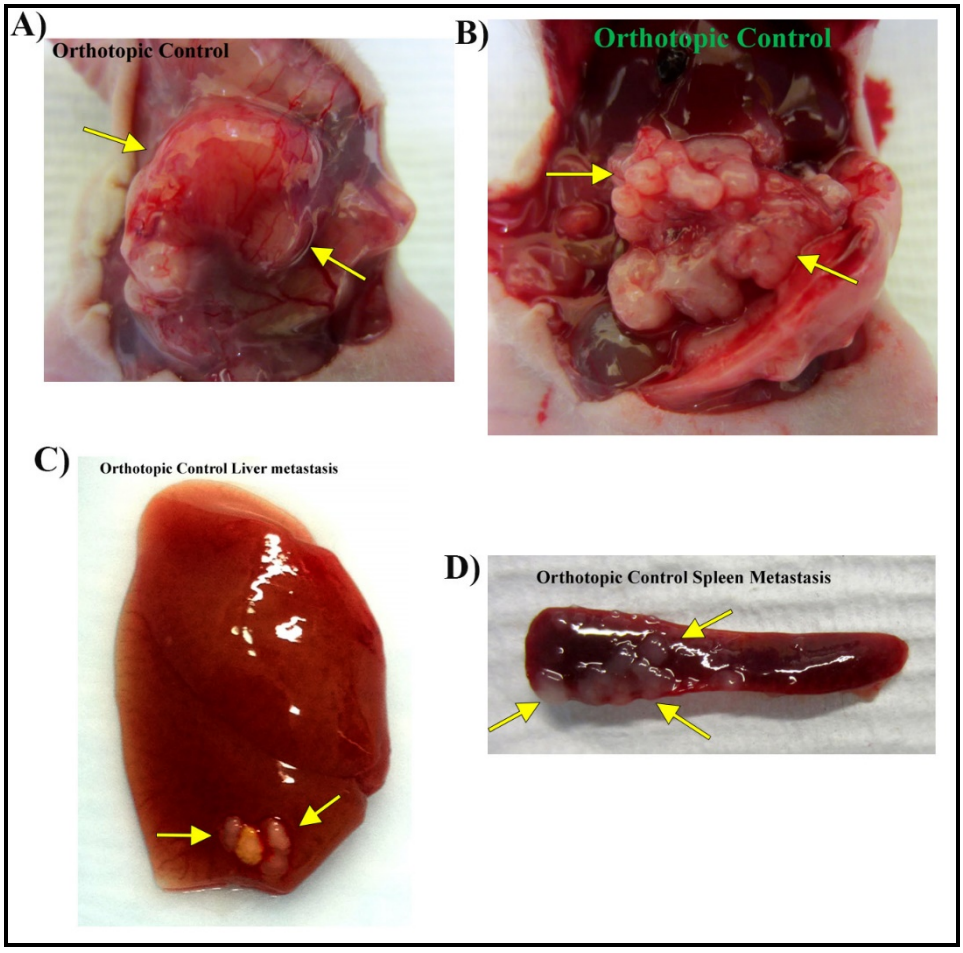

Figure 3.33: Tumour volume, liver and spleen metastasis in orthotopic control group. **(A, B)** Tumour volume was significantly higher in orthotopic controls compared to the treatment group. **(C, D)** Liver and Spleen metastasis in orthotopic controls (yellow arrows), treatment abolished liver and spleen metastasis.

3.3.1.5: Histopathological analysis of tumour sections:

Approximately an hour after the last injection, mice were sacrificed, blood was collected and tumours harvested and weighed; half were formalin fixed and half were liquid nitrogen frozen for later analysis. Following tissue processing, tumour sections were cut and stained with haematoxylin and eosin and also immunohistochemically stained with anti-PKM2, anti-LDHA, anti-Ki67 and anti-CD8 antibodies.

I found that the number of Ki67-positive cells was significantly lower in tumour sections from high-dose combination, low-dose combination and FX11 treated groups compared with the vehicle control group ($p < 0.001$, Kruskal-Wallis Test, Figures 5.14 and 5.15). The number of Ki67-positive cells was also significantly lower in tumour sections from high-dose combination treated group compared with the number of Ki67-positive cell in low-dose combination, FX11 and PKM2 activator IV treated groups ($p < 0.001$, Kruskal-Wallis Test, Figures 5.14 and 5.15). There was no significant difference in number of Ki67-positive cells between the PKM2 activator IV treated and control groups.

PKM2 and LDHA expression was also evaluated in tumour sections (Figure 5.15). PKM2 and LDHA expression was lower in tumour sections from the high-dose, low-dose combination and FX11 treated groups compared with the control group, whereas expression in sections from the PKM2 activator IV treated group was slightly lower than the control group (Figure 5.15).

Although CD8+TIL staining was not detected in the subcutaneous xenografts, high expression was detected in orthotopic tumours from the combination treatment group (Figure 5.16). These results are suggestive of immune cell reactivation in response to the combination treatment in the orthotopic model.

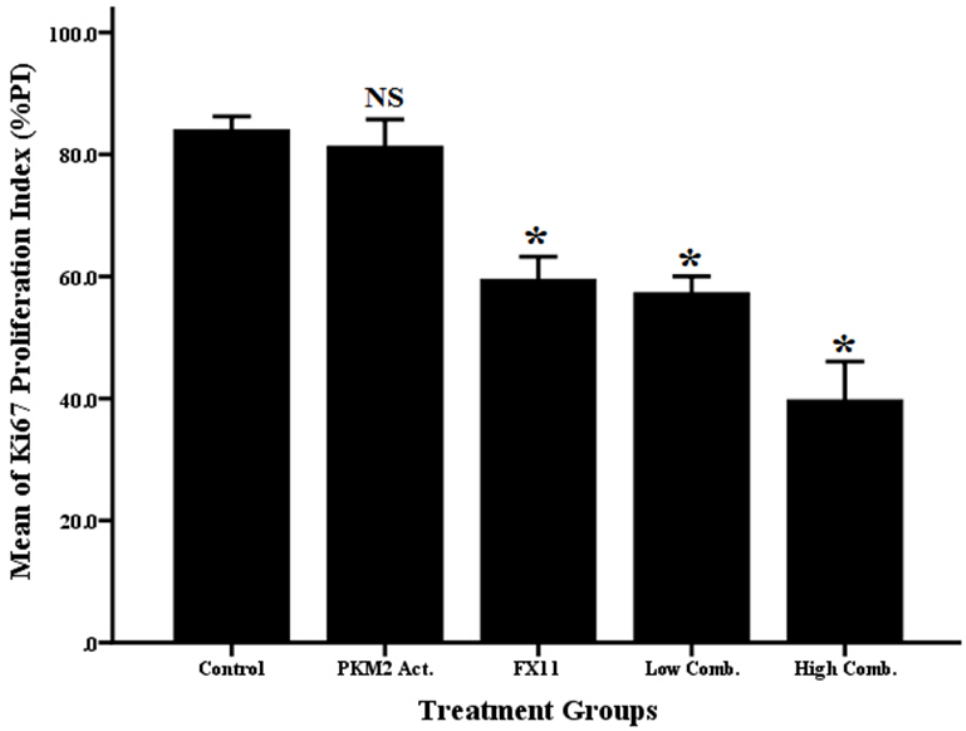

Groups	Control	PKM2 Activator IV	Lactate Dehydrogenase A inhibitor	Low Combination Treatment	High Combination Treatment
Median ± SD	83.5 ± 2.36	82.2 ± 3.58	59.2 ± 3.56	55.5 ± 2.6	40.1 ± 6.01

Figure 3.34: Ki67 proliferation index in control and different treatment groups. Significantly lower proliferation index in high-dose, low-dose combination and FX11 treated groups compared with vehicle control group in different treated groups compared to the vehicle control group. The mean number of Ki67 proliferation index significantly higher in high, low combination and FX11 treated group than in vehicle control group ($p < 0.001$, Kruskal-Wallis test, Bar chart, 95% CI). No significant differences in Ki67 proliferation index between PKM2 activator IV treated and control group.

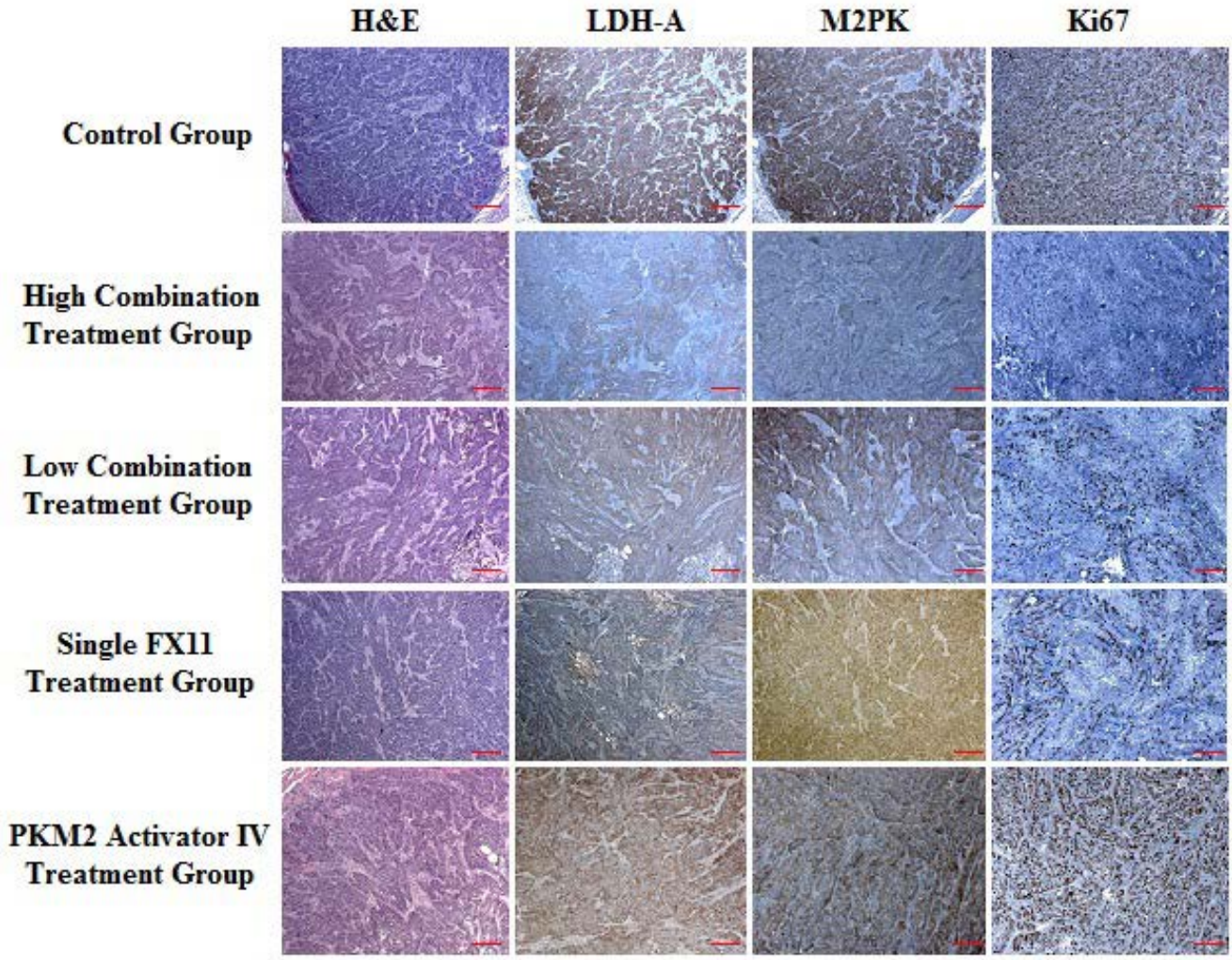

Figure 3.35: H&E staining and PKM2, LDHA and Ki67 expression in BxPc-3 pancreatic cancer xenografts in response to therapy. Lower expression of PKM2, LDHA and Ki67 were observed in the high-dose and low-dose combination therapy and FX11 treated group compared with control groups. Slightly differences in the expression of these three markers was observed between PKM2 activator IV treated and control groups (Scale bar= 100 µm).

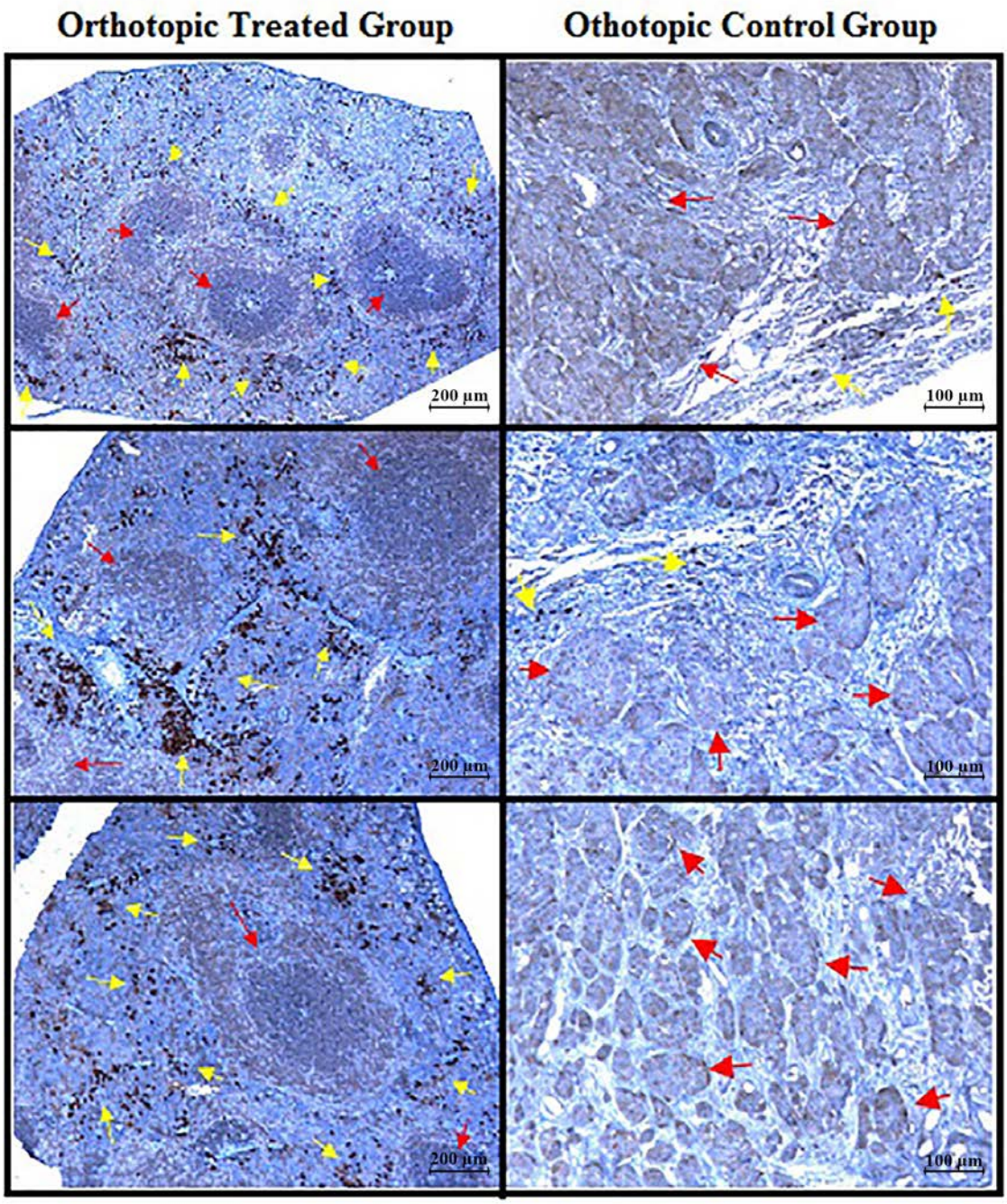

Figure 3.36: Immunohistochemical staining of CD8+TILs in orthotopic tumours. The red arrow shows tumour area and the yellow arrow shows nuclear CD8+ staining. High expression of CD8+ cells was observed in tumour sections from the combination treatment group compared with the controls.

3.3.1.6: PK and LDH activity in tumour lysate and plasma:

Activity of the PK and LDH enzymes was evaluated in mice tumour lysates and plasma using a commercially available kit (BioVision, UK). Surprisingly, we found very close or similar relative values of PK and LDH activities in both mice tumour lysates and plasma as a response to treatment. PK activity in tumour lysates and plasma was significantly higher in the high-dose, low-dose combination and PKM2 activator IV treated groups compared with the vehicle control group ($p < 0.001$, Kruskal-Wallis Test, Figure 5.17A and B). PK activity was approximately 2-fold higher in the high-dose combination and PKM2 activator IV treated groups compared with control group. No significant differences in PK activity were found between the FX11 treated and vehicle control groups. LDH activity in tumour lysates and plasma was significantly lower in the high-dose, low-dose combination and FX11 treated groups compared with vehicle control group ($p < 0.001$, Kruskal-Wallis Test, Figure 5.17 C and D). LDH activity was decreased by 60% in high-dose combination and FX11 treated groups compared with the vehicle control group. Similar activity was observed in the PKM2 activator IV treated and vehicle control groups.

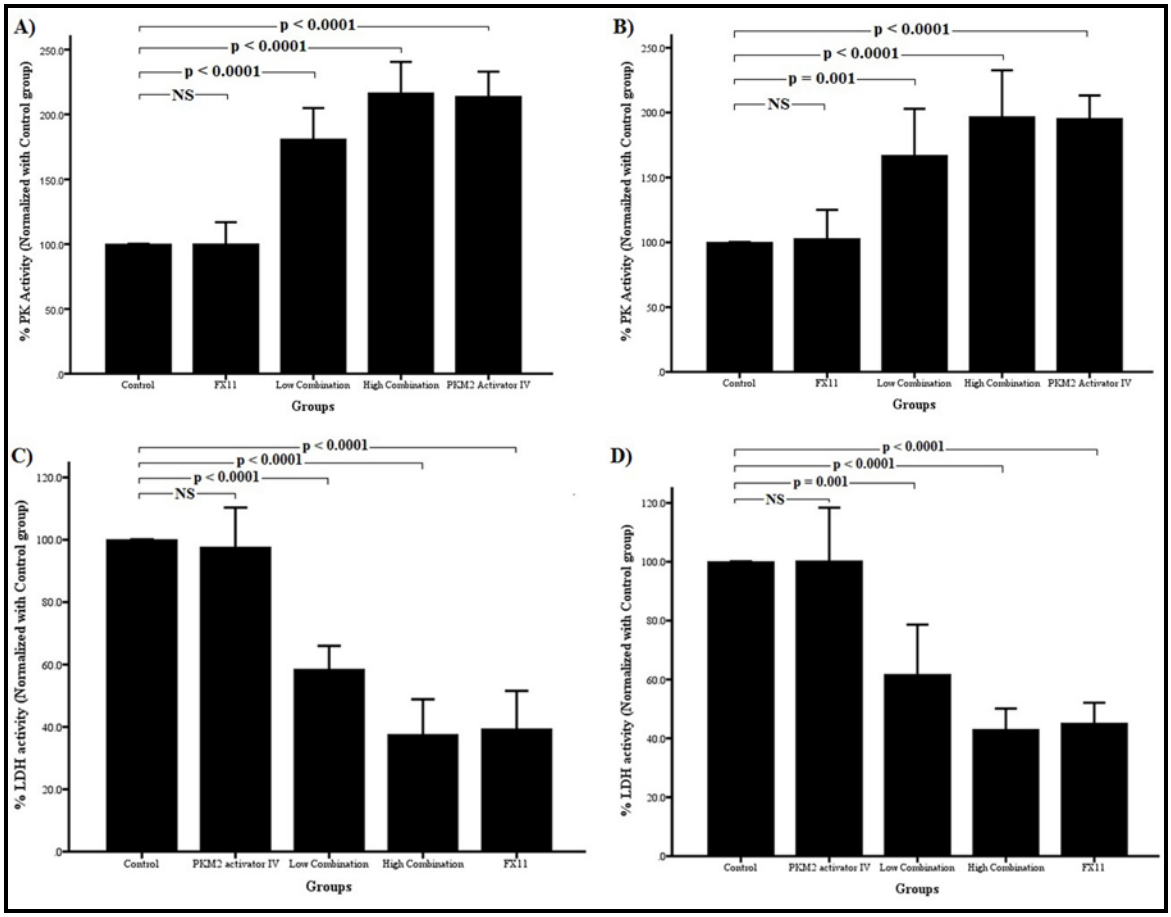

Figure 3.37: Relative values of pyruvate kinase (PK) and lactate dehydrogenase (LDH) activity in tumour lysate and plasma from mice with subcutaneous or orthotopic BxPc-3 xenografts (Bar chart, 95% CI). **A)** Relative values of PK activity in plasma 1hr post injection **B)** Relative values of PK activity in tumour lysates. **C)** Relative values of LDH activity in plasma 1hr post injection. **D)** Relative values of LDH activity in tumour lysates.

3.3.1.7: Toxicity:

Toxicity was evaluated as a measure of liver enzyme function (ALT: alanine transaminase, AST: aspartate transaminase) albumin, and change in mice weight in response to the treatment regimen. There were no significant differences in these measures between the treatment and control groups, indicating that the therapy with TEPP-46 and/or FX11 had no toxic side effects (Figure 5.18).

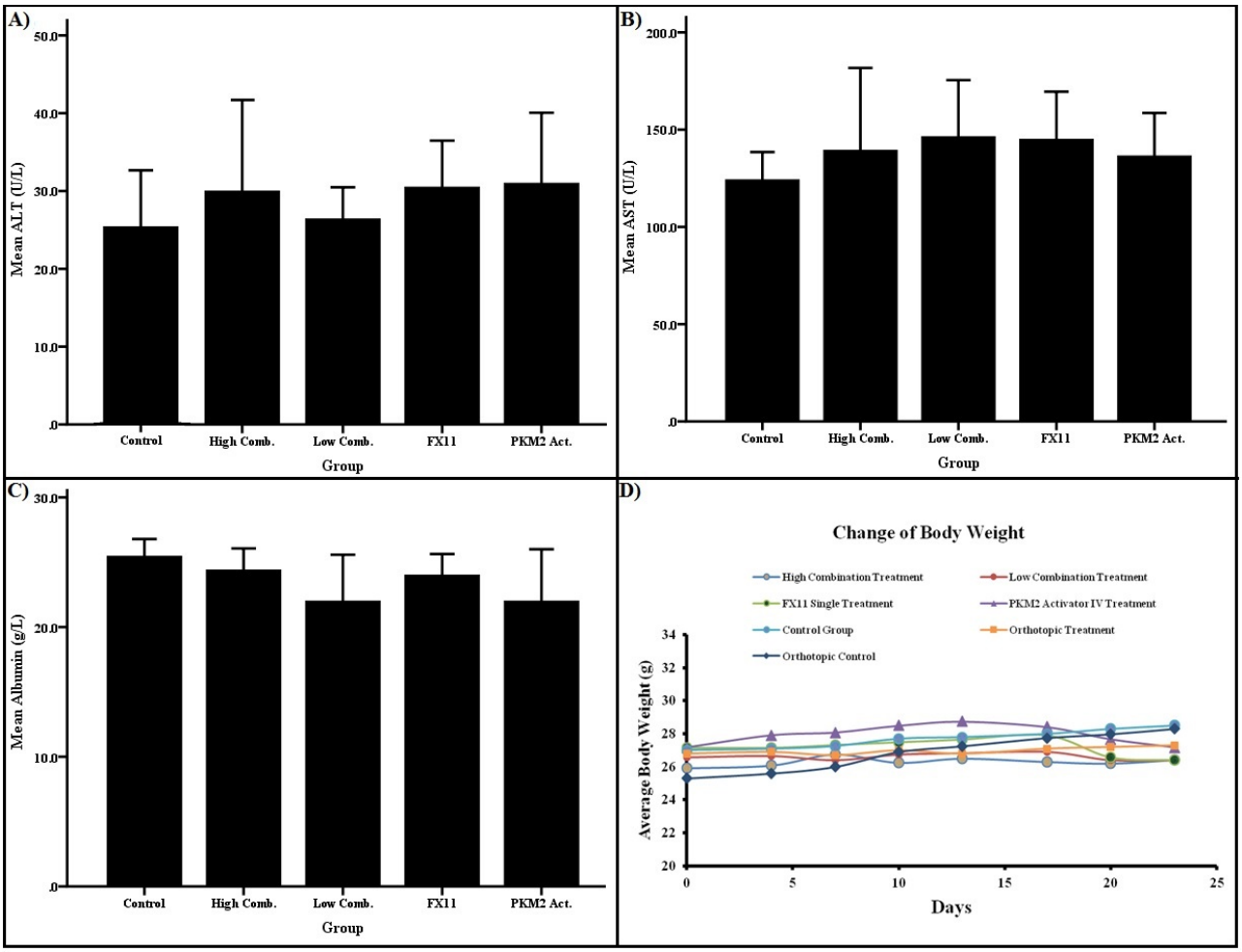

Figure 3.38: Toxicity evaluation in response to therapy (Bar chart, 95% CI). Effect of drugs on **(A)** Alanine Transaminase (ALT), **(B)** Aspartate Aminotransferase (AST), **(C)** Albumin and **(D)** body weight.

3.3.2: DISCUSSION:

Cancer cells have an altered cellular energy metabolism with an elevated glucose uptake and a concomitant increase in lactate production (51,53). Therefore, I proposed that targeting cancer cell metabolism could potentially inhibit tumour growth. Our studies demonstrate that activation/tetramerisation of PKM2 in combination with the inhibition of LDHA, impaired pancreatic cancer cell proliferation and growth both *in vitro* and *in vivo*.

Up-regulation of LDHA or PKM2 expression has been reported in several tumour types including pancreatic cancer (20,73), gastric carcinoma (200), cholangiocarcinoma (201) and non-small cell lung cancer (202), and has been proposed to have a key role in tumour initiation, progression and resistance to chemotherapy (113,203).

High expression of LDHA can increase lactate production, which is used as a source of energy by well-oxygenated tumour cells, while glucose is spared for hypoxic tumour cells (134,136). Inhibition of LDHA can reduce the ability of cancer cells to metabolize pyruvate to lactate, halting the regeneration of NAD+, which is required for sustained glycolysis, and hence resulting in the inhibition of tumour cell proliferation. Indeed, inhibition of LDHA has been reported to impair lymphoma and pancreatic cancer growth via decreasing of ATP level, inducing oxidative stress and cell death. (72).

PKM2 also plays a key role in the initiation and progression of cancer. PKM2 can occur as a dimer or a tetramer, dimeric form has been reported to predominate in tumour cells and direct glycolysis toward accumulation of glycolytic intermediates and anabolic pathway. Therefore, activation or tetramerisation of PKM2 could interfere cancer cell metabolism and proliferation.

Recently, several PKM2 activators have been developed, including TEPP-46 which has been reported to impair progression and growth of lung tumour xenografts (113). X-ray crystallography has revealed that the PKM2 activator binding site is completely different from the allosteric binding site and the activator can strengthen binding of PKM2 subunits and FBP (PKM2 allosteric activator) and lock PKM2 in tetrameric isoform (113).

Based on these findings, I hypothesised that tetramerisation of PKM2 in combination with the inhibition of LDHA can impede pancreatic tumour cell progression and growth. Indeed I demonstrate that this combination approach synergistically inhibited pancreatic cancer cell proliferation *in vitro* and significantly delayed tumour growth of pancreatic cancer xenografts in mice.

Moreover, non-metabolic function of PKM2 has been recently reported, which involves the translocation of the dimeric from of PKM2 from the cytoplasm to the nucleus, where it has been implicated to act as a transcriptional co-activator of genes such as HIF-1 and OCT-4 (52,59). *LDHA* and *PDK1* transcription induced by HIF-1, has been reported in hepatocellular and cervical carcinoma, deriving tumour progression and survival (100,177). Therefore, tetramerisation of PKM2 not only depletes glycolytic intermediates, but could also impede translocation of PKM2 into the nuclear and hence inhibit the transcription of LDHA and, consequently, cancer cell proliferation.

Indeed, our results demonstrate a decrease in number of nuclei Ki67 expression and reduction in PKM2 and LDHA expression with the combination treatment. Moreover, the number of CD8+ tumour infiltrating lymphocytes was increased in response to the combined therapy in the orthotopic xenografts. I have previously shown that high PKM2 and LDHA expression is associated with a decrease in the number of CD8+TILs and a reduced anti-immune response, which is in line with our current findings. These results suggest that the combination treatment could have reactivated immune response (CD8+TIL) against the tumour. The activation or tetramerisation of PKM2 combined with LDHA inhibition could facilitate the interaction between major histocompatibility class I (MHC I) protein with CD8+TIL and reactivate immune response against tumour cells, further contributing to tumour growth inhibition.

Moreover, the combination regimen could be safely administered without any demonstrable toxicity. There was no noticeable lethargy or inability of any treated mice to drink or eat, and there was no death or reduced body weight in the treatment groups. There were also no significant differences in plasma hepatic enzymes between treated and control groups to suggest any liver toxicity.

There are some limitations to the animal experiments, which include small number of animals in each group and short length of treatment. Moreover, due to the small size of animals, a limited amount of plasma samples was collected, which was insufficient for full biochemical analysis to assess drug toxicity (renal toxicity in particular).

In conclusion, tetramerisation of PKM2 combined with inhibition of LDHA significantly inhibits tumour growth while also re-activating anti-tumour immune response (CD8+TILs) without toxic side effects, and therefore, is a promising new therapeutic approach for pancreatic cancer.

CHAPTER 4: GENERAL DISCUSSION

4.1: DISCUSSION:

Despite significant advances in the understanding of cancer biology and the development of novel treatments, imaging and surgical techniques, the prognosis for patients with pancreatic cancer remains very poor. Pancreatic cancer is the tenth most common cancer and the fifth cause of cancer-related deaths in the UK (2). Over the last forty years, whilst most cancer survival rates have improved, the 5 -year survival rate of patients with pancreatic cancer has not changed and remains ≤ 4%. This poor prognosis can be attributed to late stage diagnosis, at which point surgical resection is no longer an option. However, patients eligible for surgery have a ~25% chance of surviving beyond 5 years (5). There are few therapies, with palliative chemotherapy as the main treatment option for patients with locally advanced or metastatic disease (6). Therefore, early diagnostic markers and new therapeutic strategies are urgently needed to improve survival rates and reduce the toxic side effects associated with current treatment. Gemcitabine and 5-fluorouracil are the standard treatment option for patients with advanced pancreatic cancer. Recently, therapy with FOLFIRINOX has shown improved survival rates compared with single-agent gemcitabine, but is accompanied by severe side-effects (6,204).

In this context, novel therapies are required. For instance, a high glycolytic rate is a common feature of cancer cells, and therefore, targeting glycolytic enzymes might be a feasible target for cancer therapy. Indeed, number of studies have combined glycolytic enzymes inhibitors, such as LDHA inhibitors (NHI-1 and NHI-2), with gemcitabine for treatment of pancreatic cancer and have shown synergistic effects in both hypoxic and normoxic culture conditions. (74). However, our work focused on the study of two important glycolytic enzymes, PKM2 and LDHA, and their potential as diagnostic markers and therapeutic target for pancreatic cancer, aiming for improvement of the prognosis and survival rate of pancreatic cancer patients.

The results of our studies showed that PKM2 and LDHA are up-regulated in pancreatic cancer and correlated with poor outcome. Interestingly, overexpression of LDHA occurred at quite an early stage along the carcinogenetic pathway from pancreatitis through cyst/PanIN to cancer, with the highest expression in the most aggressive cancers. In contrast, PKM2 expression increased progressively along the tumorigenic pathway, with the lowest in the cysts, intermediate expression in PanIN lesions and the highest in cancers. High expression of PKM2 and LDHA significantly correlated with tumour type, tumour size and a worse overall survival of pancreatic cancer patients, and poorly differentiated tumours also had higher PKM2 and LDHA expression. Moreover, high expression of PKM2 and LDHA were observed in both pancreatic cancer cell lines and plasma samples of pancreatic cancer patients compared with that from healthy volunteers. Overexpression of PKM2 and LDHA were also directly correlated with Ki-67 proliferation marker and inversely proportion with CD8-TILs.

Additionally, our findings demonstrated that the combination of PKM2 activation and LDHA inhibition treatment synergistically inhibited pancreatic cancer cell proliferation in cell culture experiments and significantly impeded tumour growth in pancreatic cancer xenograft models. Our treatment strategy significantly reduced the number of Ki-67 proliferation markers and increased the number of CD8+ TILs around tumours and abolished metastases in the animal model. The results also showed that inhibition of PKM2 by Shikonin attenuated pancreatic cancer cell proliferation and increased cancer cell death in vitro. Our results suggest that this combination therapy may be a novel therapeutic option for pancreatic cancer.

Although the exact mechanism of the differential expression pattern of PKM2 and LDHA in pancreatic cancer remains to be elucidated, it could be possible that the pre-neoplastic lesions acquire the glycolytic phenotype through LDHA overexpression and then LDHA itself or other oncogenes induce PKM2 overexpression at later stages, when cells need to proliferate at a faster pace for tumour-growth.

Indeed, up-regulation of PKM2 or LDHA has been reported in a broad spectrum of tumours and has been implicated in tumour initiation and progression (73,168,201,202,205,206). More recently, while this thesis was in preparation, two studies have shown the overexpression of both PKM2 and LDHA in tongue squamous cell carcinoma (TSCC) compared with normal tongue mucosa (206) and in thyroid cancer compared with benign goitre (176). The result of the present study concur with these findings showing significant overexpression of these two markers in pancreatic cancer tissue sections compared to the normal pancreatic tissues. High expression of PKM2 and LDHA were also observed in 8 and 9 out of the 10 pancreatic cancer cell lines, respectively.

Elevated uptake of glucose by tumour cells is associated with an increase in lactate production (59,172). Since PKM2 and LDHA are two crucial glycolytic enzymes that facilitate processes associated with the glycolytic phenotype, a very important question arises: is there an association between the expressions of these enzymes in pancreatic cancer? Our findings provide evidence that the expression of PKM2 significantly correlates with the expression of LDHA in pancreatic cancer. Therefore, the synergistic activation of these two metabolic enzymes during the initiation and progression of pancreatic cancer, might serve as a novel diagnostic biomarker for detection of pancreatic cancer. Previous studies have identified both PKM2 and LDHA as target genes for similar oncogenic transcription factors, such as HIF-1 and Myc, in various cancer types (49,51,54,207). Moreover, PKM2 interacts with HIF-1 in the nucleus and functions as a transcriptional co-activator to stimulate the expression of HIF-1 target genes, including *SLC2A1, LDHA*, and *PDK1*, in hepatocellular and cervical carcinoma cells (177,208). PKM2 and LDHA in combination seem to synergistically catalyse the glycolytic process to promote oncogenic metabolic reprogramming; however, the details and the mechanism of this association are not clear and require further investigation.

In addition to the crucial role of reprogramming cancer cell metabolism, recent findings have identified a non-enzymatic function of PKM2 in the nucleus. PKM2 can be translocated from the cytoplasm to the nucleus, acting as a transcriptional co-activator of

various target genes, such as HIF-1α and OCT-4, and it can also stimulate the expression of HIF-1 target genes, including *LDHA* and *PDK1*, in hepatocellular and cervical carcinoma cells, (51–53,57,59,101). These findings provide a further link for PKM2 in the tumorigenic process.

Indeed, PKM2 and LDHA expression has been reported both in the cytoplasm and nucleus in human glioblastoma, colorectal and gastric cancers (86,200,206). Our results demonstrate that PKM2 and LDHA are mainly expressed in the cytoplasm and partially in the nucleus. PKM2 and LDHA function as a glycolytic enzymes in the cytoplasm; however, their actual function in the nucleus is not fully understood and requires further investigation.

The high plasma activity of both PK and LDH were found in patients with pancreatic cancer compared with that from healthy donors. These results were in agreement with our immunohistochemistry study results, which shows overexpression of these two glycolytic enzymes in pancreatic cancer, and consistent with previous reports that showed significant higher levels of serum PK and LDH in pancreatic cancer patients compared with the healthy control (5,20,209). A high level (or activity) of plasma PK and LDH is correlated with poor prognosis and shorter survival rates in patients with pancreatic cancer (5,20,76,209–211). High plasma levels of PKM2 or LDHA have also been reported in several other tumour types, including gastric (21,212); lung (213,214); breast (215,216); renal cell carcinoma (217,218); and biliary tract cancer (168,219). A high plasma level of PKM2 and LDHA could be a useful marker for diagnosis of pancreatic cancer; furthermore, the plasma level of these two glycolytic enzymes could be important in monitoring the patient's response to the chemotherapy.

Immune response plays a crucial role in host immune defence against tumour growth and progression; however, the failure of the immune system to recognise and eliminate tumour cells may cause growth and spread of cancer. CD8+TILs are important components of the immune system that play a major role in the elimination and control of cancer growth and development (160). Previous studies have shown a significant direct correlation between the number of CD8+ TILs and the occurrence of apoptosis in

tumour cells (158,159). A number of studies have also shown that the number of effector CD8+ TILs is decreased in patients with melanoma, colorectal, lung and pancreatic cancer (162,220–222). Tumour cells can evade immune response by various mechanisms. For instance, the loss of major histocompatibility complex class I (MHC I) or surface antigens can prevent recognition of tumour cells by CD8+T cells. However, the ability of PKM2 and LDHA to modulate tumour immune response is unclear. The result of our studies found that the number of CD8+TIL was significantly higher in patients with weak PKM2 and LDHA expression, who also had a significantly higher survival rates, compared with those that had a higher expression. High expression of these two enzymes were prevented accumulation of CD8+TILs in or around the tumour. However, further studies are required to understand the mechanism of this association.

A previous study reported that the interaction between SOCS3 (suppressor of cytokine signaling 3) with PKM2 in dendritic cells lead to the impairment of immune response against cancer cells, while the dendritic cells are in the tumour environment, the expression of SOCS3 is upregulated by tumour-derived factors. The interaction of upregulated SOCS3 with PKM2 leads to decreased ATP production by decreasing the activity of PKM2, which ultimately causes dysfunction of dendritic cells, with reduced ability to present antigens and an impaired immune response (223).

Our results also clearly showed that the expression of LDHA negatively correlates with CD8+TILs, high expression of LDHA leads to the production of high amount of lactate and increases the acidity of tumour micro-environment, which ultimately leads to the impairment of the immune response (49). Our results are consistent with previous findings that showed that tumour cell acidity impairs CD8+ tumour specific effector T cells in both human and animal model (224). Collectively, the high expression of PKM2 and LDHA in pancreatic cancer may obstruct the interaction between the immune response and pancreatic cancer cells and contribute to poor response to the both chemo and radiotherapy.

On the other hand, a high rate of glycolysis is one of the hallmarks of tumour cells. The most important advantage of increased glycolysis in tumour cells is the production of

energy without oxygen consumption, and the generation of glycolytic intermediates such as triglycerides, phospholipids, and nucleotides, which are used as macromolecules for biosynthesis of new cells. Previous research findings have demonstrated that oncogenic tyrosine kinase fibroblast growth factor receptor-1 (FGFR-1) can regulate and phosphorylate both PKM2 and LDHA. Phosphorylation of PKM2 at tyrosine 105 (Y105) prevents tetramerisation and inactivates PKM2; however, phosphorylation of LDHA at tyrosine 10 (Y10) by FGFR-1 promotes tetramerisation and activation of LDHA (176). As a consequence of up-regulation and phosphorylation of PKM2 and LDHA, tumour cells proliferate and grow faster. Therefore, I proposed that targeting both PKM2 and LDHA enzymes could be an effective new therapeutic strategy for treatment of pancreatic cancer. Here, I clearly documented that activation or tetramerisation of PKM2 in combination with the inhibition of LDHA impaired pancreatic cancer cell proliferation *in vitro* and significantly impaired tumour growth in pancreatic cancer xenograft models.

To investigate the role of PKM2 in pancreatic cancer cell proliferation and tumour growth, firstly, the effect of PKM2 inhibition on cell proliferation was evaluated by using Shikonin as a PKM2 inhibitor. The results of our study showed that Shikonin had a strong cytotoxic effect on different types of pancreatic cancer cell lines with low IC_{50} values. Shikonin can inhibit pancreatic cancer cell proliferation by inhibiting PKM2 activity, and hence glycolysis, causing cell death by triggering programmed cell death. Our results are consistent with a previous report showing that Shikonin and its analogues can effectively inhibit cancer cell proliferation by the selective inhibition of tumour PKM2 (112).

Although Shikonin effectively inhibited pancreatic cancer cell proliferation in vitro, Shikonin was not selected for in vivo experiment. There are some reasons for non-selection of Shikonin in animal experiment models, one reason is due to multiple effects of Shikonin leading to cell death which is not purely due to the inhibition of PKM2, which our hypothesis is based on. Wiench *et al* (2012) found that Shikonin can induce apoptosis in different cancer cell lines by directly affecting mitochondrial function and disruption of mitochondrial membrane potential, leading to generation of reactive

oxygen species (ROS) and ultimately cell death (191). More recently, Gara *et al* (2015) demonstrated in prostate cancer that Shikonin can induce and activate endoplasmic reticulum stress and also increase generation of ROS and enhance pro-apoptotic signaling through affecting mitochondrial function (197).

On the other hand, the inhibition of glycolysis can be toxic to both normal and cancer cells, and the use of Shikonin can damage and kill healthy as well as cancer cells in animal models. Therefore, the PKM2 activator in combination with an LDHA inhibitor was used as a treatment strategy in the in vivo study. Activation of PKM2 may not be toxic to the normal non-proliferating cell, and inhibition of LDHA is also not associated with major side effects. In patients with hereditary LDHA deficiency, the only side-effect of the lack of LDHA is the development of myoglobinuria after intense exercise. Hence, the combination treatment strategy may be non-toxic to the normal cell and unlikely to cause major side effects.

The active form of PKM2 (tetramer) impedes tumour growth, whereas the inactive form of PKM2 (dimer) contributes to the progression and growth of tumours. Several studies have shown that the replacement of PKM2 by PKM1 can inhibit cancer cell proliferation *in vitro* and impairs tumour growth in xenograft models (59,113). In line with these observations, researchers have been interested in the development of PKM2 activators and several small molecular activators have been identified. Anastasiou *et al.* (2012) studied the effect of tetramerisation of PKM2 on tumour cell proliferation by using small molecular activators, and found that the activation of PKM2 can inhibit cancer cell proliferation through interfering with the anabolic pathway. The results of this study also showed that the activation of PKM2 decreased pools of ribose phosphate and the amino acid serine, which are key precursors of lipid, amino acid and nucleotide metabolism, both *in vitro* and *in vivo*. This research group has developed numerous PKM2 activators; TEPP-46 is an example of a potent PKM2 activator and has been shown to impaired tumour growth in the xenograft models. Moreover, x-ray crystallography studies have shown that the activator binding site differ from the allosteric binding site, and the

activator can strengthen binding of subunits and FBP (PKM2 allosteric activator) and lock PKM2 in the tetrameric form.

In a related study, Kung *et al.* (2012) found that the activation of PKM2, using a small molecular activator, known as compound 9 or PKM2 activator III, induced serine autotrophy in cancer cells and locked PKM2 in an active tetrameric form, forcing tumour cells to reprogram their metabolism, which is less metabolically flexible compared with normal cells.

Tetramerisation of PKM2 might have further effect on the attenuation of cancer cell proliferation. Recent research findings identified non-metabolic function of PKM2, in particular circumstance, dimeric form of PKM2 can translocate to the nucleus and functioning as a protein kinase to regulate gene expressions. These findings suggest that the tetramerisation of PKM2 not only depletes glycolytic intermediates, but also impedes translocation of PKM2 from the cytoplasm into the nucleus and hence can inhibit the transcription of LDHA, and consequently, the cancer cell proliferation.

Our results demonstrate that the activation of PKM2 alone did not have a significant effect on cell viability and tumour growth; however, in combination with LDHA inhibition, pancreatic cancer cell proliferation was inhibited in a synergistic manner and xenograft tumour growth was significantly impaired.

High expression and activity of LDHA in pancreatic cancer was observed in our study, which could increase the lactate production. High lactate production has some advantages to tumour cells and has an important role in the progression, metastasis and resistance to chemotherapy by changing the acidity of extracellular microenvironment. Moreover, lactate can be used as fuel by aerobic tumour cells, sparing glucose for hypoxic tumour cells. Accordingly, the inhibition of LDHA can reduce lactate production and consequently attenuate pancreatic cancer cell proliferation and growth by forcing aerobic tumour cells to use glucose as a main source of energy, depleting glucose for the hypoxic tumour cells and then resulting in tumour cell death due to depletion of glucose.

The anti-tumour effect of LDHA inhibition has been known for many years; however, the lack of highly selective and potent inhibitors has posed some difficulty. A number of moderately potent LDHA inhibitors have been identified and the effort of finding highly potent inhibitors has continued. Recently, Anne Le *et al.* (2010) studied the effect of LDHA inhibition on progression and growth of human lymphoma and pancreatic cancer cells by FX11, which is a potent LDHA inhibitor; they found that inhibition of LDHA inhibited cancer cell proliferation and growth both *in vitro* and *in vivo*. The study also reported that inhibition of LDHA can increase oxygen consumption, reduce lactate production and ATP levels, increase reactive oxygen species (ROS) and induce oxidative stress, causing inhibition of cancer cell proliferation and finally death (72). Moreover, the combination of FX11 with an inhibitor of NAD+ synthesis (FK866) has demonstrated a synergistic effect on the inhibition of P493 human lymphoma cell proliferation *in vitro* and impaired tumour growth *in vivo* (72).

In the present studies, PKM2 activator (TEPP-46) in combination with the LDHA inhibitor (FX11) was used as a therapeutic strategy for pancreatic cancer. Tetramerisation of PKM2 can inhibit the anabolic pathway and deplete glycolytic intermediates and inhibition of LDHA, on the other hand, can reduce lactate production and deplete extracellular lactate. Therefore, combination of PKM2 activation and LDHA inhibition hinders cancer cell proliferation due to interference with the anabolic pathway; well-oxygenated tumour cells are forced to use glucose as their main energy source, which may cause the death of hypoxic tumour cells. As a consequence, tumour cell proliferation and growth are inhibited; leaving a low number of surviving tumour cells in well-oxygenated regions, resulting in tumour shrinkage, providing the opportunity for surgery. Our findings also suggest that the activation of PKM2 in combination with LDHA inhibition leads to the accumulation of pyruvate inside the cell and then shunting it into the mitochondria. As a results of the shunting pyruvate into the mitochondria oxygen consumption might enhanced, ATP level reduced and finally induce oxidative stress and pancreatic cancer cell death. On the other hand, the high expression of LDHA and PKM2 could result in resistance to both chemo and radiotherapy by increasing

acidity of the extracellular microenvironment; therefore, combination of PKM2 activation and LDHA inhibition might increase tumour cell sensitivity to both chemo and radiotherapy and be an effective approach in patients with metastatic pancreatic cancer.

Our findings also demonstrate that combination of PKM2 activation and LDHA inhibition significantly decreased the number of Ki67-positive cells and reduced PKM2 and LDHA expression. Furthermore, the correlation between combination therapy and host immune response (CD8+TILs, CD8+ tumour infiltrating lymphocytes) was found. Our previous findings suggested that the high PKM2 and LDHA expression in pancreatic cancer potentially prevent accumulation of CD8+TIL cells peri- and intra-tumoural, and thus blunt the anti-tumour host immune response. Interestingly, the results of the present study were consistent with our previous findings. Higher number of CD8+TIL cells were found around orthotopic tumours that treated with the combination drugs, while there was no or negligible number of CD8+TIL cells in orthotopic control tumours. These results suggest that the combination treatment could have reactivated the immune response (CD8+TILs) against the tumour and may facilitate the interaction between major histocompatibility class I (MHC I) with CD8+TILs and reactivate immune response against tumour cells, which further contribute to the inhibition of tumour cell proliferation and growth. Furthermore, the combination therapy was well-tolerated by mice, as evaluated by weight loss and hepatic enzymes function.

To summarise, tetramerisation of PKM2 in combination with inhibition of LDHA significantly impede pancreatic cancer cell proliferation and tumour growth and might also reactivate anti-tumour immune response, inducing further cancer cell death.

A comment should be made of potential errors in the methodology of the research studies, which can include instrumental error, methodological errors, errors in preparation or addition of the regents and during assessment of the staining or counting of the stained cells. Generally, experimental error can be divided into systematic and random error. In our study, we avoided systematic error by precisely setting up the instrument and using blank and sometimes positive controls to avoid any error that may be caused by the instrument. Random errors were minimized by repeating at least twice

the same experiment and the average of these two experiments was taken and used for the interpretation of the results. If any big differences between two repeated experiments were observed a third and sometimes fourth repetition of the experiment was performed to confirm the results. To avoid bias in the assessment of immunohistochemistry staining, the stained tissue sections were assessed independently and blindly to the status and stage of the patients by two observers and any differences were resolved by conference microscope. The same strategy was used for the counting of stained Ki-67 and CD8+TIL stained cells. Finally, animal experiments were done under observation and supervision of an experienced project licence holder. Tumour sizes were measured and compared with bioluminescence images to confirm the accuracy of the tumour size measurements.

4.2: CONCLUSION:

PKM2 and LDHA are overexpressed in pancreatic cancer and significantly correlate with a poor outcome. Activation of PKM2 in combination with inhibition of LDHA synergistically inhibited pancreatic cancer cell proliferation and significantly impaired the growth of pancreatic cancer xenograft tumours. Therefore, this combination might represent a novel strategy for the treatment of pancreatic cancer. PKM2 and LDHA may contribute to the aggressiveness of pancreatic cancer and confer anergy against host anti-tumour immune response. As such, activation of PKM2 in combination with inhibition of LDHA may reactivate anti-tumour immune response and induce tumour cell death. Our results suggest that PKM2 and LDHA may serve as diagnostic and prognostic markers and as potential therapeutic targets for pancreatic cancer. Furthermore, the combination of PKM2 activation and LDHA inhibition in conjunction with chemotherapy could be an effective therapy for patients with metastatic pancreatic cancer, and might improve quality of life and survival rates.

4.3: FUTURE WORK:

The therapeutic strategy for pancreatic cancer described here is not complete and further studies are ongoing. Our project can be taken forward in a number of ways before moving to clinical trials. These include the mechanistic investigations of some cell signaling pathways disrupted by the combination of PKM2 activation and LDHA inhibition. Proteomic analysis is another planned approach to understand the effect of combination treatment on the function and levels of cell proteins, particularly the glycolytic metabolome.

Additionally, gene analysis is another important part of our ongoing project, The dimeric form of PKM2 can be translocated from the cytoplasm to nucleus and acts as a transcriptional co-activator of some genes including Stat 3, β-catenin, HIF-1 and Oct-4. The study of genes in response to combination treatment in pancreatic cancer could be important to know whether the treatment regimen has an effect on the down-regulation of those genes involved in the progression of pancreatic cancer.

Finally, in our study combination treatment inhibited pancreatic cancer cell proliferation and tumour growth and also abolished metastasis. We expect the use of combination treatment in conjunction with chemotherapy will increase the sensitivity of chemotherapy and may improve the quality of life and survival in patients with metastatic disease. Consistent with our expectation, very recently, Kim *et al* (2015) found that the knockdown of PKM2 increased the sensitivity of gemcitabine treatment in pancreatic cancer and significantly enhanced gemcitabine-enhanced cell apoptosis through the activation of caspase cascade and poly ADP-ribose polymerase (PARP) cleavage (225). In a related study, Wang *et al* (2015) found that the knockdown of PKM2 gene enhanced the sensitivity of radiotherapy in non-small cell lung cancer through increasing apoptosis rate and endoplasmic reticulum stress (226). Hence, the conjunction of combination treatment with chemotherapy could be an effective treatment for patients with metastatic pancreatic cancer and it is our future research work.

CHAPTER 5: REFERENCES

1. Stewart, B. W., Wild CP. World Cancer Report 2014. 2014.

2. Cancer Research UK. Cancer mortality statistics. Retrieved February 20, 2015 from, http://www.cancerresearchuk.org/cancer-info/cancerstats/mortality/. 2014.

3. Cancer Research UK. Pancreatic Cancer Statistics. Retrieved February 20, 2015 from, http://www.cancerresearchuk.org/cancer-info/cancerstats/types/pancreas/. 2014.

4. Maitra, A., and Hruban RH. Pancreatic cancer. Annu Rev Pathol. 2008;3:157–88.

5. Joergensen MT, Heegaard NHH, Schaffalitzky de Muckadell OB. Comparison of plasma Tu-M2-PK and CA19-9 in pancreatic cancer. Pancreas. 2010;39(2):243–7.

6. Conroy T, Desseigne F, Ychou M, Bouché O, Guimbaud R, Bécouarn Y, et al. FOLFIRINOX versus gemcitabine for metastatic pancreatic cancer. N Engl J Med. 2011;364(19):1817–25.

7. American Cancer Society. Cancer Fact and Figures 2014. Retrieved December 16, 2014 from, http://www.cancer.org/research/cancerfactsfigures/cancerfactsfigures/cancer-facts-figures-2014. 2014.

8. Brat DJ, Lillemoe KD, Yeo CJ, Warfield PB, Hruban RH. Progression of pancreatic intraductal neoplasias to infiltrating adenocarcinoma of the pancreas. The American journal of surgical pathology. 1998. p. 163–9.

9. Iacobuzio-Donahue CA, Ashfaq R, Maitra A, Adsay NV, Shen-Ong GL, Berg K, et al. Highly expressed genes in pancreatic ductal adenocarcinomas: a comprehensive characterization and comparison of the transcription profiles obtained from three major technologies. Cancer Res. 2003;63(24):8614–22.

10. Herreros-Villanueva M, Gironella M. Molecular markers in pancreatic cancer diagnosis. Clin Chim Acta. 2013;418:22–9.

11. Singh P, Srinivasan R, Wig JD. Major molecular markers in pancreatic ductal adenocarcinoma and their roles in screening, diagnosis, prognosis, and treatment. Pancreas. 2011;40(5):644–52.

12. Hruban RH, Wilentz RE, Kern SE. Genetic progression in the pancreatic ducts. Am J Pathol. 2000 Jun;156(6):1821–5.

13. Olson SH, Kurtz RC. Epidemiology of pancreatic cancer and the role of family history. J Surg Oncol. 2013;107(1):1–7.

14. Stoita A, Penman ID, Williams DB. Review of screening for pancreatic cancer in high risk individuals. World J Gastroenterol. 2011;17(19):2365–71.

15. Tersmette AC, Petersen GM, Offerhaus GJ, Falatko FC, Brune KA, Goggins M, et al. Increased risk of incident pancreatic cancer among first-degree relatives of patients with familial pancreatic cancer. Clin Cancer Res. 2001;7(3):738–44.

16. Grocock CJ, Vitone LJ, Harcus MJ, Neoptolemos JP, Raraty MGT, Greenhalf W. Familial pancreatic cancer: a review and latest advances. Adv Med Sci. 2007;52:37–49.

17. Kim DH, Crawford B, Ziegler J, Beattie MS. Prevalence and characteristics of pancreatic cancer in families with BRCA1 and BRCA2 mutations. Fam Cancer. 2009;8(2):153–8.

18. Ballehaninna UK, Chamberlain RS. The clinical utility of serum CA 19-9 in the diagnosis, prognosis and management of pancreatic adenocarcinoma: An evidence based appraisal. J Gastrointest Oncol. Pioneer Bioscience Publishing Company; 2012;3(2):105.

19. Ballehaninna, U. K., and Chamberlain RS. Serum CA 19-9 as a Biomarker for Pancreatic Cancer-A Comprehensive Review. Indian J Surg Oncol. 2011;2:88–100.

20. Ventrucci M, Cipolla A, Racchini C, Casadei R, Simoni P, Gullo L. Tumor M2-pyruvate kinase, a new metabolic marker for pancreatic cancer. Dig Dis Sci. Springer; 2004;49(7-8):1149–55.

21. Kumar Y, Tapuria N, Kirmani N, Davidson BR. Tumour M2-pyruvate kinase: a gastrointestinal cancer marker. Eur J Gastroenterol Hepatol. 2007;19:265–76.

22. Rü F, Rückert F, Pilarsky C, Grützmann R. Serum Tumor Markers in Pancreatic Cancer—Recent Discoveries. Cancers (Basel). 2010;2(2):1107–24.

23. Schulze G. The tumor marker tumor M2-PK: an application in the diagnosis of gastrointestinal cancer. Anticancer Res. 2000;20(6D):4961–4.

24. O'Brien DP, Sandanayake NS, Jenkinson C, Gentry-Maharaj A, Apostolidou S, Fourkala E-O, et al. Serum CA19-9 Is Significantly Upregulated up to 2 Years before Diagnosis with Pancreatic Cancer: Implications for Early Disease Detection. Clin Cancer Res. AACR; 2015;21(3):622–31.

25. Miura F, Takada T, Amano H, Yoshida M, Furui S, Takeshita K. Diagnosis of pancreatic cancer. HPB (Oxford). 2006;8(5):337–42.

26. Rickes S, Unkrodt K, Neye H, Ocran KW, Wermke W. Differentiation of pancreatic tumours by conventional ultrasound, unenhanced and echo-enhanced power Doppler sonography. Scand J Gastroenterol. 2002;37(11):1313–20.

27. Ben Miller IG and SR-C. Pancreatic tumours. In: Goh PH and V, editor. Radiotherap in practice-Imaging. Oxford university press; 2010. p. 105–14.

28. Kitano M, Kudo M, Maekawa K, Suetomi Y, Sakamoto H, Fukuta N, et al. Dynamic imaging of pancreatic diseases by contrast enhanced coded phase inversion harmonic ultrasonography. Gut. 2004;53(6):854–9.

29. Alexakis N, Halloran C, Raraty M, Ghaneh P, Sutton R, Neoptolemos JP. Current standards of surgery for pancreatic cancer. Br J Surg. 2004;91(11):1410–27.

30. Peddu P, Quaglia A, Kane PA, Karani JB. Role of imaging in the management of pancreatic mass. Crit Rev Oncol Hematol. 2009;70(1):12–23.

31. Takakura K, Sumiyama K, Munakata K, Ashida H, Arihiro S, Kakutani H, et al. Clinical usefulness of diffusion-weighted MR imaging for detection of pancreatic cancer: comparison with enhanced multidetector-row CT. Abdom Imaging. 2011;36(4):457–62.

32. Majumder S, Chubineh S, Birk J. Pancreatic cancer: an endoscopic perspective. Expert Rev Gastroenterol Hepatol. 2012;6(1):95–103; quiz 104.

33. Rosewicz S, Wiedenmann B. Pancreatic carcinoma. Lancet. 1997;349(9050):485–9.

34. Hewitt MJ, McPhail MJW, Possamai L, Dhar A, Vlavianos P, Monahan KJ. EUS-guided FNA for diagnosis of solid pancreatic neoplasms: a meta-analysis. Gastrointest Endosc. 2012;75(2):319–31.

35. Polkowski M, Larghi A, Weynand B, Boustière C, Giovannini M, Pujol B, et al. Learning, techniques, and complications of endoscopic ultrasound (EUS)-guided sampling in gastroenterology: European Society of Gastrointestinal Endoscopy (ESGE) Technical Guideline. Endoscopy. 2012;44(2):190–206.

36. Fritcher EGB, Kipp BR, Halling KC, Oberg TN, Bryant SC, Tarrell RF, et al. A multivariable model using advanced cytologic methods for the evaluation of indeterminate pancreatobiliary strictures. Gastroenterology. 2009;136(7):2180–6.

37. Smoczynski M, Jablonska A, Matyskiel A, Lakomy J, Dubowik M, Marek I, et al. Routine brush cytology and fluorescence in situ hybridization for assessment of pancreatobiliary strictures. Gastrointest Endosc. 2012;75(1):65–73.

38. Uchida N, Kamada H, Tsutsui K, Ono M, Aritomo Y, Masaki T, et al. Utility of pancreatic duct brushing for diagnosis of pancreatic carcinoma. J Gastroenterol. 2007;42(8):657–62.

39. Sendler A, Avril N, Helmberger H, Stollfuss J, Weber W, Bengel F, et al. Preoperative evaluation of pancreatic masses with positron emission tomography using 18F-fluorodeoxyglucose: diagnostic limitations. World J Surg. 2000;24(9):1121–9.

40. Wu L-M, Hu J-N, Hua J, Liu M-J, Chen J, Xu J-R. Diagnostic value of diffusion-weighted magnetic resonance imaging compared with fluorodeoxyglucose positron emission tomography/computed tomography for pancreatic malignancy: a meta-analysis using a hierarchical regression model. J Gastroenterol Hepatol. 2012;27(6):1027–35.

41. Bramhall SR, Neoptolemos JP. Advances in diagnosis and treatment of pancreatic cancer. Gastroenterologist. 1995;3(4):301–10.

42. Stojadinovic A, Brooks A, Hoos A, Jaques DP, Conlon KC, Brennan MF. An evidence-based approach to the surgical management of resectable pancreatic adenocarcinoma. J Am Coll Surg. 2003;196(6):954–64.

43. Gagner M, Palermo M. Laparoscopic Whipple procedure: review of the literature. J Hepatobiliary Pancreat Surg. 2009;16(6):726–30.

44. Neoptolemos JP, Dunn JA, Stocken DD, Almond J, Link K, Beger H, et al. Adjuvant chemoradiotherapy and chemotherapy in resectable pancreatic cancer: a randomised controlled trial. Lancet. 2001;358(9293):1576–85.

45. Neoptolemos JP, Stocken DD, Tudur Smith C, Bassi C, Ghaneh P, Owen E, et al. Adjuvant 5-fluorouracil and folinic acid vs observation for pancreatic cancer: composite data from the ESPAC-1 and -3(v1) trials. Br J Cancer. 2009;100(2):246–50.

46. Burris HA, Moore MJ, Andersen J, Green MR, Rothenberg ML, Modiano MR, et al. Improvements in survival and clinical benefit with gemcitabine as first-line therapy for patients with advanced pancreas cancer: a randomized trial. J Clin Oncol. 1997;15(6):2403–13.

47. Cunningham D, Chau I, Stocken DD, Valle JW, Smith D, Steward W, et al. Phase III randomized comparison of gemcitabine versus gemcitabine plus capecitabine in patients with advanced pancreatic cancer. J Clin Oncol. 2009;27(33):5513–8.

48. Billiard J, Dennison JB, Briand J, Annan RS, Chai D, Colón M, et al. Quinoline 3-sulfonamides inhibit lactate dehydrogenase A and reverse aerobic glycolysis in cancer cells. Cancer Metab. 2013;1(1):19.

49. Doherty JR, Cleveland JL. Targeting lactate metabolism for cancer therapeutics. J Clin Invest. 2013;123(9):3685–92.

50. Fiume L, Vettraino M, Stefano G Di, Manerba M, Vettraino M, Di Stefano G. Inhibition of lactate dehydrogenase activity as an approach to cancer therapy. Future Med Chem. 2014;6(4):429–45.

51. Wong N, Ojo D, Yan J, Tang D. PKM2 contributes to cancer metabolism. Cancer Letters. 2014;

52. Warner S, Carpenter K, Bearss D. Activators of PKM2 in cancer metabolism. Future Med Chem. 2014;06:1167–78.

53. Iqbal MA, Gupta V, Gopinath P, Mazurek S, Bamezai RNK. Pyruvate kinase M2 and cancer: an updated assessment. FEBS Lett. Federation of European Biochemical Societies; 2014;588(16):2685–92.

54. Miao P, Sheng S, Sun X, Liu J, Huang G. Lactate dehydrogenase a in cancer: A promising target for diagnosis and therapy. IUBMB Life. 2013. p. 904–10.

55. Boland ML, Chourasia AH, Macleod KF. Mitochondrial dysfunction in cancer. Front Oncol. 2013;3(December):292.

56. Jang M, Kim SS, Lee J. Cancer cell metabolism: implications for therapeutic targets. Exp Mol Med. Nature Publishing Group; 2013;45(10):e45.

57. Yang W, Lu Z. Regulation and function of pyruvate kinase M2 in cancer. Cancer Letters. 2013. p. 153–8.

58. Wong K-K, Engelman JA, Cantley LC. Targeting the PI3K signaling pathway in cancer. Curr Opin Genet Dev. Elsevier; 2010;20(1):87–90.

59. Wong N, De Melo J, Tang D. PKM2, a central point of regulation in cancer metabolism. Int J Cell Biol. 2013;

60. Elstrom RL, Bauer DE, Buzzai M, Karnauskas R, Harris MH, Plas DR, et al. Akt stimulates aerobic glycolysis in cancer cells. Cancer Res. AACR; 2004;64(11):3892–9.

61. Robey RB, Hay N. Is Akt the "Warburg kinase"?—Akt-energy metabolism interactions and oncogenesis. In: Seminars in cancer biology. Elsevier; 2009. p. 25–31.

62. Vousden KH, Ryan KM. p53 and metabolism. Nat Rev Cancer. Nature Publishing Group; 2009;9(10):691–700.

63. Bensaad K, Tsuruta A, Selak MA, Vidal M, Nakano K, Bartrons R, et al. TIGAR, a p53-inducible regulator of glycolysis and apoptosis. Cell. Elsevier; 2006;126(1):107–20.

64. Matoba S, Kang J-G, Patino WD, Wragg A, Boehm M, Gavrilova O, et al. p53 regulates mitochondrial respiration. Science (80-). American Association for the Advancement of Science; 2006;312(5780):1650–3.

65. López-lázaro M. The Warburg Effect : Why and How do Cancer Cells Activate Glycolysis in the Presence of Oxygen ? 2008;305–12.

66. Ganapathy-Kanniappan S, Geschwind J-FH. Tumor glycolysis as a target for cancer therapy: progress and prospects. Mol Cancer. 2013;12:152.

67. Wang Z, Wang N, Chen J, Shen J. Emerging glycolysis targeting and drug discovery from chinese medicine in cancer therapy. Evid Based Complement Alternat Med. 2012;2012:873175.

68. Xu R, Pelicano H, Zhou Y, Carew JS, Feng L, Bhalla KN, et al. Inhibition of Glycolysis in Cancer Cells : A Novel Strategy to Overcome Drug Resistance Associated with Mitochondrial Respiratory Defect and Hypoxia. 2005;(2):613–22.

69. Shuch B, Linehan WM, Srinivasan R. Aerobic glycolysis: a novel target in kidney cancer. Expert Rev Anticancer Ther. 2013;13(6):711–9.

70. Pelicano H, Martin DS, Xu R-H, Huang P. Glycolysis inhibition for anticancer treatment. Oncogene. 2006;25(34):4633–46.

71. Gupta V, Bamezai RNK. Human pyruvate kinase M2: A multifunctional protein. Protein Science. 2010. p. 2031–44.

72. Le A, Cooper CR, Gouw AM, Dinavahi R, Maitra A, Deck LM, et al. Inhibition of lactate dehydrogenase A induces oxidative stress and inhibits tumor progression. Proc Natl Acad Sci U S A. 2010;107(5):2037–42.

73. Rong Y, Wu W, Ni X, Kuang T, Jin D, Wang D, et al. Lactate dehydrogenase A is overexpressed in pancreatic cancer and promotes the growth of pancreatic cancer cells. Tumour Biol. 2013;34(3):1523–30.

74. Maftouh M, Avan a, Sciarrillo R, Granchi C, Leon LG, Rani R, et al. Synergistic interaction of novel lactate dehydrogenase inhibitors with gemcitabine against pancreatic cancer cells in hypoxia. Br J Cancer. Nature Publishing Group; 2014;110(1):172–82.

75. Jurica MS, Mesecar a, Heath PJ, Shi W, Nowak T, Stoddard BL. The allosteric regulation of pyruvate kinase by fructose-1,6-bisphosphate. Structure. 1998;6(2):195–210.

76. Kumar Y, Mazurek S, Yang S, Failing K, Winslet M, Fuller B, et al. In vivo factors influencing tumour M2-pyruvate kinase level in human pancreatic cancer cell lines. Tumour Biol. 2010;31(2):69–77.

77. Mazurek S. Pyruvate kinase type M2: a key regulator of the metabolic budget system in tumor cells. Int J Biochem Cell Biol. 2011;43(7):969–80.

78. Vander Heiden MG, Christofk HR, Schuman E, Subtelny AO, Sharfi H, Harlow EE, et al. Identification of small molecule inhibitors of pyruvate kinase M2. Biochem Pharmacol. Elsevier Inc.; 2010;79(8):1118–24.

79. Christofk HR, Vander Heiden MG, Harris MH, Ramanathan A, Gerszten RE, Wei R, et al. The M2 splice isoform of pyruvate kinase is important for cancer metabolism and tumour growth. Nature. 2008;452(7184):230–3.

80. Li YG, Zhang N. Clinical significance of serum tumour M2-PK and CA19-9 detection in the diagnosis of cholangiocarcinoma. Dig Liver Dis. 2009;41(8):605–8.

81. Mazurek S, Boschek CB, Hugo F, Eigenbrodt E. Pyruvate kinase type M2 and its role in tumor growth and spreading. Semin Cancer Biol. 2005;15(4):300–8.

82. Dombrauckas JD, Santarsiero BD, Mesecar AD. Structural basis for tumor pyruvate kinase M2 allosteric regulation and catalysis. Biochemistry. 2005;44(27):9417–29.

83. Wu S, Le H. Dual roles of PKM2 in cancer metabolism. Acta Biochim Biophys Sin. 2013;45(1):27–35.

84. Spoden G a, Rostek U, Lechner S, Mitterberger M, Mazurek S, Zwerschke W. Pyruvate kinase isoenzyme M2 is a glycolytic sensor differentially regulating cell proliferation, cell size and apoptotic cell death dependent on glucose supply. Exp Cell Res. Elsevier Inc.; 2009;315(16):2765–74.

85. Chaneton B, Gottlieb E. Rocking cell metabolism: Revised functions of the key glycolytic regulator PKM2 in cancer. Trends in Biochemical Sciences. 2012. p. 309–16.

86. Xueliang Gao, Haizhen Wang, J. Yang Jenny, Xiaowei Liu and Z-RL. Pyruvate Kinase M2 Regulates Gene Transcription by Acting as A Protein Kinas. 2012;45(5):598–609.

87. Hardt, P. D., and Ewald N. Tumor M2 pyruvate kinase: a tumor marker and its clinical application in gastrointestinal malignancy. Expert Rev Mol Diagn. 2008;8:579–85.

88. Valentini G, Chiarelli L, Fortin R, Speranza ML, Galizzi a, Mattevi a. The allosteric regulation of pyruvate kinase. J Biol Chem. 2000;275(24):18145–52.

89. Morgan HP, Zhong W, McNae IW, Michels PAM, Fothergill-Gilmore LA, Walkinshaw MD. Structures of pyruvate kinases display evolutionarily divergent allosteric strategies. R Soc Open Sci. 2014 Sep 24;1(1).

90. Suzuki K, Ito S, Shimizu-Ibuka A, Sakai H. Crystal structure of pyruvate kinase from Geobacillus stearothermophilus. J Biochem. 2008;144(3):305–12.

91. Eigenbrodt E, Reinacher M, Scheefers-Borchel U, Scheefers H, Friis R. Double role for pyruvate kinase type M2 in the expansion of phosphometabolite pools found in tumor cells. Crit Rev Oncog. 1991;3(1-2):91–115.

92. Williams R, Holyoak T, McDonald G, Gui C, Fenton AW. Differentiating a ligand's chemical requirements for allosteric interactions from those for protein binding. Phenylalanine inhibition of pyruvate kinase. Biochemistry. 2006;45(17):5421–9.

93. Chaneton B, Hillmann P, Zheng L, Martin ACL, Maddocks ODK, Chokkathukalam A, et al. Serine is a natural ligand and allosteric activator of pyruvate kinase M2. Nature. 2012;(V).

94. Keller KE, Tan IS, Lee Y-S. SAICAR Stimulates Pyruvate Kinase Isoform M2 and Promotes Cancer Cell Survival in Glucose-Limited Conditions. Science. 2012.

95. Hitosugi T, Kang S, Vander Heiden MG, Chung T-W, Elf S, Lythgoe K, et al. Tyrosine phosphorylation inhibits PKM2 to promote the Warburg effect and tumor growth. Sci Signal. NIH Public Access; 2009;2(97):ra73.

96. Anastasiou D, Poulogiannis G, Asara JM, Boxer MB, Jiang J -k., Shen M, et al. Inhibition of Pyruvate Kinase M2 by Reactive Oxygen Species Contributes to Cellular Antioxidant Responses. Science. 2011. p. 1278–83.

97. Mazurek S, Drexler HC a, Troppmair J, Eigenbrodt E, Rapp UR. Regulation of pyruvate kinase type M2 by A-Raf: a possible glycolytic stop or go mechanism. Anticancer Res. 2007;27(6B):3963–71.

98. Steták A, Veress R, Ovádi J, Csermely P, Kéri G, Ullrich A. Nuclear translocation of the tumor marker pyruvate kinase M2 induces programmed cell death. Cancer Res. 2007;67(4):1602–8.

99. Lee J, Kim HK, Han YM, Kim J. Pyruvate kinase isozyme type M2 (PKM2) interacts and cooperates with Oct-4 in regulating transcription. Int J Biochem Cell Biol. 2008;40(5):1043–54.

100. Luo W, Hu H, Chang R, Zhong J, Knabel M, O'Meally R, et al. Pyruvate kinase M2 is a PHD3-stimulated coactivator for hypoxia-inducible factor 1. Cell. Elsevier Inc.; 2011 May 27 [cited 2012 Nov 6];145(5):732–44.

101. Wang H-J, Hsieh Y-J, Cheng W-C, Lin C-P, Lin Y, Yang S-F, et al. JMJD5 regulates PKM2 nuclear translocation and reprograms HIF-1α-mediated glucose metabolism. Proc Natl Acad Sci U S A. 2014;111(1):279–84.

102. Yang W, Xia Y, Ji H, Zheng Y, Liang J, Huang W, et al. Nuclear PKM2 regulates β-catenin transactivation upon EGFR activation. Nature. 2011. p. 118–22.

103. David CJ, Chen M, Assanah M, Canoll P, Manley JL. HnRNP proteins controlled by c-Myc deregulate pyruvate kinase mRNA splicing in cancer. Nature. 2010;463(7279):364–8.

104. Yang W, Xia Y, Hawke D, Li X, Liang J, Xing D, et al. PKM2 phosphorylates histone H3 and promotes gene transcription and tumorigenesis. Cell. 2012;150(4):685–96.

105. Lv L, Xu YP, Zhao D, Li FL, Wang W, Sasaki N, et al. Mitogenic and Oncogenic Stimulation of K433 Acetylation Promotes PKM2 Protein Kinase Activity and Nuclear Localization. Mol Cell. 2013;52(3):340–52.

106. Mazurek S, S. M. Pyruvate kinase M2: A key enzyme of the tumor metabolome and its medical relevance. Biomed Res-India. 2012;23(133):133–41.

107. Christofk HR, Vander Heiden MG, Wu N, Asara JM, Cantley LC. Pyruvate kinase M2 is a phosphotyrosine-binding protein. Nature. 2008;452(7184):181–6.

108. Kefas B, Comeau L, Erdle N, Montgomery E, Amos S, Purow B. Pyruvate kinase M2 is a target of the tumor-suppressive microRNA-326 and regulates the survival of glioma cells. Neuro Oncol. 2010;12(11):1102–12.

109. Guo W, Zhang Y, Chen T, Wang Y, Xue J, Zhang Y, et al. Efficacy of RNAi targeting of pyruvate kinase M2 combined with cisplatin in a lung cancer model. J Cancer Res Clin Oncol. 2011;137(1):65–72.

110. Shi H, Li D, Zhang J, Wang Y, Yang L, Zhang H, et al. Silencing of pkm2 increases the efficacy of docetaxel in human lung cancer xenografts in mice. Cancer Sci. 2010;101(6):1447–53.

111. Müllner, S., Stark, H., Niskanen, P., Eigenbrodt, E., Mazurek, S. and Fasold H. From Target to Lead Synthesis, in Proteomics in Drug Research. (eds M Hamacher, K Marcus, K Stühler, A van Hall, B Warscheid H E Meyer), Wiley-VCH Verlag GmbH Co KGaA, Weinheim, FRG doi 101002/3527608230.ch10. 2006;

112. Chen J, Xie J, Jiang Z, Wang B, Wang Y, Hu X. Shikonin and its analogs inhibit cancer cell glycolysis by targeting tumor pyruvate kinase-M2. Oncogene. 2011;30(42):4297–306.

113. Anastasiou D, Yu Y, Israelsen WJ, Jiang J, Boxer MB, Hong BS, et al. Pyruvate kinase M2 activators promote tetramer formation and suppress tumorigenesis. Nat Chem Biol. 2012;8(10):839–47.

114. Jiang JK, Boxer MB, Vander Heiden MG, Shen M, Skoumbourdis AP, Southall N, et al. Evaluation of thieno[3,2-b]pyrrole[3,2-d]pyridazinones as activators of the tumor cell specific M2 isoform of pyruvate kinase. Bioorg Med Chem Lett. Elsevier Ltd; 2010;20(11):3387–93.

115. Boxer MB, Jiang JK, Vander Heiden MG, Shen M, Skoumbourdis AP, Southall N, et al. Evaluation of substituted N,N'-diarylsulfonamides as activators of the tumor cell specific M2 isoform of pyruvate kinase. J Med Chem. 2010;53(3):1048–55.

116. Walsh MJ, Brimacombe KR, Veith H, Bougie JM, Daniel T, Leister W, et al. 2-Oxo-N-aryl-1, 2, 3, 4-tetrahydroquinoline-6-sulfonamides as activators of the tumor cell specific M2 isoform of pyruvate kinase. Bioorg Med Chem Lett. Elsevier; 2011;21(21):6322–7.

117. Yacovan A, Ozeri R, Kehat T, Mirilashvili S, Sherman D, Aizikovich A, et al. 1-(sulfonyl)-5-(arylsulfonyl)indoline as activators of the tumor cell specific M2 isoform of pyruvate kinase. Bioorganic Med Chem Lett. 2012;22(20):6460–8.

118. Kung C, Hixon J, Choe S, Marks K, Gross S, Murphy E, et al. Small molecule activation of pkm2 in cancer cells induces serine auxotrophy. Chem Biol. 2012;19(9):1187–98.

119. Guo C, Linton A, Jalaie M, Kephart S, Ornelas M, Pairish M, et al. Discovery of 2-((1H-benzo[d]imidazol-1-yl)methyl)-4H-pyrido[1,2-a]pyrimidin-4-ones as novel PKM2 activators. Bioorg Med Chem Lett. 2013;23(11):3358–63.

120. Xu Y, Liu X-H, Saunders M, Pearce S, Foulks JM, Parnell KM, et al. Discovery of 3-(trifluoromethyl)-1H-pyrazole-5-carboxamide activators of the M2 isoform of pyruvate kinase (PKM2). Bioorg Med Chem Lett. Elsevier; 2014;24(2):515–9.

121. Granchi C, Bertini S, Macchia M, Minutolo F. Inhibitors of lactate dehydrogenase isoforms and their therapeutic potentials. Curr Med Chem. 2010;17(7):672–97.

122. Granchi C, Roy S, Giacomelli C, MacChia M, Tuccinardi T, Martinelli A, et al. Discovery of N-hydroxyindole-based inhibitors of human lactate dehydrogenase isoform A (LDH-A) as starvation agents against cancer cells. J Med Chem. 2011;54(6):1599–612.

123. Yu Y, Deck JA, Hunsaker LA, Deck LM, Royer RE, Goldberg E, et al. Selective active site inhibitors of human lactate dehydrogenases A4, B4, and C4. Biochem Pharmacol. 2001;62(1):81–9.

124. Read JA, Winter VJ, Eszes CM, Sessions RB, Brady RL. Structural basis for altered activity of M- and H-isozyme forms of human lactate dehydrogenase. Proteins Struct Funct Genet. 2001;43(2):175–85.

125. Baumgart E, Fahimi HD, Stich A, Völkl A. L-lactate dehydrogenase A4- and A3B isoforms are bona fide peroxisomal enzymes in rat liver: Evidence for involvement in intraperoxisomal nadh reoxidation. J Biol Chem. 1996;271(7):3846–55.

126. McClelland GB, Khanna S, González GF, Butz CE, Brooks GA. Peroxisomal membrane monocarboxylate transporters: Evidence for a redox shuttle system? Biochem Biophys Res Commun. 2003;304(1):130–5.

127. Elustondo P a, White AE, Hughes ME, Brebner K, Pavlov E, Kane D a. Physical and functional association of lactate dehydrogenase (LDH) with skeletal muscle mitochondria. J Biol Chem. 2013;288:25309–17.

128. Lemire J, Mailloux RJ, Appanna VD. Mitochondrial lactate dehydrogenase is involved in oxidative-energy metabolism in human astrocytoma cells (CCF-STTG1). PLoS One. 2008;3(2):1–10.

129. Brooks GA, Dubouchaud H, Brown M, Sicurello JP, Butz CE. Role of mitochondrial lactate dehydrogenase and lactate oxidation in the intracellular lactate shuttle. Proc Natl Acad Sci U S A. 1999;96(3):1129–34.

130. Kim JW, Dang C V. Multifaceted roles of glycolytic enzymes. Trends Biochem Sci. Elsevier; 2015;30(3):142–50.

131. Dai RP, Yu FX, Goh SR, Chng HW, Tan YL, Fu JL, et al. Histone 2B (H2B) expression is confined to a proper NAD+/NADH redox status. J Biol Chem. 2008;283(40):26894–901.

132. Kohlmann A, Zech SG, Li F, Zhou T, Squillace RM, Commodore L, et al. Fragment growing and linking lead to novel nanomolar lactate dehydrogenase inhibitors. J Med Chem. 2013;56(3):1023–40.

133. Zhao D, Zou SW, Liu Y, Zhou X, Mo Y, Wang P, et al. Lysine-5 acetylation negatively regulates lactate dehydrogenase a and is decreased in pancreatic cancer. Cancer Cell. 2013;23(4):464–76.

134. Draoui N, Feron O. Lactate shuttles at a glance: from physiological paradigms to anti-cancer treatments. Dis Model Mech. 2011;4:727–32.

135. Sonveaux P, Végran F, Schroeder T, Wergin MC, Verrax J, Rabbani ZN, et al. Targeting lactate-fueled respiration selectively kills hypoxic tumor cells in mice. J Clin Invest. American Society for Clinical Investigation; 2008 Dec 1 [cited 2015 Jan 11];118(12):3930–42.

136. Semenza GL. Tumor metabolism : cancer cells give and take lactate. Cancer. American Society for Clinical Investigation; 2008;118(12):3835–7.

137. Sheng SL, Liu JJ, Dai YH, Sun XG, Xiong XP, Huang G. Knockdown of lactate dehydrogenase A suppresses tumor growth and metastasis of human hepatocellular carcinoma. FEBS J. Wiley Online Library; 2012;279(20):3898–910.

138. Xue J-J, Chen Q-Y, Kong M-Y, Zhu C-Y, Gen Z-R, Wang Z-L. Synthesis, cytotoxicity for mimics of catalase: Inhibitors of lactate dehydrogenase and hypoxia inducible factor. Eur J Med Chem. Elsevier; 2014;80:1–7.

139. Manerba M, Vettraino M, Fiume L, di Stefano G, Sartini A, Giacomini E, et al. Galloflavin (CAS 568-80-9): A Novel Inhibitor of Lactate Dehydrogenase. ChemMedChem. 2012;7(2):311–7.

140. Farabegoli F, Vettraino M, Manerba M, Fiume L, Roberti M, Di Stefano G. Galloflavin, a new lactate dehydrogenase inhibitor, induces the death of human breast cancer cells with different glycolytic attitude by affecting distinct signaling pathways. Eur J Pharm Sci. 2012;47(4):729–38.

141. Dragovich PS, Fauber BP, Corson LB, Ding CZ, Eigenbrot C, Ge H, et al. Identification of substituted 2-thio-6-oxo-1,6-dihydropyrimidines as inhibitors of human lactate dehydrogenase. Bioorganic Med Chem Lett. 2013;23(11):3186–94.

142. Granchi C, Calvaresi EC, Tuccinardi T, Paterni I, Macchia M, Martinelli A, et al. Assessing the differential action on cancer cells of LDH-A inhibitors based on the N-hydroxyindole-2-carboxylate (NHI) and malonic (Mal) scaffolds. Org Biomol Chem. 2013;11(38):6588–96.

143. Moorhouse AD, Spiteri C, Sharma P, Zloh M, Moses JE. Targeting glycolysis: a fragment based approach towards bifunctional inhibitors of hLDH-5. Chem Commun (Camb). 2011;47(1):230–2.

144. Ward RA, Brassington C, Breeze AL, Caputo A, Critchlow S, Davies G, et al. Design and synthesis of novel lactate dehydrogenase a inhibitors by fragment-based lead generation. J Med Chem. 2012;55(7):3285–306.

145. Zhou M, Zhao Y, Ding Y, Liu H, Liu Z, Fodstad O, et al. Warburg effect in chemosensitivity: targeting lactate dehydrogenase-A re-sensitizes taxol-resistant cancer cells to taxol. Mol Cancer. 2010;9:33.

146. Zhao Y, Liu H, Liu Z, Ding Y, LeDoux SP, Wilson GL, et al. Overcoming trastuzumab resistance in breast cancer by targeting dysregulated glucose metabolism. Cancer Res. 2011;71(13):4585–97.

147. Alberts B, Johnson A LJ and RM. Molecular Biology of The Cell. 5th ed. New York ; Abingdon : Garland Science; 2008.

148. Henderson L, Bortone DS, Lim C ZA. Classic Broken Cell and Newer Live Cell Methods for Cell Cycle Assessment. Am J Physiol Cell Physiol. 2013;

149. Blow JJ, Dutta A. Preventing re-replication of chromosomal DNA. Nat Rev Mol Cell Biol. Nature Publishing Group; 2005;6(6):476–86.

150. Williams G, Stoeber K. Cell cycle markers in clinical oncology. Curr Opin Cell Biol. CURRENT BIOLOGY LTD; 2007;19(6):672–9.

151. Williams GH, Stoeber K. The cell cycle and cancer. J Pathol. 2012;226(2):352–64.

152. Kontzoglou K, Palla V, Karaolanis G, Karaiskos I, Alexiou I, Pateras I, Konstantoudakis K SM. Correlation between Ki67 and Breast Cancer Prognosis. Oncology. 2013;84(4):219–25.

153. Urruticoechea A, Smith I E and DM. Proliferation Marker Ki67 in Early Breast Cancer. J Clin Oncol. 2005;23:7212–20.

154. Dowsett M, Nielsen TO, A'Hern R, Bartlett J, Coombes RC, Cuzick J, et al. Assessment of Ki67 in breast cancer: recommendations from the International Ki67 in Breast Cancer working group. J Natl Cancer Inst. 2011;103(22):1656–64.

155. Jonat W, Arnold N. Is the Ki-67 labelling index ready for clinical use? Ann Oncol. 2011;22(3):500–2.

156. Ademmer K, Ebert M, Müller-Ostermeyer F, Friess H, Büchler MW, Schubert W, et al. Effector T lymphocyte subsets in human pancreatic cancer: detection of CD8+CD18+ cells and CD8+CD103+ cells by multi-epitope imaging. Clin Exp Immunol. 1998 Apr;112(1):21–6.

157. Deschoolmeester V, Baay M, Van Marck E, Weyler J, Vermeulen P, Lardon F, et al. Tumor infiltrating lymphocytes: an intriguing player in the survival of colorectal cancer patients. BMC Immunol. 2010 Jan;11:19.

158. Mahmoud SM a, Paish EC, Powe DG, Macmillan RD, Grainge MJ, Lee AHS, et al. Tumor-infiltrating CD8+ lymphocytes predict clinical outcome in breast cancer. J Clin Oncol. 2011;29(15):1949–55.

159. Ikeguchi M, Oi K, Hirooka Y, Kaibara N. CD8+ lymphocyte infiltration and apoptosis in hepatocellular carcinoma. Eur J Surg Oncol. 2004;30(1):53–7.

160. Murphy KM, T. T. WM. Antigen recognition by B-cell and T-cell receptors. In: Janeway's immunobiology. 8 ed. Garland Science, New york, NY; 2012. p. 138–51.

161. Trapani J a, Smyth MJ. Functional significance of the perforin/granzyme cell death pathway. Nat Rev Immunol. 2002 Oct [cited 2013 Feb 28];2(10):735–47.

162. Yu X, Ji S, Xu J, Yao W, Qu B, Zhu W, et al. CD8 + T Cells Are Compromised In Human Pancreatic Cancer. 2012;2(1):2–5.

163. OpenStax College. Adaptive Immune Response [Internet]. 2013. Available from: http://cnx.org/content/m44821/latest/?collection=col11448/latest

164. Buchwalow B I BW. Immunohistochemistry: basics and methods. Heidelberg ; London : Springer; 2010.

165. Gillett CE. Immunohistochemistry. In: Susan A. Brooks AH, editor. Breast Cancer Researh Protocols. 2006. p. 191–200.

166. Ramos-Vara JA. Principles and methods of immunohistochemistry. In: Gautier J-C, editor. Drug Safety Evaluation Methods and Protocols. 2011. p. 83–96.

167. IHC World. Immunohistchemistry:Introduction to Immunohistochemistry. Retrived February 5, 2013 from:http://www.ihcworld.com/_intro/ihc-methods.htm.

168. Dhar DK, Olde Damink SWM, Brindley JH, Godfrey A, Chapman MH, Sandanayake NS, et al. Pyruvate kinase M2 is a novel diagnostic marker and predicts tumor progression in human biliary tract cancer. Cancer. 2013 Feb;119(3):575–85.

169. Allison. LA. Fundamental Molecular Biology. Malden, MA ; Oxford : Blackwell Pub.; 2007. 251-258 p.

170. Yang Y, Ma H. Western Blotting and ELISA Techniques. Researcher. 2009;1(2):67–86.

171. Moore C. Introduction to Western Blotting Western Blotting. MorphoSys UK Ltd; 2009.

172. Singh S, Tan M, Rameshwar P. Cancer Metabolism: Targeting metabolic pathways in cancer therapy. Cancer Lett. 2015;356:147–8.

173. Kumar Y, Gurusamy K, Pamecha V, Davidson BR. Tumor M2-pyruvate kinase as tumor marker in exocrine pancreatic cancer a meta-analysis. Pancreas. 2007;35(2):114–9.

174. Goonetilleke KS, Mason JM, Siriwardana P, King NK, France MW, Siriwardena AK. Diagnostic and prognostic value of plasma tumor M2 pyruvate kinase in periampullary cancer: evidence for a novel biological marker of adverse prognosis. Pancreas. 2007 Apr;34(3):318–24.

175. He T-L, Zhang Y-J, Jiang H, Li X, Zhu H, Zheng K-L. The c-Myc–LDHA axis positively regulates aerobic glycolysis and promotes tumor progression in pancreatic cancer. Med Oncol. Springer; 2015;32(7):1–8.

176. Kachel P, Trojanowicz B, Sekulla C, Prenzel H, Dralle H, Hoang-Vu C. Phosphorylation of pyruvate kinase M2 and lactate dehydrogenase A by fibroblast growth factor receptor 1 in benign and malignant thyroid tissue. BMC Cancer. BioMed Central Ltd; 2015;15(1):140.

177. Yang W, Zheng Y, Xia Y, Ji H, Chen X, Guo F, et al. ERK1/2-dependent phosphorylation and nuclear translocation of PKM2 promotes the Warburg effect. Nat Cell Biol. Nature Publishing Group; 2012;14(12):1295–304.

178. Hitosugi T, Kang S, Vander Heiden MG, Chung T-W, Elf S, Lythgoe K, et al. Tyrosine phosphorylation inhibits PKM2 to promote the Warburg effect and tumor growth. Sci Signal. NIH Public Access; 2009;2(97):ra73.

179. Wang Y, Zhang X, Zhang Y, Zhu Y, Yuan C, Qi B, et al. Overexpression of pyruvate kinase M2 associates with aggressive clinicopathological features and unfavorable prognosis in oral squamous cell carcinoma. Cancer Biol Ther. Taylor & Francis; 2015;(just-accepted):0.

180. Sun X, Sun Z, Zhu Z, Li C, Zhang J, Xu H, et al. Expression of SIP1 is strongly correlated with LDHA and shows a significantly poor outcome in gastric cancer. Tumor Biol. Springer; 2015;1–10.

181. Rajeshkumar N V., Dutta P, Yabuuchi S, de Wilde RF, Matrinez G V., Le a., et al. Therapeutic targeting of the Warburg effect in pancreatic cancer relies on an absence of p53 function. Cancer Research. 2015. 713-745 p.

182. Li Z, Yang P, Li Z. The multifaceted regulation and functions of PKM2 in tumor progression. Biochim Biophys Acta. Elsevier B.V.; 2014;

183. Jiang Y, Li X, Yang W, Hawke DH, Zheng Y, Xia Y, et al. PKM2 Regulates Chromosome Segregation and Mitosis Progression of Tumor Cells. Mol Cell. 2014;53(1):75–87.

184. Parra-Bonilla G, Alvarez DF, Alexeyev M, Vasauskas A, Stevens T. Lactate Dehydrogenase A Expression Is Necessary to Sustain Rapid Angiogenesis of Pulmonary Microvascular Endothelium. PLoS One. 2013;8(9).

185. Crane CA, Austgen K, Haberthur K, Hofmann C, Moyes KW, Avanesyan L, et al. Immune evasion mediated by tumor-derived lactate dehydrogenase induction of NKG2D ligands on myeloid cells in glioblastoma patients. Proc Natl Acad Sci. 2014;1413933111 – .

186. Liu W-R, Tian M-X, Yang L-X, Lin Y-L, Jin L, Ding Z-B, et al. PKM2 promotes metastasis by recruiting myeloid-derived suppressor cells and indicates poor prognosis for hepatocellular carcinoma. Oncotarget. Impact Journals, LLC; 2015;6(2):846.

187. Lockney NA, Zhang M, Lu Y, Sopha SC, Washington MK, Merchant N, et al. Pyruvate Kinase Muscle Isoenzyme 2 (PKM2) Expression Is Associated with Overall Survival in Pancreatic Ductal Adenocarcinoma. J Gastrointest Cancer. 2015;2.

188. Lim JY, Yoon SO, Seol SY, Hong SW, Kim JW, Choi SH, et al. Overexpression of the M2 isoform of pyruvate kinase is an adverse prognostic factor for signet ring cell gastric cancer. World J Gastroenterol. 2012;18:4037–43.

189. Zhang X, He C, He C, Chen B, Liu Y, Kong M, et al. Nuclear PKM2 expression predicts poor prognosis in patients with esophageal squamous cell carcinoma. Pathol Res Pract. 2013;209:510–5.

190. Li J, Yang Z, Zou Q, Yuan Y, Liang L, Zeng G, et al. PKM2 and ACVR 1C are prognostic markers for poor prognosis of gallbladder cancer. Clin Transl Oncol. 2014;16:200–7.

191. Wiench B, Eichhorn T, Paulsen M, Efferth T. Shikonin directly targets mitochondria and causes mitochondrial dysfunction in cancer cells. Evidence-Based Complement Altern Med. Hindawi Publishing Corporation; 2012;2012:726025.

192. Chang I-C, Huang Y-J, Chiang T-I, Yeh C-W, Hsu L-S. Shikonin induces apoptosis through reactive oxygen species/extracellular signal-regulated kinase pathway in osteosarcoma cells. Biol Pharm Bull.; 2010;33(5):816–24.

193. Hou Y, Xu J, Liu X, Xia X, Li N, Bi X. Shikonin induces apoptosis in the human gastric cancer cells HGC-27 through mitochondria-mediated pathway. Pharmacogn Mag. India: Medknow Publications & Media Pvt Ltd; 2015;11(42):250–6.

194. Hou Y, Guo T, Wu C, He X, Zhao M. Effect of shikonin on human breast cancer cells proliferation and apoptosis in vitro. Yakugaku Zasshi. The Pharmaceutical Society of Japan; 2006;126(12):1383–6.

195. Yeh C-C, Kuo H-M, Li T-M, Lin J-P, Yu F-S, Lu H-F, et al. Shikonin-induced apoptosis involves caspase-3 activity in a human bladder cancer cell line (T24). In Vivo (Brooklyn). 2007;21(6):1011–9.

196. Hao Z, Qian J, Yang J. Shikonin induces apoptosis and inhibits migration of ovarian carcinoma cells by inhibiting the phosphorylation of Src and FAK. Oncol Lett. Spandidos Publications; 2015;9(2):629–33.

197. Gara RK, Srivastava VK, Duggal S, Bagga JK, Bhatt M, Sanyal S, et al. Shikonin selectively induces apoptosis in human prostate cancer cells through the endoplasmic reticulum stress and mitochondrial apoptotic pathway. J Biomed Sci. BioMed Central Ltd; 2015;22(1):26.

198. Wu Z, Wu L, Li L, Tashiro S, Onodera S, Ikejima T. p53-Mediated Cell Cycle Arrest and Apoptosis Induced by Shikonin via a Caspase-9-Dependent Mechanism in Human Malignant Melanoma A375-S2 Cells. J Pharmacol Sci. 2004;94(2):166–76.

199. Yeh Y-C, Liu T-J, Lai H-C. Shikonin Induces Apoptosis, Necrosis, and Premature Senescence of Human A549 Lung Cancer Cells through Upregulation of p53 Expression. Evidence-Based Complement Altern Med. 2015;2015:1–13.

200. Kolev Y, Uetake H, Takagi Y, Sugihara K. Lactate dehydrogenase-5 (LDH-5) expression in human gastric cancer: association with hypoxia-inducible factor (HIF-1α) pathway, angiogenic factors production and poor prognosis. Ann Surg Oncol. Springer; 2008;15(8):2336–44.

201. Yu Y, Liao M, Liu R, Chen J, Feng H, Fu Z. Overexpression of lactate dehydrogenase-A in human intrahepatic cholangiocarcinoma: its implication for treatment. World J Surg Oncol. 2014;12:78.

202. Koukourakis MI, Giatromanolaki A, Sivridis E, Bougioukas G, Didilis V, Gatter KC, et al. Lactate dehydrogenase-5 (LDH-5) overexpression in non-small-cell lung cancer tissues is linked to tumour hypoxia, angiogenic factor production and poor prognosis. Br J Cancer. Nature Publishing Group; 2003;89(5):877–85.

203. Yao Y, Wang H, Li B. LDH5 overexpression is associated with poor survival in patients with solid tumors: a meta-analysis. Tumor Biol. 2014;35:6973–81.

204. Gourgou-Bourgade S, Bascoul-Mollevi C, Desseigne F, Ychou M, Bouché O, Guimbaud R, et al. Impact of FOLFIRINOX compared with gemcitabine on quality of life in patients with metastatic pancreatic cancer: Results from the PRODIGE 4/ACCORD 11 randomized trial. J Clin Oncol. 2013;31(1):23–9.

205. Tamada M, Suematsu M, Saya H. Pyruvate kinase M2: Multiple faces for conferring benefits on cancer cells. Clinical Cancer Research. 2012. p. 5554–61.

206. Yuan C, Li Z, Wang Y, Qi B, Zhang W, Ye J, et al. Overexpression of metabolic markers PKM2 and LDH5 correlates with aggressive clinicopathological features and adverse patient prognosis in tongue cancer. Histopathology. 2014;65(5):595–605.

207. Sun Q, Chen X, Ma J, Peng H, Wang F, Zha X, et al. Mammalian target of rapamycin up-regulation of pyruvate kinase isoenzyme type M2 is critical for aerobic glycolysis and tumor growth. Proc Natl Acad Sci U S A. 2011;108(10):4129–34.

208. Luo W, Semenza GL. Pyruvate kinase M2 regulates glucose metabolism by functioning as a coactivator for hypoxia-inducible factor 1 in cancer cells. Oncotarget. 2011;2(7):551–6.

209. Tas F, Aykan F, Alici S, Kaytan E, Aydiner A, Topuz E. Prognostic factors in pancreatic carcinoma: serum LDH levels predict survival in metastatic disease. Am J Clin Oncol. 2001;24(6):547–50.

210. Dai Y-D. Prognostic factors in patients with pancreatic cancer. Exp Ther Med. 2011;423–32.

211. Stocken DD, Hassan a B, Altman DG, Billingham LJ, Bramhall SR, Johnson PJ, et al. Modelling prognostic factors in advanced pancreatic cancer. Br J Cancer. 2008;99:883–93.

212. Lee H, Yuh Y, Kim S. Serum lactate dehydrogenase (LDH) level as a prognostic factor for the patients with advanced gastric cancer. In: ASCO Annual Meeting Proceedings. 2009. p. e15621.

213. Schneider J, Neu K, Grimm H, Velcovsky H-G, Weisse G, Eigenbrodt E. Tumor M2-pyruvate kinase in lung cancer patients: immunohistochemical detection and disease monitoring. Anticancer Research. 2002. p. 311–8.

214. Hermes A, Gatzemeier U, Waschki B, Reck M. Lactate dehydrogenase as prognostic factor in limited and extensive disease stage small cell lung cancer - A retrospective single institution analysis. Respir Med. Elsevier Ltd; 2010;104(12):1937–42.

215. Lüftner D, Mesterharm J, Akrivakis C, Geppert R, Petrides PE, Wernecke KD, et al. Tumor type M2 pyruvate kinase expression in advanced breast cancer. Anticancer Res. 1999;20(6D):5077–82.

216. Mishra S, Sharma DC, Sharma P. Studies of biochemical parameters in breast cancer with and without metastasis. Indian J Clin Biochem. 2004;19(1):71–5.

217. Wechsel HW, Petri E, Bichler KH, Feil G. Marker for renal cell carcinoma (RCC): the dimeric form of pyruvate kinase type M2 (Tu M2-PK). Anticancer Res. 1998;19(4A):2583–90.

218. Armstrong AJ, George DJ, Halabi S. Serum lactate dehydrogenase predicts for overall survival benefit in patients with metastatic renal cell carcinoma treated with inhibition of mammalian target of rapamycin. J Clin Oncol. 2012;30:3402–7.

219. Sasaki T, Isayama H, Nakai Y, Togawa O, Kogure H, Ito Y, et al. Prognostic factors in patients with advanced biliary tract cancer receiving chemotherapy. Cancer Chemother Pharmacol. Springer; 2011;67(4):847–53.

220. Rosenberg SA, Sherry RM, Morton KE, Scharfman WJ, Yang JC, Topalian SL, et al. Tumor progression can occur despite the induction of very high levels of self/tumor antigen-specific CD8+ T cells in patients with melanoma. J Immunol. 2005;175(9):6169–76.

221. Salama P, Phillips M, Platell C, Iacopetta B. Low expression of Granzyme B in colorectal cancer is associated with signs of early metastastic invasion. Histopathology. 2011;59(2):207–15.

222. Zhang Y, Huang S, Gong D, Qin Y, Shen Q. Programmed death-1 upregulation is correlated with dysfunction of tumor-infiltrating CD8+ T lymphocytes in human non-small cell lung cancer. Cell Mol Immunol. 2010;7(5):389–95.

223. Zhang Z, Liu Q, Che Y, Yuan X, Dai L, Zeng B, et al. Antigen presentation by dendritic cells in tumors is disrupted by altered metabolism that involves pyruvate kinase M2 and its interaction with SOCS3. Cancer Res. 2010;70(1):89–98.

224. Calcinotto A, Filipazzi P, Grioni M, Iero M, De Milito A, Ricupito A, et al. Modulation of microenvironment acidity reverses anergy in human and murine tumor-infiltrating T lymphocytes. Cancer Res. AACR; 2012;72(11):2746–56.

225. Kim DJ, Park YS, Kang MG, You Y-M, Jung Y, Koo H, et al. Pyruvate kinase isoenzyme M2 is a therapeutic target of gemcitabine-resistant pancreatic cancer cells. Exp Cell Res. Elsevier; 2015;336(1):119–29.

226. Wang S, Ma Y, Wang P, Song Z, Liu B, Sun X, et al. Knockdown of PKM2 Enhances Radiosensitivity of Non-small cell Lung Cancer. Cell Biochem Biophys. Springer; 2015;1–6.

APPENDIX 1

Pyruvate Kinase-M2 (PKM2) as a Novel Diagnostic Marker and Therapeutic Target for Pancreatic Cancer

Goran Hamid Mohammad[1,2], Dipok Kumar Dhar[1, 3], Stephen P. Pereira[1]

[1]UCL Institute for Liver and Digestive Health, Royal Free Hospital Campus, University College London, London, UK, [2]Chemistry Department, School of Science, University of Sulaimani, Sulaimanyah, Kurdistan Region, Iraq, [3]King Faisal Specialist Hospital and Research Centre, Riyadh, Saudi Arabia

Introduction

Pancreatic ductal adenocarcinoma (PDAC) is diagnosed at a late and incurable stage, leaving patients with a 5-year survival rate of <4%. Therefore new diagnostic and treatment strategies are necessary. For example, pyruvate kinase type M2 (PKM2) and lactate dehydrogenase A (LDHA) are important glycolytic enzymes, which play a role in the initiation and progression of PDAC and could therefore serve as potential targets for therapy.

Aims

•To evaluate the expression of PKM2 & LDHA in pancreatic pre-neoplastic lesions and cancers & correlate with patient outcome.

•To evaluate the potential of PKM2 & LDHA as novel targets for therapy in PDAC.

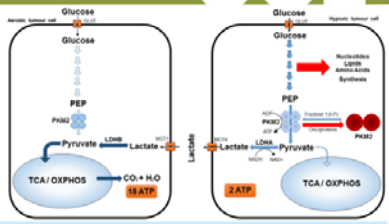

Fig 1. Cancer cell metabolism. Hypoxic tumour cells utilize high amounts of glucose, producing lactate; however, aerobic tumour cells can use lactate as an energy source and spare glucose for hypoxic tumour cells.

Methods

- PKM2, LDHA, CD8+ & Ki-67 assessed in 124 PDAC, 11 Ampullary, 49 pancreatic cysts, 19 PanIN, 21 Pancreatitis, 42 normal pancreas by IHC.
- PKM2 & LDHA also assessed by Western blotting in 10 human pancreatic cancer cell lines.
- Targeting of PKM2 & LDHA by TEPP-46 & FX11 alone or in combination both in vitro and in vivo in subcutaneous & orthotopic pancreatic cancer xenograft models.

Results

- PKM2 & LDHA overexpressed with progressive increase in PKM2 expression during tumour progression.
- High LDHA expression in pancreatitis, pre-neoplastic & tumour tissues
- High expression of PKM2 & LDHA in pancreatic cancer cell lines.
- Plasma PK and LDH concentrations higher in pancreatic cancer compared to healthy controls (45.5 vs 21.6 U/L and 685 vs 194 U/L, P < 0.0001).

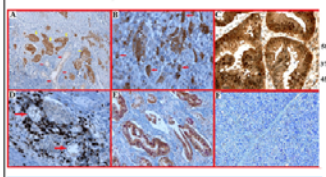

Fig 2. PKM2 & LDHA expression (A) Well differentiated area of tumour showing weak PKM2 expression (red arrow), high expression in poorly differentiated areas (brown colour, yellow arrow). (B) Heterogeneous expression of PKM2 with predominant expression in proliferating cells (red arrow). (C) Strong cytoplasmic & nuclear expression of LDHA. (D) Well differentiated tumours with strong CD8+ T-lymphocytes infiltration. (E) High PKM2 expression in Ki-67+ cells. (F) Normal pancreas.

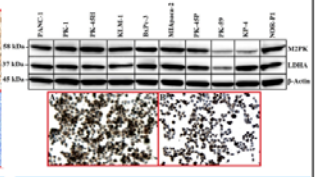

Fig 3. PKM2 & LDHA expression in pancreatic cancer cell lines (upper panel). Immunostaining of Miapaca-2 cells with PKM2 (A) & LDHA (B) (lower panel). Strong cytoplasmic & nuclear staining in proliferating cells.

- PKM2 & LDHA expression correlated with tumour size & differentiation (p= 0.047, Chi-square test).
- Increased CD8+ TIL in tumours with low PKM2 or LDHA expression (p=0.0001, p=0.005 respectively).
- Patients with tumours that had strong PKM2 & LDHA expression, had significantly worse survival than those with weak PKM2 &/or LDHA expression (7.0 months vs. 27.9 months, respectively, p = 0.003, log rank test, Fig 4).

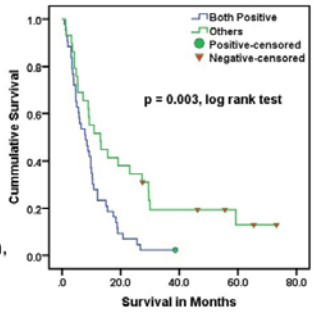

Fig 4. Overall patient survival in relation to PKM2 & LDHA expression.

- TEPP-46 & FX11 combination treatment synergistically reduced cell proliferation in vitro in 10 pancreatic cancer cell lines
- Maximum inhibitory effect in BxPc-3 cells (IC50=30.32 μM & CI = 0.45)

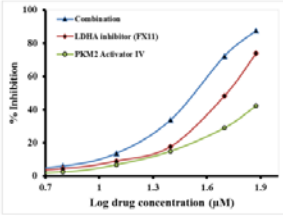

Fig 5. Effect of single & combination treatment on BxPc-3 cell lines.

- Combination therapy significantly delayed tumour growth compared to vehicle control in both subcutaneous & orthotopic xenografts ($p < 0.0001$).
- Significant reduction in tumour growth compared with controls ($p < 0.0001$).

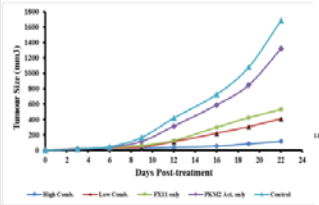

Fig 6. Tumour growth of subcutaneous xenografts

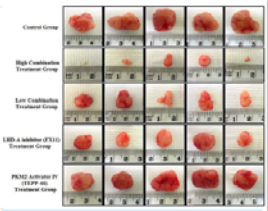

Fig 7. Effect of single & combination treatment on subcutaneous tumours after 21 days of treatment compared with controls.

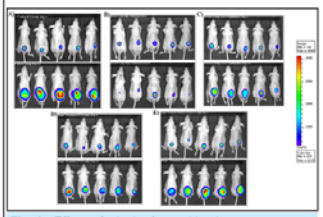

Fig 8. Effect of single & combination treatment on subcutaneous tumour growth. (A) vehicle-control group. (B) High combination treated group. (C) Low combination treated group. (D) LDHA inhibitor treated group. (E) PKM2 activator treated group (at start & 21 days of therapy).

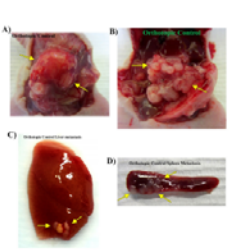

Fig 9. Tumour volume, liver & spleen metastasis in orthotopic control group.

- Combination treatment reduced M2PK, LDHA & Ki-67 ($P < 0.0001$), increased CD8+TIL and abolished metastases in the orthotopic model.

Conclusions

- M2PK & LDHA are overexpressed in pancreatic cancer and associated with poor patient outcome.
- Activation of M2PK in combination with LDHA inhibition synergistically inhibits pancreatic cancer cell proliferation & impairs tumour growth in pancreatic cancer xenograft models.

Acknowledgements: This work was supported by NIH grant P01 CA084203, The Pancreatic Cancer Research Fund, The Jason Boas Foundation and the UCLH/UCL Comprehensive Biomedical Centre.

Table 1: TNM classification of pancreatic cancer according to the American Joint Committee on Cancer (AJCC).

I- Classification according to tumour size (T)	
TX	The tumour cannot be assessed.
T0	No evidence of a primary tumour.
Tis	Cancer in situ (few tumour cells found)
T1	Tumour inside pancreas and less than 2 cm in size.
T2	Tumour still inside pancreas but the size of it larger than 2 cm.
T3	The tumour has started to grow into the near surrounding pancreas tissue but it has not extended to the nerves or blood vessels.
T4	The tumour has spread further outside the pancreas to the nearest large blood vessels or nerves
II- Classification according to lymph nodes (N)	
NX	Regional lymph nodes cannot be assessed
N0	The tumour has not extended to the regional lymph nodes
N1	The tumour has extended to the regional lymph nodes
III- Classification according to metastasis (M)	
M0	The cancer has not spread to distant lymph nodes or to the other organ such as lung, liver, brain, etc.
M1	The cancer has spread (Metastasis) to other organs.

Table 2: Staging of pancreatic cancer according to the American Joint Committee on Cancer (AJCC).

Stages	Meaning	TNM system
Stage 0	The tumour is just on the outer layer of pancreatic duct cells and it is not gone down to the deeper tissue layers and it is not spread.	Tis,N0,M0
Stage IA	The tumour inside pancreas with less than 2 cm in size and it has not extended to distant or near lymph nodes.	T1,N0,M0
Stage IB	The tumour inside pancreas with larger than 2 cm in size and it has not extended to distant or near lymph nodes.	T2,N0,M0
Stage IIA	The tumour has started to grow into near surrounding tissues outside pancreas but it has not extended to large blood vessels or near lymph nodes.	T3,N0,M0
Stage IIB	The tumour is either inside the pancreas or extended to surrounding but it has not spread to the main nerves or large blood vessels. The tumour has extended to the near lymph nodes but not distant.	T1-3,N1,M0
Stage III	The tumour has spread to surrounding of pancreas and it has extended to near large blood vessels or main nerves. It may or may not extend to near lymph nodes and it has not extended to distant sites.	T4,Any N,M0
Stage IV	The cancer has extended and metastasized to the other distant organs such as liver and lung.	Any T, Any N,M1

A) Optimization of Shikonin concentration, the figures show the effect of Shikonin treatment on PK-1 cell viability (%):

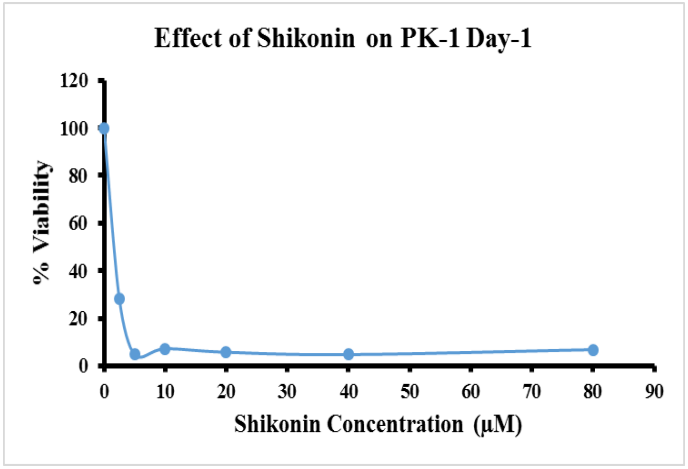

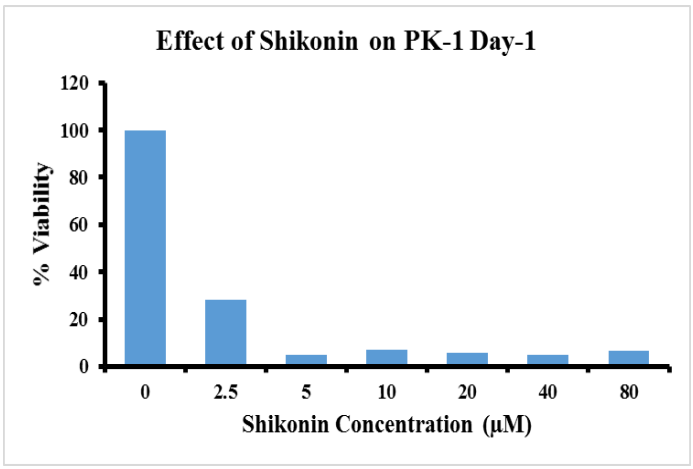

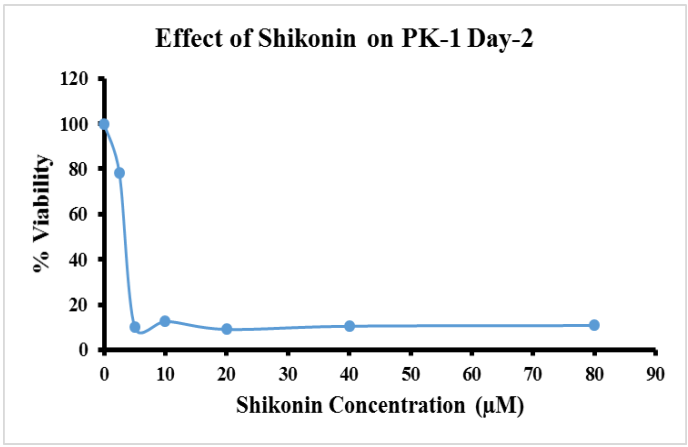

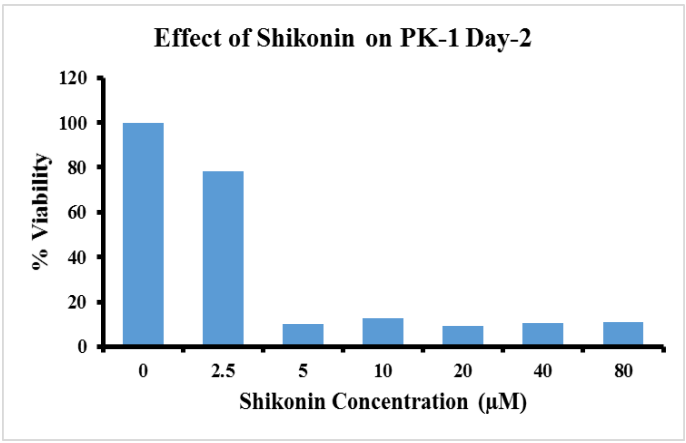

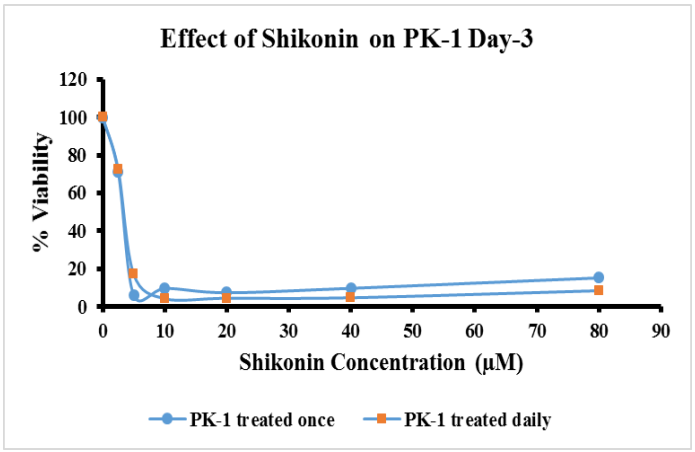

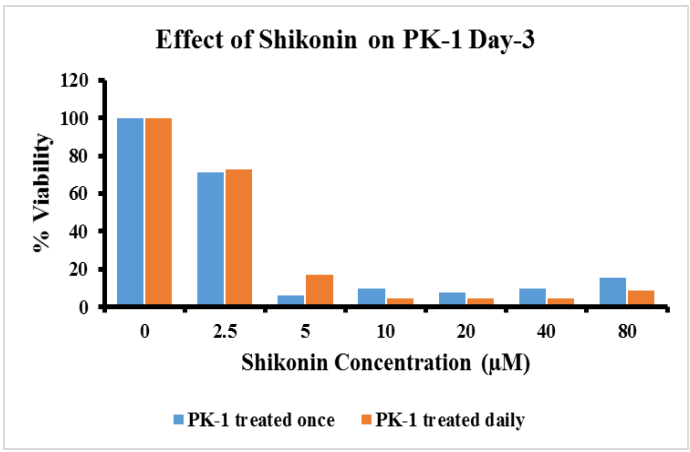

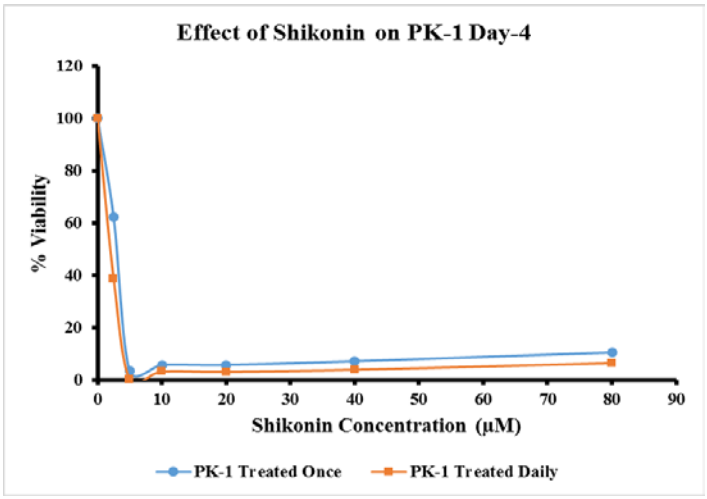
Effect of Shikonin on PK-1 Day-4
% Viability
120
100
80
60
40
20
0
0
10
20
30
40
50
60
70
80
90
Shikonin Concentration (µM)
PK-1 Treated Once
PK-1 Treated Daily

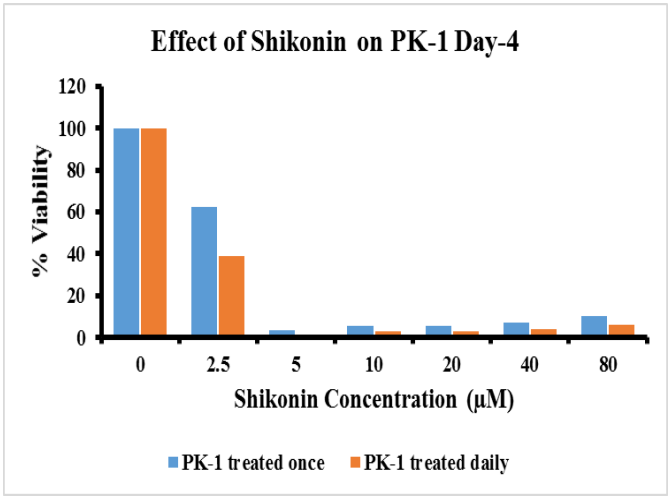
Effect of Shikonin on PK-1 Day-4
% Viability
120
100
80
60
40
20
0
0
2.5
5
10
20
40
80
Shikonin Concentration (µM)
PK-1 treated once
PK-1 treated daily

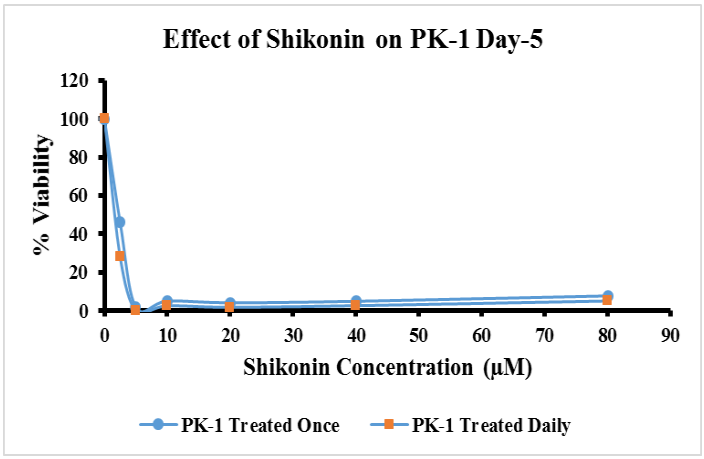
Effect of Shikonin on PK-1 Day-5
% Viability
120
100
80
60
40
20
0
0
10
20
30
40
50
60
70
80
90
Shikonin Concentration (µM)
PK-1 Treated Once
PK-1 Treated Daily

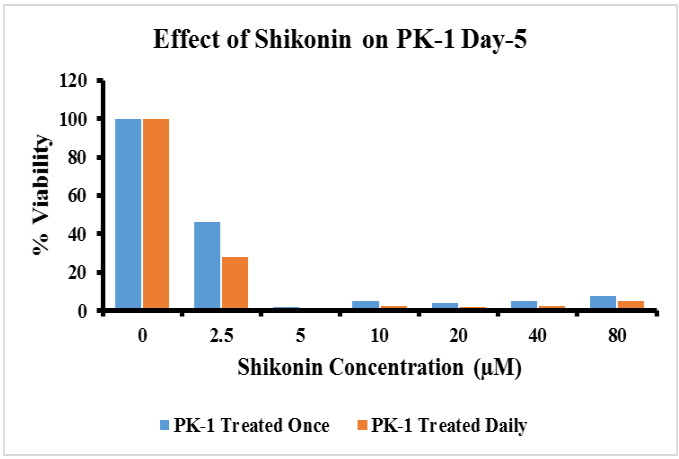
Effect of Shikonin on PK-1 Day-5
% Viability
120
100
80
60
40
20
0
0
2.5
5
10
20
40
80
Shikonin Concentration (µM)
PK-1 Treated Once
PK-1 Treated Daily

B) Optimization of PKM2 activator and LDHA inhibitor combination ratio, the tables show the effect of single and combination treatment on cell viability (%):

24 hrs

FX11 Concentration (µM) \ PKM2 Activator IV Concentration (µM)	0	6.25	12.5	25	50	100
0	100	99.8	96.28	92.5	88.87	80.05
2.5	97.76	91.54	93.4	86.64	95.47	84.96
5	90.4	88.26	94.21	90	92.18	80.83
10	87.88	97.78	86	92.22	91.39	80.44
20	83.37	82.54	85.16	78.83	82.2	71.78
40	78.76	87	87.48	84.57	75.04	71.45
60	76.73	85.44	86.26	79.63	74.06	70.2
100	57.63	64.3	56	53.3	49.25	42.84

48 hrs

FX11 Concentration (µM) \ PKM2 Activator IV Concentration (µM)	0	6.25	12.5	25	50	100
0	100	99.13	96.84	90.54	84.41	73.62
2.5	93.91	88.62	97.23	97.88	90.15	70.33
5	88.43	80.01	95.59	93.79	87.88	68.48
10	88.10	99.12	78.16	95.30	92.49	68.34
20	85.50	89.27	94.47	77.93	81.91	63.00
40	75.01	89.66	84.84	78.07	65.19	50.51
60	59.85	66.50	66.63	55.15	44.37	38.82
100	23.36	31.41	32.67	26.17	24.01	17.74

72 hrs

FX11 Concentration (µM) \ PKM2 Activator IV Concentration (µM)	0	6.25	12.5	25	50	100
0	100	99.92	96.61	81.10	70.64	46.70
2.5	96.57	88.65	93.72	77.68	67.79	55.42
5	90.69	70.50	78.69	69.59	61.73	53.73
10	85.84	93.52	64.51	73.75	50.80	49.05
20	80.90	94.29	81.23	51.76	40.35	42.00
40	72.99	72.40	70.92	57.29	30.37	29.77
60	45.30	51.93	47.55	32.00	18.92	26.56
100	13.08	18.49	17.44	11.54	7.21	5.03

96 hrs

FX11 Concentration (µM) \ PKM2 Activator IV Concentration (µM)	0	6.25	12.5	25	50	100
0	100	92.12	87.24	72.74	56.45	41.40
2.5	95.12	91.46	88.70	67.77	52.19	40.75
5	88.74	72.08	88.73	62.05	51.14	39.79
10	83.47	92.06	61.22	66.68	52.51	31.25
20	80.79	87.71	83.66	49.96	49.05	36.25
40	71.54	83.20	84.40	45.04	25.54	26.83
60	43.76	48.96	45.68	28.03	17.82	14.79
100	12.50	16.96	16.13	10.62	6.29	3.52